Analyse von Alterungsmechanismen im Hinblick auf die Effizienz von Haushaltskältegeräten

zur Erlangung des akademischen Grades
DOKTOR DER INGENIEURWISSENSCHAFTEN
(Dr.-Ing.)
der Fakultät für Maschinenbau
der Universität Paderborn

genehmigte
DISSERTATION

von
Dipl.-Ing. Andreas Paul
aus Geseke

Tag des Kolloquiums:	10. Juli 2023
Referent:	Prof. Dr.-Ing. habil. Jadran Vrabec
Korreferentin:	Prof. Dr. Tina Kasper

Danksagung

Die vorliegende Dissertation entstand in der Zeit von 2014 bis 2023 im Rahmen meiner Tätigkeit als wissenschaftlicher Mitarbeiter am Lehrstuhl für Thermodynamik und Energietechnik und am Lehrstuhl für Technische Thermodynamik der Universität Paderborn. In diesen Jahren haben mich eine Vielzahl von Freunden, Arbeitskollegen, Studenten oder Projektpartnern fachlich und freundschaftlich auf meinem Weg zur Promotion begleitet, bei denen ich mich an dieser Stelle bedanken möchte.

Als erstes möchte ich meinem Doktorvater, Herrn Prof. Dr. Jadran Vrabec, meinen ganz besonderen Dank aussprechen, ohne dessen Unterstützung diese Arbeit nicht möglich gewesen wäre. Er hat mich stets bei meinem Promotionsvorhaben gefördert und stand mir mit seinem fachlichen Rat zur Seite.

Ich möchte mich auch bei Frau Prof. Dr. Tina Kasper für die Übernahme des Korreferats meiner Arbeit und die Unterstützung in den letzten Jahren meiner Promotion bedanken. Mein weiterer Dank gehört Prof. Dr. Eugeny Kenig für den Vorsitz der Prüfungskommission und Dr. Steffen Jesinghausen als Beisitzer.

Ein ganz besonderer und herzlicher Dank gehört Andreas Elsner. Mit seiner stets ruhigen und freundlichen Art ist es mir immer ein besonderes Vergnügen mit ihm zu arbeiten. Er hat mich bereits in der Zeit als wissenschaftliche Hilfskraft begleitet und ich habe von seinem detaillierten und methodischen Vorgehen viel gelernt.

Durch seine weitsichtige Entscheidung, alte Haushaltskältegeräte seit den 1990er Jahren aufzubewahren, hat Prof. Dr. Dieter Gorenflo in besonderer Weise den Grundstein für diese Dissertation gelegt, wofür ich mich bei ihm bedanken möchte. Des Weiteren möchte ich mich bei Dr. Gerrit Sonnenrein für die vielen strategischen Gespräche, bei Elmar Baumhögger, der mir bei der Entwicklung von Versuchsaufbauten konstruktiv geholfen hat, den Mitarbeitern der Werkstatt Rüdiger Pflock, Norbert Temborius und Dennis Themm für die Fertigung der Versuchsaufbauten und ihre Verbesserungsvorschläge bedanken. Darüber hinaus bedanke ich mich bei Jutta Jäger für ihre großartige Unterstützung bei administrativen Angelegenheiten.

Die interdisziplinäre Zusammenarbeit mit verschiedenen Universitäten und Industriepartnern waren mir eine besondere Freude. Hier gehört mein Dank Dr. Jasmin Geppert, Dr. Christian Hüppe, Prof. Dr. Rainer Stamminger, Wolfgang Becker, Heike Hölscher, Dr. Ragnar Stoll, Dr. Hendrik Wagner, Dr. Wenke Wollny, Dr. Ulrich Gries, Alfred Freiberger, Nicola Brzoska-Steinhaus und Lukas Schleelein für die stets konstruktive und angenehme Zusammenarbeit.

Die Jahre als wissenschaftlicher Mitarbeiter am Lehrstuhl für Technische Thermodynamik bzw. Lehrstuhl für Thermodynamik und Energietechnik werden mir aufgrund der sehr guten kollegialen Zusammenarbeit mit meinen Arbeitskollegen, Kommilitonen und studentischen Mitarbeitern positiv in Erinnerung bleiben. Daher möchte ich mich an dieser Stelle auch bei ihnen allen ganz herzlich bedanken.

Abschließend möchte ich mich bei meiner Familie für die Unterstützung in diesen Jahren bedanken. Sie war mir stets ein großer Rückhalt.

Paderborn, im Juli 2023

Andreas Paul

Zusammenfassung

Die Energieaufnahme von Haushaltskältegeräten ist seit den 1990er Jahren erheblich gesunken. Dieser Wert wird von den Herstellern im Neuzustand der Geräte unter Normbedingungen bestimmt. Wie jedes technische System unterliegen jedoch auch Haushaltskältegeräte einem Alterungsprozess, der zu einem Anstieg der Energieaufnahme über die Zeit führt. Im Rahmen dieser Dissertation wurde auf der Grundlage von 100 Messungen der Energieaufnahme, die an 32 Geräten über einen Zeitraum von 21 Jahren durchgeführt wurden, ein Alterungsmodell entwickelt. Dieses Modell ist das erste, das mit Hilfe von Daten der Energieaufnahme real gealterter Geräte entwickelt wurde. Es beschreibt einen Anstieg der Energieaufnahme von 27 % über die durchschnittliche Einsatzzeit eines Haushaltskältegeräts von 16 Jahren. Der stärkste Anstieg erfolgt in den ersten fünf Betriebsjahren. Durch Diffusionsvorgänge in dem im Gehäuse verbauten Polyurethan-Schaum wird das im Zellgas vorhandene Kohlenstoffdioxid durch Luft ersetzt. Hierdurch steigt die Wärmeleitfähigkeit des Schaums um ca. 33 % an, wodurch sich die Energieaufnahme der Geräte erhöht. Des Weiteren wurde der Einsatz von Paraffinen als Phasenwechselmaterial in Haushaltskältegeräten untersucht. Durch deren Einsatz konnte die Energieaufnahme gesenkt und die Funktionalität der Geräte gesteigert werden. Hierfür sind detaillierte Kenntnisse der Materialkenndaten der Paraffine notwendig. Die Wärmeleitfähigkeit der verschiedenen Paraffin-Stoffgruppen in der festen Phase ist jedoch bisher nur unzureichend untersucht worden. Daher wurde ein Messaufbau entwickelt, mit dem die Wärmeleitfähigkeit von festem Paraffin bestimmt werden kann, und es wurden entsprechende Messungen durchgeführt.

Abstract

The energy consumption of household refrigeration appliances has decreased significantly since the 1990s. This value is determined by the manufacturers under standard conditions when the appliances are new. However, like any other technical system, these appliances are also subject to an aging process that leads to an increase of energy consumption over the time of usage. As part of this thesis, an aging model was developed on the basis of 100 standard energy consumption measurements carried out on 32 appliances over a period of 21 years. This model is the first to be developed on the basis of energy consumption data from real aged appliances. It describes an increase of energy consumption by 27 % over 16 years, which is the average period of use of a household refrigeration appliance. The largest increase occurs in the first five years of use. Diffusion processes in the polyurethane foam installed in the cabinet of the appliances result in an exchange of carbon dioxide with air. This gas exchange increases the thermal conductivity of the foam by approximately 33 %, which rises the energy consumption of the appliances. Furthermore, the use of paraffins, as one type of phase change materials, in household refrigeration appliances was investigated. The use of these materials made it possible to reduce energy consumption and increase the functionality of the appliances. This application of paraffins requires detailed knowledge of their material characteristics. However, the thermal conductivity of paraffins in the solid state has so far only been investigated insufficiently. Therefore, a measurement setup for determining the thermal conductivity of solid paraffins was developed and corresponding measurements were carried out.

Publikationsliste

Paul, A., Moczarski, L., Gieselmann, M., Reineke, M., Elsner, A., Baumhögger, E., Sonnenrein, G., Vrabec, J., 2019. Bestimmung von Wärmeverlusten in Haushaltskältegeräten. Deutsche Kälte-Klima Tagung 45, Ulm, Deutschland, 20.-22. November 2019, Deutsche Kälte- und Klimatechnischer Verein e. V., (Konferenzbeitrag mit Peer-Review). ISBN: 978-3-932715-52-5.

Hueppe, C., Geppert, J., Stamminger, R., Wagner, H., Hoelscher, H., Vrabec J., Paul, A., Elsner, A., Becker, W., Gries, U., Freiberger, A., 2020. Age-related efficiency loss of household refrigeration appliances: Development of an approach to measure the degradation of insulation properties. Applied Thermal Engineering 173, 115113. DOI: https://doi.org/10.1016/j.applthermaleng.

Sonnenrein, G., Baumhögger, E., Elsner, A., Neukötter, M., Paul, A., Vrabec, J., 2020. Improving the performance of household refrigerating appliances through the integration of phase change materials in the context of the new global refrigerator standard IEC 62552:2015. International Journal of Refrigeration 119, 448-456. DOI: https://doi.org/10.1016/j.ijrefrig.2020.07.025.

Hueppe, C., Geppert, J., Moenninghoff-Juessen, J., Wolff. L., Stamminger, R., Paul, A., Elsner, A., Vrabec, J., Wagner, H., Hoelscher, H., Becker, W., Gries, U., Freiberger, A., 2021. Investigating the real life energy consumption of refrigeration appliances in Germany: Dynamic modelling of consumer behaviour. Energy Policy 155, 112275. DOI: https://doi.org/10.1016/j.enpol.2021.112275.

Paul, A., Baumhögger, E., Elsner, A., Moczarski, L., Reineke, M., Sonnenrein, G., Hueppe, C., Stamminger, R., Hoelscher, H., Wagner, H., Gries, U., Freiberger, A., Becker, W., Vrabec, J., 2021. Determining the heat flow through the cabinet walls of household refrigerating appliances. International Journal of Refrigeration 121, 235-242. DOI: https://doi.org/10.1016/j.ijrefrig.2020.10.007.

Paul, A., Baumhögger, E., Elsner, A., Reineke, M., Sonnenrein, G., Hueppe, C., Stamminger, R., Hoelscher, H., Wagner, H., Gries, U., Becker, W., Vrabec, J., 2022. Impact of aging on the energy efficiency of household refrigerating appliances. Applied Thermal Engineering 205, 117992.
DOI: https://doi.org/10.1016/j.applthermaleng.2021.117992.

Paul, A., Baumhögger, E., Elsner, A., Reineke, M., Kasper, T., Schumacher, D., Vrabec, J., Hueppe, C., Stamminger, R., Hoelscher, H., Stoll, R., Wagner, H., Gries, U., Becker, W., 2023. Alterungsmechanismen von Haushaltskältegeräten. Deutsche Kälte-Klima Tagung 48, Magdeburg, Deutschland, 16.-18. November 2022, Deutsche Kälte- und Klimatechnischer Verein e. V., (Konferenzbeitrag mit Peer-Review). ISBN: 978-3-932715-55-6.

Paul, A., Baumhögger, E., Dewerth, M. O., Elsner, A., Dindar, I. H., Sonnenrein, G., Vrabec, J., 2023. Thermal conductivity of solid paraffins and several n-docosane compounds with graphite. Journal of Thermal Analysis and Calorimetry 148, 5687-5694. DOI: https://doi.org/10.1007/s10973-023-12107-2.

Inhaltsverzeichnis

Symbole und Formelzeichen

Lateinische Buchstaben

Symbol	Einheit	Bedeutung
A	m²	Mittlere Oberfläche des Gehäuses
A_{Heiz}	m²	Heizfläche
a	-	Normierter Energieaufnahme-Offset des Alterungsmodells
AE	kWh/a	Jährliche Energieaufnahme des Haushaltskältegeräts
A_C	-	Ausgleichsfaktor für Entfrosten
BI	-	Bonusfaktor für Einbaugeräte
B_c	-	Ausgleichsfaktor für Aufstellungsart
b	a	Zeitkorrekturfaktor
C	-	Modellierungsparameter für Kombigeräte
CC	-	Bonusfaktor für Geräte bestimmter Klimaklassen
CH	kWh/a	Bonus auf die Energieaufnahme für Geräte mit einem Kaltlagerfach
COP	-	Leistungszahl
$c_{v,Luft}$	kJ/(kg·K)	Isochore Wärmekapazität von Luft
$c_{p,Eis}$	kJ/(kg·K)	Isobare Wärmekapazität von Eis
D	-	Ausgleichsfaktor für Anzahl der Türen
$E(\tau)$	kWh/d	Energieaufnahme zum Zeitpunkt τ
E_0	kWh/d	Energieaufnahme zum Zeitpunkt der ersten Messung
E_{aux}	kWh/d	Hilfsenergie für Abtauheizungen
E_{daily}	kWh/d	Tägliche Energieaufnahme aus Messungen der Norm-Energieaufnahme
E_H	kWh/a	Jährliche Energieaufnahme des Haushaltskältegeräts
E_p	kWh/d	Hypothetischer Energieaufnahme zum Zeitpunkt der Produktion
E_{St}	kWh/a	Jährliche Energieaufnahme des hypothetischen Referenzgeräts

EEI	-	Index der Energieeffizienz
EEI_{1994}	-	Index der Energieeffizienz bis zum 28.02.2021
EEI_{2019}	-	Index der Energieeffizienz ab dem 01.03.2021
FF_c	-	Bonusfaktor für die Art des Abtauvorgangs des Gefrierfachs
g	-	Startwert des Alterungsmodells
k	W/(m^2·K)	Wärmedurchgangskoeffizient
$k \cdot A$	W/K	$k \cdot A$-Wert
L	-	Lastfaktor
M	kWh/(a·l)	Energieaufnahmekorrektur des Referenzgeräts
M_c	kWh/(a·l)	Energieaufnahmekorrektur für die Fachgröße des Referenzgeräts
m_{Eis}	kg	Masse der Eiszugabe
m_{Luft}	kg	Masse der Luft im Lagerraum
N	kWh/a	Grundenergieaufnahme des Referenzgeräts
N_c	kWh/a	Grundenergieaufnahme für ein Fach des Referenzgeräts
P	W	Heizleistung
P_{el}	W	elektrische Heizleistung
P_{Pumpe}	W	Antriebsleistung der Umwälzpumpe
$\dot{Q}$	W	Wärmestrom
$\dot{Q}_{Geh.}$	W	In das Gehäuse eintretender Wärmestrom
r	%	Anfängliche Alterungsrate
SAE	kWh/a	Jährliche Energieaufnahme des hypothetischen Referenzgeräts
s	mm	Materialstärke der Probe
s_a	mm	Mittlere Schichtstärke der eingeschlossenen Luft
s_f	mm	Materialstärke der Wärmeleitfolie
T_a	°C	Umgebungstemperatur
T_c	°C	Lagertemperatur im Fach
T_{Eis}	°C	Schmelztemperatur von Wasser
$T_{Eis,1}$	°C	Lagertemperatur des Eises
T_i	°C	Temperatur im Inneren des Gehäuses

T_{m*}	°C	Mittlere Lagertemperatur
T_R	°C	Reglerstellung
V	l	Nutzinhalt des gesamten Geräts
V_c	l	Nutzinhalt des Fachs
V_{eq}	l	Nutzinhalt des hypothetischen Referenzgeräts
x	-	Korrekturfaktor für Treibgas

Griechische Buchstaben

Symbol	Einheit	Bedeutung
α	W/(m²·K)	Wärmeübergangskoeffizient
α_a	W/(m²·K)	Wärmeübergangskoeffizient auf der Außenseite
α_i	W/(m²·K)	Wärmeübergangskoeffizient auf der Innenseite
ΔCOP	-	Veränderung der Leistungszahl
$\Delta E_0(\tau)$	-	Vorläufiges Alterungsmodell
$\Delta E_p(\tau)$	-	Alterungsmodell
Δe_{ir}	%	Jährlicher Anstieg der Energieaufnahme
Δh_s	kJ/kg	Schmelzenthalpie von Wasser
ΔT	K	Temperaturdifferenz
$\Delta \tau_s$	h	Abtauzeit
θ_i	h^{-1}	Prüfgröße
λ	W/(m·K)	Wärmeleitfähigkeit
λ_a	W/(m·K)	Wärmeleitfähigkeit der eingeschlossenen Luft
λ_f	W/(m·K)	Wärmeleitfähigkeit der Wärmeleitfolie
λ_G	W/(m·K)	Anteil der Wärmeleitfähigkeit des Polyurethan-Hartschaums durch die Zellgase
λ_K	W/(m·K)	Anteil der Wärmeleitfähigkeit des Polyurethan-Hartschaums durch Konvektion in den Schaumzellen
λ_M	W/(m·K)	Anteil der Wärmeleitfähigkeit des Polyurethan-Hartschaums durch die Polyurethan-Matrix
λ_{PUR}	W/(m·K)	Wärmeleitfähigkeit des Polyurethan-Hartschaums
λ_R	W/(m·K)	Anteil der Wärmeleitfähigkeit des Polyurethan-Hartschaums durch Wärmestrahlung

τ	a	Gerätealter
τ_B	h	Dauer des Temperaturanstiegs

1 Einleitung

Durch den starken Anstieg der Weltbevölkerung in den letzten hundert Jahren [1] hat die Bedeutung von Haushaltskältegeräten (wie z.B. Kühlschränken, Gefriergeräten und deren Kombinationen) zur Konservierung von Lebensmitteln deutlich an Bedeutung hinzugewonnen. Lebensmittel unterliegen verschiedensten biologischen und chemischen Prozessen, die zu ihrem Verderb führen. Dieser wird durch die Vermehrung von Mikroorganismen, Reaktionen der im Lebensmittel vorhandenen Enzyme oder Reaktionen von Luftsauerstoff mit dem Lebensmittel verursacht [2]. Da die genannten Prozesse abhängig von der Temperatur sind, verlangsamen sie sich deutlich bzw. kommen zum Erliegen, wenn die Temperatur gesenkt wird. Private Haushalte nutzen diesen Zusammenhang zur signifikanten Verlängerung der Haltbarkeit von Lebensmitteln in Haushaltskältegeräten [3].

In den OECD-Mitgliedsstaaten werden 13,4 % des Stromverbrauchs privater Haushalte durch das Kühlen und Gefrieren von Lebensmitteln verursacht [4]. Der Anteil der Haushaltskältegeräte am Stromverbrauch in privaten Haushalten in Deutschland lag im Jahr 2018 bei 22,4 %. Auf den Gesamtstromverbrauch Deutschlands bezogen sind dies 5,4 % [5, 6]. Diese Energiemenge entspricht absolut gesehen einem Verbrauch von 28,896 TWh elektrischer Energie, führt zu CO_2-Emissionen von 13.523.328 t und hatte 8,634 Mrd. € an Energiekosten für die privaten Haushalte Deutschlands im Jahr 2018 zur Folge [5-9]. Aufgrund des durchgehenden ganztägigen Betriebs über durchschnittlich 16 Jahre [10] und der nahezu vollständigen Marktdurchdringung von 99,9 % [8] haben Haushaltskältegeräte ein großes Potenzial zur Reduzierung des Stromverbrauchs beizutragen.

1.1 EU-Energielabel

Seitens der Europäischen Union wurde im Jahr 1994 das EU-Energielabel (Richtlinie 94/75/EWG) mit dem Ziel eingeführt, die Energieaufnahme von Haushaltskältegeräten in Europa zu senken [11]. Seit ihrem Bestehen wurde die Richtlinie mehrfach überarbeitet und an die aktuelle Marktsituation angepasst (siehe Abbildung 1). So wurden beispielsweise zunächst 2003 die Effizienzklassen A+ und A++ [12] und 2010 die Klasse A+++ eingeführt [13]. Für eine Bereinigung der Klassen sorgte die Überarbeitung der Richtlinie 2021 [14]. Mit zunehmender Steigerung der Energieeffizienz der Haushaltkältegeräte wurden die Klassen A bis G angepasst und die Klassen A+ bis A+++ gestrichen. Ein hocheffizientes Gerät der alten Klasse A+++ wird in der Richtlinie von 2021 nur noch in die Klasse C eingeordnet.

Neben dem Energielabel geben die Richtlinien ein EU-Datenblatt vor, welches die wichtigsten technischen Daten der Haushaltskältegeräte beinhaltet. In diesem Datenblatt müssen bestimmte Informationen enthalten sein, die zur Bestimmung der Energieeffizienzklasse benötigt werden [13, 14].

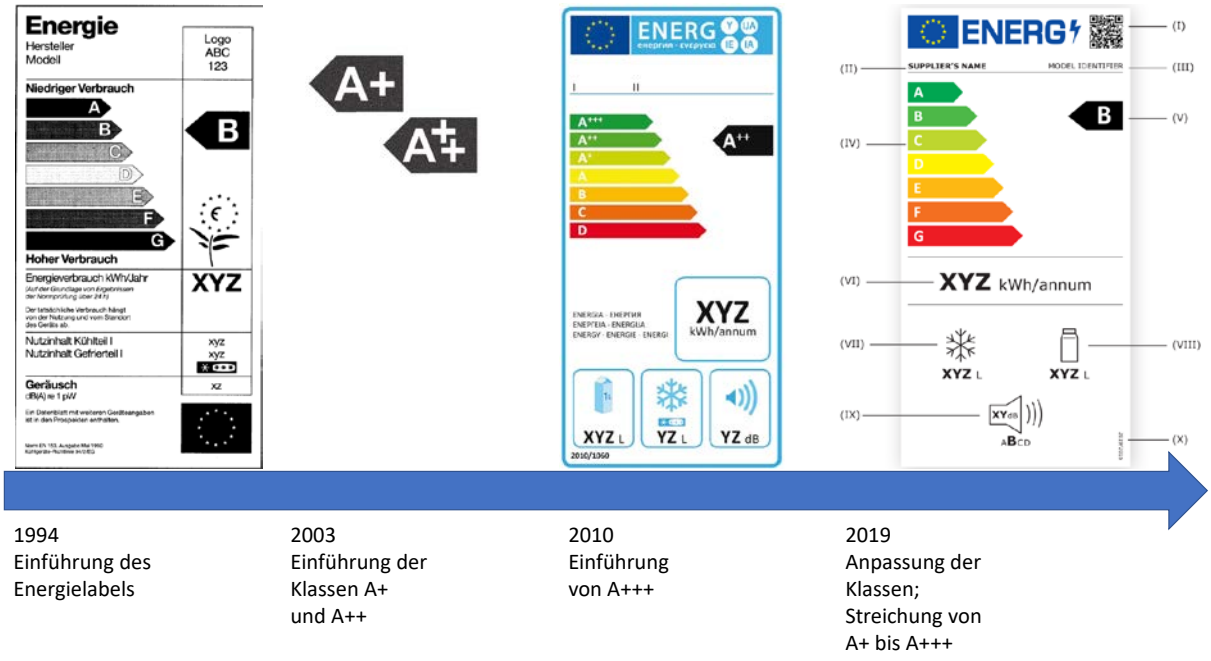

1994
Einführung des Energielabels

2003
Einführung der Klassen A+ und A++

2010
Einführung von A+++

2019
Anpassung der Klassen; Streichung von A+ bis A+++

Abbildung 1: Entwicklung des EU-Energielabels.

Das Energielabel klassifiziert über den Index der Energieeffizienz (EEI) die Haushaltskältegeräte anhand von Bauform, Nutzinhalt und Energieaufnahme. Je niedriger der EEI eines Geräts ist, desto energieeffizienter wird es eingeschätzt. Hierzu werden die Spezifikationen eines Haushaltskältegeräts mit denen eines imaginären Referenzgeräts verglichen. In den älteren Richtlinien wurde der EEI_{1994} mit den Gleichungen (1) bis (3) berechnet. Die Größen in den Gleichungen (1) bis (3) sind in Tabelle 1 beschrieben.

$$EEI_{1994} = \frac{E_H}{E_{St}} \cdot 100 \tag{1}$$

$$E_{St} = V_{eq} \cdot M + N + CH \tag{2}$$

$$V_{eq} = \left[\sum_{c=1}^{c=n} \left(V_c \cdot \frac{(25 - T_c)}{20} \cdot FF_c \right)\right] \cdot CC \cdot BI \tag{3}$$

Der Aufbau der Berechnungsmethoden wurde in der Vergangenheit von verschiedenen Stellen kritisiert [10, 15-18]. So wurden zum Beispiel auf dem deutschen Markt Geräte der Klimaklasse T (Tropen, Einsatz bis zu einer Umgebungstemperatur von 43 °C) vermehrt angeboten, obwohl diese Klimaklasse für die in Deutschland vorherrschenden klimatischen Bedingungen nicht notwendig ist [15]. Einer der möglichen Gründe hierfür war der Bonusfaktor CC von 1,2, der diese Art von Geräten bei der Berechnung des EEI begünstigt [10, 17, 18]. Des Weiteren darf die an einem Gerät gemessene Energieaufnahme den gelabelten Wert um bis zu 15 % [19] bzw. 10 % [20] überschreiten. Dies sollte ursprünglich Fertigungstoleranzen ausgleichen, wurde aber auch von einigen Herstellern bei der Berechnung des EEI ausgenutzt.

Tabelle 1: Größen zur Berechnung des EEI_{1994} [11].

Faktor	Bedingung	Wert
E_H	Jährliche Energieaufnahme des Haushaltskältegeräts	
E_{St}	Jährliche Energieaufnahme des hypothetischen Referenzgeräts	
V_{eq}	Nutzinhalt des hypothetischen Referenzgeräts	
M	Energieaufnahmekorrektur des Referenzgeräts	
N	Grundenergieaufnahme des Referenzgeräts	
CH	Bonus auf die Energieaufnahme von 50 kWh/a für Geräte mit einem Kaltlagerfach mit einem Nutzinhalt von mindestens 15 Litern	
FF_c	Gefrierfach mit No-Frost	1,2
	Sonstige Lagerfächer	1
CC	Geräte mit Klimaklasse T (Tropen)	1,2
	Geräte mit Klimaklasse ST (Subtropen)	1,1
	Geräte mit Klimaklasse N und SN (Normal und Erweitert Normal)	1
BI	Einbaugeräte mit einer Breite von weniger als 58 cm	1,2
	Sonstige Geräte	1
T_c	Lagertemperatur im Fach	
V_c	Nutzinhalt des Fachs	

Mit dem Inkrafttreten des EU-Energielabels mit der delegierten Verordnung (EU) Nr. 2019/2016 am 01.03.2021 änderte sich die Berechnung des EEI und dieser wird nun über die Gleichungen (4) bis (6) bestimmt [14]. Durch diese Änderungen lassen sich die Ergebnisse der alten und neuen Berechnungen nicht direkt miteinander vergleichen. Der numerische Wert des Index EEI_{2019} ist für ein gegebenes Gerät stets höher als der des Index EEI_{1994}.

$$EEI_{2019} = \frac{AE}{SAE} \tag{4}$$

$$AE = 365 \cdot \frac{E_{daily}}{L} + E_{aux} \tag{5}$$

$$SAE = C \cdot D \cdot \left[\sum_{c=1}^{c=n} \left(A_c \cdot B_c \cdot \frac{V_c}{V} \cdot \left(N_C + V \cdot \frac{(T_a - T_c)}{20} \cdot M_c \right) \right)\right] \tag{6}$$

Tabelle 2: Größen zur Berechnung des EEI_{2019} [14].

Faktor	Bedingung
AE	Jährliche Energieaufnahme des Haushaltskältegeräts
E_{daily}	Tägliche Energieaufnahme nach Norm-Energieverbrauchsmessungen
L	Lastfaktor der durch die Zufuhr warmer Lebensmittel zusätzlich im Betrieb abzuführenden Wärme
E_{aux}	Hilfsenergie für Abtauheizungen
SAE	Jährliche Energieaufnahme des hypothetischen Referenzgeräts
C	Modellierungsparameter für Kombigeräte
D	Ausgleichsfaktoren für Anzahl der Türen
A_C	Ausgleichsfaktor für Entfrosten
B_c	Ausgleichsfaktor für Aufstellungsart (Freistehend/Einbaugerät)
V_c	Nutzinhalt des Fachs
V	Nutzinhalt des gesamten Geräts
N_c	Grundenergieaufnahme für ein Fach des Referenzgeräts
T_a	Umgebungstemperatur 24 °C
T_c	Lagertemperatur im Fach
M_c	Energieaufnahmekorrektur für die Fachgröße des Referenzgeräts

Auf Grundlage der Ökodesign-Richtlinien wurde der Verkauf von Haushaltskältegeräten, die einen bestimmten EEI überschreiten, verboten [21, 22]. Diese Anforderungen wurden, wie in Tabelle 3 dargestellt, über die letzten Jahre mehrfach angepasst.

Tabelle 3: Entwicklung des maximal erlaubten EEI und der dazugehörigen Energieeffizienzklassen seit 2010 [21, 22].

Gültig ab:	maximal erlaubter EEI (%)	erlaubte Energieeffizienzklassen für Geräte mit Kompressionskältemaschinen
01.07.2010	EEI_{1994} < 55	A+++ bis A
01.07.2012	EEI_{1994} < 44	A+++ bis A+
01.07.2014	EEI_{1994} < 42	A+++ bis A+
01.03.2021	EEI_{2019} ≤ 125	A bis F
01.03.2024	EEI_{2019} ≤ 100	A bis E

In Tabelle 4 sind die Aufteilungen der Energieeffizienzklassen in den verschiedenen Richtlinien gegenübergestellt.

Tabelle 4: Einteilung der Energieeffizienzklassen innerhalb der verschiedenen Richtlinien [11-14].

Energie-effizienz-klasse	Index der Energieeffizienz (EEI) [%]			
	Richtlinie 94/75/EWG (1994)	Richtlinie 2003/66/EG (2003)	Delegierte Verordnung (EU) Nr. 1060/2010 (2010)	Delegierte Verordnung (EU) Nr. 2019/2016 (2019)
A+++	Klasse nicht definiert	Klasse nicht definiert	EEI_{1994} < 22	Klasse nicht definiert
A++	Klasse nicht definiert	EEI_{1994} < 30	22 ≤ EEI_{1994}< 33	Klasse nicht definiert
A+	Klasse nicht definiert	30 ≤ EEI_{1994} < 42	33 ≤ EEI_{1994}< 44/42*	Klasse nicht definiert
A	EEI_{1994} < 55	42 ≤ EEI_{1994} < 55	44/42* ≤ EEI_{1994}< 55	EEI_{2019} ≤ 41
B	55 ≤ EEI_{1994} < 75	55 ≤ EEI_{1994} < 75	55 ≤ EEI_{1994} < 75	41 < EEI_{2019}≤ 51
C	75 ≤ EEI_{1994} < 90	75 ≤ EEI_{1994} < 90	75 ≤ EEI_{1994} < 95	51 < EEI_{2019}≤ 64
D	90 ≤ EEI_{1994} < 100	90 ≤ EEI_{1994} < 100	95 ≤ EEI_{1994} < 110	64 < EEI_{2019}≤ 80
E	100 ≤ EEI_{1994} < 110	100 ≤ EEI_{1994} < 110	110 ≤ EEI_{1994} < 125	80 < EEI_{2019}≤ 100
F	110 ≤ EEI_{1994} < 125	110 ≤ EEI_{1994} < 125	125 ≤ EEI_{1994} < 150	100 < EEI_{2019}≤ 125
G	125 ≤ EEI_{1994}	125 ≤ EEI_{1994}	150 ≤ EEI_{1994}	EEI_{2019} > 125

* Dieser Wert wurde bei der Einführung der delegierten Verordnung (EU) Nr. 1060/2010 zunächst mit 44 angegeben und zum 01.07.2012 auf 42 reduziert.

1.2 Bestimmung der Norm-Energieaufnahme

Haushaltskältegeräte werden innerhalb der Europäischen Union in einem stark reglementierten Markt zum Kauf angeboten. Normen, die die technische Überprüfung der verschiedenen Geräteparameter unter reproduzierbaren Bedingungen beschreiben, bilden die Grundlage für diese Reglementierung. Seit dem Jahr 1990 wurden mehrere Normen eingeführt, überarbeitet und gebündelt. Die historische Zusammenfassung dieser Normen und der EU-Richtlinien ist in Abbildung 2 dargestellt.

In den 1990er Jahren hatte prinzipiell jeder Gerätetyp (Kühlschränke, Gefriergeräte und Kühl-Gefrier-Kombinationen) seine eigene Norm, die die Bestimmung der

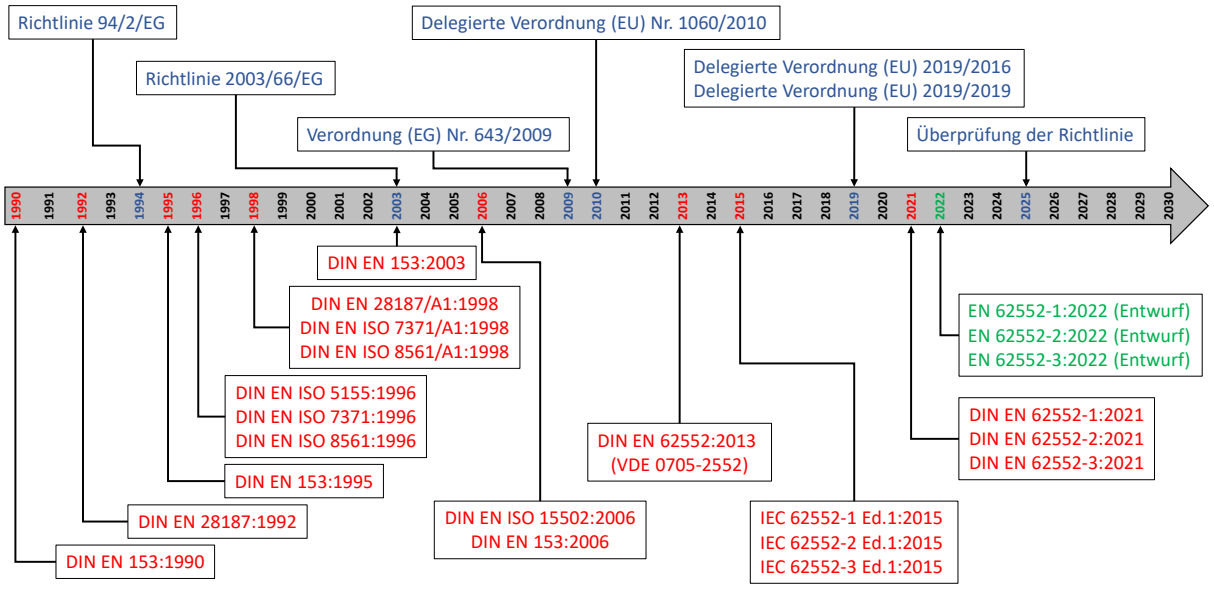

Abbildung 2: Zeitlicher Verlauf der Einführung von den im Bereich Haushaltskältegeräte gültigen Normen und Richtlinien in Deutschland.

Geräteparameter regelte. Diese verschiedenen Normen wurden im Jahr 2006 in der DIN EN ISO 15502:2006 [19] zusammengefasst. Die verschiedenen Versionen der DIN EN 153 stellten das Bindeglied zwischen den Normen und den Richtlinien dar. In den Richtlinien wurde stets darauf verwiesen, dass die Energieaufnahme nach der DIN EN 153 bestimmt wird und in der zum gegebenen Zeitpunkt aktuellen DIN EN 153 wurde dann auf die entsprechende Norm weiterverwiesen [23]. Das grundsätzliche Vorgehen war bis zur Einführung der Normenreihe IEC 62552:2015 innerhalb der verschiedenen Vorgängernormen gleich.

Für die Untersuchung des Alterungsverhaltens von Haushaltskältegeräten ist ein methodisches Vorgehen notwendig. Dies wird durch die Anwendung der in den Normen beschriebenen Messverfahren erreicht. Jedoch liegen in diesem methodischen Vorgehen durch die Einführung neuer Normen leichte Abweichungen in der Erfassung der Messdaten vor. Daher wird zunächst im Folgenden das Vorgehen zur Bestimmung der Norm-Energieaufnahme in vereinfachter Form dargestellt.

In den Normen bis zur Einführung der IEC 62552:2015 sind die Messstellen in den verschiedenen Lagerfächern unterschiedlich ausgeführt. In Lagerfächern für frische Lebensmittel müssen drei Temperatursensoren mit Metallzylinder (meistens aus Kupfer oder Messing) abhängig von der Fachgeometrie positioniert werden. Die Raumtemperatur wird auf der halben Gerätehöhe ebenfalls mit Metallzylindern gemessen. Die Metallzylinder dienen durch ihre thermische Masse der Pufferung und Glättung von kurzzeitigen Temperaturschwankungen an den Messstellen. Kaltlagerfächer und Gefrierfächer werden mit sogenannten Prüfpaketen aus einer Mischung aus Zellulose, Kochsalz und Wasser beladen. Diese Prüfpakete simulieren das thermophysikalische Verhalten von magerem Rindfleisch. Durch die Variation der Menge an Kochsalz kann der Gefrierpunkt der Pakete auf -1 °C für Gefrierfächer oder -5 °C für Kaltlagerfächer eingestellt werden. Durch die unterschiedlichen Gefrierpunkte

wird sichergestellt, dass die Prüfpakete immer im sensiblen Temperaturbereich im jeweiligen Lagerfach eingesetzt werden können und es nicht zu einem Phasenwechsel im Paket kommt, der das Messergebnis verfälschen würde. [19]

Einige Prüfpakete werden mit Temperatursensoren ausgerüstet (M-Pakete) und haben eine Abmessung von 100x100x50 mm^3 sowie eine Masse von 500 g. Der Temperatursensor wird mittig im Paket platziert und die M-Pakete müssen immer mit ihrer 100x100 mm^2 Grundfläche horizontal im Gerät positioniert werden. [19]

Kaltlagerfächer werden in Abhängigkeit von ihrem Nutzinhalt mit mindestens zwei Prüfpaketen und bis maximal zehn Prüfpaketen ausgestattet. Von den Prüfpaketen müssen mindestens zwei als M-Pakete ausgeführt werden. [19]

Die Gefrierfächer werden mit so vielen Stapeln an Prüfpaketen ausgestattet, wie es räumlich möglich ist. Hierbei können die Stapel aus 500 g oder aus 1000 g Prüfpaketen (200x100x50 mm^3) bestehen. Die Stapel werden bündig an den Wänden platziert und folgen den Konturen des Fachs. Sollte zwischen den Stapeln noch Platz sein, müssen auch freistehende Stapel eingesetzt werden, jedoch muss zwischen den Stapeln ein Freiraum von mindestens 15 mm verbleiben. Die M-Pakete werden in die Stapel integriert und sind dort zu platzieren, wo die wärmsten Stellen während des Betriebs zu erwarten sind. Dies sind in der Regel die Ecken des Lagerfachs im Bereich der Türdichtung oder der Abtauheizung. [19]

Für die Bestimmung der Energieaufnahme muss in zwei aufeinanderfolgenden Zeiträumen jeweils ein stabiler Betriebszustand vorliegen. Für diesen stabilen Betriebszustand dürfen über einen Zeitraum von mindestens 24 h und einer ganzen Anzahl an Kompressorzyklen keine Veränderungen der Lagertemperaturen und der Energieaufnahme auftreten. Bei Geräten mit einer No-Frost Funktion kann so der Auswertezeitraum, je nach Betriebsverhalten, teilweise auf bis zu neun Tage anwachsen. Für die Bestimmung der Lagertemperaturen in Lagerfächern für frische Lebensmittel wird der arithmetische Mittelwert der Temperaturen an den Messstellen berechnet und für die Kaltlagerfächer und Gefrierfächer die maximale Temperatur im Fach innerhalb eines Auswertezeitraums bestimmt. [19]

Mit der Umstellung auf die Normenreihe IEC 62552:2015 [20] änderte sich das Vorgehen in vielen Bereichen grundlegend. Die Normenreihe besteht aus drei separaten Teilen [24-26] und beschreibt eine Reihe von Prüfmethoden, die zur Bestimmung einzelner technischer Aspekte eines Haushaltskältegeräts, wie z.B. die Energieaufnahme, die Lagertemperaturen oder die Geräteperformance, optimiert sind. Im ersten Teil, der IEC 62552-1:2015, werden die grundlegenden Begrifflichkeiten erklärt und die Positionierung der Messstellen geregelt [24]. Die IEC 62552-2:2015 beschreibt verschiedene Prüfungen, die einzelne technische Parameter untersuchen [25]. Abschließend legt die IEC 62552-3:2015 das Vorgehen zur Bestimmung der Energieaufnahme und des Nutzinhalts eines Geräts fest [26]. Diese Normenreihe ist dazu gedacht, weltweit angewendet zu werden. Jedes Land oder Staatengemeinschaft soll über nationale Richtlinien die Untersuchungen definieren, die für die dort vermarkteten Geräte vom Hersteller durchgeführt werden müssen.

Im Bereich der Kaltlagerfächer und Gefrierfächer änderte sich das Vorgehen zur Bestimmung der Fachtemperaturen grundlegend. Hier werden nun die Temperaturen ebenfalls mit Metallzylindern gemessen und für die Auswertung werden arithmetische Mittelwerte über die Messstellen gebildet. [24, 26]

Auch die Festlegung des Auswertezeitraums unterscheidet sich von den Vorgängernormen. Für die Bestimmung des Auswertezeitraums werden drei aufeinanderfolgenden Gruppen von mindestens drei Kompressorzyklen gebildet. Innerhalb dieser Gruppen müssen bestimmte Stabilitätskriterien erfüllt sein, damit ein stabiler Betriebszustand vorliegt. [24, 26]

Die Ausführung der Messstellen in den verschiedenen Lagerfächern eines Haushaltskältegeräts wird für die jeweilige Norm in Tabelle 5 gezeigt.

Tabelle 5: Vergleich der Ausführung der Messstellen für die Ermittlung der Energieaufnahme unter den verschiedenen Normen [19, 20, 24-26].

Lagerfach	Norm		
	DIN EN ISO 15502:2006 (und Vorgängernormen)	DIN EN 62552:2013	Normenreihe IEC 62552:2015
Umgebungstemperatur	Metallzylinder		
Speisekammerfach	Metallzylinder		
Weinlagerfach	Nicht definiert	M-Pakete (-5 °C)	M-Pakete (-5 °C)
Kellerfach	Metallzylinder		
Lagerfach für frische Lebensmittel	Metallzylinder		
Kaltlagerfach	M-Pakete (-5 °C)		Metallzylinder
Null-Sterne- und Eisbereiterfach	M-Pakete (-1 °C)		Metallzylinder
Ein-Stern-Fach	M-Pakete (-1 °C)		Metallzylinder
Zwei-Sterne-Fach	M-Pakete (-1 °C)		Metallzylinder
Drei-Sterne-Fach	M-Pakete (-1 °C)		Metallzylinder
Gefrierfach (Vier-Sterne-Fach)	M-Pakete (-1 °C)		Metallzylinder

Trotz dieser notwendigen Anpassungen der Messmethoden in den Normen an die neuen Gegebenheiten am Markt werden Alterungsmechanismen an Haushaltskältegeräten nicht in den Normen berücksichtigt. Die Geräte werden im Neuzustand vermessen und auf Grundlage dieses Messwerts wird das Label der Geräte bestimmt.

2 Alterung von Haushaltskältegeräten

Wie bei jedem technischen System unterliegen auch Haushaltskältegeräte (wie z.B. Kühlschränke, Gefriergeräte und deren Kombinationen) über ihre Lebensdauer einem Alterungsprozess, der zu einem Anstieg der Energieaufnahme führt. Im Jahr 1990 wurde im Rahmen einer Untersuchung für die Australian Consumers' Association kein nennenswerter Anstieg der Energieaufnahme über einen Zeitraum von einem Jahr festgestellt [27]. Elsner et al. stellten hingegen im Jahr 2013 einen Anstieg der Energieaufnahme von 25 % bis 36 % über einen Zeitraum von 18 Jahren an Haushaltskältegeräten fest [28]. Diese Geräte wurden zwischen 1994 und 1995 gefertigt und gehörten zu den ersten FCKW-freien Geräten auf dem deutschen Markt [28-30]. Eine im Rahmen der Überarbeitung der Verordnung des EU-Energielabels von 2019 in Auftrag gegebene Studie nennt die Isolierung, die Türdichtungen, die Innenraumelemente und den Verdichter als Hauptursachen für die Alterung [10]. Aufgrund der unzureichenden Datenlage wird in der Studie von einem Anstieg der Energieaufnahme von 10 % bei einer durchschnittlichen Betriebszeit von 16 Jahren ausgegangen. Die durchschnittliche Betriebszeit besteht aus einer Hauptbetriebszeit von 12-13 Jahren und einer Sekundärbetriebszeit von 3-4 Jahren (z.B. in einer Garage) [10].

Die wesentlichen Teilsysteme eines Haushaltskältegeräts sind das Gehäuse mit den Türen und die Kompressionskältemaschine.

2.1 Verdichteralterung

Die zentrale Teilkomponente der in einem Haushaltskältegerät verbauten Kompressionskältemaschine ist der Verdichter. Im Haushaltskältebereich werden im Wesentlichen Hubkolben-Verdichter eingesetzt. Deren Alterungsverhalten lässt sich aus tribologischen Untersuchungen der relevanten Materialpaarungen ableiten. Dazu werden Proben der Materialpaarungen (Werkstoffe, Kältemaschinenöle und Kältemittel) in einem Prüfstand aneinander gerieben [31, 32]. Anschließende mikroskopische Untersuchungen zum Verschleiß dieser künstlich gealterten Materialien lassen Rückschlüsse auf den Kältemittelfluss im realen Verdichterbetrieb zu. Ein aus den Ergebnissen einer solchen Untersuchung erstelltes Modell von Garland und Hadfield aus dem Jahr 2004 zeigt eine Zunahme der relativen Verdichterlaufzeit von 30-39 % über einen Zeitraum von 15 Jahren [32]. Dies würde theoretisch einer allein durch die Alterung des Verdichters bedingten Erhöhung der Energieaufnahme um ca. 30 % entsprechen. Die Ergebnisse von Elsner et al. [28] zeigten ebenfalls einen Anstieg der Energieaufnahme um ca. 30 % nach 18 Jahren Betrieb, jedoch wurde dieser Wert für das Gesamtsystem Haushaltskältegerät ermittelt, die die Alterung der Isolierung und der Türdichtungen beinhaltet. Daher scheinen die Ergebnisse von Garland und Hadfield zu hoch zu sein.

Zur genaueren Untersuchung des Einflusses der Verdichteralterung auf die Energieaufnahme wurden im Rahmen dieser Arbeit Kalorimetermessungen an

Verdichtern durchgeführt. Hierzu wurde zunächst bei acht Verdichtern (von drei verschiedenen Verdichtertypen) die Leistungszahl COP nach der DIN EN 13771-1:2003 [33] auf einem Kalorimeterprüfstand (Methode A) vermessen und diese Verdichter wurden anschließend in Haushaltskältegeräte eingebaut. Nach einer Betriebszeit von zwei Jahren wurden die Verdichter wieder aus den Haushaltskältegeräten ausgebaut und erneut auf dem Kalorimeterprüfstand untersucht. Die Ergebnisse dieser Untersuchung sind in Tabelle 6 gezeigt.

Tabelle 6: Ergebnisse der Kalorimetermessungen der untersuchten Verdichter.

	Marke	Gerätetyp	Verdichtertyp (Secop)	Betriebszeit [Jahre]	COP_1	COP_2	ΔCOP
R03	Siemens	KI81RAD30	DLX4.8KK	2,00	1,77	1,83	3,4 %
R08	Siemens	KI81RAD30	DLX4.8KK	2,17	1,76	1,84	4,2 %
R09	Siemens	KI81RAD30	DLX4.8KK	2,17	1,76	1,75	- 0,1 %
Durchschnitt aller DLX4.8KK Verdichter				2,11	1,76	1,81	2,5 %
C18	Bosch	KIS86AF30	DLX7.5KK	2,17	1,98	1,99	0,2 %
C19	Bosch	KIS86AF30	DLX7.5KK	2,17	1,98	1,98	0,1 %
Durchschnitt aller DLX7.5KK Verdichter				2,17	1,98	1,98	0,1 %
F06	Siemens	GS36NVW3V	HZK95AA	2,00	1,93	1,96	1,4 %
F09	Siemens	GS36NVW3V	HZK95AA	2,17	1,95	1,92	- 1,5 %
F10	Siemens	GS36NVW3V	HZK95AA	2,17	1,93	1,93	0,1 %
Durchschnitt aller HZK95AA Verdichter				2,11	1,93	1,93	0,0 %
Durchschnitt aller Verdichter				2,13	1,88	1,90	0,9 %

Die acht untersuchten Verdichter zeigen im Durchschnitt eine leichte Verbesserung des COP von 0,9 % über die betrachtete Betriebszeit. Die Ergebnisse sind im Wesentlichen durch das Einlaufen der Lager und Ventile zu erklären. Diese Schlussfolgerung ist aus dem im Abbildung 3 dargestellten zeitlichen Verlauf des COP eines auf einem Kalorimeterprüfstand einlaufenden Verdichters abgeleitet. Die experimentellen Ergebnisse zur Verdichteralterung belegen, dass der Verdichter in den ersten zwei Betriebsjahren keinen wesentlichen Beitrag für den Anstieg der Energieaufnahme leistet. Die im Folgenden beschriebenen Alterungsprozesse anderer Komponenten haben so erhebliche Folgen, dass auch in der übrigen Betriebszeit nur von einem geringen Beitrag des Verdichters zum Alterungsverhalten des Gesamtsystems ausgegangen wird.

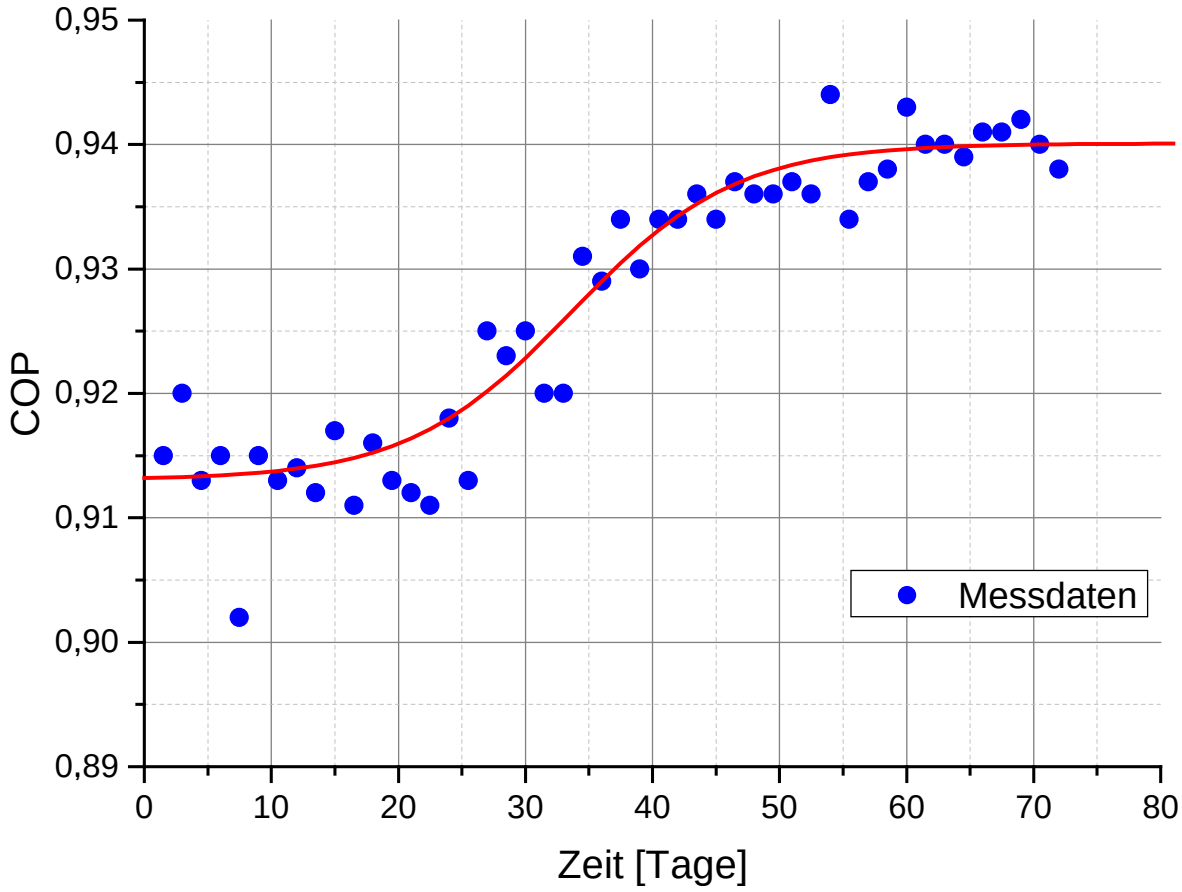

Abbildung 3: Einlaufverhalten eines Verdichters auf einem Kalorimeterprüfstand.

2.2 PUR-Schaum

Das Gehäuse eines Haushaltskältegeräts besteht an der Außenseite in den meisten Fällen aus einem ca. 1 mm dünnen Metallblech, einem 40-60 mm starken Kernmaterial, das zur Isolierung dient, und auf der Innenseite aus einem ca. 0,6-2 mm dünnen Innenbehälter (Inliner), der aus High-Impact-Polystyrene (HIPS) tiefgezogenen wird. Für die Isolierung wird bei den meisten Haushaltskältegeräten Polyurethanschaum (PUR-Schaum) verwendet, darüber hinaus werden in hochpreisigen energieeffizienteren Geräten auch lokal platzierte Vakuum-Isolations-Paneele (VIP) eingesetzt. Für die Funktion des Gehäuses spielt der PUR-Schaum die wichtigste Rolle. Neben der Isolierung des Lagerraums gegenüber der Umgebung versteift er das Gehäuse und verbindet durch seine Adhäsions- und Kohäsionskräfte die verschiedenen Bestandteile des Gehäuses miteinander [34].

In der Fertigung der Haushaltskältegeräte werden aufbauend auf dem Inliner zunächst die Rohrleitungen, die Kabel und die evtl. vorhandenen VIP fixiert. Dann wird das Außengehäuse provisorisch befestigt und der sich ergebende Innenraum des Gehäuses mit PUR-Schaum ausgeschäumt. Dies geschieht, indem zwei vorkommissionierte Komponenten miteinander vermischt werden. Dies sind zum einen polymeres Methylendiphenylisocyanat und eine Mischung aus Polyolen,

Katalysatoren, Stabilisatoren, Treibmitteln, Hilfsstoffen, Wasser und Cyclopentan. Bei der Vermischung dieser Komponenten laufen eine Vielzahl von in der Summe exothermen Reaktionen ab. Das Cyclopentan dient durch seine Verdampfung der Kühlung der Reaktionsprodukte und als physikalisches Aufschäummittel. In Bezug auf die Alterung ist die Reaktion von Wasser mit Isocyanat zu Kohlenstoffdioxid und Harnstoff besonders bedeutsam. Das Kohlenstoffdioxid schäumt das Polyurethan auf und reichert sich in den Schaumzellen an. Unmittelbar nach der Fertigung der Haushaltskältegeräte besteht das im PUR-Schaum eingeschlossene Zellgas daher aus Cyclopentan, Kohlenstoffdioxid und geringen Mengen von Sauerstoff und Stickstoff [34-38].

Die Wärmeleitfähigkeit des PUR-Schaums λ_{PUR} lässt sich über Gleichung (7) berechnen und setzt sich aus den Anteilen der Wärmeleitfähigkeit in der Kunststoffmatrix λ_M, der Wärmeleitfähigkeit des Zellgases λ_G, Wärmeübertragung durch Wärmestrahlung zwischen den Zellwänden λ_R und Wärmeübertragung durch Konvektion in den Schaumzellen λ_K zusammen. Hierbei hat die Wärmeleitfähigkeit der Zellgase mit über 50 % den größten Anteil an der gesamten Wärmeleitfähigkeit des PUR-Schaums. Dagegen ist die Wärmeübertragung durch Wärmestrahlung und Konvektion in den Schaumzellen der in Haushaltskältegeräten eingesetzten PUR-Schäumen zu vernachlässigen [34, 35].

$$\lambda_{PUR} = \lambda_M + \lambda_G + \lambda_R + \lambda_K \tag{7}$$

Im Zeitraum von 1997 bis 2003 veröffentlichten Wilkes et al. mehrere Studien, die den Anstieg der Wärmeleitfähigkeit von in Haushaltskältegeräten verwendeten PUR-Schäumen nachwiesen [39-43]. Hierzu wurde die Wärmeleitfähigkeit von mit verschieden Treibmitteln und Rezepturen hergestellten PUR-Schaum-Probekörpern über die Zeit vermessen und auf die Wärmeleitfähigkeit eines mit R11 hergestellten PUR-Schaum-Probekörpers als Referenzsystem normiert [42]. Aus diesen Messdaten leitete Johnson ein Alterungsmodell zur Beschreibung der Energieaufnahme von Haushaltskältegeräten ab. Dieses Modell beschreibt den jährlichen Anstieg der Energieaufnahme Δe_{ir} und liefert einen Gesamtanstieg von 21 % über einen Zeitraum von 20 Jahren, siehe Gleichung (8). In dieser Gleichung stellt r die anfängliche Alterungsrate, x einen Korrekturfaktor und τ das Gerätealter dar. Die Größen r und x sind vom dem im Schaum verwendeten Treibmittel abhängige Konstanten.

$$\Delta e_{ir} = r \cdot \left(\frac{20 - \tau}{20}\right)^x \tag{8}$$

Im Vergleich zu den Ergebnissen von Elsner et al. mit einem Anstieg der Energieaufnahme von 25 bis 32 % nach 18 Jahren [28] zeigt das Alterungsmodell von Johnson einen um etwa 5 bis 12 % geringeren Anstieg der Energieaufnahme. Dieses Alterungsmodell wird in Kapitel 2.3 mit weiteren aus der Literatur bekannten Modellen vergleichend diskutiert.

Die Alterung von PUR-Schäumen besteht aus einem komplexen Zusammenspiel verschiedener Prozesse und Effekte, die zu einer Veränderung der Wärmeleitfähigkeit des Schaums führen. So wird die Wärmeleitfähigkeit unter anderem von der Zusammensetzung des Zellgases, der Temperatur und dem Druck in den Schaumzellen beeinflusst [35, 44, 45]. Da eine quantitative Beschreibung der einzelnen Effekte aufgrund ihrer zeitlichen Überlagerung nur schwer möglich ist, wird der Alterungsprozess im nachfolgenden qualitativ diskutiert. Ein mit experimentellen Beobachtungen deutlich konsistenteres Bild wäre über die messtechnische Erfassung des Drucks in den Schaumzellen möglich. Dies ist jedoch aktuell aufgrund der geringen Größe der Schaumzellen von rund 170 nm sowie der Beschaffenheit des Schaums nicht möglich und ist Gegenstand der aktuellen Forschung. Jedoch scheint der Zellgasdruck nach aktuellem Stand nur eine untergeordnete Rolle zu spielen.

Aufgrund des Konzentrationsgradienten zwischen dem Zellgas und der Umgebung diffundiert das Kohlenstoffdioxid über die Zeit aus den Zellen heraus und Luft (Sauerstoff und Stickstoff) diffundiert hinein. Durch die höhere Wärmeleitfähigkeit von Sauerstoff und Stickstoff im Vergleich zu Kohlenstoffdioxid kommt es zu einem Anstieg der Wärmeleitfähigkeit des Zellgases und so auch zu einem Anstieg der Wärmeleitfähigkeit des PUR-Schaums. Darüber hinaus steigt die Wärmekapazität des Zellgases durch den Gasaustausch ebenfalls an. Hierdurch verändert sich der in dem Gehäuse einfallende Wärmestrom leicht. Jedoch wird die absolute Wärmekapazität eines Haushaltskältegeräts durch die Masse der Glasböden dominiert, so dass dieser Effekt nur eine untergeordnete Rolle spielt. In Tabelle 7 sind die Diffusionskoeffizienten, die Wärmeleitfähigkeit und die Wärmekapazitäten der Gasspezies aufgelistet.

Tabelle 7: Diffusionskoeffizienten, Wärmeleitfähigkeiten und spezifische Wärmekapazitäten der im PUR-Schaum relevanten Zellgase bei 20 °C [35].

Stoff	Diffusionskoeffizient	Wärmeleitfähigkeit	Wärmekapazität	
			isochor	isobar
	[m²/s]	[mW/(m·K)]	[kJ/(kg·K)]	[kJ/(kg·K)]
Kohlenstoffdioxid (CO_2)	$1{,}20 \cdot 10^{-10}$	17,1	0,6524	0,8460
Sauerstoff (O_2)	$3{,}06 \cdot 10^{-11}$	25,9	0,6577	0,9189
Stickstoff (N_2)	$4{,}66 \cdot 10^{-12}$	25,4	0,7431	1,0413
Cyclopentan (CP)	$2{,}51 \cdot 10^{-14}$	10,9	1,2490	1,7866

Durch eine Analyse der Gaszusammensetzung und einer Messung der Wärmeleitfähigkeit an PUR-Schaum-Probekörpern kann der Anstieg der Wärmeleitfähigkeit und der Austausch der Zellgase nachgewiesen werden. So steigt die Wärmeleitfähigkeit des PUR-Schaums von anfangs 19,5 mW/(m·K) auf ca. 26 mW/(m·K) an. Die Ergebnisse solcher Untersuchungen hängen stark von der Beschaffenheit des Probekörpers ab. In Abbildungen 4 und 5 sind die zeitlichen Verläufe der Wärmeleitfähigkeit und der Zellgaszusammensetzung von Probekörpern dargestellt. Aufgrund der komplexen Gehäusegeometrie wird sich der Anstieg der Wärmeleitfähigkeit des in einem realen Haushaltskältegerät verbauten PUR-Schaums von diesen Ergebnissen im zeitlichen Verlauf unterscheiden.

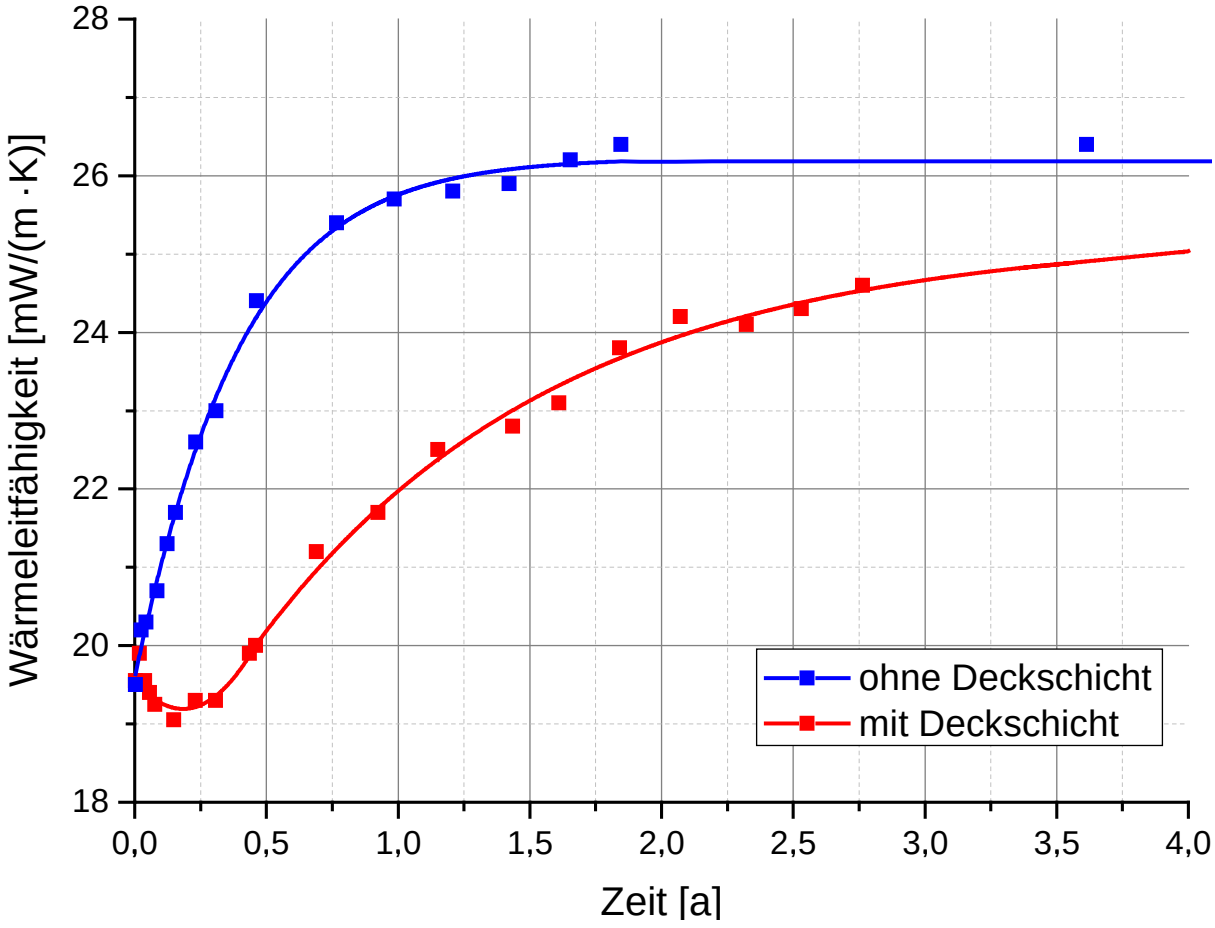

Abbildung 4: Wärmeleitfähigkeitsanstieg von verschiedenen PUR-Schaum-Probekörpern.

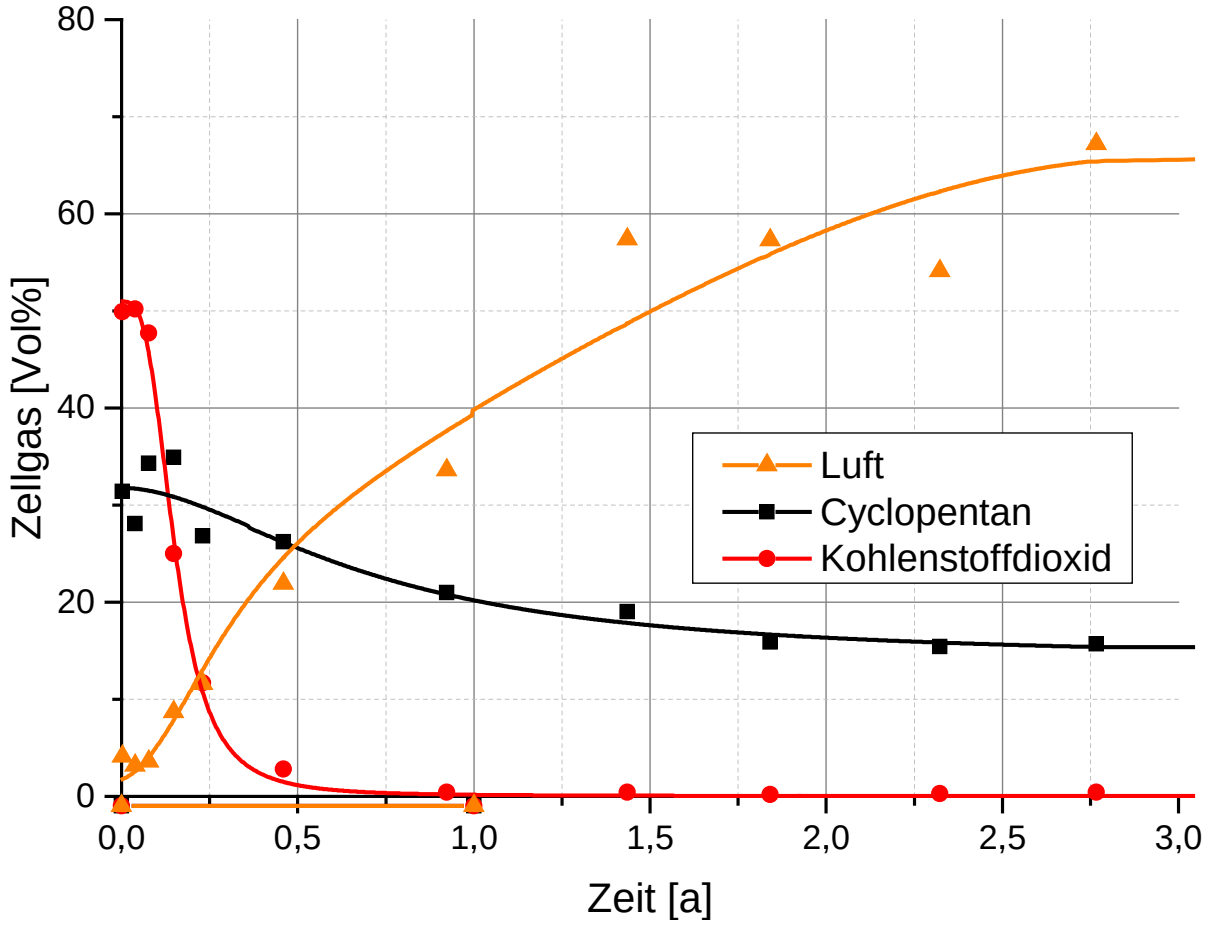

Abbildung 5: Zellgasdiffusion von PUR-Schaum-Probekörpern ohne Deckschicht.

2.3 Bestimmung des in das Gehäuse einfallenden Wärmestroms

Der Wärmestrom $\dot{Q}_{Geh.}$, der in das Gehäuse eines Haushaltskältegeräts einfällt, kann vereinfacht über die Gleichung (9) aus dem Produkt des Wärmedurchgangskoeffizienten k, der mittleren Oberfläche des Gehäuses A und der Temperaturdifferenz ΔT zwischen der Umgebung T_a und dem Innenraum T_i berechnet werden [34].

$$\dot{Q}_{Geh.} = k \cdot A \cdot \Delta T = k \cdot A \cdot (T_a - T_i) \tag{9}$$

Hierbei geht der Wärmedurchgangskoeffizient k und die mittlere Oberfläche des Gehäuses A nach Gleichung (10) ein. Der konvektive Wärmeübergang an der Innen- und Außenseite des Gehäuses wird mit den Wärmeübergangskoeffizienten α_a und α_i, die Wärmeleitung durch das Gehäuse mit der jeweiligen Materialstärke d und der Wärmeleitfähigkeit λ, der verwendeten Materialien berücksichtigt [34].

$$\frac{1}{k \cdot A} = \frac{1}{\alpha_a \cdot A_a} + \sum_{j=1}^{n} \left[\frac{d_j}{\lambda_j \cdot A_j} \right] + \frac{1}{\alpha_i \cdot A_i} \tag{10}$$

Dieser Wärmestrom lässt sich mit Hilfe von Heat-Flow-Sensoren und den Versuchsaufbauten der Reverse-Heat-Leak-Methode, der B-Methode und der Latent-Heat-Sink-Methode bestimmen [35, 46-53]. Im Rahmen dieser Dissertation wurden die B-Methode und die Latent-Heat-Sink-Methode entwickelt. Im Folgenden werden zunächst die Methoden beschrieben und dann ihre Eignung und notwendige Anpassungen für die Untersuchung von in Kühlgeräten eingesetzten Isolationsmaterialien unter dem Gesichtspunkt der Alterung betrachtet.

Heat-Flow-Sensoren

Prinzipiell lässt sich der Wärmestrom, der durch das Gehäuse in den Lagerraum eintritt, mit Hilfe von Heat-Flow-Sensoren messen. Die Funktionsweise dieser Sensoren wurde 1994 von Lassue et al. beschrieben [46]. Der Einsatz dieses Verfahrens wurden von Melo et al. und Thiessen et al. an Haushaltskältegeräten untersucht [47, 48]. Die Sensoren werden auf dem Gehäuse platziert und es wird der lokal in das Gehäuse eintretende Wärmestrom gemessen. Der lokale Wärmestrom kann jedoch abhängig von Hersteller, Marke, Gerätetyp und der Anordnung von Kabeln, Rohrleitungen und des Verdampfers punktuell stark variieren und repräsentiert daher nicht den globalen Wärmestrom in einem spezifischen Gehäuse. Zur Bestimmung des Gesamtwärmestroms müsste daher das Gehäuse großflächig mit Sensoren bestückt werden. Hierdurch würde der Arbeits- und Materialaufwand für dieses Messverfahren stark steigen, was ihren Einsatz in Bezug auf Alterungseffekte uninteressant macht.

Reverse-Heat-Leak-Methode

Die Reverse-Heat-Leak-Methode wurde von verschiedenen Autoren untersucht, modifiziert und verbessert [47, 49-52], und wird aktuell auch in vielen Forschungs- und Entwicklungsabteilungen von Kältegeräteherstellern eingesetzt. Im Gegensatz zu den üblichen Temperaturverhältnissen im Lagerraum eines Haushaltskältegeräts wird dem Lagerraum mit elektrischen Heizelementen Wärme zugeführt, bis eine konstante mittlere Temperatur von 40 °C im Lagerraum erreicht wird. Gleichzeitig wird die Umgebungstemperatur auf 16 °C abgesenkt, so dass sich ein Wärmestrom von innen nach außen einstellt. Die elektrische Heizleistung P_{el}, die benötigt wird, um eine stabile Temperatur innerhalb des Lagerraums aufrechtzuerhalten, steht über Gleichung (11) in direktem Zusammenhang mit dem Wärmestrom durch das Gehäuse $\dot{Q}_{Geh.}$. Durch Umstellung der Gleichung (11) kann der für ein Gehäuse charakteristische $k \cdot A$-Wert bestimmt werden, siehe Gleichung (12) [34].

$$P_{el} = \dot{Q}_{Geh.} = k \cdot A \cdot (T_i - T_a) \tag{11}$$

$$k \cdot A = \frac{P_{el}}{(T_i - T_a)} \tag{12}$$

Die Messergebnisse, die mit dieser Methode erhalten werden, hängen (stark) von den verwendeten Versuchsparametern bzw. den Randbedingungen ab und sind keine Absolutwerte. Da es aufgrund der Messmethode zu einer Temperaturschichtung im Lagerraum kommt, wird der Einsatz von Ventilatoren im Lagerraum notwendig, um eine homogenere Temperaturverteilung zu erreichen. Jedoch stellt sich so eine

erzwungene Konvektion im Lagerraum ein, wodurch die Wärmeübergangskoeffizient an den Innenwänden des Lagerraums ansteigt und so das Ergebnis beeinflusst. Außerdem unterscheidet sich die Temperaturdifferenz zwischen dem Lagerraum und der Umgebung von der realen Haushaltsnutzung. Im realen Einsatz stellt sich die größte Temperaturdifferenz im unteren Teil des Lagerraums des Kühlschranks ein, bei den Messungen mit der Reverse-Heat-Leak-Methode liegt die größte Temperaturdifferenz im oberen Teil des Lagerraums (siehe Abbildung 6) [34].

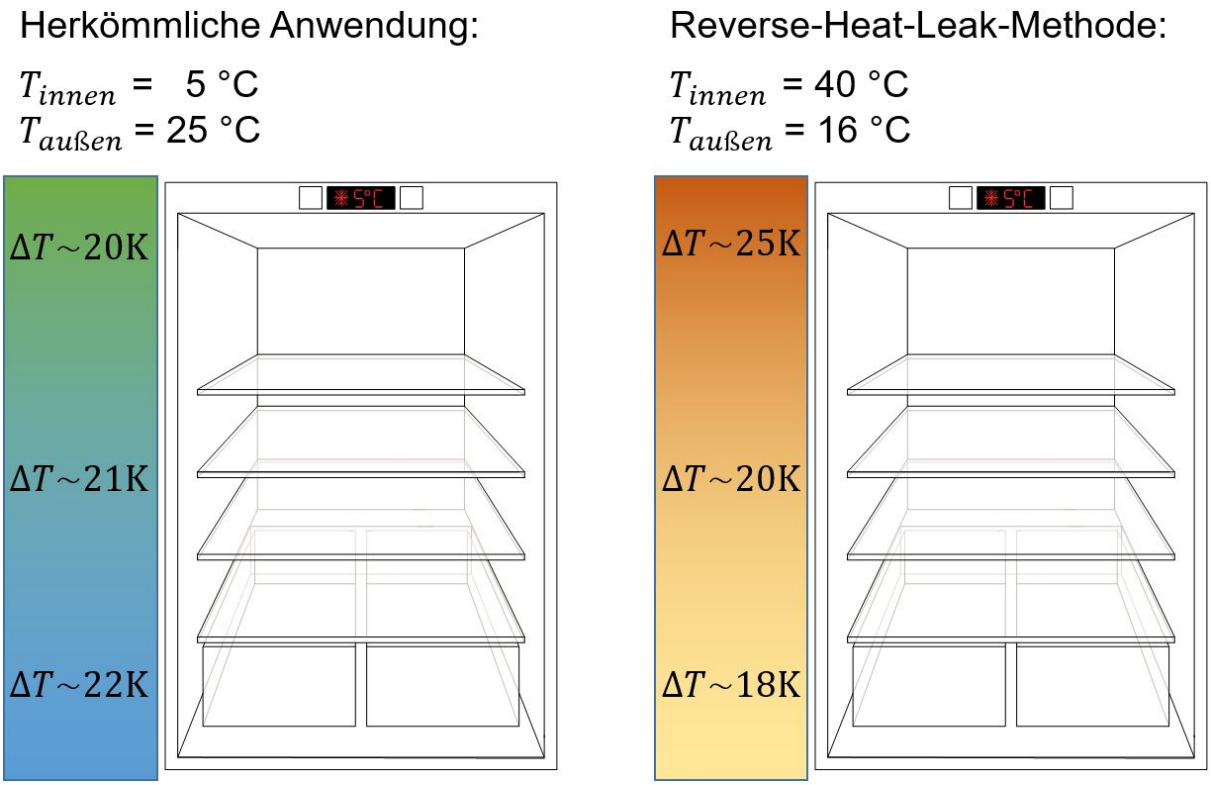

Abbildung 6: Temperaturgradienten an einem Kühlschrank während der herkömmlichen Anwendung und der Messung mit der Reverse-Heat-Leak Messung. ΔT gibt die Differenz zwischen Innen- und Außentemperatur an.

B-Methode

Bei der sogenannten B-Methode [53] handelt es sich um einen modifizierten Temperature-Rise-Test in Anlehnung an die IEC 62552-2:2015 [25]. Das Gerät wird nach der IEC 62552-1:2015 mit Messstellen bestückt [24]. Zu einem bestimmten Zeitpunkt wird das zuvor im stabilen Kühlbetrieb laufende Gerät ausgeschaltet und die Zeit gemessen, die der Lagerraum zum Aufwärmen benötigt. Über eine definierte Prüfgröße θ_i kann der Anstieg der Temperatur im Lagerraum beschrieben werden, siehe Gleichung (13). Wird die Gleichung (13) nun um das Verhältnis von Wärmedurchgang und Wärmekapazität mit Gleichung (14) erweitert, kann der $k \cdot A$-Wert mittels der Gleichung (15) bestimmt werden. In die Rechnung gehen die Masse der Luft im Lagerraum m_{Luft}, die isochore Wärmekapazität der Luft $c_{v,Luft}$, die Dauer des Temperaturanstiegs τ_B, die Innen- T_i und die Außentemperatur T_a zu Beginn und am Ende des Temperaturanstiegs ein [53].

$$\theta_i = \frac{1}{\tau_B} \cdot \ln\left(\frac{T_i(0) - T_a(0)}{T_i(\tau_B) - T_a(\tau_B)}\right) \tag{13}$$

$$\theta_i = \frac{k \cdot A}{m_{Luft} \cdot c_{v,Luft}} \tag{14}$$

$$k \cdot A = m_{Luft} \cdot c_{v,Luft} \cdot \int_0^{\tau_B} \left[\frac{1}{\tau_B} \cdot \ln\left(\frac{T_i(0) - T_a(0)}{T_i(\tau_B) - T_a(\tau_B)}\right)\right] d\tau \tag{15}$$

Dieses Messverfahren ist daher gut in die bestehenden Normprüfungen nach der Normenreihe IEC 62552:2015 [24-26] zu integrieren. Da es sich jedoch um ein neues Verfahren handelt, muss die Einsatzfähigkeit dieser Methode erst noch nachgewiesen werden. So wird derzeit das thermische Verhalten der im Gehäuse befindlichen Einbauten (wie z.B. die Glasböden oder Schubladen) in der Berechnung nicht berücksichtigt, obwohl sie aufgrund ihrer deutlich größeren absoluten Wärmekapazität das Aufwärmen der Luft beeinflussen.

Latent-Heat-Sink-Methode

Bei der Latent-Heat-Sink-Methode wird der Lagerraum bei ausgeschalteter Kältemaschine über einen Eiswasserbehälter gekühlt. Durch eine Umwälzpumpe wird eine Temperaturschichtung im Eiswasserbehälter während des Versuchs verhindert. Über die Abtauzeit einer definierten Menge an Eis kann der $k \cdot A$-Wert bestimmt werden. Hierzu müssen zunächst alle Böden aus dem Lagerraum entfernt werden, um Platz für den zu Beginn nur mit flüssigem Wasser gefüllten Eiswasserbehälter zu schaffen. Das Gerät wird zunächst über die Kältemaschine mit ausgeschalteter Umwälzpumpe in einen stabilen Betriebszustand gebracht. Zu einem definierten Zeitpunkt wird die Kältemaschine ausgeschaltet, die Umwälzpumpe eingeschaltet und eine kleine Menge Eis in den Behälter gegeben. Ist diese Eismenge nahezu abgetaut, kommt es zu einem Anstieg der Temperatur im Eiswasserbehälter. Da während des Abtauens immer eine gewisse Restmenge an Eis im Behälter verbleibt, muss mit einer zweiten, größeren Eiszugabe m_{Eis} gearbeitet werden. Die Abtauzeit dieser zweiten Eismenge $\Delta\tau_S$ wird zur Bestimmung des $k \cdot A$-Werts herangezogen. In Abbildung 7 ist der Temperaturverlauf des Eiswassers über die Versuchszeit dargestellt.

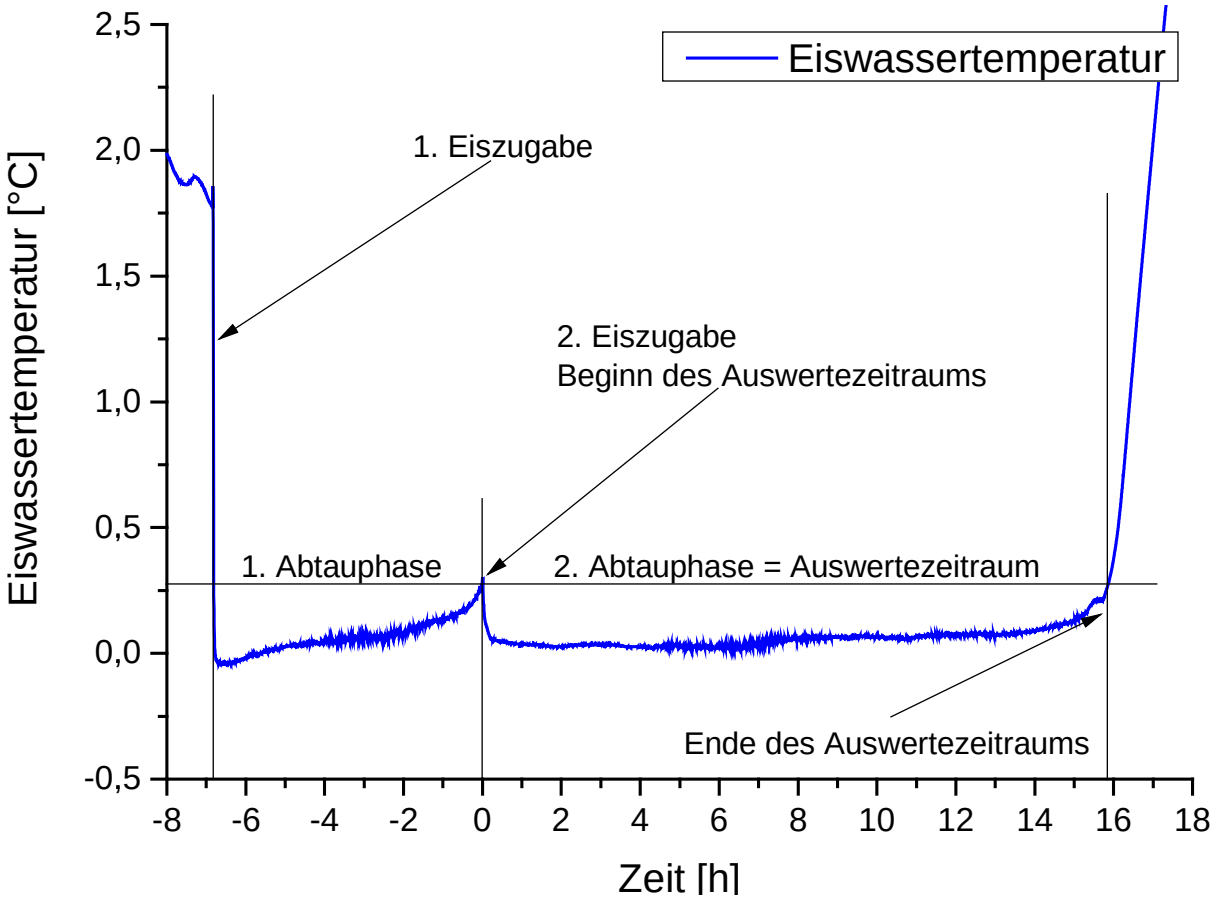

Abbildung 7: Verlauf der Eiswassertemperatur während des Versuchs.

Durch eine Energiebilanz des Eisbehälters kann der $k \cdot A$-Wert mittels Gleichung (16) bestimmt werden. Die Rechnung bezieht sich in der dargestellten Gleichung auf den $k \cdot A$-Wert zwischen der Umgebungs- T_a und der mittleren Lagertemperatur während der zweiten Abtauphase T_{m*}. Eine mögliche Unterkühlung wird über die Differenz der Schmelztemperatur von T_{Eis}=0 °C und der Temperatur, bei der das Eis vor dem Versuch gelagert wurde $T_{Eis,1}$, berücksichtigt. Außerdem werden die Schmelzenthalpie Δh_s und die isobare Wärmekapazität des Eises $c_{p,Eis}$ als Stoffdaten benötigt. Die Antriebsleistung der Umwälzpumpe P_{Pumpe} wird während des Versuchs vollständig dissipiert und wird ebenfalls messtechnisch erfasst.

$$k \cdot A = \frac{m_{Eis} \cdot \left[\Delta h_s + c_{p,Eis} \cdot \left(T_{Eis} - T_{Eis,1}\right)\right]}{\left(T_a - T_{m*}\right) \cdot \Delta\tau_s} - \frac{P_{Pumpe}}{\left(T_a - T_{m*}\right)} \qquad (16)$$

Die Eismengen der ersten und zweiten Eiszugabe und die zu Beginn des Versuchs im Eiswasserbehälter befindliche Menge an flüssigem Wasser müssen abhängig von der Umgebungstemperatur aufeinander abgestimmt werden. Durch die große thermische Masse im Eisbehälter besitzt diese Messmethode eine deutlich höhere Messgenauigkeit als die zuvor beschriebenen Methoden.

Mithilfe dieser Messmethode konnte ein Anstieg des $k \cdot A$-Werts von vier Neugeräten von durchschnittlich 9 % über einen Zeitraum von 14 Monaten festgestellt werden. Die Ergebnisse dieser Messungen sind in Abbildung 8 gezeigt.

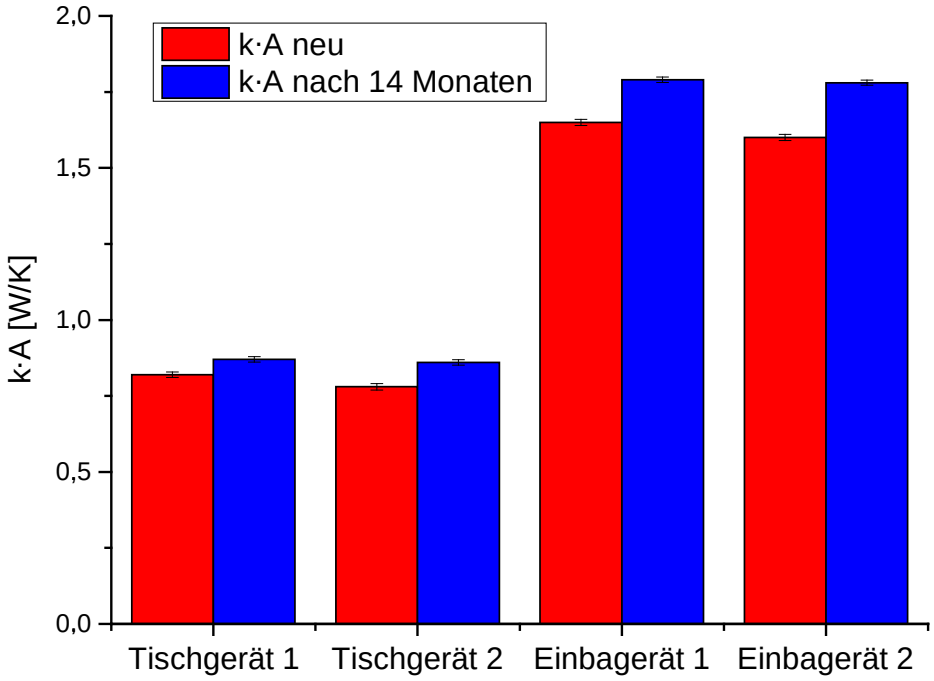

Abbildung 8: Anstieg des $k \cdot A$-Werts von Neugeräten nach 14 Monaten der mit der Latent-Heat-Sink-Methode ermittelt wurde.

Bewertung der Messmethoden

Die beschriebenen Messmethoden haben unterschiedliche Vor- und Nachteile in ihrer Anwendung. Zum jetzigen Zeitpunkt hat sich bei den Herstellern die Reverse-Heat-Leak-Methode durchgesetzt. Jedoch kann diese Methode den alterungsbedingten Anstieg des $k \cdot A$-Werts aufgrund der im Vergleich zum normalen Betrieb unterschiedlichen Anströmung der Luft an das Gehäuse nur unzureichend beschreiben. Daher wurden im Rahmen dieser Dissertation mit der B-Methode und der Latent-Heat-Sink-Methode zwei neue Messverfahren entwickelt, die den Anstieg des $k \cdot A$-Werts unter realen Bedingungen nachweisen können. So zeichnet sich die B-Methode durch ihre leichte Integrierbarkeit in bestehende Versuchsprogramme nach der IEC 62552:2015 und die Latent-Heat-Sink-Methode durch eine deutlich höhere Messgenauigkeit aus.

2.4 Bestimmung des Anstiegs der Energieaufnahme an real gealterten Haushaltskältegeräten

Bisherige Modelle zur Beschreibung des alterungsbedingten Anstiegs der Energieaufnahme von Haushaltskältegeräten beruhen nur auf Funktionen, die für einzelne Systemkomponenten angepasst und dann auf das Gesamtsystem extrapoliert wurden [32, 54, 55]. An Messungen der Energieaufnahme des Gesamtsystems Haushaltskältegerät angepasste Alterungsmodelle waren im Vorfeld zu dieser Dissertation nicht vorhanden.

Die Verwendung der auf dem EU-Energielabel angegebenen Energieaufnahme als Ausgangsbasis für ein Alterungsmodell von Haushaltskältegeräten ist nicht möglich,

da aufgrund von Fertigungstoleranzen die reale Energieaufnahme eines spezifischen Geräts um bis zu 10 % vom gelabelten Wert abweichen darf. Zur Erstellung des Alterungsmodells wurden im Rahmen dieser Untersuchungen über 100 Messungen der Norm-Energieaufnahme an 32 unter realen Bedingungen gealterten Haushaltskältegeräten durchgeführt. Die Geräte wurden zunächst im Labor im Neuzustand untersucht und dann nach einer Betriebszeit von bis zu 21 Jahren erneut vermessen. Die Wiederholungsmessungen wurden immer unter den gleichen Norm-Bedingungen wie bei der ersten Messung durchgeführt. Dies bedeutet, dass ältere Geräte, die vor 2016 hergestellt wurden, nach der DIN EN ISO 15502:2006 [19] und der DIN EN 153:2006 [23] vermessen wurden. Durch die Verwendung der im Kapitel 1.2 vorgestellten, normierten Messmethoden konnte eine Reproduzierbarkeit der Energieaufnahme sichergestellt werden. Eine Umrechnung der Ergebnisse der verschiedenen Normen untereinander ist, wie in Kapitel 1.2 dargestellt, nicht ohne weiteres möglich. Daher wurden die relativen Zeitverläufe der Energieaufnahme betrachtet.

Da die Energieaufnahme unmittelbar nach der Herstellung nicht gemessen werden konnte, musste dieser Wert für die Erstellung eines Alterungsmodells aus den vorhandenen Daten und Informationen zum Produktionsdatum abgeschätzt werden. Dazu wurde zunächst eine vorläufige Funktion erstellt. Hierzu wurde die zu dem Zeitpunkt τ gemessene Energieaufnahme $E(\tau)$ auf die Energieaufnahme der ersten Messung E_0 jedes einzelnen Geräts normiert, siehe Gleichung (17), und anschließend die in Gleichung (18) gezeigte Funktion an diese normierten Daten angepasst. Dies ist in Abbildung 9 dargestellt.

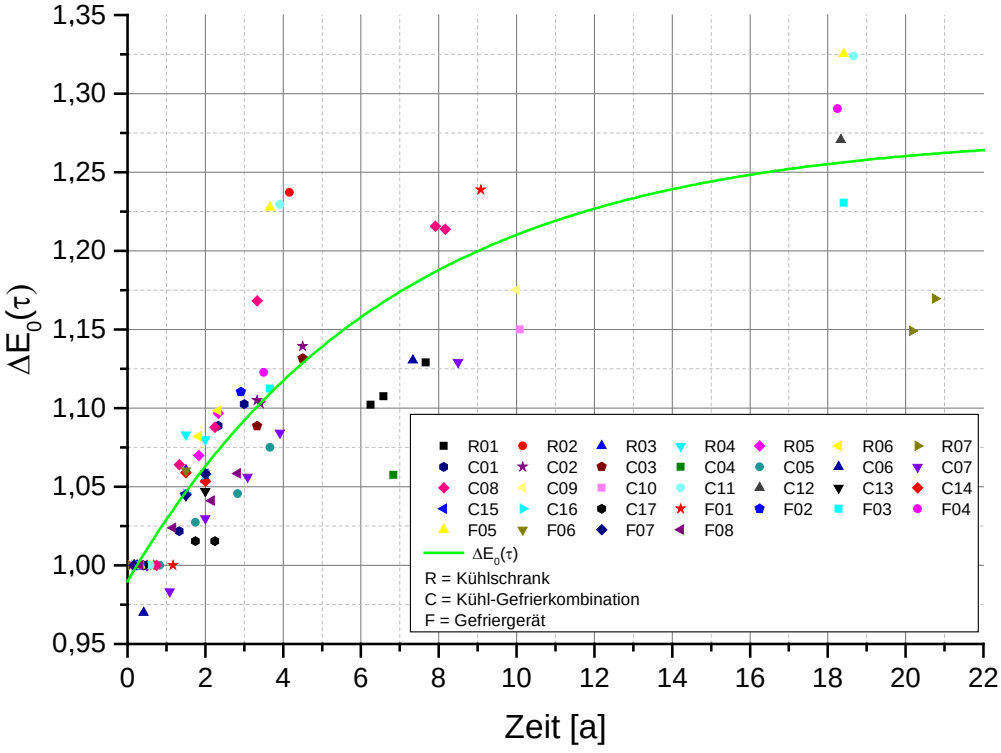

Abbildung 9: Normierte Energieaufnahme (Symbole) und vorläufige Alterungsfunktion (Linie).

$$\Delta E_0(\tau) = \frac{E(\tau)}{E_0} \tag{17}$$

$$\Delta E_0(\tau) = g + a \cdot \left[1 - \mathrm{e}^{-\left(\frac{\tau}{b}\right)}\right] = 0{,}990 + 0{,}285 \cdot \left[1 - \mathrm{e}^{-\left(\frac{\tau}{6{,}749}\right)}\right] \tag{18}$$

Über die Gleichung (18) lässt sich mit Hilfe von Gleichung (19) die hypothetische Energieaufnahme zum Produktionszeitpunkt der Geräte E_p berechnen. Auf diese Energieaufnahme wurden die Messdaten erneut normiert und die finale Alterungsfunktion erstellt, siehe Gleichung (20). Der Verlauf dieser Funktion ist in Abbildung 10 dargestellt.

$$E_p = E_0 \cdot \left[1 - \left(\Delta E_0(\tau) - \Delta E_0(\tau = 0)\right)\right] \tag{19}$$

$$\Delta E_p(\tau) = 1 + 0{,}295 \cdot \left[1 - \mathrm{e}^{-\left(\frac{\tau}{6{,}517}\right)}\right] \tag{20}$$

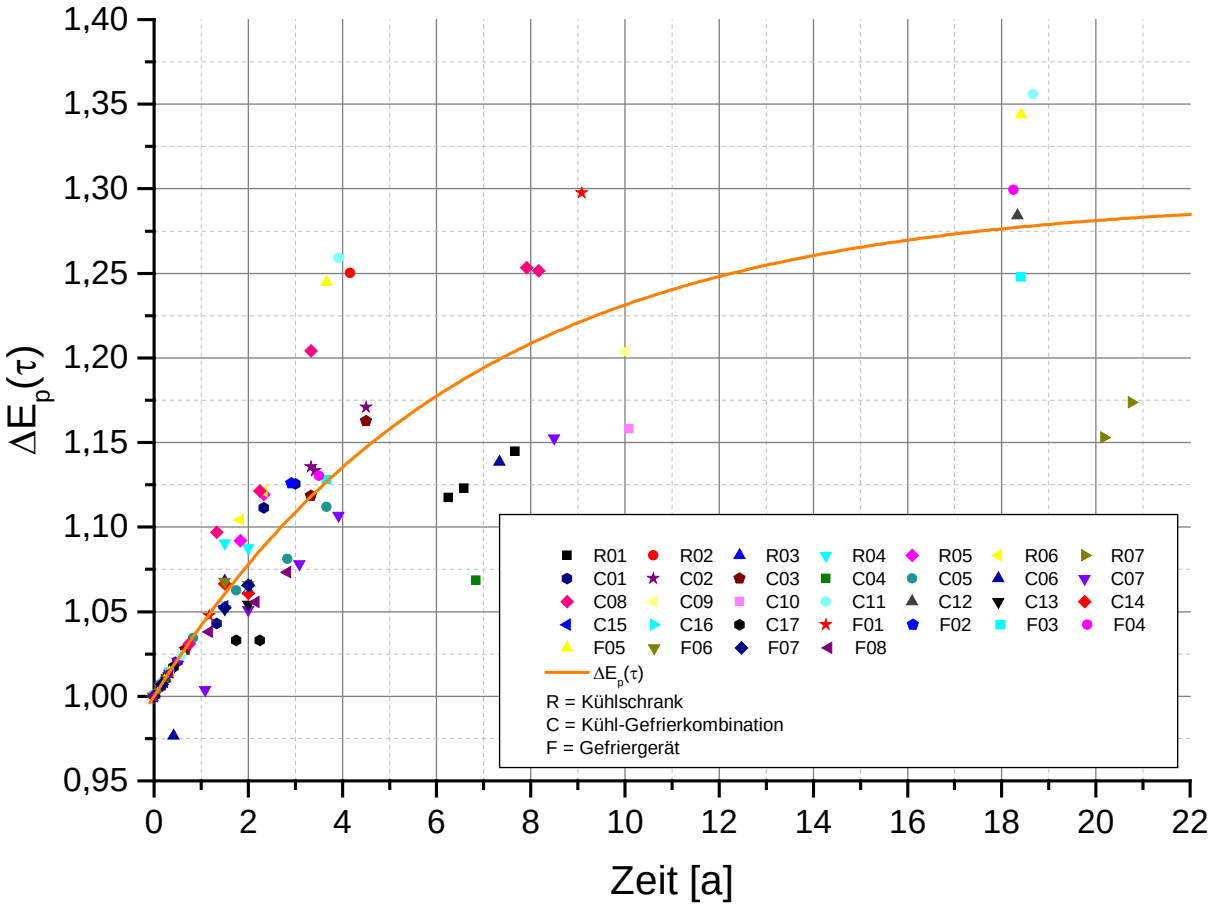

Abbildung 10: Korrigierte Energieaufnahme (Symbole) und konsolidiertes Alterungsmodell $\Delta E_p\ (\tau)$ (Linie).

Das beschriebene Alterungsmodell zeigt den größten Anstieg der Energieaufnahme in den ersten fünf Jahren nach der Produktion. In diesem Zeitraum steigt die Energieaufnahme im Schnitt um 15,8 % an. Über den durchschnittlichen Betriebszeitraum eines Haushaltskältegeräts von 16 Jahren [10] steigt die Energieaufnahme um 27 % an. Dies entspricht einem durchschnittlichen Mehrverbrauch von 18 % über diesen Zeitraum. Bei deutlich älteren Geräten ist der

weitere Anstieg der Energieaufnahme vernachlässigbar. Da die in dieser Studie untersuchten Geräte von unterschiedlicher Bauart und Fertigungsqualität sind, streuen ihre Alterungsergebnisse. Dennoch folgen sie im Wesentlichen dem beschriebenen Verlauf des vorliegenden Alterungsmodells. Die Streuung beträgt in den ersten drei Jahren nach der Produktion ± 5 % und steigt bei einem Gerätealter von > 15 Jahren auf bis zu ± 15 % an.

In Abbildung 11 ist der Vergleich des entwickelten Alterungsmodells mit den bereits in der Literatur beschriebenen Modellen von Johnson, Garland und Hadfield sowie der EU-Studie zu sehen. Das im Rahmen dieser Dissertation entwickelte Alterungsmodell zeigt in den ersten 14 Betriebsjahren der Kältegeräte einen deutlich höheren Anstieg der Energieaufnahme als die Modelle aus der Literatur. Speziell der in der EU-Studie angenommene Anstieg der Energieaufnahme von 10 % über 16 Jahre ist deutlich zu gering.

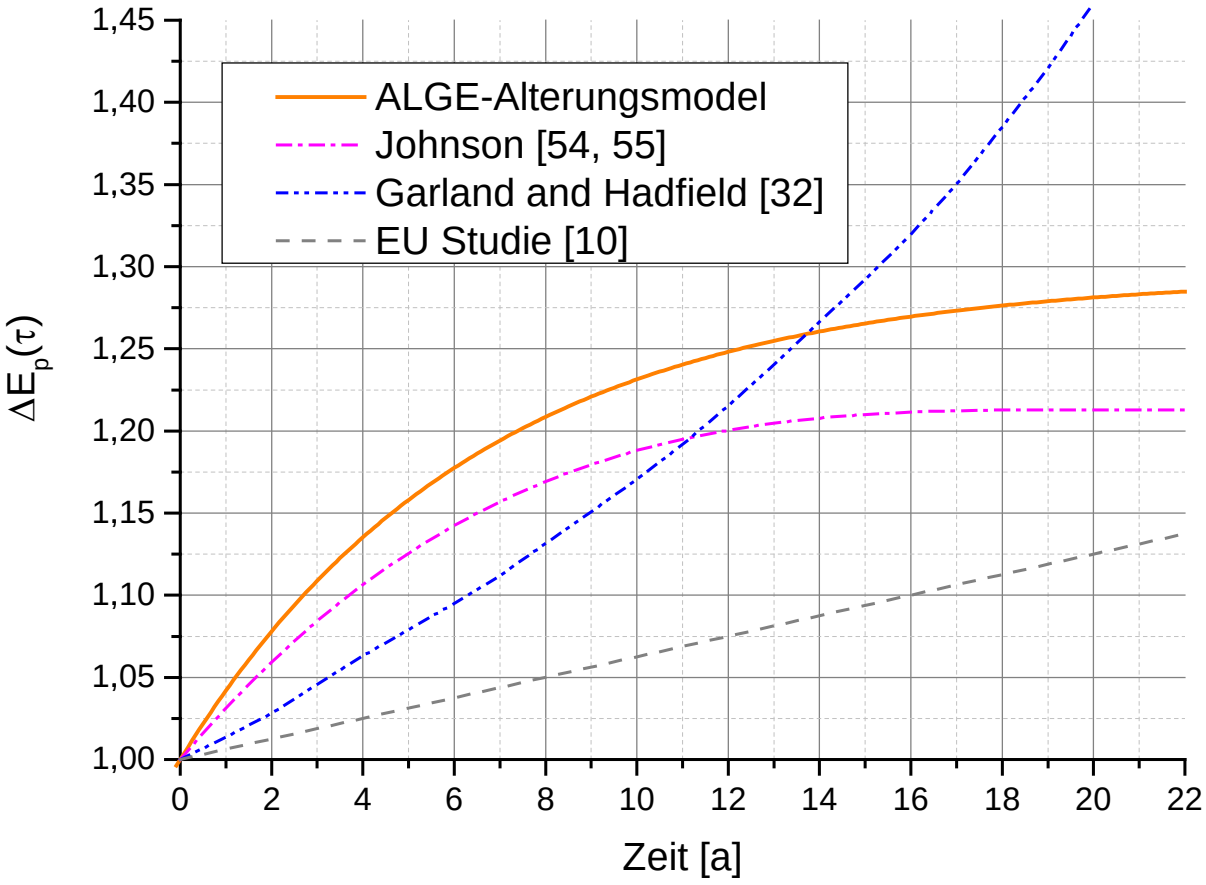

Abbildung 11: Vergleich verschiedener Alterungsmodelle für die elektrische Energieaufnahme von Haushaltskältegeräten.

Im Vergleich zum Modell von Johnson [54, 55] ist ebenfalls ein deutlich stärkerer Anstieg der Energieaufnahme über die gesamte Beobachtungszeit festzustellen. Das Johnson-Modell basiert auf den Arbeiten von Wilkes [39-43], in denen die Wärmeleitfähigkeit von PUR-Schaumproben über einen Zeitraum von 13 Jahren gemessen wurde. Daher berücksichtigt das Johnson-Modell nur die Alterung des PUR-Schaums. Jedoch verläuft die von Johnson beschriebene Funktion grundsätzlich mathematisch ähnlich zu dem in dieser Dissertation entwickelten Modell.

Dem Alterungsmodell von Garland und Hadfield [32] liegt ein grundlegend anderer mathematischer Verlauf für den Anstieg der Energieaufnahme zu Grunde. Innerhalb der ersten 14 Jahre liegt der Verlauf des Garland und Hadfield-Modells unterhalb des hier einwickelten Modells und steigt dann ab einem Gerätealter von 14 Jahren auf deutlich höhere Werte an. Dieses Modell basiert auf tribologischen Untersuchungen und beschränkt sich daher ausschließlich auf den Verdichter als Alterungsquelle in einem Haushaltskältegerät.

Beide Literaturmodelle geben die Alterung für eines der Teilsysteme im Haushaltskältegerät wieder. Durch eine gewichtete Kombination der Modelle von Johnson sowie von Garland und Hadfield sollte eine Umrechnung in das hier entwickelte Modell möglich sein, wobei der Schwerpunkt der Gerätealterung im PUR-Schaum liegen wird. Hierbei müsste eine Anpassung der älteren Modelle aus den frühen 2000er Jahren auf die aktuell in Haushaltskältegeräten eingesetzten Systeme und Werkstoffe durchgeführt werden. Jedoch besteht zum jetzigen Zeitpunkt noch keine ausreichende Datenbasis für das hier entwickelte Alterungsmodells, um dies durchzuführen. Durch weiterführende Messungen der Energieaufnahme sollte es möglich werden.

2.5 Einfluss des Verbraucherverhaltens auf die Energieaufnahme von Haushaltskältegeräten

Die reale Energieaufnahme eines Haushaltskältegeräts kann deutlich von der unter Normbedingungen erfassten Energieaufnahme auf dem EU-Energielabel abweichen und hängt stark vom individuellen Verhalten des Verbrauchers ab. Im Rahmen dieser Dissertation wurde daher an einer Verbraucherbefragung mitgearbeitet, die die wesentlichen Einflussgrößen auf die reale Energieaufnahme identifizieren sollte.

Der Verbrauchereinfluss lässt sich grundsätzlich in ein indirektes (IUB) und ein direktes Verbraucherverhalten (DUB) klassifizieren. Einflussgrößen wie z.B. die eingestellte Lagertemperatur, die Anzahl der Türöffnungen, das Einlagern warmer Speisen und die wöchentliche Einlagerungsmenge zählen zum direkten Verbraucherverhalten. Der Aufstellungsort des Geräts und die hierdurch beeinflussten Größen, wie z.B. die Umgebungstemperatur oder das mögliche Aufstellen neben einer Wärmequelle (wie z.B. Heizung, Backofen, Fenster mit direkter Sonneneinstrahlung), zählen zum indirekten Verbraucherverhalten. Die Hersteller oder auch Verbraucherschutz-organisationen geben oft in den Betriebsanleitungen der Geräte oder in Zeitschriftenartikeln Handlungsempfehlungen an die Verbraucher heraus, um negativen Einflüssen entgegenzuwirken und so die Energieaufnahme zu senken. Die Ergebnisse sind in Tabelle 8 aufgeführt.

Tabelle 8: Ergebnisse der Verbraucherbefragung zu den Einflussgrößen auf die Energieaufnahme von Haushaltskältegeräten [56].

Verbraucherempfehlung			Umsetzung der Empfehlung	Auswertbare Befragte
Indirektes Verbraucherverhalten (IUB)				
Umgebungstemperatur am Aufstellort		Sommer	12,0 %	706
T_a ≈ 19 °C (±1 K); $T_{a,min}$ ≥ 16 °C; $T_{a,max}$ ≤ 25 °C		Winter	38,4 %	
Keine Aufstellung in Nähe zu externen Wärmequellen			77,9 %	706
Direktes Verbraucherverhalten (DUB)				
Lagertemperatur	Kühlteil:	5 °C ≤ T_R≤ 7 °C	59,9 %	706
	Gefrierteil:	T_R ≤ -18 °C	64,1 %	540
		T_R ≤ -16 °C	76,5 %	
Türöffnungen	Kühlschrank:	≤ 10 Öffnungen/Tag	53,6 %	166
	Kühl-Gefrierkombination:	≤ 12 Öffnungen/Tag	53,3 %	540
Kein Einlagern warmer Speisen			54,2 %	706
Einlagerung von Lebensmittel ≤ 10 Liter/Woche			88,4 %	706

Eines der wesentlichen Ergebnisse dieser Untersuchungen ist, dass diese Handlungsempfehlungen von einem Großteil der Verbraucher aus unterschiedlichen Gründen nicht umgesetzt werden, was sich negativ auf die Energieaufnahme im Feld auswirkt. Teilweise sind jedoch einzelne dieser Empfehlungen für einen individuellen privaten Haushalt auch nicht umsetzbar. Für die Reduzierung des Stromverbrauchs privater Haushalte ergeben sich hier weitere Ansätze. Durch aktive Informationskampagnen von Herstellern, Verbraucherschutzorganisationen oder staatlichen Stellen ist eine Sensibilisierung der Bevölkerung für diese Problematik möglich. Aus volkswirtschaftlicher Sicht könnte so, vor dem Hintergrund der vollständigen Marktdurchdringung von Haushaltskältegeräten, der Nettostromverbrauch signifikant reduziert werden.

3 Einsatz von Phasenwechselmaterialien in Haushaltskältegeräten

Der Einsatz von Phasenwechselmaterialien (PCM) in Haushaltskältegeräten bietet mehrere Vorteile. Er würde es erlauben, die Energieaufnahme, um bis zu 17 % zu senken [57], die Geräte als Energiespeicher zu verwenden und darüber hinaus die Lagerbedingungen zu verbessern [57-61]. So können zum Beispiel die Temperaturschwankungen im Lagerraum von 4 K auf 0,5 K reduziert, die Zeit zum Abkühlen von Lebensmitteln um 33 % gesenkt und die Zeit bis zu einem kritischen Temperaturanstieg bei einem Stromausfall um 145 % verlängert werden [61].

Für den Einsatz in Haushaltskältegeräten muss das PCM genau auf den Anwendungsfall und die technischen Randbedingungen angepasst werden. Das PCM muss über eine Lebensmittelverträglichkeit verfügen, zyklenstabil sein, es sollte kein Korrosionsverhalten zu den im Gerät verbauten Werkstoffen aufweisen und zu einer möglichst geringen Unterkühlung beim Erstarren neigen. Darüber hinaus sollten Stoffdaten wie die Schmelzenthalpie, Schmelztemperatur oder die Wärmeleitfähigkeit des PCM bekannt sein. Innerhalb des in Haushaltskältegeräten relevanten Temperaturbereichs von ca. -30 °C bis 50 °C können eutektische Wasser-Salz-Lösungen, Clathrate, Polyethylenglycol, Fettsäuren, Nitrate, Wasser und Paraffine eingesetzt werden [62]. Trotz der relativ geringen Schmelzenthalpie besitzen Paraffine in diesem Anwendungsgebiet mehrere Vorteile: in Abhängigkeit von ihrer molekularen Kettenlänge ist die Schmelztemperatur wählbar, sie zeigen eine geringe Neigung zur Unterkühlung, sind lebensmittelgeeignet, zyklenstabil und führen nicht zu Korrosion.

Jedoch sind nicht alle diese Stoffdaten, wie die Wärmeleitfähigkeit, in der Vergangenheit ausreichend untersucht worden. Es ist zwar bekannt, dass die Wärmeleitfähigkeit von Paraffinen vergleichsweise gering ist und sich dies durch Zugabe von Graphit verbessern lässt [57, 58, 62-64]. Allerdings ist die exakte Wärmeleitfähigkeit der verschiedenen Paraffine zum größten Teil nur für die flüssige Phase und nur für einige wenige Paraffine für die feste Phase bekannt [65].

3.1 Messung der Wärmeleitfähigkeit von Paraffinen

Im Rahmen dieser Dissertation wurde daher ein Messaufbau zur Bestimmung der Wärmeleitfähigkeit entwickelt und die Wärmeleitfähigkeit von reinem n-Octadecan, reinem n-Eicosan sowie verschiedenen Proben von n-Docosan in seiner Reinform und Mischungen aus n-Docosan mit 5 Massen% und 10 Massen% Graphit (Compound) in der festen Phase vermessen. Der verwendete Messaufbau ist ein modifizierter Aufbau des Guarded-Hot-Plate-Verfahrens und wird in Abbildung 12 dargestellt.

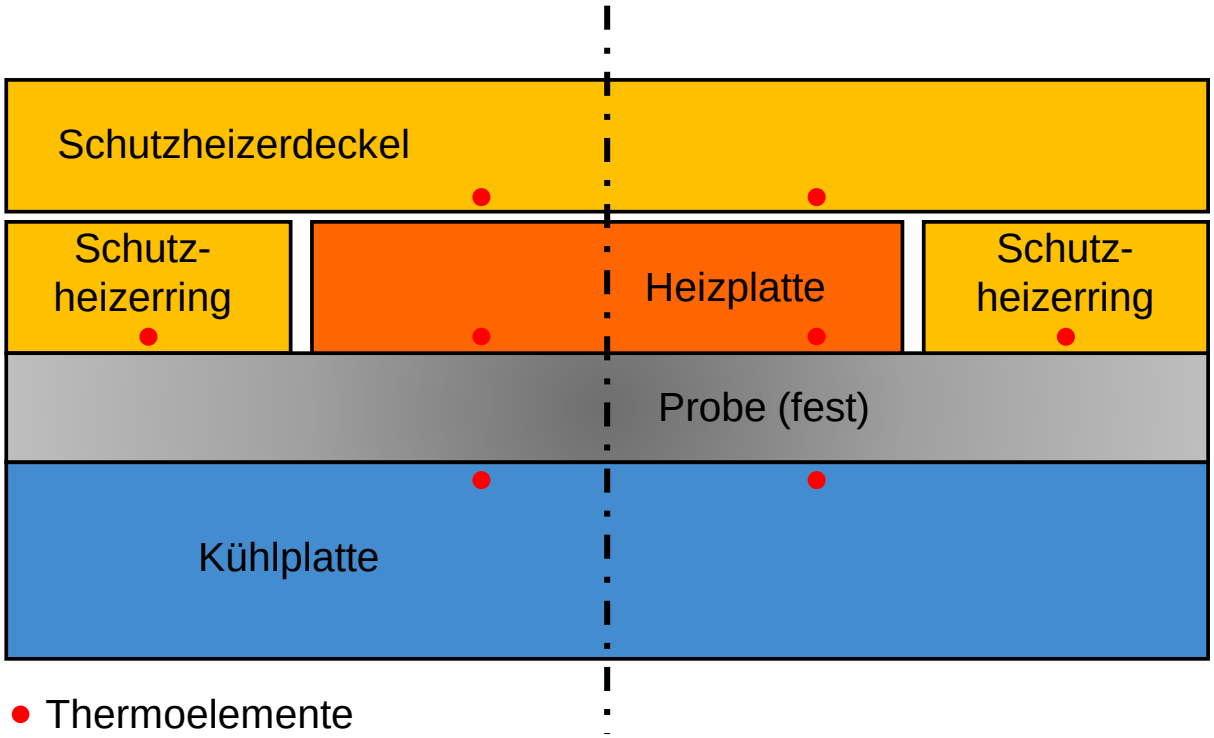

Abbildung 12: Messaufbau des hier entwickelten modifizierten Guarded-Hot-Plate-Verfahrens.

Die Probe wird zwischen einer Heiz- und einer Kühlplatte platziert. Die Kühlplatte wird mithilfe eines Temperierbads auf einer Temperatur von 5 °C gehalten und die Heizplatte wird mit elektrischen Heizelementen auf eine höhere Temperatur geregelt. Um eine Wärmeübertragung der Heizplatte an die Umgebung zu verhindern, wird um die Heizplatte ein Schutzheizerring und über der Heizplatte ein Schutzheizerdeckel platziert, die auf die gleiche Temperatur wie die Heizplatte geregelt werden. Durch den Temperaturgradienten zwischen der Heiz- und Kühlplatte stellt sich über die Heizerfläche A_{Heiz} ein gerichteter Wärmestrom durch die Probe ein.

Zur Minimierung der Lufteinschlüsse zwischen der Probe und der Heiz- und Kühlplatte wird jeweils eine Wärmeleitfolie ober- und unterhalb der Probe platziert. Der Wärmestrom $\dot{Q}$ durch die Probe entspricht der Leistung des elektrischen Heizelements P und kann mithilfe des Fourierschen Gesetzes beschrieben werden:

$$\dot{Q} = P = \frac{1}{\left[2 \cdot \left(\frac{s_f}{\lambda_f} + \frac{s_a}{\lambda_a}\right) + \frac{s}{\lambda}\right]} \cdot A_{Heiz} \cdot \Delta T \qquad (21)$$

Die Gleichung (21) kann nach der Wärmeleitfähigkeit der Probe λ umgestellt werden, siehe Gleichung (22).

$$\lambda = \frac{s}{\frac{\Delta T \cdot A}{P} - 2 \cdot \left(\frac{s_f}{\lambda_f} + \frac{s_a}{\lambda_a}\right)} \qquad (22)$$

Die durch die restlichen Lufteinschlüsse verursachte Luftschicht geht über ihre mittlere Stärke s_a und die Wärmeleitfähigkeit der Luft λ_a in die Gleichung ein. Die mittlere Stärke der Luftschicht wird in Kalibriermessungen ermittelt. Die Höhe der Probe s und der Wärmeleitfolie s_f können gemessen werden und die Wärmeleitfähigkeit der Folie λ_f ist bekannt.

Wie bereits beschrieben, waren vor dieser Untersuchung nur ungenaue Angaben zur Wärmeleitfähigkeit von festen Paraffinen bekannt. Lediglich für n-Hexadecan, n-Octadecan und n-Eicosan wurden von Vélez et al. [66] und Sasaguchi et al. [67] (teilweise auch von Sharma et al. [68]) die Wärmeleitfähigkeit von festen Paraffinen bestimmt. Die Werte von Vélez et al. und Sasaguchi et al. konnten durch die Untersuchungen in dieser Arbeit bestätigt und um die Wärmeleitfähigkeit von festem n-Docosan erweitert werden. Für die Wärmeleitfähigkeit von flüssigen Paraffinen ist bereits bekannt, dass die Wärmeleitfähigkeit mit steigender molekularer Kettenlänge zunimmt [69]. Daher sind die im Rahmen dieser Dissertation gemessenen Werte deutlich kohärenter als die Ergebnisse von Abhat [70], Li et al. (2013) [64], Li et al. (2014) [71], Sari et al. [63] und in Teilen Sharma et al. [68]. In Abbildung 13 sind die Ergebnisse dieser Untersuchung gezeigt.

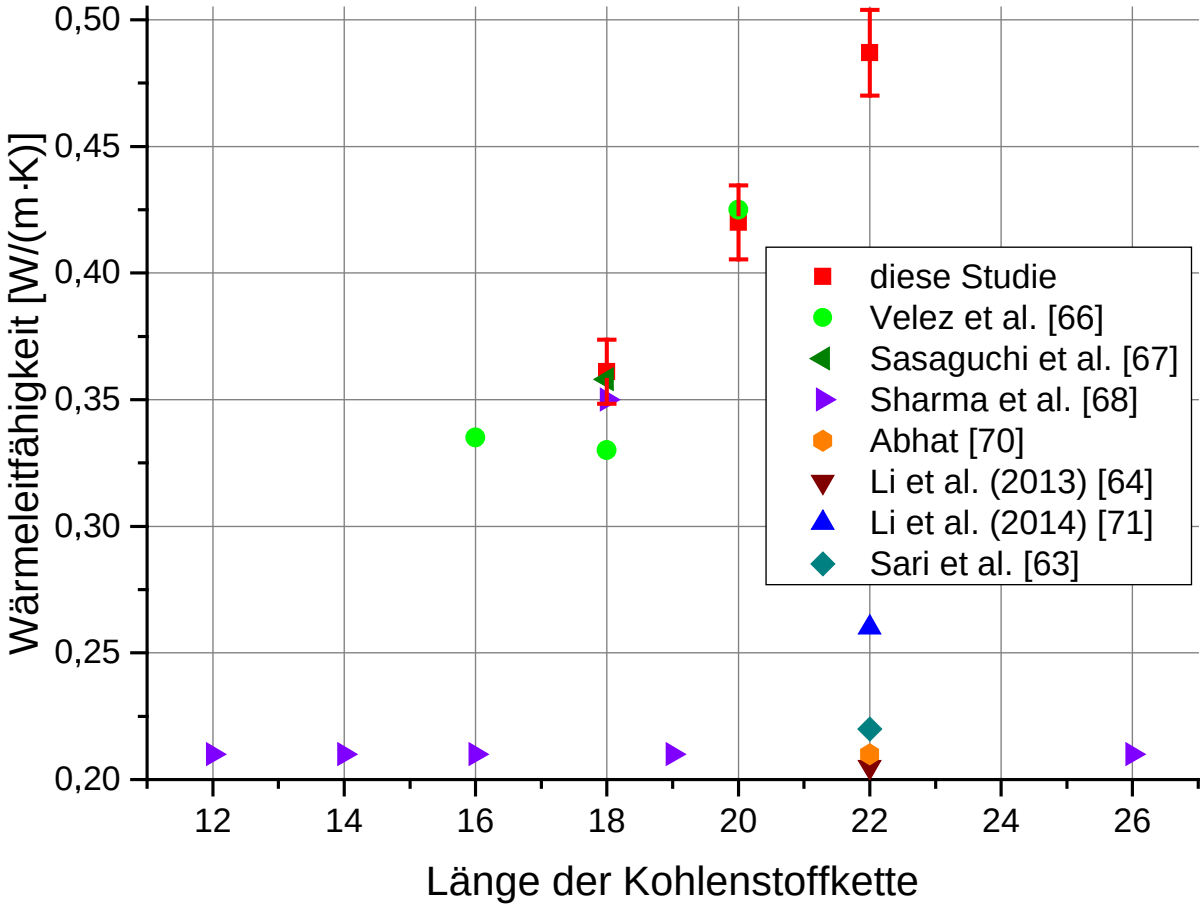

Abbildung 13: Vergleich der publizierten Daten für die Wärmeleitfähigkeit verschiedener Paraffine mit den Ergebnissen dieser Arbeit.

In Abbildung 14 ist der Einfluss des Massenanteils an Graphit und der verwendeten Graphitpartikelgrößen auf die Wärmeleitfähigkeit von n-Docosan-Compound gezeigt. Mit steigendem Massenanteil erhöht sich die Wärmeleitfähigkeit von 0,49 W/(m·K) auf bis zu 1,41 W/(m·K). Eine kugelförmige Partikelgröße von 200 und 600 µm stellte sich als optimal heraus. Bei kleineren Partikeln bilden sich nur unzureichende wärmeleitende Graphit-Mikrostrukturen im Compound aus. Das verwendete Graphit mit einer Partikelgröße von 1000 µm war eher stabförmig, wodurch sich ebenfalls keine ausreichenden Wärmebrücken ausbilden konnten. Im Vergleich zu früheren Untersuchungen von Sari et al. [63] und Li et al. (2013) [64] wurde eine deutlich höhere Wärmeleitfähigkeit des Compounds festgestellt, die wie zuvor beschrieben deutlich besser in das physikalische Gesamtbild passt.

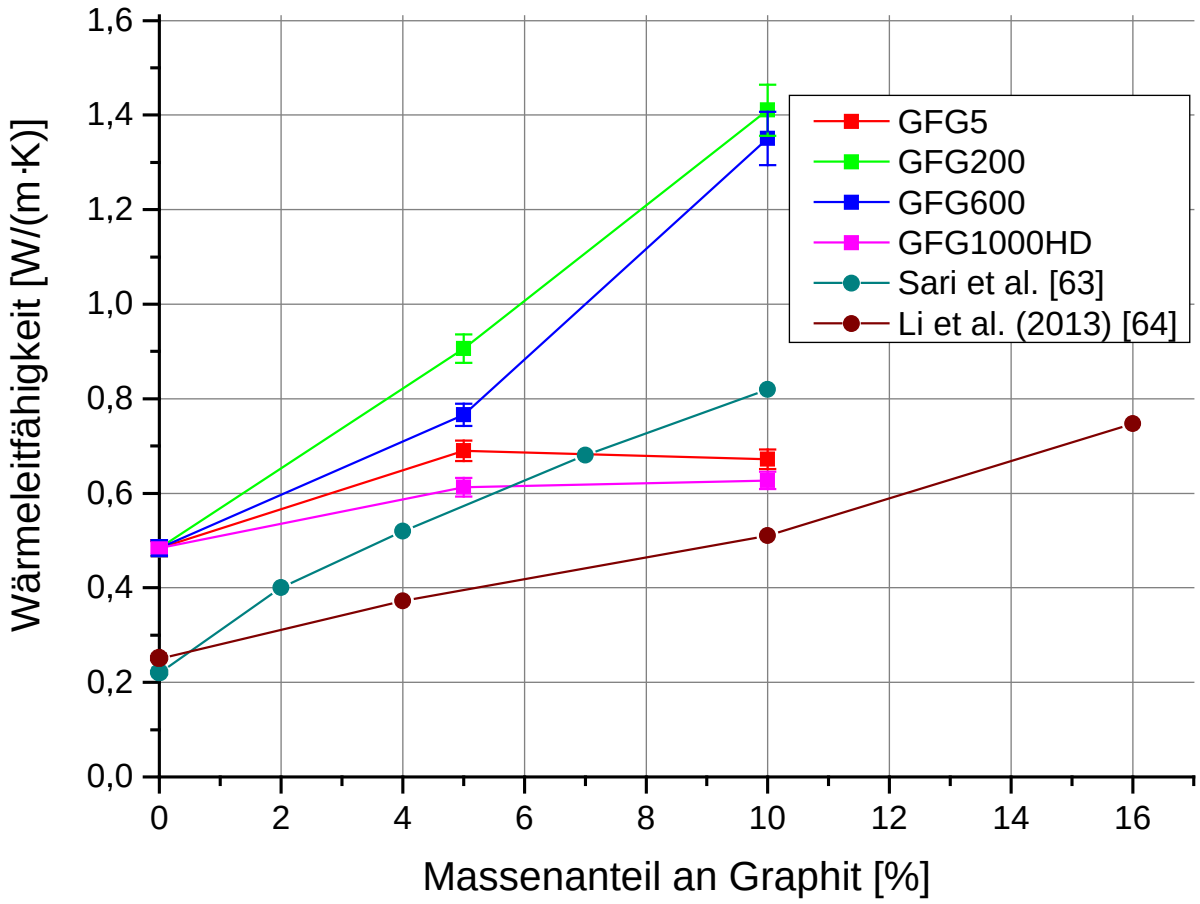

Abbildung 14: Wärmeleitfähigkeit von n-Docosan-Graphit-Compounds in Abhängigkeit von Partikelgröße und variierendem Graphitgehalt im Vergleich zu Literaturergebnissen.

4 Zusammenfassung

In dieser Dissertation wurde der alterungsbedingte Anstieg der Energieaufnahme von Haushaltskältegeräten (wie z.B. Kühlschränke, Gefriergeräte und deren Kombinationen) und dessen Ursachen untersucht. Darüber hinaus wurde der Einsatz von Phasenwechselmaterialien in Haushaltskältegeräten genauer betrachtet, sowie thermophysikalische Eigenschaften von PCM, insbesondere die Wärmeleitfähigkeit, untersucht. Mit den Erkenntnissen dieser Dissertation ist es nun möglich die Energieaufnahme von Haushaltskältegeräten besser zu prognostizieren. Dies ist sowohl auf Ebene der privaten Haushalte möglich, wo mit den vorliegenden Erkenntnissen der Austauschzeitpunkt der Geräte bestimmt werden kann. Auf Seiten der Hersteller von Haushaltskältegeräten und der Zulieferer der Teilsysteme ist mit den hier gewonnen Ergebnissen ein deutlich energieeffizienteres und alterungsbeständiges Design von Haushaltskältegeräten möglich. Prinzipiell könnte mit einem alterungsbeständigeren Design (18 %) und dem Einsatz von Phasenwechselmaterialien (17 %) die Energieaufnahme, bezogen auf die Betriebsdauer von Haushaltskältegeräten, um bis zu 35 % reduziert werden. Dies entspricht auf der volkswirtschaftlichen Ebene ca. 1,9 % des deutschen Nettostromverbrauchs der zukünftig eingespart werden könnte.

Mit den in dieser Dissertation gezeigten Ergebnissen konnte die Problematik des alterungsbedingten Anstiegs der Energieaufnahme nachgewiesen werden. Darüber hinaus ist es nun möglich, die Alterung in zukünftigen Überarbeitungen des EU-Energielabels zu berücksichtigen.

Im ersten Teil dieser Arbeit (Kap. 2) wurde zunächst das Alterungsverhalten von Haushaltskältegeräten analysiert. In diesem Zusammenhang konnte auf Grundlage von 100 einzelnen Messungen der Norm-Energieaufnahme an 32 Haushaltskältegeräten, die unter realen Bedingungen gealtert sind, ein Alterungsmodell entwickelt werden. Die Messdaten wurden über einen Zeitraum von 21 Jahren gewonnen. Dieses Modell beschreibt den durchschnittlichen Anstieg der Energieaufnahme über diesen Zeitraum. Der größte Anstieg der Energieaufnahme von +15,8 % erfolgt in den ersten fünf Betriebsjahren. Innerhalb der primären Einsatzzeit von 12 bis 13 Jahren steigt die Energieaufnahme um ca. +25 % und in der durchschnittlichen Gesamteinsatzzeit von 16 Jahren um +27 %. Für ältere Geräte kann ein weiterer Anstieg der Energieaufnahme vernachlässigt werden. Als Hauptursache für den Anstieg der Energieaufnahme stellte sich der im Gehäuse verbaute PUR-Schaum heraus. Durch die Konzentrationsunterschiede zwischen Zellgas und der Umgebung diffundiert das nach der Produktion des Schaums im Zellgas enthaltene Kohlenstoffdioxid aus den Zellen hinaus und Luft in die Zellen hinein. Da die Wärmeleitfähigkeit der Luft höher ist als die von Kohlenstoffdioxid, steigt die Wärmeleitfähigkeit des PUR-Schaums infolgedessen an. Dies wurde an PUR-Schaum-Proben untersucht, bei denen ein Anstieg der Wärmeleitfähigkeit von anfangs 19,5 mW/(m·K) um 33 % auf 26 mW/(m·K) innerhalb eines Zeitraums von drei Jahren festgestellt werden konnte. Ebenfalls wurde der Einfluss der Alterung der Verdichter untersucht. In Vergleichsmessungen von acht Verdichtern, die über einen Zeitraum von zwei Jahren in einem Haushaltskältegerät

betrieben wurden, konnte kein nennenswertes Alterungsverhalten festgestellt werden. Vielmehr steigt der COP der Verdichter aufgrund von eingelaufenen Ventilen und Lagern leicht an. Hierdurch reduziert sich theoretisch die Energieaufnahme leicht. Allerdings spielen sich diese Effekte innerhalb der laborüblichen Messfehler für die Energieaufnahmemessungen ab und sind daher kaum nachzuweisen.

Der Einsatz von Phasenwechselmaterialien in Haushaltskältegeräten (siehe Kap. 3) bietet in Bezug auf die Senkung der Energieaufnahme und der Steigerung der Funktionalität ein großes Entwicklungspotenzial. Als Phasenwechselmaterial haben Paraffine mehrere Vorteile, jedoch sind deren thermophysikalische Eigenschaften oft nur unzureichend bekannt. Im Rahmen dieser Dissertation wurde daher die Wärmeleitfähigkeit von Paraffinen in ihrer festen Phase näher untersucht. Hierbei wurde festgestellt, dass die in der Literatur veröffentlichten Werte zum größten Teil nicht korrekt sind. Die Wärmeleitfähigkeit von Paraffinen lässt sich durch Zugabe von Graphit erhöhen. Dabei haben sich eher kugelförmige Partikel mit einem Durchmesser von 200 bis 600 µm als optimal herausgestellt.

Der Einsatz von Paraffinen als Phasenwechselmaterial zur Steigerung der Funktionalität und zur Senkung der Energieaufnahme bietet weiterhin ein erhebliches Potential in Haushaltskältegeräten. Diese Ansätze werden in aktuellen Geräten jedoch noch kaum umgesetzt. Im Rahmen dieser Dissertation konnten daher weitere Anwendungsmöglichkeiten aufgezeigt und die Stoffdaten, wie z.B. die Wärmeleitfähigkeit, von Paraffinen detaillierter klassifiziert werden.

5 Literaturverzeichnis

[1] Statista, 2022. Entwicklung der Weltbevölkerungszahl von Christi Geburt bis zum Jahr 2021. URL: https://de.statista.com/statistik/daten/studie/1694/umfrage/entwicklung-der-weltbevoelkerungszahl/, Zuletzt aufgerufen 16.02.2023.

[2] Ternes, W., Täufel, A., Tunger, L., Zobel, M., 2005. Lebensmittel-Lexikon. B. Behr`s Verlag GmbH & Co. KG, Hamburg, ISBN: 3-89947-165-2.

[3] Krämer, J., 2002. Lebensmittel-Mikrobiologie. 4. Auflage, Verlag Eugen Ulmer GmbH & Co., Stuttgart, ISBN: 3-8252-1421-4.

[4] Organisation for Economic Cooperation and Development, OECD, 2003. COOL APPLIANCES: Policy Strategies for Energy Efficient Homes. URL: http://library.umac.mo/ebooks/b13623886.pdf, Zuletzt aufgerufen am 16.02.2023.

[5] Umwelt Bundesamt, 2022. Energieverbrauch privater Haushalte. URL: https://www.umweltbundesamt.de/daten/private-haushalte-konsum/wohnen/energieverbrauch-privater-haushalte#direkte-treibhausgas-emissionen-privater-haushalte-sinken, Zuletzt aufgerufen am 16.02.2023.

[6] Umwelt Bundesamt, 2022. Stromverbrauch. URL: https://www.umweltbundesamt.de/daten/energie/stromverbrauch, Zuletzt aufgerufen am 16.02.2023.

[7] Umwelt Bundesamt, 2020. Bilanz 2019: CO2-Emissionen pro Kilowattstunde Strom sinken weiter. URL: https://www.umweltbundesamt.de/presse/pressemitteilungen/bilanz-2019-co2-emissionen-pro-kilowattstunde-strom, Zuletzt aufgerufen am 16.02.2023.

[8] Statistisches Bundesamt, 2023. Ausstattung privater Haushalte mit elektrischen Haushalts- und sonstigen Geräten – Deutschland. URL: https://www.destatis.de/DE/Themen/Gesellschaft-Umwelt/Einkommen-Konsum-Lebensbedingungen/Ausstattung-Gebrauchsgueter/Tabellen/liste-haushaltsgeraete-d.html;jsessionid=3DAEC628A118E9B1A8CACAE97FE0AC09.internet8732, Zuletzt aufgerufen am 16.02.2023.

[9] BUNDESMINISTERIUM FÜR WIRTSCHAFT UND ENERGIE, 2020. Alle Tarife mengengewichteter Elektrizitätspreis für Haushaltskunden. URL: https://www.bmwi.de/Redaktion/DE/Infografiken/Energie/strompreisbestandteile.html, Zuletzt aufgerufen am 16.02.2023.

[10] Van Holsteijn en Kemna B.V (VHK)., Association pour la Recherche et le Développement des Méthodes et Processus Industriels (ARMINES), 2016. Commission Regulation (EC) No. 643/2009 with regard to ecodesign requirements for household refrigeration appliances and Commission Delegated Regulation (EU) No. 1060/2010 with regard to energy labelling of household refrigeration appliances, FINAL REPORT.

[11] Europäische Gemeinschaft, 1994. Richtlinie 94/2/EG der Kommission vom 21. Januar 1994 zur Durchführung der Richtlinie 92/75/EWG betreffend die Energieetikettierung für elektrische Haushaltskühl- und –Gefriergeräte sowie entsprechende Kombinationsgeräte. Amtsblatt der Europäischen Gemeinschaft, Nr. L 45/1.

[12] Europäischen Union, 2003. Richtlinie 2003/66/EG der Kommission vom 3. Juli 2003 zur Änderung der Richtlinie 94/2/EG zur Durchführung der Richtlinie 92/75/EWG des Rates betreffend die Energieetikettierung für elektrische Haushaltskühl- und -gefriergeräte sowie entsprechende Kombinationsgeräte. Amtsblatt der Europäischen Union, L 170/10.

[13] Europäischen Union, 2010. Deligierte Verordnung (EU) Nr. 1060/2010 der Kommission vom 28. September 2010 zur Ergänzung der Richtlinie 2010/30/EU des Europäischen Parlaments und des Rates im Hinblick auf die Kennzeichnung von Haushaltskühlgeräten in Bezug auf den Energieverbrauch. Amtsblatt der Europäischen Union, L 314/17.

[14] Europäischen Union, 2019. Deligierte Verordnung (EU) 2019/2016 der Kommission vom 11. März 2019 zur Ergänzung der Verordnung (EU) 2017/1369 des Europäischen Parlaments und des Rates im Hinblick auf die Energieverbrauchskennzeichnung von Kühlgeräten und zur Aufhebung der Delegierten Verordnung (EU) Nr. 1060/2010 der Kommission. Amtsblatt der Europäischen Union, L 315/102.

[15] Michel, A., 2015. Household refrigeration: What is the good EEI formula?. URL: https://ecodesign-fridges.eu/sites/ecodesign-fridges.eu/files/Topten_input_HH-cold_stakeholder_meeting.pdf. Zuletzt aufgerufen am 15.02.2023.

[16] Siderius, H.-P., 2015. NL comments on the Interim report “Ecodesign & Labelling Review Household Regriferation”. URL: https://ecodesign-fridges.eu/sites/ecodesign-fridges.eu/files/NL%20-%20Comments%20interim%20report%20-%20draft%20150715.pdf. Zuletzt aufgerufen am 15.02.2023.

[17] Michel, A., Attali, S., Bush, E., 2015. Energy efficiency of White Goods in Europe: monitoring the market with sales data. URL: https://ecodesign-fridges.eu/sites/ecodesign-fridges.eu/files/TOPTEN%20Latest%20market%20analysis%20whitegoods%20(excl%20freezers)%203%20June.pdf. Zuletzt aufgerufen am 15.02.2023.

[18] Van Holsteijn en Kemna BV, 2015. Minutes of the 1st Stakeholder meeting Ecodesign & Labelling Review household refrigeration appliances. URL: https://ecodesign-fridges.eu/sites/ecodesign-fridges.eu/files/Final%20Minutes%20of%20the%201st%20Stakeholder%20meeting%2001072015.pdf. Zuletzt aufgerufen am 15.02.2023.

[19] Normausschuss Kältetechnik (FNKÄ) im DIN, 2006. DIN EN ISO 15502:2006. Haushalt-Kühl-/Gefriergeräte. Eigenschaften und Prüfverfahren (ISO 15502:2005); Deutsche Fassung EN ISO 15502:2005.

[20] Normausschuss Kältetechnik (FNKÄ) im DIN, 2013. DIN EN 62552:2013. Haushalt-Kühl-/Gefriergeräte. Eigenschaften und Prüfverfahren (IEC 62552:2007, modifiziert + corrigendum Mar. 2008); Deutsche Fassung EN 62552:2013.

[21] Europäischen Union, 2009. Verordnung (EG) Nr. 643/2009 der Kommission vom 22. Juli 2009 zur Durchführung der Richtlinie 2005/32/EG des Europäischen Parlaments und des Rates im Hinblick auf die Festlegung von Anforderungen an die umweltgerechte Gestaltung von Haushaltskühlgeräten. Amtsblatt der Europäischen Union, L 191/53.

[22] Europäischen Union, 2019. Europäischen Union, 2019. Verordnung (EU) 2019/2019 der Kommission vom 1. Oktober 2019 zur Festlegung von Ökodesign-Anforderungen an Kühlgeräte gemäß der Richtlinie 2009/125/EG des Europäischen Parlaments und des Rates und zur Aufhebung der Verordnung (EG) Nr. 643/2009 der Kommission. Amtsblatt der Europäischen Union, L 315/187.

[23] Normausschuss Kältetechnik (FNKÄ) im DIN, 2006. DIN EN 153:2006. Verfahren zur Messung der Aufnahme elektrischer Energie und damit zusammenhängender Eigenschaften für netzbetriebene Haushalt-Kühlgeräte, -Tiefkühlgeräte, -Gefriergeräte und deren Kombinationen; Deutsche Fassung EN 153:2006.

[24] IEC 62552:2015, 2015. IEC 62552-1:2015 Household Refrigerating Appliances – Characteristics and Test Methods – Part 1: General requirements. International Electrotechnical Commission (IEC).

[25] IEC 62552:2015, 2015. IEC 62552-2:2015 Household Refrigerating Appliances – Characteristics and Test Methods – Part 2: Performance requirements. International Electrotechnical Commission (IEC).

[26] IEC 62552:2015, 2015. IEC 62552-3:2015 Household Refrigerating Appliances – Characteristics and Test Methods – Part 3: Energy consumption and volumes. International Electrotechnical Commission (IEC).

[27] Australian Consumers' Association, 1990. Energy Consumption of Refrigerators and Freezers Used Under Normal Conditions of Use. Choice, Sydney, Australia.

[28] Elsner, A., Müller, M., Paul, A., Vrabec, J., 2013. Zunahme des Stromverbrauchs von Haushaltskältegeräten durch Alterung. Deutsche Kälte-Klima Tagung 40, Hannover, Germany, November 20-22.

[29] Stiftung Warentest, 1994. Umwelt geschont – Strom gespart. test 1994, Nr. 3, p. 36-39.

[30] Stiftung Warentest, 1994. Auch ohne Ozonkiller. test 1994, Nr. 6, p. 24-25.

[31] Kloos, K. H., Broszeit, E.; Hess, F. J., 1978. Tribologische Wirkung von Kältemitteln. Materialwissenschaft und Werkstofftechnik 9, 445-451.

[32] Garland, N. P., Hadfield, M., 2005. Environmental implications of hydrocarbon refrigerants applied to the hermetic compressor. Material and Design 26, 578-586.

[33] DIN-Normenausschuss Kältetechnik (FNKä), 2017. DIN EN 13771-1:2017. Compressors and condensing units for refrigeration – Performance testing and test methods – Part 1: Refrigerant compressors. German version EN 13771-1:2017.

[34] Paul, A., Baumhoegger, E., Elsner, A., Moczarski, L., Reineke, M., Sonnenrein, G., Hueppe, C., Stamminger, R., Hoelscher, H., Wagner, H., Gries, U., Freiberger, A., Becker, W., Vrabec, J., 2021. Determining the heat flow through the cabinet walls of household refrigerating appliances. International Journal of Refrigeration 121, 235–242.

[35] Wagner, K-E., 2002. Simulation und Optimierung des Wärmedämmvermögens von PUR Hartschaum, Wärme- und Stofftransport sowie mechanische Verformung, Dissertation, Stuttgart (Germany): http://dx.doi.org/10.18419/opus-1579.

[36] Engels, H.-W., Pirkl, H.-G., Albers, R., Albach, R. W., Krause, J., Hoffmann, A., Casselmann, H., Dormish, J., 2013. Polyurethane: vielseitige Materialien und nachhaltige Problemlöser für aktuelle Anforderungen. Angewandte Chemie 125, 9596-9616.

[37] Tucker, B. W., 1992. Rigid polyurethane foams with low thermal conductivities, patent document, US005169877A, PCT, 08.12.1992.

[38] Berardi, U., Madzarevic, J., 2020. Microstructural analysis and blowing agent concentration in aged polyurethane and polyisocyanurate foams. Applied Thermal Engineering 164, 114440.

[39] Wilkes K. E., Yarbrough D. W., Weaver F. J., 1997. Aging of polyurethane foam insulation in simulated refrigerator walls. International Conference on Ozone Protection Technologies, Baltimore Maryland, November 12-13.

[40] Wilkes K. E., Gabbard, W. A., Weaver, F. J., 1999. Aging of polyurethane foam insulation in simulated refrigerator panels: One-year results with third-generation blowing agents. The Earth Technologies Forum, Washington D.C., September 27-29.

[41] Wilkes K. E., Gabbard, W. A., Weaver, F. J., Booth, J. R., 2001. Aging of polyurethane foam insulation in simulated refrigerator panels: Two-year results with third-generation blowing agents. Journal of Cellular Plastics 37, 400-428.

[42] Wilkes, K. E., Yarbrough, D. W., Gabbard, W. A., Nelson, G. E., Booth, J. R., 2002. Aging of polyurethane foam insulation in simulated refrigerator panels: Three-year results with third-generation blowing agents. Journal of Cellular Plastics 38, 317-339.

[43] Wilkes, K. E., Yarbrough, D. W., Nelson, G. E., Booth, J. R., 2003. Aging of polyurethane foam insulation in simulated refrigerator panels: Four-year results with third-generation blowing agents. The Earth Technologies Forum, Washington D.C., April 22-24.

[44] Paul, A., Baumhögger, E., Elsner, A., Reineke, M., Sonnenrein, G., Hueppe, C., Stamminger, R., Hoelscher, H., Wagner, H., Gries, U., Becker, W., Vrabec, J., 2022. Impact of aging on the energy efficiency of household refrigerating appliances. Applied Thermal Engineering 205, 117992.

[45] Zhang, H., Fang, W.-Z., Li, Y.-M., Tao, W.-Q., 2017. Experimental study of the thermal conductivity of polyurethane foams. Applied Thermal Engineering 115, 528–538.

[46] Lassue, S., Guths, S., Leclercq, D., Duthoit, B., 1993. Contribution to the experimental study of natural convection by heat flux measurement an anemometry using thermoelectric effects. Experimental Heat Transfer, Fluid Mechanics and Thermodynamics 1993, 831-838.

[47] Melo, C., da Selva, L. W., Pereira, R. H., 2000. Experimental evaluation of the heat transfer through the walls of household refrigerators. Eighth International Refrigeration Conference at Purdue University, West Lafayette, IN, USA, July 25-28, 353-360.

[48] Thiessen, S., Knabben, F. T., Melop, C., 2014. Experimental evaluation of the heat fluxes through the walls of a domestic refrigerator. 15th Brazilian Congress of Thermal Sciences an Engineering, Belem, PA, Brazil, November 10-13.

[49] Stovall, T., 2012. Closed Cell Foam Insulation: A review of long term thermal performance, Oak Ridge National Laboratory report ORNL/TM-2012/583.

[50] Lieghton, D. L., 2011. Investigation of household refrigerator with alternative low global warming potential refrigerants. Master thesis, University of Maryland, USA.

[51] Sim, J. S., Ha, J. S., 2011. Experimental study of heat transfer characteristics for a refrigerator by using reverse heat loss method. International Communications in Heat and Mass Transfer 38, 572-576.

[52] Hermes, C., Melo, C., Knabben. F., 2013. Alternative test method to assess the energy performance of frost-free refrigerating appliances. Applied Thermal Engineering 50, 1029-1034.

[53] Hueppe, C., Geppert, J., Stamminger, R., Wagner, H., Hoelscher, H., Vrabec, J., Paul, A., Elsner, A., Becker, W., Gries, U., Freiberger, A., 2020. Age-related efficiency loss of household refrigeration appliances: Development of an approach to measure the degradation of insulation properties. Applied Thermal Engineering 173, 115113.

[54] Johnson, R. W., 2000. The effect of blowing agent on refrigerator/-freezer TEWI. Polyurethanes conference, Boston, MA, October 8–11.

[55] Johnson, R. W., 2004. The effect of blowing agent choice on energy use and global warming impact of a refrigerator. International Journal of Refrigeration 27, 794-799.

[56] Hueppe, C., Geppert, J., Moenninghoff-Juessen, J., Wolff. L., Stamminger, R., Paul, A., Elsner, A., Vrabec, J., Wagner, H., Hoelscher, H., Becker, W., Gries, U., Freiberger, A., 2021. Investigating the real life energy consumption of refrigeration appliances in Germany: Dynamic modelling of consumer behaviour. Energy Policy, 155, 112275.

[57] Sonnenrein, G., Elsner, A., Baumhögger, E., Morbach, A., Fieback, K., Vrabec, J., 2015. Reducing the power consumption of household refrigerators through the integration of latent heat storage elements in wire-and-tube condensers. International Journal of Refrigeration 51, 154-160.

[58] Sonnenrein, G., Baumhögger, E., Elsner, A., Fieback, K., Morbach, A., Paul, A., Vrabec, J., 2015. Copolymer-bound phase change materials for household refrigerating appliances: experimental investigation of power consumption, temperature distribution and demand side management potential. International Journal of Refrigeration 60, 166-173.

[59] Azzouz, K., Leducq, D., Gobin, D., 2008. Performance enhancement of a household refrigerator by addition of latent heat storage. International Journal of Refrigeration 31, 892–901.

[60] Azzouz, K., Leducq, D., Gobin, D., 2009. Enhancing the performance of household refrigerators with latent heat storage: an experimental investigation. International Journal of Refrigeration 32, 1634–1644.

[61] Sonnenrein, G., Baumhögger, E., Elsner, A., Morbach, A., Neukötter, M., Paul, A., Vrabec, J., 2020. Improving the performance of household refrigerating appliances through the integration of phase change materials in the context of the new global refrigerator standard IEC 62552:2015. International Journal of Refrigeration 119, 448-456.

[62] Mehling, H., Cabeza, L. F., 2008. Heat and cold storage with PCM: An up to date introduction into basics and applications. Springer. Berlin, Heidelberg. ISBN 978-3-540-68557-9.

[63] Sari, A., Karaipekli, A., 2007. Thermal conductivity and latent heat thermal energy storage characteristics of paraffin/expanded graphite composite as phase change material. Applied Thermal Engineering 27, 1271-1277.

[64] Li, M., Wu, Z., 2013. Thermal properties of the graphite/n-docosane composite PCM. Journal of Thermal Analysis and Calorimetry 111, 77-83.

[65] Paul, A., Baumhögger, E., Dewerth, M. O., Elsner, A., Dindar, I. H., Sonnenrein, G., Vrabec, J., 2023. Thermal conductivity of solid paraffins and several n-docosane compounds with graphite. Journal of Thermal Analysis and Calorimetry.

[66] Vélez, C., Khayet, M., Ortiz de Zárate, J. M., 2015. Temperature dependent thermal properties of solid/liquid phase change even-numbered n-alkanes: n-Hexadecane, n-octadecane and n-eicosane. Applied Energy 143, 383-394.

[67] Sasaguchi, K., Viskanta, R., 1989. Phase Change Heat Transfer during melting and solidification of melt around cylindrical heat source(s)/sink(s). Journal of Energy Resources Technology 111, 43-49.

[68] Sharma, S. D., Sagara, K., 2005. Latent Heat Storage Materials and Systems: A Review. International Journal of Green Energy 2, 1-56.

[69] Poling, B. E., Prausnitz, J. M., O´Connell, J. P., 2001. The properties of gases and liquids. McGraw-Hill. New York. ISBN 0 07 149999 7.

[70] Abhat, A., 1983. Low Temperature Latent Heat Thermal Energy Storage: Heat Storage Materials. Solar Energy 30, 313 332.

[71] Li, J. F., Lu, W., Zeng, Y. B., Luo, Z. P., 2014. Simultaneous enhancement of latent heat and thermal conductivity of docosane-based phase change material in the presence of spongy graphene. Solar Energy Materials & Solar Cells 128, 48-51.

6 Wissenschaftliche Publikationen

Publikationen, die im Rahmen der vorliegenden Dissertation angefertigt wurden:

1. Paul, A., Baumhögger, E., Elsner, A., Reineke, M., Sonnenrein, G., Hueppe, C., Stamminger, R., Hoelscher, H., Wagner, H., Gries, U., Becker, W., Vrabec J., 2022. Impact of aging on the energy efficiency of household refrigerating appliances. Applied Thermal Engineering, 205, 117992.

2. Hueppe, C., Geppert, J., Moenninghoff-Juessen, J., Wolff. L., Stamminger, R., Paul, A., Elsner, A., Vrabec, J., Wagner, H., Hoelscher, H., Becker, W., Gries, U., Freiberger, A., 2021. Investigating the real life energy consumption of refrigeration appliances in Germany: Dynamic modelling of consumer behaviour. Energy Policy 155, 112275.

3. Paul, A., Baumhögger, E., Elsner, A., Moczarski, L., Reineke, M., Sonnenrein, G., Hueppe, C., Stamminger, R., Hoelscher, H., Wagner, H., Gries, U., Freiberger, A., Becker, W., Vrabec, J., 2021. Determining the heat flow through the cabinet walls of household refrigerating appliances. International Journal of Refrigeration 121, 235-242.

4. Hueppe, C., Geppert, J., Stamminger, R., Wagner, H., Hoelscher, H., Vrabec, J., Paul, A., Elsner, A., Becker, W., Gries, U., Freiberger, A., 2020. Age-related efficiency loss of household refrigeration appliances: Development of an approach to measure the degradation of insulation properties. Applied Thermal Engineering 173, 115113.

5. Paul, A., Baumhögger, E., Dewerth, M. O., Elsner, A., Dindar, I. H., Sonnenrein, G., Vrabec, J., 2023. Thermal conductivity of solid paraffins and several n-docosane compounds with graphite. Journal of Thermal Analysis and Calorimetry 148, 5687-5694. DOI: https://doi.org/10.1007/s10973-023-12107-2.

6. Sonnenrein, G., Baumhögger, E., Elsner, A., Neukötter, M., Paul, A., Vrabec, J., 2020. Improving the performance of household refrigerating appliances through the integration of phase change materials in the context of the new global refrigerator standard IEC 62552:2015. International Journal of Refrigeration 119, 448-456.

6.1 Impact of aging on the energy efficiency of household refrigerating appliances

Paul, A., Baumhögger, E., Elsner, A., Reineke, M., Sonnenrein, G., Hueppe, C., Stamminger, R., Hoelscher, H., Wagner, H., Gries, U., Becker, W., Vrabec, J., 2022. Applied Thermal Engineering 205, 117992.

In dieser Studie wurde der alterungsbedingte Anstieg der Energieaufnahme von Haushaltskältegeräten und die Ursachen für diesen Anstieg untersucht. Hierfür wurden 100 Messungen der Norm-Energieaufnahme an 32 Haushaltskältegeräten verschiedener Bauart durchgeführt. Aus den Ergebnissen dieser Messungen wurde ein Alterungsmodell entwickelt. Dieses ist das erste Modell, welches auf Messdaten der Energieaufnahme real gealterter Geräte beruht. Frühere Alterungsmodelle wurden lediglich an das Alterungsverhalten einzelner Systemkomponenten angepasst. Innerhalb der ersten fünf Jahre steigt die Energieaufnahme im Mittel um 15,8 % an und bei einem Gerätealter von 16 Jahre liegt der Anstieg bei 27 %. Als Hauptursache für diesen Alterungseffekt stellte sich der im Gehäuse verbaute Polyurethan-Hartschaum heraus, dessen Wärmeleitfähigkeit aufgrund von Diffusionsvorgängen über einen Zeitraum von drei Jahren um 26 % ansteigt. Eine Alterung der Verdichter konnte nicht festgestellt werden.

Der Autor dieser Dissertation hat die vorliegende Publikation verfasst, die Versuchsaufbauten ausgearbeitet, die Versuche durchgeführt und ausgewertet. Andreas Elsner, Gerrit Sonnenrein und Michael Reineke haben bei der Durchführung der Versuche unterstützt. Bei der Mess- und Regelungstechnik für die Versuchsdurchführung wirkten Andreas Elsner und Elmar Baumhögger mit. Ein Teil der Haushaltskältegeräte wurde durch Wolfgang Becker von der BSH Hausgeräte GmbH bereitgestellt. Heike Hölscher und Hendrik Wagner haben die Messungen zur Wärmeleitfähigkeit des Polyurethan-Hartschaums und Ulrich Gries hat die Messungen der COP-Werte der Verdichter durchgeführt. Christian Hüppe und Rainer Stamminger unterstützten die Arbeiten zu dieser Publikation im Rahmen des durch das BMWi geförderten Projekts ALGE. An der Überarbeitung des Manuskripts waren Andreas Elsner und Jadran Vrabec beteiligt. Während der gesamten Arbeit wurde der Autor von Jadran Vrabec betreut.

Applied Thermal Engineering 205 (2022) 117992

Contents lists available at ScienceDirect

Applied Thermal Engineering

journal homepage: www.elsevier.com/locate/apthermeng

Impact of aging on the energy efficiency of household refrigerating appliances

Andreas Paul [a], Elmar Baumhögger [a], Andreas Elsner [a], Michael Reineke [a], Christian Hueppe [b], Rainer Stamminger [b], Heike Hoelscher [c], Hendrik Wagner [c], Ulrich Gries [d], Wolfgang Becker [e], Jadran Vrabec [f,*]

[a] Thermodynamics and Energy Technology, University of Paderborn, Warburger Str. 100, 33098 Paderborn, Germany
[b] University of Bonn, Institute of Agricultural Engineering – Section Household and Appliance Engineering, Nussallee 5, 53115 Bonn, Germany
[c] BASF Polyurethanes GmbH, Elastogranstr. 60, 49448 Lemförde, Germany
[d] Secop GmbH, Mads-Clausen-Str. 7, 24939 Flensburg, Germany
[e] BSH Home Appliances GmbH, Robert-Bosch-Str. 100, 89537 Giengen an der Brenz, Germany
[f] Thermodynamics and Process Engineering, Technische Universität Berlin, Ernst-Reuter-Platz 1, 10587 Berlin, Germany

ARTICLE INFO

Keywords:
Household refrigerating appliances
Energy efficiency
Aging
Electrical energy consumption

ABSTRACT

The parameters required to calculate the energy efficiency of household refrigerating appliances (i.e. refrigerators, freezers and their combinations) are determined by standard measurements. According to regulations, these measurements are carried out when the appliances are new. It is known from previous studies that various technical aging mechanisms can increase electrical energy consumption by up to 36% over a product lifespan of 18 years. In order to determine the time dependence of the energy consumption of household refrigerating appliances, repeated measurements are carried out in this work. Eleven new appliances are examined under standard measurement conditions. After just two years of operation, an additional energy consumption of up to 11% is determined. Furthermore, 21 older appliances that had previously been measured in new condition are tested again after up to 21 years of operation. For these older appliances, an average increase of energy consumption of 28% is found. For individual appliances, the maximum increase is 36%. An aging model is developed on the basis of these measurement results, which may help to predict the aging-related increase of energy consumption of household refrigerating appliances. This model shows an average increase in energy consumption of 27% for an appliance age of 16 years. Supplemental performance tests of eight compressors do not show any significant aging effects related to these devices after two years of operation. Furthermore, measurements of the thermal conductivity of aged polyurethane foam test samples are carried out and an increase of its thermal conductivity of 26% over a period of about three years is determined.

1. Introduction

The electrical energy consumption of household refrigerating appliances (i.e. refrigerators, freezers and their combinations) has continuously decreased since the 1990s [1]. Although it is relatively small for individual household refrigerating appliances, the entire fleet makes up a large proportion of the total electrical energy consumption because of the almost complete market penetration and year-round operation of these appliances. The launch of the EU energy label in 1994 accelerated this process further. With this label, it is possible for the customer to assess the energy efficiency of an appliance in relation to its energy consumption and the usable storage volume. On average, 13.4% of the electrical energy consumption of private households in the OECD member states is caused by cooling and freezing food [2]. In Germany, this share was even 22.4% in 2018 (cf. Fig. 1), which corresponds to 5.4% of the total national electrical energy consumption [3-5].

Like all technical systems, household refrigerating appliances are subject to aging. Since the failure of individual components can lead to the failure of the entire system, individual components, such as compressor [6] or door hinges [7], are subjected to defined tests in order to predict their failure probability and thus ultimately the reliability of the refrigerating appliance. The typical contributions of the individual components to the total electrical energy consumption of household refrigerating appliances are described in the ASHRAE handbook as listed in Table 1 [8].

* Corresponding author.

https://doi.org/10.1016/j.applthermaleng.2021.117992
Received 29 July 2021; Received in revised form 13 December 2021; Accepted 20 December 2021
Available online 30 December 2021

Nomenclature

a	Normalized energy consumption offset of the aging function
A	Surface (m^2)
A_a	Outer surface (m^2)
A_i	Inner surface (m^2)
A_{HIPS}	Average surface of the HIPS inner liner (m^2)
A_{PUR}	Average surface of the PUR foam (m^2)
A_{st}	Average surface of the steel case (m^2)
b	Time correction factor (a)
COP	Coefficient of performance
dE_i	Difference between the measured electrical energy consumption of two individual measurements (kWh/d)
d_{HIPS}	Material thickness of the HIPS inner liner (mm)
d_{PUR}	Material thickness of the PUR foam (mm)
d_{st}	Material thickness of the steel case (mm)
dT_i	Difference between the measured storage temperatures of two individual measurements (K)
E	Electrical energy consumption (kWh/d)
$E(\tau)$	Electrical energy consumption at the time τ (kWh/d)
E_0	Electrical energy consumption at the first measurement (kWh/d)
E_P	Corrected electrical energy consumption immediately after production (kWh/d)
g	Parameter of the aging model
k	Heat transfer coefficient ($W/(m^2 \cdot K)$)
$k{\cdot}A$	$k{\cdot}A$ value (W/K)
P	Mechanical drive power (W)
P_{el}	Electrical drive power (W)
P_{ecs}	Power of the electrical control system (W)
$\dot{Q}_0$	Heat flow in the evaporator (W)
$\dot{Q}_{cab}$	Heat flow into the cabinet (W)
r	Initial aging rate of the blowing agent (%)
x	Correction factor
α_a	Outer heat transfer coefficient ($W/(m^2 \cdot K)$)
α_i	Inner heat transfer coefficient ($W/(m^2 \cdot K)$)
δE	Total uncertainty of the energy measurement (%)
δE_e	Uncertainty of the energy measurement system (%)
δE_t	Contribution of the temperature measurement uncertainty to the energy measurement uncertainty (%)
δT_t	Temperature measurement uncertainty (K)
Δe_{ir}	Annual increase rate of electrical energy consumption (%)
ΔCOP	Improvement of the COP (%)
ΔE	Increase of the electrical energy consumption
$\Delta E_0(\tau)$	Preliminary aging model
$\Delta E_p(\tau)$	Aging model
ΔT	Temperature difference (K)
η_m	Motor efficiency (%)
λ	Thermal conductivity ($W/(m \cdot K)$)
λ_{HIPS}	Thermal conductivity of HIPS ($W/(m \cdot K)$)
λ_{PUR}	Thermal conductivity of PUR foam ($W/(m \cdot K)$)
λ_{st}	Thermal conductivity of steel ($W/(m \cdot K)$)
τ	Time (a)
τ_c	Time of an operating cycle (h)
Indices	
0	Related to the electrical energy consumption during the first measurement
p	Related to the electrical energy consumption immediately after production

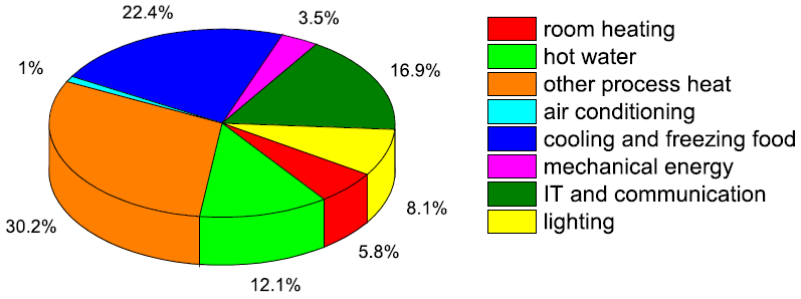

Fig. 1. Distribution of the electrical energy consumption in private households in Germany [4].

Table 1
Typical contributions of the system components to the total electrical energy consumption of household refrigerating appliances [8].

System component	Proportion of energy consumption
fan motor	2–10%
external heater	0–6%
defrost heater	4–10%
wall insulation	45–55%
door gasket region	25–30%

In 1990, the Australian Consumers' Association investigated energy consumption data of household refrigerating appliances over a period of one year and did not find any increase due to aging [9]. In contrast, comparative studies with respect to CFC-free appliances by Elsner et al. from 2012 showed an increase of energy consumption of 25–36% over a period of 18 years. The examined appliances were among the first CFC-free household refrigerating appliances to hit the market in 1994 and 1995, respectively [10-12].

A study commissioned as part of the development of the EU energy label regulation of 2019 mentions the insulation foam material, door gaskets, interior elements and compressor as primary causes for aging and assumes that aging could lead to an increase of energy consumption of 10% over an estimated average operating time of 16 years, consisting of a primary operating period of 12–13 years and a secondary operating period of 3–4 years (e.g. in a garage) [13].

In his dissertation, Harrington examined the influence of various parameters on energy consumption. This includes the influence of temperature and humidity in the storage compartment, ambient temperature, evaporator defrosting, door openings, the general choice of the model and the influence of consumer behavior. However, he did not

consider ageing of the product [14].

Based on a consumer survey with 706 participants, Hueppe et al. investigated the influence of consumer behavior on energy consumption in Germany. The study showed that 32.5% of the energy consumption was influenced by consumer behavior, e.g. door openings or choice of the installation site [15].

Technical properties of household refrigerating appliances, such as the energy consumption, are determined according to standards under laboratory conditions with a focus on comparability and reproducibility. Energy consumption measurements are carried out at standardized ambient temperatures mostly without user influence [7,16-21] or with only little [22]. The ambient temperatures during these measurements are higher than the average room temperature in a kitchen. A study by Moretti in 2000 has shown that the impact of user influence on energy consumption can be compensated by a higher ambient temperature during standard measurements [23]. The real energy consumption in a household depends very much on the individual user [15], which can vary greatly from household to household [14].

Household refrigerating appliances essentially consist of a compression refrigeration cycle and an insulated cabinet. With respect to energy consumption, this demands a refrigeration cycle that is as energy-efficient as possible and the lowest possible heat flow entering the cabinet through the walls and the door gaskets. Consequently, the components which influence the energy consumption most need to be investigated with respect to changes over lifetime.

1.1. Theoretical calculation of energy consumption

The change of the electrical energy consumption of real household refrigerating appliances can be deduced from the change of the thermal conductivity of the polyurethane (PUR) foam. The energy consumption E of a household refrigerating appliance can be calculated by integrating the mechanical drive power $P(\tau_c)$ and the power of the electrical control system $P_{ecs}(\tau_c)$ over the time of an operating cycle:

$$E = \int \frac{P(\tau_c)}{\eta_m} d\tau_c + \int P_{ecs}(\tau_c) d\tau_c \tag{1}$$

In the case of mechanical drive power, the motor efficiency factor η_m must be considered in the calculation. Fig. 2 shows an example of the electrical drive power of three different appliances. The behavior is not uniform such that the theoretical calculation of the energy consumption is not straightforward.

Due to cyclical switching (on and off) of the compressor, the mechanical drive power is not constant during an operating cycle. It can be determined by dividing the heat flow absorbed by the evaporator $\dot{Q}_0$ by the coefficient of performance COP according to:

$$P = \frac{\dot{Q}_0}{COP} \tag{2}$$

The product of the heat transfer coefficient k, the average surface of the cabinet A and the mean temperature difference between the storage room and the ambient ΔT, yields the heat flow into the cabinet $\dot{Q}_{cab}$, which is balanced by $\dot{Q}_0$:

$$\dot{Q}_{cab} = k \cdot A \cdot \Delta T = \dot{Q}_0 \tag{3}$$

The product of the heat transfer coefficient and the average surface of the cabinet is summarized by the $k{\cdot}A$ value. The $k{\cdot}A$ value can be calculated from the heat transfer coefficient on the inside and outside of the cabinet, the outer and the inner surface of the cabinet and the average surface, material thickness and thermal conductivity of the respective materials:

$$\frac{1}{k \cdot A} = \frac{1}{\alpha_a \cdot A_a} + \frac{d_{st}}{\lambda_{st} \cdot A_{st}} + \frac{d_{PUR}}{\lambda_{PUR} \cdot A_{PUR}} + \frac{d_{HIPS}}{\lambda_{HIPS} \cdot A_{HIPS}} + \frac{1}{\alpha_i \cdot A_i} \tag{4}$$

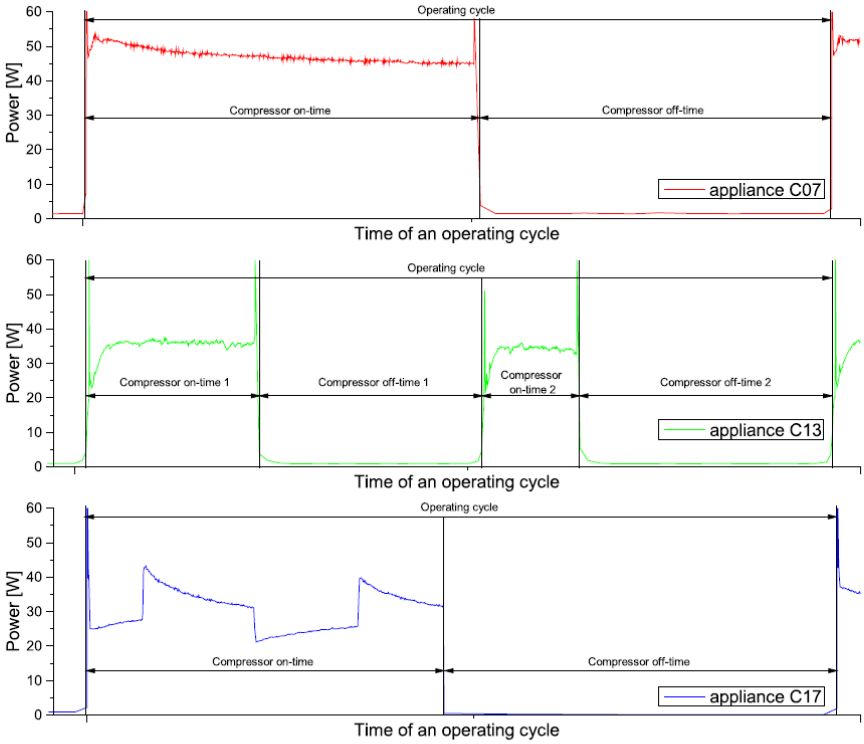

Fig. 2. Course of the electrical power over time for one operating cycle of three different appliances.

The thermal conductivity of the PUR foam λ_{PUR} influences the heat flow into the cabinet $\dot{Q}_{cab}$ and increases over time. In order to relate the thermal conductivity to the energy consumption E, the exact cabinet geometry and structure, motor efficiency η_m, power of the electrical control system $P_{ecs}(\tau_c)$ and the COP of the refrigeration cycle must be known, which is usually only possible for a manufacturer's proprietary product.

1.2. Compressor

A reciprocating compressor is typically used in modern household refrigeration appliances. The aging behavior of compressors can be deduced from tribological studies of the relevant material pairings. For this purpose, samples of the material pairings (materials, compressor oil and refrigerant) are rubbed against each other in a test stand [24,25]. Microscopic examinations of the artificially aged materials allow for conclusions to be drawn about the refrigerant flow during real compressor operation. It is expected that the damage caused by friction will lead to a leakage mass flow passing from the high pressure side to the low pressure side. As a result, the compressor has to compensate for this loss, which leads to an increase in relative running time. Research by Garland and Hadfield from 2004 shows an increase in relative running time from 30-39% over a period of 15 years [25]. This corresponds to an increase of power consumption of ~30% solely induced by compressor aging. The results of Elsner et al. [10] also showed an increase of the energy consumption of approx. 30% after 18 years of operation, but this value was determined for entire household refrigerating appliances, including the aging of the cabinet wall insulation and the door gaskets. Hence the results of Garland and Hadfield appear to be overestimated.

Furthermore, electrolytic processes can cause copper ions from the materials inside the compressor housing to dissolve in the refrigerant-oil mixture and deposit at various locations in the compression refrigeration circuit. This so-called copper plating process, which has been studied since the 1950s [26], can lead to a reduction of mass flow, which entails to a reduction of cooling capacity and an increase of energy consumption. In the course of the conversion to CFC-free refrigerants between 1990 and 2007, further investigations were carried out [27]. In 2007, Kaufmann et al. proposed several measures to prevent copper plating [28]. In compressors currently used in household refrigerating appliances, copper plating only plays a minor role. For the next generation of modern refrigerants with a low global warming potential and their lubricants, studies of compatibility with the materials used in the compressor were carried out by Majurin et al., showing that some pairs may bear reliability risks [29].

Since a defect of the compressor always leads to a total failure of the entire household refrigerating appliance, accelerated life tests are carried out with compressors in order to estimate their life expectancy [30-33]. The actual long-term performance behavior of modern hermetic compressors over several years of real operating conditions has so far only been insufficiently investigated. Most manufacturers test their appliances immediately after production for a period of a few hours on fully automated test stands in order to identify production issues.

1.3. Door gaskets

In the ASHRAE handbook from 2010, the proportion of the heat flow entering the storage compartment through the door gaskets is listed to be 25-30% of the total heat flow [8]. Because of the usual material composition of polyvinyl chloride with plasticizer, aging effects are also to be expected in the subsystem door gasket [34]. However, studies by Litt et al. from 1993 showed no clear influence on the energy consumption by exchanging old door gaskets with new ones [35]. Using numerical simulations, Kim et al. examined the heat transfer characteristics near the door gaskets and compared the results with experimental studies [36].

1.4. Wall insulation

With 45-55% of the total energy consumption of household refrigerating appliances, the heat flow through the cabinet walls makes up the largest share [8]. The cabinet usually consists of a thin galvanized sheet steel layer of approximately 1 mm on the outside, an insulation with a thickness of 40–60 mm made of PUR foam and an inner liner made of high impact polystyrene (HIPS), which is approximately 0.6–2 mm thick [37]. The basics of heat transfer in PUR foam were examined by Wagner in his dissertation [38].

Since the 1990s, the cabinet walls of household refrigerating appliances essentially consist of PUR which is foamed with cyclopentane as a blowing agent. Cyclopentane evaporates during exothermic reactions and thus cools the emerging PUR foam. A large number of reactions takes place in parallel during that foaming process. With respect to the aging process, the formation of carbon dioxide (CO_2) as a result of the reaction between water and isocyanate is crucial. Both cyclopentane and CO_2 serve as blowing agents and foam the PUR up. Immediately after the foaming process, the gas enclosed in the cells of the PUR foam essentially consists of these two gas species only. Due to composition differences between the cell gas and the ambient air, CO_2 diffuses out of the foam cells and nitrogen (N_2) and oxygen (O_2) diffuse into the foam cells. Since nitrogen and oxygen have a larger thermal conductivity than CO_2, the total thermal conductivity of the PUR foam increases over time. In most appliances, diffusion takes place through the inner liner made of HIPS, since the outer case is made of steel, which is impermeable for these gases. The diffusive exchange of the three gas species (CO_2, N_2 and O_2) takes place at different rates due to their varying diffusion coefficients, while cyclopentane diffusion is practically negligible [39-41].

Before 1990, CFC-11 was predominantly used as a physical blowing agent for PUR foam [42-44]. As water is not required for these reactions, no CO_2 is generated so that these older PUR foams are more resistant to aging than modern PUR foams. The increase of thermal conductivity of PUR foams used in household refrigerating appliances has been the subject of publications by Wilkes et al. [45-49] and Hueppe et al. [50], while Albrecht investigated PUR foams in the context of building construction [51]. Wilkes compared the thermal conductivity of PUR foams made with cyclopentane to PUR foams made with CFC-11. Over a period of three years, an increase of the thermal conductivity of 16.7% was found. The results by Hueppe et al. [50] show an increase of 15.1% over a period of 1.15 years, with significantly more modern PUR foams being examined.

To determine the quality of the insulation of the appliance housing, the reverse heat leak method [52-56], the use of heat flow sensors [53,57,58], the b-method [50] and the latent heat sink method [37] are described in the literature. The increase of the $k{\cdot}A$ value of a household refrigerator cabinet over time has until now only been investigated with the latent heat sink method. Paul et al. [37] found an increase of 6.1–11.3% for the $k{\cdot}A$ value over a period of 14 months looking at four cabinets.

Aging mechanisms are also known in other refrigeration applications. In 2018, Capo et al. examined the aging of refrigerated transport equipment and showed that the overall insulation coefficient of nine different refrigerated vehicles increases by up to 65% in the first twelve years. In the following 6 years, this value changed only slightly [59]. In principle, diffusion is much less problematic in the sandwich profiles used in refrigerated vehicles than in household refrigerating appliances, as the PUR foam in the sandwich profiles used for the vehicles is surrounded on both sides by a metal layer that acts as a diffusion barrier.

1.5. Energy consumption model

On the basis of Wilkes' results, Johnson in 2000 published a function that describes the annual increase rate of energy consumption (Δe_{ir}) of household refrigerating appliances [60]:

$$\Delta e_{ir} = r \cdot \left(\frac{20-\tau}{20}\right)^{x} \quad (5)$$

In this equation, r is the initial aging rate of the blowing agent, τ the appliance age and x a correction factor depending on the blowing agent. Johnson revised this model in 2004 and depicted the increase of energy consumption graphically. This function attains a limiting value of 21% for an appliance age of 20 years [61].

Although there are some data on the increase of the energy consumption of refrigeration appliances with age, there is no systematic investigation about the origin of this increase and especially there is no comprehensive model which combines all those effects and allows to describe the average loss of electrical energy efficiency over age. It is therefore the aim of this paper to complement the available information with new and systematically gathered data and to incorporate them into a generalized model for the age-dependent efficiency of refrigeration appliances.

2. Test setup

All measurements were carried out in climatic chambers with an ambient temperature fluctuation of ±0.5 K and an air humidity of 50%. As the employed measuring systems were modernized several times during the study period from 1994 to 2020, the system-related measurement uncertainty changed over this extensive period of time.

2.1. Methodology

To determine the aging behavior of household refrigerating appliances (i.e. refrigerators, freezers and their combinations), the electrical energy consumption of 21 appliances from different manufacturers and appliance categories [62] was measured after their production and repeatedly after several years of operation. The individual measurements were consistently carried out according to the standards applicable in the year of production. These are the standards DIN EN ISO 15502:2006 [16] in conjunction with DIN EN 153:2006 [63], DIN EN 62552:2013 [7] and the series of standards IEC 62552:2015 [17-19]. Furthermore, 11 new household refrigerating appliances were examined several times over a period of two years following the IEC 62552:2015 series of standards [17-19]. For better comparability of the results according to the various standards, a uniform ambient temperature of 25 °C was used for all measurements. In the supplemental material, Tables SM1 to SM32 list all appliances with the respective standards or test programs which were used during the measurements. All energy consumption results were interpolated to the respective compartment target temperatures as defined in the standards.

2.2. Temperature measurement

Temperatures were sampled by thermocouple differential measurements, where each measuring junction had its own reference junction in a separate ice water bath. In the period from 1994 to 2008, the measurement signal was recorded by an Acurex Cooperation system consisting of an Autodata Ten/5 datalogger and an Autodata 1016 scanner with a measurement uncertainty of ±0.3 K. After 2008, the measurement signal of the thermocouples was processed by a combination of a pre-amplifier LTC1050 (Linear Technologies) with adjusted gain of 1000 and an analog-to-digital converter system OMB DAQ 55/56 (Omega Technologies), limiting the offset drift to ±0.025 K. By calibrating each thermocouple individually and applying a polynomial correction, the measurement uncertainty was reduced from ±1% x ΔT to ±0.5% x ΔT.

2.3. Energy measurement and power supply

Until 2012, the system GTU 0610 from ASEA BROWN BOVERI was used with a measurement uncertainty of ±1%. Since 2012, a single-phase large-range energy meter of the type EZI 1 from ZES Zimmer - Electronic Systems was used, resulting in a reduced measurement uncertainty of ±0.5% and a better resolution.

The GTU 0610 was inserted between the power supply and the appliance during the test (measurement site) via the conventional 2-wire connection method. Using the new EZI 1 system, the appliances were equipped with a 4-wire connection allowing for a separate current and voltage measurement. Both systems have a pulse output, each pulse corresponds to an energy quantity of 2812.5 Ws for GTU 0610 and 144 Ws for EZI 1. Each pulse was recorded in time and date. The final energy consumption follows from the summation of the pulses during the relevant time period.

In the early years of this investigation, the supply voltage for the test appliances was conditioned with a voltage stabilizer Skz D 241102 from Siemens. From 2012 onwards, an electronic power source ACS-6000-PS from HBS Electronic was used.

2.4. Measurement uncertainty

Table 2 shows the specific measurement uncertainty of the various measurement systems used in this study.

Due to the interpolation of energy consumption measurements at two temperatures to a target temperature, the temperature measurement uncertainty also influences the total measurement uncertainty of energy consumption, cf. Fig. 3. This influence was determined individually for each interpolated measuring point by:

$$\delta E_t = \sqrt{\sum \left(\frac{dE_i}{dT_i}\right)^2 \cdot \delta T_t^2} \quad (6)$$

In this equation, δE_t is the uncertainty of the energy measurement due to the uncertainty of the temperature measurement δT_t, dE_i is the difference between the measured energy consumption of the two individual measurements and dT_i the difference between the measured storage temperatures of the two individual measurements. The total uncertainty of the energy measurement δE is given by the sum of the uncertainty of the energy measurement system δE_e and the interpolation uncertainty δE_t:

$$\delta E = \delta E_e + \delta E_t \quad (7)$$

2.5. Thermal conductivity of aged PUR foam samples

As a continuation of the measurements by Hueppe et al. [50], further values of the thermal conductivity of PUR foam up to an age of 2.76 years were determined in this work. The same measurement setup and methodology was used as in the original study [50].

Table 2
Measured properties and their uncertainties.

Measured quantity	System	Time period	Measuring device	Uncertainty
Temperature	Acurex	1994 to 2008	Thermocouples	±0.3 K
	DAQ	2008 to 2020	Thermocouples	±0.1 K
Energy consumption	GTU	1994 to 2012		±1.0%
	EZI	2012 to 2020		±0.5%
Power supply	Siemens	1994 to 2012		±1.0%
	ACS	2012 to 2020		±0.1%
Time		1994 to 2020	Personal computer	±0.1 s/day

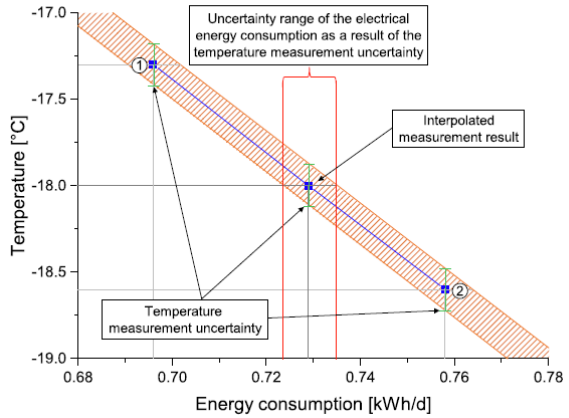

Fig. 3. Influence of the temperature uncertainty on the measurement uncertainty of the electrical energy consumption (example).

2.6. Coefficient of performance of the compressor

Compressor measurements were carried out according to DIN EN 13771-1:2003 [64] with a calorimeter test stand (method A). The compressors were measured at the beginning of the study and then installed in eight appliances (cf. supplemental material Tables SM33 to SM40). After 2.00-2.17 years of real operation, during which the electrical energy consumption of the appliances was regularly measured, the compressors were removed and studied again. The *COP*was determined from the electrical drive power P_{el} and the heat flow in the evaporator $\dot{Q}_0$. The measurement accuracy of the heat flow was ±0.3%, that of the electrical drive power ±0.1% and the resulting *COP* uncertainty was ±0.4%.

3. Results

To determine the influence of aging on the electrical energy consumption of household refrigerating appliances, standard measurements were carried out. With these data, a model was created that describes the change of energy consumption depending on the age of the appliance.

The energy consumption at the production date cannot be derived from the value on the energy label as this is not the true value of an individual appliance. Due to e.g. manufacturing tolerances, the energy consumption stated on the energy label may deviate by up to 10% from the real energy consumption of a specific appliance [62]. Because it was not possible to measure the energy consumption immediately after manufacturing, an estimate of this value had to be extrapolated from the existing data and information on the production date in order to create a consolidated aging model. For this purpose, a preliminary function was created to normalize the energy consumption of the first measurement. The aging function is an average of 32 appliances of different types. At present, it is not possible to determine an aging function for individual appliance models, as the available data for such a purpose are insufficient.

3.1. Measurement results

In a first step, each individual measuring point $E(\tau)$ of the interpolated energy consumption was divided by the energy consumption at the time of the first measurement E_0, creating a normalized function of appliance age τ:

$$\Delta E_0(\tau) = \frac{E(\tau)}{E_0} \tag{8}$$

The results of 100 measurements standardized in this way are shown in Fig. 4. A detailed list of the results for each of the 32 appliances can be found in the supplemental material (Tables SM1 to SM32).

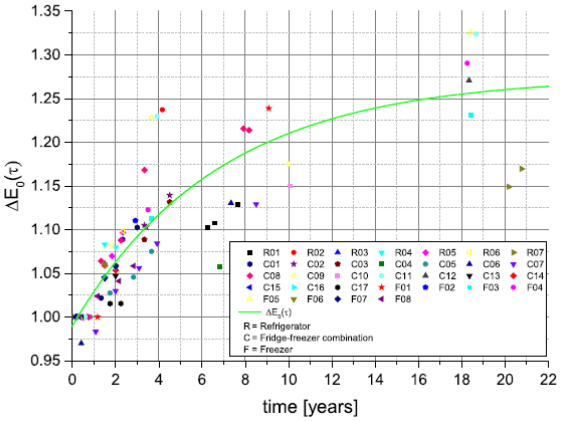

Fig. 4. Normalized energy consumption (symbols) and preliminary aging function (line).

3.2. Aging function

Using measurement data, a preliminary aging function with the reference point of the first measurement was generated on the basis of an error function:

$$\Delta E_0(\tau) = g + a \cdot \left[1 - e^{-\left(\frac{\tau}{b}\right)}\right] \tag{9}$$

Its parameters a, b and g were adjusted by minimization of the root mean square (RMS) difference between the measured energy consumption and the function. This resulted in a course that is depicted in Fig. 4, cf. supplemental material for its parameter values (Equation SM1). Since the preliminary aging function shown in Fig. 4 relates to the first measurement that was carried out in an already aged appliance state, it starts with a value of $g_0 = 0.990$ due to aging processes in the PUR foam, which begin immediately after production.

Using the preliminary aging function, it can be extrapolated to the hypothetical energy consumption at the production date of the appliances with:

$$E_p = E_0 \cdot [1 - (\Delta E_0(\tau) - \Delta E_0(\tau = 0))] \tag{10}$$

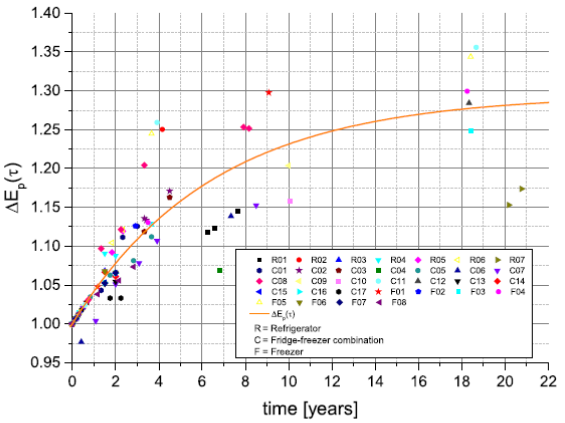

Fig. 5. Corrected energy consumption (symbols) and consolidated aging function $\Delta E_p(\tau)$ (line).

This correction was applied to all data sets. As a result, the data points of the normalized energy consumption in Fig. 5 shift slightly upwards.

The curve fitting procedure was repeated with the new standardized energy consumption data set, yielding the consolidated aging model, cf. Fig. 5:

$$\Delta E_p(\tau) = 1 + 0.295 \cdot \left[1 - e^{-\left(\frac{\tau}{0.37\tau}\right)}\right] \quad (11)$$

3.3. Thermal conductivity measurements of PUR foam samples

As shown in Fig. 6, the thermal conductivity λ of the PUR foam samples increases from the initial 19.5 mW/(m·K) by 26% to 24.6 mW/(m·K) over a period of 2.76 years. Due to the different diffusion coefficients of the gas species CO_2, N_2 and O_2, mass transport takes place at different rates [38]. The composition of the gas species changes over time and with it the conductive heat transfer, which entails a slightly decreased thermal conductivity of the PUR foam during the first ~0.27 years after production.

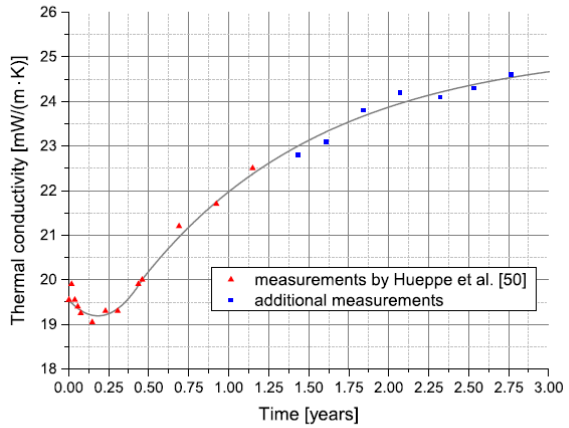

Fig. 6. Thermal conductivity measurements of PUR foam samples (symbols) and guide to the eye (line).

3.4. Calorimeter measurements

The results of the calorimeter measurements are shown in Table 3. The *COP* tends to improve slightly over the period under review. Four compressors displayed a small improvement of the *COP*, three had nearly no change and only one device slightly deteriorated by −1.5%. Overall, an average improvement of the *COP* of 0.9% was found for the eight examined appliances. Based on these results, it can be assumed that there is a negligible influence on the aging behavior of household refrigerating appliances.

4. Discussion

The present data clearly show that the increase of electrical energy consumption is most pronounced in the first five years after production. After the average operating time of a household refrigerating appliance of 16 years [13], there is an increase of energy consumption of 27%. For the primary operating time of 12–13 years the increase is about 25%. In the case of significantly older appliances, the further increase of energy consumption is negligible.

Since the appliances examined in this study are of different

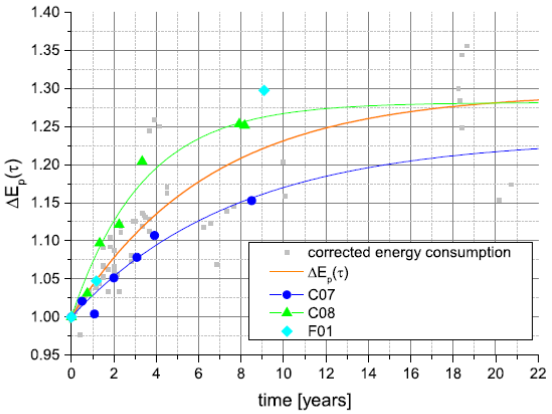

Fig. 7. Comparison between individual appliances C07, C08 and F01 and the average aging function.

Table 3
Results of the calorimeter measurements.

	Refrigerator brand	Refrigerator type	Compressor type (Secop)	Operating time (years)	COP_1	COP_2	ΔCOP
R03	Siemens	KI81RAD30	DLX4.8KK	2.00	1.77	1.83	3.4%
R08	Siemens	KI81RAD30	DLX4.8KK	2.17	1.76	1.84	4.2%
R09	Siemens	KI81RAD30	DLX4.8KK	2.17	1.76	1.75	− 0.1%
Average over all DLX4.8KK compressors				**2.11**	**1.76**	**1.81**	**2.5%**
C18	Bosch	KIS86AF30	DLX7.5KK	2.17	1.98	1.99	0.2%
C19	Bosch	KIS86AF30	DLX7.5KK	2.17	1.98	1.98	0.1%
Average over all DLX7.5KK compressors				**2.17**	**1.98**	**1.98**	**0.1%**
F06	Siemens	GS36NVW3V	HZK95AA	2.00	1.93	1.96	1.4%
F09	Siemens	GS36NVW3V	HZK95AA	2.17	1.95	1.92	− 1.5%
F10	Siemens	GS36NVW3V	HZK95AA	2.17	1.93	1.93	0.1%
Average over all HZK95AA compressors				**2.11**	**1.93**	**1.93**	**0.0%**
Average over all compressors				**2.13**	**1.88**	**1.90**	**0.9%**

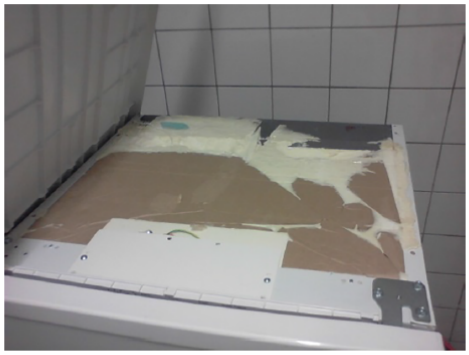

Fig. 8. Missing diffusion barrier at the cabinet of appliance F01.

construction type and production processing quality, their aging results are scattered. Nonetheless, they essentially follow the mathematical course described in this paper. The largest individual data sets are available for the two appliances C07 and C08, each with six measuring points, which is sufficient to adjust the aging function accordingly. As can be seen in Fig. 7, the measured energy consumption follows the course of the aging model given by Eq. (11).

Another appliance that stands out is F01. The aging of this appliance led to an increase of 30% with respect to energy consumption in just nine years. The reason for this is the missing diffusion barrier in parts of the outer housing, cf. Fig. 8.

A comparison of the present aging model with other literature models is shown in Fig. 9. Compared to the model of Johnson [52], a significantly larger increase of energy consumption was observed in this study. The Johnson model is based on the work by Wilkes [45-49], who measured the thermal conductivity of PUR foam samples over a period of 13 years, i.e. their aging function is an extrapolation beyond that point in time. Furthermore, this model assumes aging of the PUR foam only.

The study of Garland and Hadfield [25] reports a different function for the increase of energy consumption, cf. Fig. 9. During the first 14 years, the model values are below the present data, but increase to significantly higher values for an appliance age over 14 years. In the underlying tribological investigation, a metal ball was rolled over a metal plate in a refrigerant-oil environment. This model is greatly simplified and limited to the compressor as the sole source of aging in a household refrigerating appliance.

In practice, no significant change of the compressor *COP* was found

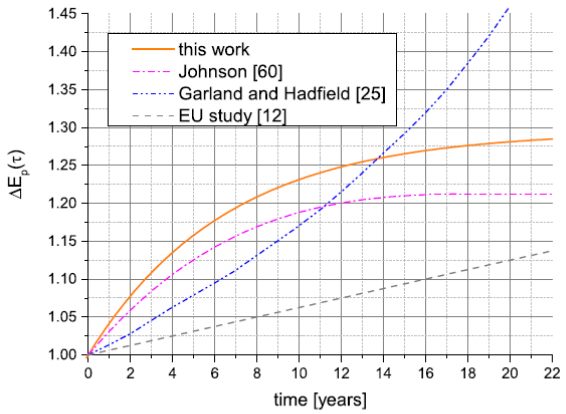

Fig. 9. Comparison of different aging models for electrical energy consumption.

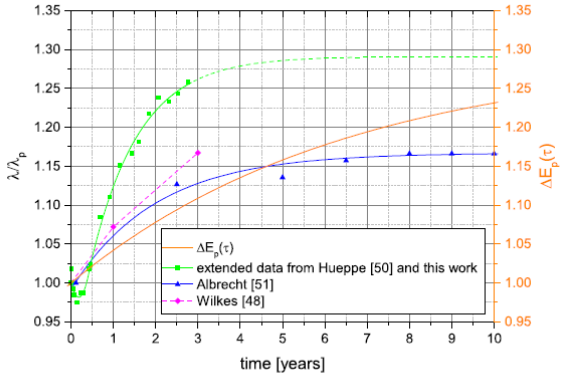

Fig. 10. Comparison of the aging model with the thermal conductivity increase of the PUR foam.

during the calorimeter measurements performed in this study. Essentially, this is likely to be due to better sealing valves and running-in of the bearings in the compressor. In addition, it is difficult to deduce the aging of household refrigerating appliances by solely observing the relative compressor run time. Because it indicates the ratio of the compressor on-time to the total time of a compressor cycle, the relative runtime might not change over the course of time, while both of the absolute values will do so in most cases.

The results of this study show that a 10% increase of energy consumption over a period of 16 years as assumed in the EU study [13] is a significantly too low estimate, also when compared to the other aging models from the literature.

A direct comparison of the increase of energy consumption with the increase of the thermal conductivity of the PUR foam is shown in Fig. 10. The data on the thermal conductivity from the work of Albrecht [51] and the present thermal conductivity measurements were also normalized in this diagram to the first measuring point of the data sets and they differ significantly from each another. This is essentially due to the different technical fields of application of the examined PUR foams.

With the additional measurements of the thermal conductivity carried out in this study, the aging process of the PUR foam can be better quantified. Approximately for five years after production, the thermal conductivity will rise and assume a limiting value of 25.2 mW/(m·K), which is an increase of ~29% compared to the thermal conductivity at the time of production.

The thermal conductivity data published by Hueppe et al. [50] and in this study are significantly higher than those of Wilkes [48]. Since the data published by Wilkes are based on a foam made with CFC-11, a direct comparison of the two data sets is only possible to a limited extent.

In addition to the increase of the energy consumption due to technical aging that is addressed in this paper, the individual user behavior does influence the real energy consumption of household refrigerating appliances, as described by Harrington [14], Hueppe et al. [15] and Moretti [23]. In households with a high user induced heat load, the relative increase of the energy consumption due to technical aging will therefore be lower than in households with only a few door openings.

5. Conclusions

An aging model was derived from a solid data base of 100 electrical energy consumption values from a total of 32 appliances that were run under real operating conditions. It is the first function of its kind that was developed on the basis of to true electrical energy consumption data. Older predictions of energy consumption derived from data on individual system components show significant differences to the aging

model described in this study.

A 27% increase of the energy consumption over an average operating time of a household refrigerating appliance of 16 years is shown. For extremely old appliances with an age of around 20 years, the energy consumption increases by up to 28%. The aging model describes the average increase of the energy consumption of 32 different appliances. In the first three years, the difference between individual measurement points and the average aging function is within ±5%. As the measured values are scattered due to different production processing quality, design, size and other parameters, the increase of energy consumption in the later years of the appliances (older than 15 years) can deviate from the aging model by up to ±15%.

These findings should sensitize the stakeholders (manufactures, consumer organisations, standardisation bodies and legislators) for aging processes related to household refrigerating appliances. It is now possible to better determine the economic and energetic replacement time of the appliances for the customer and the overall economic impact caused by aging household refrigerating appliances.

In the coming years, further measurements will be carried out on the appliances that have been running for two years during this study. Furthermore, the currently poor data situation for an appliance age between 10 and 18 years has to be improved by additional measurements on older appliances. These data will help to render the aging model more precise.

Declaration of Competing Interest

The authors declare that they have no known competing financial interests or personal relationships that could have appeared to influence the work reported in this paper.

Acknowledgements

This work was carried out as part of the ALGE research project funded by the German Federal Ministry for Economic Affairs and Energy as part of the 6th energy research program (project funding reference number: 03ET1544A-E).

Appendix A. Supplementary material

Supplementary data to this article can be found online at https://doi.org/10.1016/j.applthermaleng.2021.117992.

References

[1] V. Graichen, S. Gores, G. Penninger, W. Zimmer, V. Cook, B. Schlomann, T. Fleiter, A. Striegel, W. Eichhammer, H.-J. Ziesing, Energieeffizienz in Zahlen. Endbericht zum Umweltforschungplan des Bundesministeriums für Umwelt, Naturschutz und Reaktorsicherheit – Projekt 3708 41 121 UBA-FB 00 1469, Dessau-Roßlau, 2011.
[2] Organisation for Economic Co-operation and Development, OECD.: COOL APPLIANCES: Policy Strategies for Energy Efficient Homes, 2003, URL: http://li-brary.umac.mo/ebooks/b13623886.pdf.
[3] Umwelt Bundesamt, Stromverbrauch, 2020. URL: https://www.umweltbundesamt.de/daten/energie/stromverbrauch.
[4] Umwelt Bundesamt, Energieverbrauch privater Haushalte, 2020. URL: https://www.umweltbundesamt.de/daten/private-haushalte-konsum/wohnen/energieverbrauch-privater-haushalte#direkte-treibhausgas-emissionen-privater-haushalte-sinken.
[5] Statista, Haushaltsgroßgeräte, 2018, URL: https://de.statista.com/statistik/studie/id/7683/dokument/haushaltsgrossgeraete-statista-dossier/.
[6] DIN-Normenausschuss Kältetechnik (FNKä), DIN EN 13771-1:2017. Compressors and condensing units for refrigeration – Performance testing and test methods – Part 1: Refrigerant compressors. German version EN 13771-1:2017, 2017.
[7] DKE Deutsche Kommission Elektrotechnik Elektronik Informationstechnik im DIN und VDE Normenausschuss Kältetechnik (FNKä) im DIN, DIN EN 62552:2013. Household refrigerating appliances – Characteristics and test methods (IEC 62552: 2007, modified + corrigendum Mar. 2008). German version EN 62552:2013, 2013.
[8] 2010 ASHRAE Handbook: Refrigeration. SI edition. ASHRAE, Atlanta, GA, 2010. ISBN 1933742828.
[9] Australian Consumers' Association, Energy Consumption of Refrigerators and Freezers Used Under Normal Conditions of Use. Choice, Sydney, Australia, 1990.
[10] A. Elsner, M. Müller, A. Paul, J. Vrabec, Zunahme des Stromverbrauchs von Haushaltskältegeräten durch Alterung. Deutsche Kälte-Klima Tagung 40, Hannover, Germany, 2013, November 20-22.
[11] Stiftung Warentest, Umwelt geschont – Strom gespart. test 1994, Nr. 3, 1994, p. 36-39.
[12] Stiftung Warentest, Auch ohne Ozonkiller. test 1994, Nr. 6, 1994, p. 24-25.
[13] Van Holsteijn en Kemna B.V (VHK)., Association pour la Recherche et le Développement des Méthodes et Processus Industriels (ARMINES), Commission Regulation (EC) No. 643/2009 with regard to ecodesign requirements for household refrigeration appliances and Commission Delegated Regulation (EU) No. 1060/2010 with regard to energy labelling of household refrigeration appliances, FINAL REPORT, 2016.
[14] L. Harrington, Prediction of the energy consumption of refrigerators during use. Dissertation, Melbourne (Australia), 2018, URL: https://minerva-access.unimelb.edu.au/handle/11343/213357.
[15] C. Hueppe, J. Geppert, J. Moenninghoff-Juessen, L. Wolff, R. Stamminger, A. Paul, A. Elsner, J. Vrabec, H. Wagner, H. Hoelscher, W. Becker, U. Gries, A. Freiberger, Investigating the real life energy consumption of refrigeration appliances in Germany: Are present policies sufficient? Energy Policy 155 (2021) 112275, https://doi.org/10.1016/j.enpol.2021.112275.
[16] Normausschuss Kältetechnik (FNKÄ) im DIN, DIN EN ISO 15502:2006. Household refrigerating appliances – Characteristics and test methods (ISO 15502:2005). German version EN ISO 15502:2005, 2006.
[17] IEC 62552:2015, IEC 62552-1:2015 Household Refrigerating Appliances – Characteristics and Test Methods – Part 1: General requirements. International Electrotechnical Commission (IEC), 2015.
[18] IEC 62552:2015, IEC 62552-2:2015 Household Refrigerating Appliances – Characteristics and Test Methods – Part 2: Performance requirements. International Electrotechnical Commission (IEC), 2015.
[19] IEC 62552:2015, IEC 62552-3:2015 Household Refrigerating Appliances – Characteristics and Test Methods – Part 3: Energy consumption and volumes. International Electrotechnical Commission (IEC), 2015.
[20] AS/NZS 4474.1:2007, Performance of household electrical appliances – Refrigerating appliances energy consumption and performance. Standards Australia, 2007.
[21] AHAM HRF-1-2008, Energy and internal volume of refrigerating appliances, Association of home appliance manufacturers (AHAM), 2008.
[22] JIS C 9801:2006, Household refrigerating appliances – Characteristics and test methods, Japanese Standards Association (JSA), 2006.
[23] F. Moretti, Refrigeration energy label standard measurements linked to energy consumption in daily use, in: P. Bertoldi, A. Ricci, A. de Almeida (Eds.), Energy Efficiency in Household Appliances and Lighting, Springer Berlin Heidelberg, Berlin, Heidelberg, 2001, pp. 389–394, https://doi.org/10.1007/978-3-642-56531-1_44.
[24] K.H. Kloos, E. Broszeit, F.J. Hess, Tribologische Wirkung von Kältemitteln, Materialwiss. Werkstofftech. 9 (12) (1978) 445–451.
[25] N.P. Garland, M. Hadfield, Environmental implications of hydrocarbon refrigerants applied to the hermetic compressor, Mater. Des. 26 (7) (2005) 578–586.
[26] H. Steinle, Über die Kupferplattierung in Kältemaschinen, Kältetechnik 3 (8) (1951) 194–197.
[27] R.G. Doerr, S. Kujak, Compatibility of refrigerants and lubricants with motor materials, in: Proceedings of Electrical/Electronics Insulation Conference, Chicago, 1993, October 04-07.
[28] R.E. Kauffman, Determine the mechanism for copper plating and methods for its elimination from HVAC systems, ASHRAE Research project 1249 – RP, 2007.
[29] J.A. Majurin, W. Gilles, S.J. Staats, Materials compatibility of HVACR system materials with low GWP refrigerants, in: 15th International refrigeration and air conditioning conference, Purdue, July 14-17, 2014, 2132.
[30] I.M.G. Almeida, C.R.F. Barbosa, F.A.O. Fontes, Methods of wear tests for hermetic reciprocating compressors: an overview, HOLOS 4 (2016) 86–104.
[31] B. Vetsch, G. Feichter, A. Bachmann, S.S. Bertsch, Design and realization of an automated test-stand for variable capacity household compressors, in: 24th International compressor engineering conference, Purdue, July 11-14, 2016, 1100.
[32] S. Woo, D. O'Neal, Improving the reliability of a domestic refrigerator compressor subjected to repetitive loading, in: 24th International compressor engineering conference, Purdue, July 9-12, 1101, 2018.
[33] S.-W. Woo, D.L. O'Neal, Study on Improving the Reliability of a Domestic Refrigerator Compressor Subjected to Repetitive Loading, in: S.M. Lawan, M.M. A. Rafique (Eds.), Recent Developments in Engineering Research, Vol. 9, Book Publisher International, Hooghly, 2020.
[34] E.B. Rabinovitch, J.W. Summers, The effect of physical aging on properties of rigid polyvinyl chloride, J. Vinyl Technol. 14 (3) (1992) 126–130.
[35] B. Litt, A. Megowan, Maintenance doesńt necessarily lower energy use. Home energy magazine, 1993, URL: http://www.homeenergy.org/show/article/nav/refrigerators/page/4/id/914.
[36] H.S. Kim, J.S. Sim, J.S. Ha, A study on the heat transfer characteristics near the magnetic door gasket of a refrigerator, Int. Commun. Heat Mass Transfer 38 (9) (2011) 1226–1231.
[37] A. Paul, E. Baumhögger, A. Elsner, L. Moczarski, M. Reineke, G. Sonnenrein, C. Hueppe, R. Stamminger, H. Hoelscher, H. Wagner, U. Gries, A. Freiberger, W. Becker, J. Vrabec, Determining the heat flow through the cabinet walls of household refrigerating appliances, Int. J. Refrig. 121 (2021) 235–242.
[38] K-E. Wagner, Simulation und Optimierung des Wärmedämmvermögens von PUR Hartschaum, Wärme- und Stofftransport sowie mechanische Verformung, Dissertation, Stuttgart (Germany), 2002: https://doi.org/10.18419/opus-1579.

[39] H.-W. Engels, H.-G. Pirkl, R. Albers, R.W. Albach, J. Krause, A. Hoffmann, H. Casselmann, J. Dormish, Polyurethane: vielseitige Materialien und nachhaltige Problemlöser für aktuelle Anforderungen, Angew. Chem. 125 (36) (2013) 9596–9616.
[40] B.W. Tucker, Rigid polyurethane foams with low thermal conductivities, patent document, US005169877A, PCT, 08.12.1992, 1992.
[41] U. Berardi, J. Madzarevic, Microstructural analysis and blowing agent concentration in aged polyurethane and polyisocyanurate foams, Appl. Therm. Eng. 164 (2020) 114440, https://doi.org/10.1016/j.applthermaleng.2019.114440.
[42] P. Kjeldsen, M.H. Jensen, Release of CFC-11 from disposal of polyurethane foam waste, Environ. Sci. Technol. 35 (14) (2001) 3055–3063.
[43] C. Scheutz, P. Kjeldsen, Determination of the fraction of blowing agent released from refrigerator/freezer foam after decommissioning the product, Environment and Resources DTU, Technical university of Denmark, 2002.
[44] B. Yazici, Z.S. Can, B. Calli, Prediction of future disposal of end-of-life refrigerators containing CFC-11, Waste Manage. 34 (1) (2014) 162–166.
[45] K.E. Wilkes, D.W. Yarbrough, F.J. Weaver, Aging of polyurethane foam insulation in simulated refrigerator walls, in: International Conference on Ozone Protection Technologies, Baltimore Maryland, November 12-13, 1997.
[46] K.E. Wilkes, W.A. Gabbard, F.J. Weaver, Aging of polyurethane foam insulation in simulated refrigerator panels: One-year results with third-generation blowing agents, The Earth Technologies Forum, Washington D.C., 1999, September 27-29.
[47] K.E. Wilkes, W.A. Gabbard, F.J. Weaver, J.R. Booth, Aging of polyurethane foam insulation in simulated refrigerator panels: Two-year results with third-generation blowing agents, J. Cell. Plast. 37 (5) (2001) 400–428.
[48] K.E. Wilkes, D.W. Yarbrough, W.A. Gabbard, G.E. Nelson, J.R. Booth, Aging of polyurethane foam insulation in simulated refrigerator panels: Three-year results with third-generation blowing agents, J. Cell. Plast. 38 (4) (2002) 317–339.
[49] K.E. Wilkes, D.W. Yarbrough, G.E. Nelson, J.R. Booth, Aging of polyurethane foam insulation in simulated refrigerator panels: Four-year results with third-generation blowing agents, The Earth Technologies Forum, Washington D.C., 2003, April 22-24.
[50] C. Hueppe, J. Geppert, R. Stamminger, H. Wagner, H. Hoelscher, J. Vrabec, A. Paul, A. Elsner, W. Becker, U. Gries, A. Freiberger, Age-related efficiency loss of household refrigeration appliances: Development of an approach to measure the degradation of insulation properties, Appl. Therm. Eng. 173 (2020) 115113, https://doi.org/10.1016/j.applthermaleng.2020.115113.
[51] W. Albrecht, Änderung der Wärmeleitfähigkeit von zehn Jahre alten PUR-Hartschaumplatten mit gasdiffusionsoffenen Deckschichten, Bauphysik 25 (5) (2003) 317–319.
[52] T. Stovall, Closed Cell Foam Insulation: A review of long term thermal performance, Oak Ridge National Laboratory report ORNL/TM-2012/583, 2012.
[53] C. Melo, L.W. da Selva, R.H. Pereira, Experimental evaluation of the heat transfer through the walls of household refrigerators, in: Eighth International Refrigeration Conference at Purdue University, West Lafayette, IN, USA, July 25-28, 2000, 353-360.
[54] D.L. Lieghton, Investigation of Household Refrigerator with Alternative Low Global Warming Potential Refrigerants, Master thesis, University of Maryland, USA, 2011.
[55] J.S. Sim, J.S. Ha, Experimental study of heat transfer characteristics for a refrigerator by using reverse heat loss method, Int. Commun. Heat Mass Transfer 38 (5) (2011) 572–576.
[56] C.J.L. Hermes, C. Melo, F.T. Knabben, Alternative test method to assess the energy performance of frost-free refrigerating appliances, Appl. Therm. Eng. 50 (1) (2013) 1029–1034.
[57] S. Lassue, S. Guths, D. Leclercq, B. Duthoit, Contribution to the experimental study of natural convection by heat flux measurement an anemometry using thermoelectric effects, Experimental Heat Transfer, Fluid Mechanics and Thermodynamics, 1993, 831-838.
[58] S. Thiessen, F.T. Knabben, C. Melop, Experimental evaluation of the heat fluxes through the walls of a domestic refrigerator, in: 15th Brazilian Congress of Thermal Sciences an Engineering, Belem, PA, Brazil, 2014, November 10-13.
[59] C. Capo, F. Latchan, T. Michineau, J.M. Petit, R. Revellin, J. Bonjour, G. Cavalier, Factors affecting the ageing of refrigerated transport equipment. 5th IIR Conference on Sustainability and the Cold Chain, Beijing, China, 2018, April 6–8.
[60] R.W. Johnson, The effect of blowing agent on refrigerator/-freezer TEWI, in: Polyurethanes conference, Boston, MA, 2000, October 8–11.
[61] R.W. Johnson, The effect of blowing agent choice on energy use and global warming impact of a refrigerator, Int. J. Refrig. 27 (7) (2004) 794–799.
[62] European Commission, Commission delegated regulation (EU) No 1060/2010 of 28 September 2010, Supplementing directive 2010/30/EU of the European Parliament and of the Council with regard to energy labelling of household refrigerating appliances, 2010.
[63] Normausschuss Kältetechnik (FNKÄ) im DIN, 2006. DIN EN 153:2006. Methods of measuring the energy consumption of electric mains operated household refrigerators, frozen food storage cabinets, food freezers and their combinations, together with associated characteristics. German version EN 153:2006.
[64] Normausschuss Kältetechnik (FNKÄ) im DIN, 2003. DIN EN 13771-1:2003. Compressors and condensing units for refrigeration – Performance testing and test methods – Part 1: Refrigerant compressors. German version EN 13771-1:2003.

Supplemental material

Nomenclature

COP	Coefficient of performance
$E(\tau)$	Electrical energy consumption at the time τ (kWh/d)
E_p	Corrected energy consumption immediately after production (kW/24h)
P_{el}	Electrical drive power (W)
$\dot{Q}_{ev}$	Evaporator heat flow (W)
T_a	Ambient temperature (°C)
T_{ccma}	Time averaged chill compartment temperature (°C)
$T_{cc,max}$	Maximum chill compartment temperature (°C)
T_{ev}	Evaporation temperature (°C)
T_{cond}	Condensation temperature (°C)
T_{fma}	Time averaged frozen food compartment temperature (°C)
$T_{f,max}$	Maximum frozen food compartment temperature (°C)
T_{ma}	Time averaged fresh food compartment temperature (°C)
T_{sh}	Superheating temperature (°C)
δE	Uncertainty of the energy measurement (%)
τ	Aging time (a)
τ_{op}	Actual appliance operation time (a)
ΔCOP	Improvement of the COP (%)
ΔE_0	Preliminary aging model
ΔE_p	Aging model

Preliminary aging function

$$\Delta E_0(\tau) = \left[0.990 + 0.285 \cdot \left(1 - \mathrm{e}^{-\left(\frac{\tau}{6.749}\right)}\right)\right] \quad \text{(SM1)}$$

Electrical energy consumption measurements

Table SM1: Results energy consumption measurements for R01.

Nr.:			R01					
Brand:			Bosch					
Type:			KSV36VL40/03					
Standard:			DIN EN ISO 15502:2006 and DIN EN 153:2006					
serial number:			252120269268000788					
Production date:			12/2012					
Storage volume (fresh food / chill / frozen food):		[l]	(346 / - / -)					
Measurement:			1	2	3	4	5	6
Date of measurement:			04/2013	03/2019	07/2019	08/2020		
Aging time	τ	[a]	0.33	6.25	6.58	7.67		
Time averaged fresh food compartment temperature	T_{ma}	[°C]	5.00	5.00	5.00	5.00		
Maximum chill compartment temperature	$T_{cc,max}$	[°C]						
Maximum frozen food compartment temperature	$T_{f,max}$	[°C]						
Energy consumption at the time τ	$E(\tau)$	[kW/24h]	0.168	0.205	0.206	0.210		
Uncertainty of the energy measurement	δE	[%]	1.0	1.0	1.0	1.0		
Preliminary aging model	ΔE_0		1.000	1.102	1.108	1.129		
Corrected energy consumption immediately after production	E_p	[kW/24h]	0.183					
Aging model	ΔE_p		1.014	1.117	1.123	1.145		
Note:								

Table SM2: Results energy consumption measurements for R02.

Nr.:			R02					
Brand:			Siemens					
Type:			KI 18RA60/01					
Standard:			DIN EN ISO 15502:2006 and DIN EN 153:2006					
serial number:			258030341386000847					
Production date:			03/2008					
Storage volume (fresh food / chill / frozen food):		[l]	(155 / - / -)					
Measurement:			1	2	3	4	5	6
Date of measurement:			06/2008	05/2012				
Aging time	τ	[a]	0.25	4.17				
Time averaged fresh food compartment temperature	T_{ma}	[°C]	5.00	5.00				
Maximum chill compartment temperature	$T_{cc,max}$	[°C]						
Maximum frozen food compartment temperature	$T_{f,max}$	[°C]						
Energy consumption at the time τ	$E(\tau)$	[kW/24h]	0.266	0.329				
Uncertainty of the energy measurement	δE	[%]	3.1	1.5				
Preliminary aging model	ΔE_0		1.000	1.237				
Corrected energy consumption immediately after production	E_p	[kW/24h]	0.263					
Aging model	ΔE_p		1.011	1.250				
Note:								

Table SM3: Results energy consumption measurements for R03.

Nr.:			R03					
Brand:			Siemens					
Type:			KI81RAD30					
Standard:			IEC 62552:2013					
serial number:			258050362166024031					
Production date:			05/2018					
Storage volume (fresh food / chill / frozen food):		[l]	(319 / - / -)					
Measurement:			1	2	3	4	5	6
Date of measurement:			07/2018	11/2019	05/2020			
Aging time	τ	[a]	0.17	1.50	2.00			
Time averaged fresh food compartment temperature	T_{ma}	[°C]	4.00	4.00	4.00			
Time averaged chill compartment temperature	T_{ccma}	[°C]						
Time averaged frozen food compartment temperature	T_{fma}	[°C]						
Energy consumption at the time τ	$E(\tau)$	[kW/24h]	0.347	0.368	0.366			
Uncertainty of the energy measurement	δE	[%]	1.0	1.0	1.0			
Preliminary aging model	ΔE_0		1.000	1.061	1.055			
Corrected energy consumption immediately after production	E_p	[kW/24h]	0.345					
Aging model	ΔE_p		1.007	1.068	1.062			
Note: Also used for the investigation of the compressor aging.								

Table SM4: Results energy consumption measurements for R04.

Nr.:			R04					
Brand:			Siemens					
Type:			KI81RAD30					
Standard:			IEC 62552:2013					
serial number:			258050362166024024					
Production date:			05/2018					
Storage volume (fresh food / chill / frozen food):		[l]	(319 / - / -)					
Measurement:			1	2	3	4	5	6
Date of measurement:			07/2018	11/2019	05/2020			
Aging time	τ	[a]	0.17	1.50	2.00			
Time averaged fresh food compartment temperature	T_{ma}	[°C]	4.00	4.00	4.00			
Time averaged chill compartment temperature	T_{ccma}	[°C]						
Time averaged frozen food compartment temperature	T_{fma}	[°C]						
Energy consumption at the time τ	$E(\tau)$	[kW/24h]	0.337	0.365	0.364			
Uncertainty of the energy measurement	δE	[%]	1.0	1.0	1.0			
Preliminary aging model	ΔE_0		1.000	1.083	1.080			
Corrected energy consumption immediately after production	E_p	[kW/24h]	0.335					
Aging model	ΔE_p		1.007	1.091	1.088			
Note:								

Table SM5: Results energy consumption measurements for R05.

Nr.:			R05					
Brand:			Exquisit					
Type:			KS 16-1 RVA+++					
Standard:			IEC 62552:2013					
serial number:			VB0131Z0015JBGB71E21590					
Production date:			01/2018					
Storage volume (fresh food / chill / frozen food):		[l]	(134 / - / -)					
Measurement:			1	2	3	4	5	6
Date of measurement:			07/2018	11/2019	05/2020			
Aging time	τ	[a]	0.50	1.83	2.33			
Time averaged fresh food compartment temperature	T_{ma}	[°C]	4.00	4.00	4.00			
Time averaged chill compartment temperature	T_{ccma}	[°C]						
Time averaged frozen food compartment temperature	T_{fma}	[°C]						
Energy consumption at the time τ	$E(\tau)$	[kW/24h]	0.186	0.199	0.204			
Uncertainty of the energy measurement	δE	[%]	1.0	1.0	1.0			
Preliminary aging model	ΔE_0		1.000	1.070	1.097			
Corrected energy consumption immediately after production	E_p	[kW/24h]	0.182					
Aging model	ΔE_p		1.021	1.092	1.119			
Note:								

Table SM6: Results energy consumption measurements for R06.

Nr.:			R06					
Brand:			Exquisit					
Type:			KS 16-1 RVA+++					
Standard:			IEC 62552:2013					
serial number:			VB0131Z0015JBGB71E21589					
Production date:			01/2018					
Storage volume (fresh food / chill / frozen food):		[l]	(134 / - / -)					
Measurement:			1	2	3	4	5	6
Date of measurement:			7/2018	11/2019	05/2020			
Aging time	τ	[a]	0.50	1.83	2.33			
Time averaged fresh food compartment temperature	T_{ma}	[°C]	4.00	4.00	4.00			
Time averaged chill compartment temperature	T_{ccma}	[°C]						
Time averaged frozen food compartment temperature	T_{fma}	[°C]						
Energy consumption at the time τ	$E(\tau)$	[kW/24h]	0.183	0.198	0.201			
Uncertainty of the energy measurement	δE	[%]	1.0	1.0	1.0			
Preliminary aging model	ΔE_0		1.000	1.082	1.098			
Corrected energy consumption immediately after production	E_p	[kW/24h]	0.179					
Aging model	ΔE_p		1.021	1.104	1.1201			
Note:								

Table SM7: Results energy consumption measurements for R07.

Nr.:			R07					
Brand:			Liebherr					
Type:			KSB3640-25A Index 25A/001					
Standard:			DIN EN ISO 15502:2006 and DIN EN 153:2006					
serial number:			17.850.864.3					
Production date:			01.11.1999					
Storage volume (fresh food / chill / frozen food):		[l]	(193 / 76 / -)					
Measurement:			1	2	3	4	5	6
Date of measurement:			12/1999	01/2020	08/2020			
Aging time	τ	[a]	0.08	20.18	20.76			
Time averaged fresh food compartment temperature	T_{ma}	[°C]	5.00	5.00	5.00			
Maximum chill compartment temperature	$T_{cc,max}$	[°C]	2.10	2.92	2.98			
Maximum frozen food compartment temperature	$T_{f,max}$	[°C]						
Energy consumption at the time τ	$E(\tau)$	[kW/24h]	0.772	0.887	0.903			
Uncertainty of the energy measurement	δE	[%]	3.1	1.0	1.0			
Preliminary aging model	ΔE_0		1.000	1.149	1.170			
Corrected energy consumption immediately after production	E_p	[kW/24h]	0.769					
Aging model	ΔE_p		1.004	1.153	1.174			
Note:								

Table SM8: Results energy consumption measurements for C01.

Nr.:			C01					
Brand:			Homa					
Type:			FN2-45					
Standard:			IEC 62552:2013					
serial number:			---					
Production date:			08/2017					
Storage volume (fresh food / chill / frozen food):		[l]	(209 / - / 95)					
Measurement:			1	2	3	4	5	6
Date of measurement:			02/2018	12/2018	12/2019	08/2020		
Aging time	τ	[a]	0.50	1.33	2.33	3.00		
Time averaged fresh food compartment temperature	T_{ma}	[°C]	4.00	4.00	4.00	4.00		
Time averaged chill compartment temperature	T_{ccma}	[°C]						
Time averaged frozen food compartment temperature	T_{fma}	[°C]	-18.60	-18.13	-19.48	-18.98		
Energy consumption at the time τ	$E(\tau)$	[kW/24h]	0.507	0.518	0.552	0.559		
Uncertainty of the energy measurement	δE	[%]	1.0	1.0	1.0	1.0		
Preliminary aging model	ΔE_0		1.000	1.022	1.089	1.103		
Corrected energy consumption immediately after production	E_p	[kW/24h]	0.497					
Aging model	ΔE_p		1.021	1.043	1.112	1.126		
Note:								

Table SM9: Results energy consumption measurements for C02.

Nr.:			C02					
Brand:			Haier					
Type:			BCD-185TNGK					
Standard:			IEC 62552:2013					
serial number:			BK0YF00A800B8G4JB3RX 20160425BX33 / 4006 999 999					
Production date:			04/2016					
Storage volume (fresh food / chill / frozen food):		[l]	(128 / - / 62)					
Measurement:			1	2	3	4	5	6
Date of measurement:			12/2016	08/2019	09/2019	10/2020		
Aging time	τ	[a]	0.67	3.33	3.42	4.50		
Time averaged fresh food compartment temperature	T_{ma}	[°C]	3.80	4.00	4.00	4.00		
Time averaged chill compartment temperature	T_{ccma}	[°C]						
Time averaged frozen food compartment temperature	T_{fma}	[°C]	-18.00	-18.44	-18.50	-20.43		
Energy consumption at the time τ	$E(\tau)$	[kW/24h]	0.438	0.484	0.483	0.499		
Uncertainty of the energy measurement	δE	[%]	1.0	1.0	1.0	1.0		
Preliminary aging model	ΔE_0		1.000	1.105	1.103	1.139		
Corrected energy consumption immediately after production	E_p	[kW/24h]	0.426					
Aging model	ΔE_p		1.028	1.136	1.133	1.171		
Note:								

Table SM10: Results energy consumption measurements for C03.

Nr.:			C03					
Brand:			Haier					
Type:			A3FE742CMJ					
Standard:			IEC 62552:2013					
serial number:			BB09W0E9P00BDG3U0004					
Production date:			28.03.2016					
Storage volume (fresh food / chill / frozen food):		[l]	(280 / 34 / 155)					
Measurement:			1	2	3	4	5	6
Date of measurement:			12/2016	08/2019	10/2020			
Aging time	τ	[a]	0.68	3.35	4.52			
Time averaged fresh food compartment temperature	T_{ma}	[°C]	3.98	3.74	3.21			
Time averaged chill compartment temperature	T_{ccma}	[°C]	0.48	0.05	0.30			
Time averaged frozen food compartment temperature	T_{fma}	[°C]	-18.00	-18.00	-1800			
Energy consumption at the time τ	$E(\tau)$	[kW/24h]	0.700	0.762	0.792			
Uncertainty of the energy measurement	δE	[%]	1.0	1.0	1.0			
Preliminary aging model	ΔE_0		1.000	1.189	1.131			
Corrected energy consumption immediately after production	E_p	[kW/24h]	0.681					
Aging model	ΔE_p		1.028	1.119	1.163			
Note:								

Table SM11: Results energy consumption measurements for C04.

Nr.:			C04					
Brand:			Profilo					
Type:			BD2058L3AV					
Standard:			DIN EN ISO 15502 and DIN EN 153					
serial number:			222050620687000000					
Production date:			05/2012					
Storage volume (fresh food / chill / frozen food):		[l]	(400 / - / 110)					
Measurement:			1	2	3	4	5	6
Date of measurement:			08/2012	03/2019				
Aging time	τ	[a]	0.25	6.84				
Time averaged fresh food compartment temperature	T_{ma}	[°C]	5.00	5.00				
Maximum chill compartment temperature	$T_{cc,max}$	[°C]						
Maximum frozen food compartment temperature	$T_{f,max}$	[°C]	-18.52	-18.29				
Energy consumption at the time τ	$E(\tau)$	[kW/24h]	0.696	0.736				
Uncertainty of the energy measurement	δE	[%]	1.0	1.0				
Preliminary aging model	ΔE_0		1.000	1.057				
Corrected energy consumption immediately after production	E_p	[kW/24h]	0.689					
Aging model	ΔE_p		1.101	1.069				
Note:								

Table SM12: Results energy consumption measurements for C05.

Nr.:			C05					
Brand:			Siemens					
Type:			KG39EAI40					
Standard:			According DIN EN ISO 15502 and DIN EN 153					
serial number:			101775					
Production date:			11/2011					
Storage volume (fresh food / chill / frozen food):		[l]	(247 / - / 92)					
Measurement:			1	2	3	4	5	6
Date of measurement:			09/2012	08/2013	09/2014	07/2015		
Aging time	τ	[a]	0.84	1.75	2.84	3.67		
Time averaged fresh food compartment temperature	T_{ma}	[°C]	4.82	5.00	5.00	5.00		
Maximum chill compartment temperature	$T_{cc,max}$	[°C]						
Maximum frozen food compartment temperature	$T_{f,max}$	[°C]	-18.00	-18.24	-18.57	-18.81		
Energy consumption at the time τ	$E(\tau)$	[kW/24h]	0.440	0.452	0.460	0.473		
Uncertainty of the energy measurement	δE	[%]	1.0	1.0	1.0	1.0		
Preliminary aging model	ΔE_0		1.000	1.027	1.045	1.075		
Corrected energy consumption immediately after production	E_p	[kW/24h]	0.425					
Aging model	ΔE_p		1.034	1.063	1.081	1.112		
Note: With drawers in frozen food compartment.								

Table SM13: Results energy consumption measurements for C06.

Nr.:			C06					
Brand:			Liebherr					
Type:			CBNPes 3756 Index 20B / 001					
Standard:			According DIN EN ISO 15502 and DIN EN 153					
serial number:			28.646.416.9					
Production date:			12.12.2011					
Storage volume (fresh food / chill / frozen food):		[l]	(207 / 67 / 89)					
Measurement:			1	2	3	4	5	6
Date of measurement:			02/2012	05/2012	04/2019			
Aging time	τ	[a]	0.14	0.39	7.31			
Time averaged fresh food compartment temperature	T_{ma}	[°C]	5.00	5.00	4.83			
Maximum chill compartment temperature	$T_{cc,max}$	[°C]	2.92	3.23	2.92			
Maximum frozen food compartment temperature	$T_{f,max}$	[°C]	-18.08	-18.23	-18.00			
Energy consumption at the time τ	$E(\tau)$	[kW/24h]	0.529	0.513	0.598			
Uncertainty of the energy measurement	δE	[%]	1.0	1.0	1.0			
Preliminary aging model	ΔE_0		1.000	0.970	1.130			
Corrected energy consumption immediately after production	E_p	[kW/24h]	0.526					
Aging model	ΔE_p		1.034	0.975	1.137			
Note: With drawers in frozen food compartment.								

Table SM14: Results energy consumption measurements for C07.

Nr.:			C07					
Brand:			Liebherr					
Type:			CUPesf 3503 Index 21A/001					
Standard:			According DIN EN ISO 15502 and DIN EN 153					
serial number:			44.482.126.1					
Production date:			18.08.2011					
Storage volume (fresh food / chill / frozen food):		[l]	(232 / - / 91)					
Measurement:			1	2	3	4	5	6
Date of measurement:			02/2012	09/2012	08/2013	09/2014	07/2015	02/2020
Aging time	τ	[a]	0.46	1.05	1.96	3.05	3.88	8.47
Time averaged fresh food compartment temperature	T_{ma}	[°C]	5.00	5.00	5.00	5.00	5.00	5.00
Maximum chill compartment temperature	$T_{cc,max}$	[°C]						
Maximum frozen food compartment temperature	$T_{f,max}$	[°C]	-19.19	-18.44	-18.32	-18.44	-18.37	-18.89
Energy consumption at the time τ	$E(\tau)$	[kW/24h]	0.604	0.594	0.622	0.638	0.655	0.682
Uncertainty of the energy measurement	δE	[%]	1.0	1.0	1.0	1.0	1.0	1.0
Preliminary aging model	ΔE_0		1.000	0.983	1.030	1.056	1.084	1.129
Corrected energy consumption immediately after production	E_p	[kW/24h]	0.593					
Aging model	ΔE_p		1.019	1.002	1.050	1.077	1.105	1.151
Note: With drawers in frozen food compartment.								

Table SM15: Results energy consumption measurements for C08.

Nr.:			C08					
Brand:			Miele					
Type:			KD 12622 S edt/cs					
Standard:			According DIN EN ISO 15502 and DIN EN 153					
serial number:			120016542					
Production date:			13.05.2011					
Storage volume (fresh food / chill / frozen food):		[l]	(199 / - / 54)					
Measurement:			1	2	3	4	5	6
Date of measurement:			02/2012	09/2012	08/2013	09/2014	04/2019	07/2019
Aging time	τ	[a]	9	16	27	40	95	98
Time averaged fresh food compartment temperature	T_{ma}	[°C]	4.00	4.00	4.00	4.00	4.00	4.00
Maximum chill compartment temperature	$T_{cc,max}$	[°C]						
Maximum frozen food compartment temperature	$T_{f,max}$	[°C]	-17.20	-16.59	-16.84	-17.04	-18.33	-18.02
Energy consumption at the time τ	$E(\tau)$	[kW/24h]	0.547	0.582	0.595	0.639	0.665	0.664
Uncertainty of the energy measurement	δE	[%]	1.0	1.0	1.0	1.0	1.0	1.0
Preliminary aging model	ΔE_0		1.000	1.064	1.088	1.168	1.216	1.214
Corrected energy consumption immediately after production	E_p	[kW/24h]	0.531					
Aging model	ΔE_p		1.031	1.097	1.121	1.204	1.253	1.251
Note: With drawers in frozen food compartment.								
Strong fluctuations in the frozen food compartment temperatures during the measurements, therefore a uniform interpolation of 4 °C in the fresh food compartment was chosen.								

Table SM16: Results energy consumption measurements for C09.

Nr.:			C09					
Brand:			Bosch					
Type:			KGN34A13					
Standard:			DIN EN ISO 15502 and DIN EN 153					
serial number:			100063					
Production date:			03/2009					
Storage volume (fresh food / chill / frozen food):		[l]	(189 / - / 94)					
Measurement:			1	2	3	4	5	6
Date of measurement:			10/2009	03/2019				
Aging time	τ	[a]	0.59	10.00				
Time averaged fresh food compartment temperature	T_{ma}	[°C]	4.30	4.55				
Maximum chill compartment temperature	$T_{cc,max}$	[°C]						
Maximum frozen food compartment temperature	$T_{f,max}$	[°C]	-18.00	-18.00				
Energy consumption at the time τ	$E(\tau)$	[kW/24h]	0.753	0.885				
Uncertainty of the energy measurement	δE	[%]	1.5	1.0				
Preliminary aging model	ΔE_0		1.000	1.175				
Corrected energy consumption immediately after production	E_p	[kW/24h]	0.735					
Aging model	ΔE_p		1.024	1.204				
Note:								

Table SM17: Results energy consumption measurements for C10.

Nr.:			C10					
Brand:			Bauknecht					
Type:			KV Optima/1					
Standard:			DIN EN ISO 15502 and DIN EN 153					
serial number:			500208008183					
Production date:			04/2002					
Storage volume (fresh food / chill / frozen food):		[l]	(217 / - / 22)					
Measurement:			1	2	3	4	5	6
Date of measurement:			06/2002	05/2012				
Aging time	τ	[a]	0.17	10.09				
Time averaged fresh food compartment temperature	T_{ma}	[°C]	3.72	3.52				
Maximum chill compartment temperature	$T_{cc,max}$	[°C]						
Maximum frozen food compartment temperature	$T_{f,max}$	[°C]	-18.00	-18.00				
Energy consumption at the time τ	$E(\tau)$	[kW/24h]	0.493	0.567				
Uncertainty of the energy measurement	δE	[%]	2.0	1.5				
Preliminary aging model	ΔE_0		1.000	1.150				
Corrected energy consumption immediately after production	E_p	[kW/24h]	0.490					
Aging model	ΔE_p		1.007	1.158				
Note:								

Table SM18: Results energy consumption measurements for C11.

Nr.:			C11					
Brand:			Siemens					
Type:			KT 15 L 03-02					
Standard:			DIN EN ISO 15502 and DIN EN 153					
serial number:			070165786					
Production date:			09/1993					
Storage volume (fresh food / chill / frozen food):		[l]	(140 / - / 19)					
Measurement:			1	2	3	4	5	6
Date of measurement:			04/1994	08/1997	05/2012			
Aging time	τ	[a]	0.58	3.92	18.68			
Time averaged fresh food compartment temperature	T_{ma}	[°C]	5.00	5.00	5.00			
Maximum chill compartment temperature	$T_{cc,max}$	[°C]						
Maximum frozen food compartment temperature	$T_{f,max}$	[°C]	-18.40	-19.75	-18.98			
Energy consumption at the time τ	$E(\tau)$	[kW/24h]	0.741	0.911	0.981			
Uncertainty of the energy measurement	δE	[%]	3.3	3.1	2.2			
Preliminary aging model	ΔE_0		1.000	1.229	1.324			
Corrected energy consumption immediately after production	E_p	[kW/24h]	0.724					
Aging model	ΔE_p		1.024	1.259	1.356			
Note:								

Table SM19: Results energy consumption measurements for C12.

Nr.:			C12					
Brand:			Siemens					
Type:			KT 15 L 04-03					
Standard:			DIN EN ISO 15502 and DIN EN 153					
serial number:			0701165799					
Production date:			01/1994					
Storage volume (fresh food / chill / frozen food):		[l]	(140 / - / 19)					
Measurement:			1	2	3	4	5	6
Date of measurement:			04/1994	05/2012				
Aging time	τ	[a]	0.25	18.34				
Time averaged fresh food compartment temperature	T_{ma}	[°C]	4.50	5.00				
Maximum chill compartment temperature	$T_{cc,max}$	[°C]						
Maximum frozen food compartment temperature	$T_{f,max}$	[°C]	-18.00	-18.89				
Energy consumption at the time τ	$E(\tau)$	[kW/24h]	0.729	0.926				
Uncertainty of the energy measurement	δE	[%]	3.0	2.3				
Preliminary aging model	ΔE_0		1.000	1.271				
Corrected energy consumption immediately after production	E_p	[kW/24h]	0.721					
Aging model	ΔE_p		1.010	1.284				
Note:								

Table SM20: Results energy consumption measurements for C13.

Nr.:			C13					
Brand:			Siemens					
Type:			KI86SAD40					
Standard:			IEC 62552:2013					
serial number:			258050361208002136					
Production date:			05/2018					
Storage volume (fresh food / chill / frozen food):		[l]	(188 / - / 74)					
Measurement:			1	2	3	4	5	6
Date of measurement:			07/2018	11/2019	05/2020			
Aging time	τ	[a]	0.17	1.50	2.00			
Time averaged fresh food compartment temperature	T_{ma}	[°C]	4.00	4.00	4.00			
Time averaged chill compartment temperature	T_{ccma}	[°C]						
Time averaged frozen food compartment temperature	T_{fma}	[°C]	-18.43	-18.30	-18.28			
Energy consumption at the time τ	$E(\tau)$	[kW/24h]	0.382	0.399	0.400			
Uncertainty of the energy measurement	δE	[%]	1.0	1.0	1.0			
Preliminary aging model	ΔE_0		1.000	1.045	1.047			
Corrected energy consumption immediately after production	E_p	[kW/24h]	0.379					
Aging model	ΔE_p		1.007	1.052	1.054			
Note:								

Table SM21: Results energy consumption measurements for C14.

Nr.:			C14					
Brand:			Siemens					
Type:			KI86SAD40					
Standard:			IEC 62552:2013					
serial number:			258050361208002112					
Production date:			05/2018					
Storage volume (fresh food / chill / frozen food):		[l]	(188 / - / 74)					
Measurement:			1	2	3	4	5	6
Date of measurement:			07/2018	11/2019	05/2020			
Aging time	τ	[a]	0.17	1.50	2.00			
Time averaged fresh food compartment temperature	T_{ma}	[°C]	4.00	4.00	4.00			
Time averaged chill compartment temperature	T_{ccma}	[°C]						
Time averaged frozen food compartment temperature	T_{fma}	[°C]	-18.61	-18.51	-18.61			
Energy consumption at the time τ	$E(\tau)$	[kW/24h]	0.373	0.395	0.393			
Uncertainty of the energy measurement	δE	[%]	1.0	1.0	1.0			
Preliminary aging model	ΔE_0		1.000	1.059	1.054			
Corrected energy consumption immediately after production	E_p	[kW/24h]	0.370					
Aging model	ΔE_p		1.007	1.066	1.061			
Note:								

Table SM22: Results energy consumption measurements for C15.

Nr.:			C15					
Brand:			Bosch					
Type:			KIS86AF30					
Standard:			IEC 62552:2013					
serial number:			258050270702003634					
Production date:			05/2018					
Storage volume (fresh food / chill / frozen food):		[l]	(191 / - / 74)					
Measurement:			1	2	3	4	5	6
Date of measurement:			07/2018	11/2019	05/2020			
Aging time	τ	[a]	0.17	1.50	2.00			
Time averaged fresh food compartment temperature	T_{ma}	[°C]	4.00	4.00	4.00			
Time averaged chill compartment temperature	T_{ccma}	[°C]						
Time averaged frozen food compartment temperature	T_{fma}	[°C]	-18.59	-18.64	-18.72			
Energy consumption at the time τ	$E(\tau)$	[kW/24h]	0.568	0.594	0.601			
Uncertainty of the energy measurement	δE	[%]	1.0	1.0	1.0			
Preliminary aging model	ΔE_0		1.000	1.046	1.058			
Corrected energy consumption immediately after production	E_p	[kW/24h]	0.564					
Aging model	ΔE_p		1.007	1.053	1.066			
Note:								

Table SM23: Results energy consumption measurements for C16.

Nr.:			C16					
Brand:			Bosch					
Type:			KIS86AF30					
Standard:			IEC 62552:2013					
serial number:			258050270702003627					
Production date:			05/2018					
Storage volume (fresh food / chill / frozen food):		[l]	(191 / - / 74)					
Measurement:			1	2	3	4	5	6
Date of measurement:			07/2018	11/2019	05/2020			
Aging time	τ	[a]	0.17	1.50	2.00			
Time averaged fresh food compartment temperature	T_{ma}	[°C]	4.00	4.00	4.00			
Time averaged chill compartment temperature	T_{ccma}	[°C]						
Time averaged frozen food compartment temperature	T_{fma}	[°C]	-18.66	-18.67	-18.50			
Energy consumption at the time τ	$E(\tau)$	[kW/24h]	0.571	0.597	0.604			
Uncertainty of the energy measurement	δE	[%]	1.0	1.0	1.0			
Preliminary aging model	ΔE_0		1.000	1.046	1.058			
Corrected energy consumption immediately after production	E_p	[kW/24h]	0.567					
Aging model	ΔE_p		1.007	1.053	1.065			
Note:								

Table SM24: Results energy consumption measurements for C17.

Nr.:			C17					
Brand:			LG					
Type:			GBB 60 NSZHE					
Standard:			IEC 62552:2013					
serial number:			802WRHNKX137					
Production date:			02/2018					
Storage volume (fresh food / chill / frozen food):		[l]	(223 / 27 / 93)					
Measurement:			1	2	3	4	5	6
Date of measurement:			07/2018	11/2019	05/2020			
Aging time	τ	[a]	0.41	1.75	2.25			
Time averaged fresh food compartment temperature	T_{ma}	[°C]	4.00	4.00	4.00			
Time averaged chill compartment temperature	T_{ccma}	[°C]	0.49	0.49	0.44			
Time averaged frozen food compartment temperature	T_{fma}	[°C]	-18.18	-18.09	-18.09			
Energy consumption at the time τ	$E(\tau)$	[kW/24h]	0.325	0.330	0.330			
Uncertainty of the energy measurement	δE	[%]	1.0	1.0	1.0			
Preliminary aging model	ΔE_0		1.000	1.015	1.015			
Corrected energy consumption immediately after production	E_p	[kW/24h]	0.320					
Aging model	ΔE_p		1.017	1.033	1.033			
Note:								

Table SM25: Results energy consumption measurements for F01.

Nr.:			F01					
Brand:			Exquisit					
Type:			GS 270 NFA+					
Standard:			DIN EN ISO 15502 and DIN EN 153					
serial number:			VB0188 00004D JN11ZS4 0071					
Production date:			05.02.2010					
Storage volume (fresh food / chill / frozen food):		[l]	(- / - / 188)					
Measurement:			1	2	3	4	5	6
Date of measurement:			04/2011	03/2019				
Aging time	τ	[a]	1.15	7.92				
Time averaged fresh food compartment temperature	T_{ma}	[°C]						
Maximum chill compartment temperature	$T_{cc,max}$	[°C]						
Maximum frozen food compartment temperature	$T_{f,max}$	[°C]	-18.00	-18.00				
Energy consumption at the time τ	$E(\tau)$	[kW/24h]	0.729	0.903				
Uncertainty of the energy measurement	δE	[%]	1.5	1.0				
Preliminary aging model	ΔE_0		1.000	1.239				
Corrected energy consumption immediately after production	E_p	[kW/24h]	0.696					
Aging model	ΔE_p		1.047	1.297				
Note:								

Table SM26: Results energy consumption measurements for F02.

Nr.:			F02					
Brand:			Samsung					
Type:			Rz80eepn					
Standard:			DIN EN ISO 15502 and DIN EN 153					
serial number:			D01741AS600007 L					
Production date:			07/2009					
Storage volume (fresh food / chill / frozen food):		[l]	(- / - / 277)					
Measurement:			1	2	3	4	5	6
Date of measurement:			10/2009	05/2012				
Aging time	τ	[a]	0.33	2.92				
Time averaged fresh food compartment temperature	T_{ma}	[°C]						
Maximum chill compartment temperature	$T_{cc,max}$	[°C]						
Maximum frozen food compartment temperature	$T_{f,max}$	[°C]	-18.00	-18.00				
Energy consumption at the time τ	$E(\tau)$	[kW/24h]	1.068	1.186				
Uncertainty of the energy measurement	δE	[%]	2.1	1.5				
Preliminary aging model	ΔE_0		1.000	1.110				
Corrected energy consumption immediately after production	E_p	[kW/24h]	1.054					
Aging model	ΔE_p		1.014	1.126				
Note:								

Table SM27: Results energy consumption measurements for F03.

Nr.:			F03					
Brand:			Liebherr					
Type:			GS1784 03 00511					
Standard:			According DIN EN ISO 15502 and DIN EN 153					
serial number:			12.639.240.9					
Production date:			22.11.1993					
Storage volume (fresh food / chill / frozen food):		[l]	(- / - / 125)					
Measurement:			1	2	3	4	5	6
Date of measurement:			04/1994	08/1997	05/2012			
Aging time	τ	[a]	0.36	3.69	18.45			
Time averaged fresh food compartment temperature	T_{ma}	[°C]						
Maximum chill compartment temperature	$T_{cc,max}$	[°C]						
Maximum frozen food compartment temperature	$T_{f,max}$	[°C]	-18.00	-18.00	-18.00			
Energy consumption at the time τ	$E(\tau)$	[kW/24h]	0.951	1.058	1.170			
Uncertainty of the energy measurement	δE	[%]	2.6	2.4	2.2			
Preliminary aging model	ΔE_0		1.000	1.112	1.231			
Corrected energy consumption immediately after production	E_p	[kW/24h]	0.937					
Aging model	ΔE_p		1.015	1.129	1.249			
Note: With drawers in frozen food compartment.								

Table SM28: Results energy consumption measurements for F04.

Nr.:			F04					
Brand:			Liebherr					
Type:			GS1784 03 00711					
Standard:			According DIN EN ISO 15502 and DIN EN 153					
serial number:			12.729.489.4					
Production date:			17.01.1994					
Storage volume (fresh food / chill / frozen food):		[l]	(- / - / 125)					
Measurement:			1	2	3	4	5	6
Date of measurement:			04/1994	08/1997	05/2012			
Aging time	τ	[a]	0.20	3.54	18.30			
Time averaged fresh food compartment temperature	T_{ma}	[°C]						
Maximum chill compartment temperature	$T_{cc,max}$	[°C]						
Maximum frozen food compartment temperature	$T_{f,max}$	[°C]	-18.00	-18.00	-18.00			
Energy consumption at the time τ	$E(\tau)$	[kW/24h]	0.849	0.953	1.096			
Uncertainty of the energy measurement	δE	[%]	2.6	2.4	1.8			
Preliminary aging model	ΔE_0		1.000	1.123	1.290			
Corrected energy consumption immediately after production	E_p	[kW/24h]	0.842					
Aging model	ΔE_p		1.009	1.132	1.301			
Note: With drawers in frozen food compartment.								

Table SM29: Results energy consumption measurements for F05.

Nr.:			F05					
Brand:			Foron					
Type:			GS11.1.7.					
Standard:			According DIN EN ISO 15502 and DIN EN 153					
serial number:			401000535					
Production date:			12/1993					
Storage volume (fresh food / chill / frozen food):		[l]	(- / - / 91)					
Measurement:			1	2	3	4	5	6
Date of measurement:			04/1994	08/1997	05/2012			
Aging time	τ	[a]	0.33	3.67	18.43			
Time averaged fresh food compartment temperature	T_{ma}	[°C]						
Maximum chill compartment temperature	$T_{cc,max}$	[°C]						
Maximum frozen food compartment temperature	$T_{f,max}$	[°C]	-18.00	-18.00	-18.00			
Energy consumption at the time τ	$E(\tau)$	[kW/24h]	1.011	1.241	1.340			
Uncertainty of the energy measurement	δE	[%]	2.3	2.9	1.7			
Preliminary aging model	ΔE_0		1.000	1.228	1.325			
Corrected energy consumption immediately after production	E_p	[kW/24h]	0.997					
Aging model	ΔE_p		1.014	1.245	1.344			
Note: With drawers in frozen food compartment.								

Table SM30: Results energy consumption measurements for F06.

Nr.:			F06					
Brand:			Siemens					
Type:			GS36NVW3V					
Standard:			According IEC 62552:2013					
serial number:			508050381845002197					
Production date:			05/2018					
Storage volume (fresh food / chill / frozen food):		[l]	(- / - / 242)					
Measurement:			1	2	3	4	5	6
Date of measurement:			07/2018	11/2019	05/2020			
Aging time	τ	[a]	0.17	1.50	2.00			
Time averaged fresh food compartment temperature	T_{ma}	[°C]						
Time averaged chill compartment temperature	T_{ccma}	[°C]						
Time averaged frozen food compartment temperature	T_{fma}	[°C]	-20.00	-20.00	-20.00			
Energy consumption at the time τ	$E(\tau)$	[kW/24h]	0.581	0.616	0.615			
Uncertainty of the energy measurement	δE	[%]	1.0	1.0	1.0			
Preliminary aging model	ΔE_0		1.000	1.060	1.059			
Corrected energy consumption immediately after production	E_p	[kW/24h]	0.577					
Aging model	ΔE_p		1.007	1.068	1.066			
Note: Interpolation to -20 °C as target time averaged frozen food compartment temperature. Also used for the investigation of the compressor aging.								

Table SM31: Results energy consumption measurements for F07.

Nr.:			F07					
Brand:			Siemens					
Type:			GS36NVW3V					
Standard:			According IEC 62552:2013					
serial number:			508050381845002173					
Production date:			05/2018					
Storage volume (fresh food / chill / frozen food):		[l]	(- / - / 242)					
Measurement:			1	2	3	4	5	6
Date of measurement:			07/2018	11/2019	05/2020			
Aging time	τ	[a]	0.17	1.50	2.00			
Time averaged fresh food compartment temperature	T_{ma}	[°C]						
Time averaged chill compartment temperature	T_{ccma}	[°C]						
Time averaged frozen food compartment temperature	T_{fma}	[°C]	-20.00	-20.00	-20.00			
Energy consumption at the time τ	$E(\tau)$	[kW/24h]	0.602	0.629	0.637			
Uncertainty of the energy measurement	δE	[%]	1.0	1.0	1.0			
Preliminary aging model	ΔE_0		1.000	1.045	1.058			
Corrected energy consumption immediately after production	E_p	[kW/24h]	0.598					
Aging model	ΔE_p		1.007	1.052	1.066			
Note: Interpolation to -20 °C as target time averaged frozen food compartment temperature.								

Table SM32: Results energy consumption measurements for F08.

Nr.:			F08					
Brand:			Homa					
Type:			BD1-145					
Standard:			IEC 62552:2013					
serial number:			---					
Production date:			10/2017					
Storage volume (fresh food / chill / frozen food):		[l]	(- / - / 145)					
Measurement:			1	2	3	4	5	6
Date of measurement:			02/2018	12/2018	12/2019	08/2020		
Aging time	τ	[a]	0.33	1.17	2.17	2.84		
Time averaged fresh food compartment temperature	T_{ma}	[°C]						
Time averaged chill compartment temperature	T_{ccma}	[°C]						
Time averaged frozen food compartment temperature	T_{fma}	[°C]	-18.00	-18.00	-18.00	-18.00		
Energy consumption at the time τ	$E(\tau)$	[kW/24h]	0.462	0.473	0.481	0.489		
Uncertainty of the energy measurement	δE	[%]	1.0	1.0	1.0	1.0		
Preliminary aging model	ΔE_0		1.000	1.024	1.041	1.058		
Corrected energy consumption immediately after production	E_p	[kW/24h]	0.456					
Aging model	ΔE_p		1.014	1.038	1.056	1.073		
Note:								

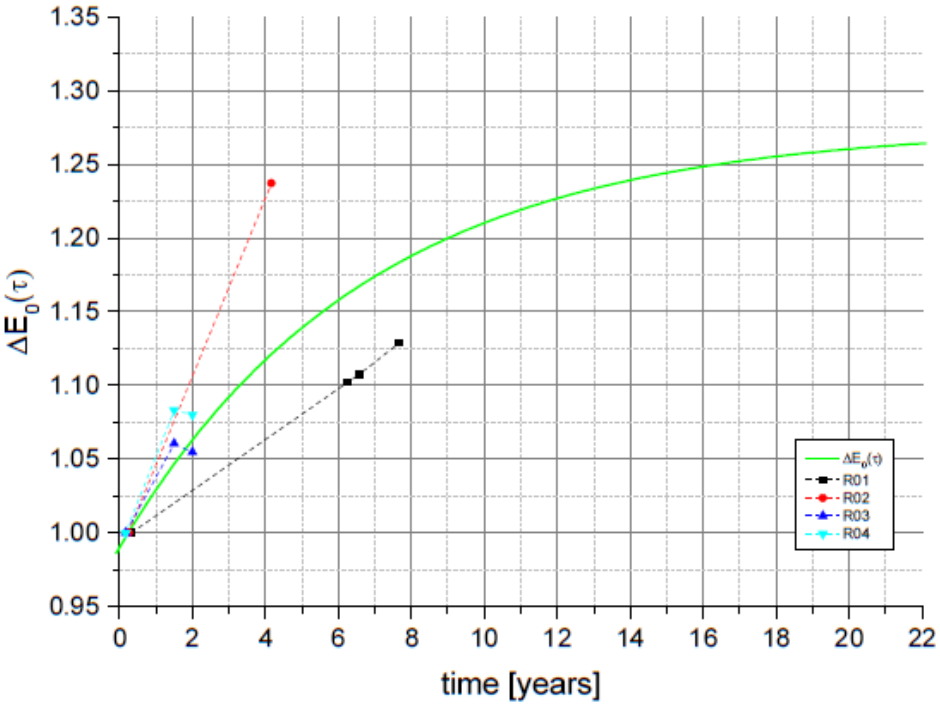

Figure SM1: Normalized energy consumption for the appliances R01 to R04 (symbols) and preliminary aging function (line).

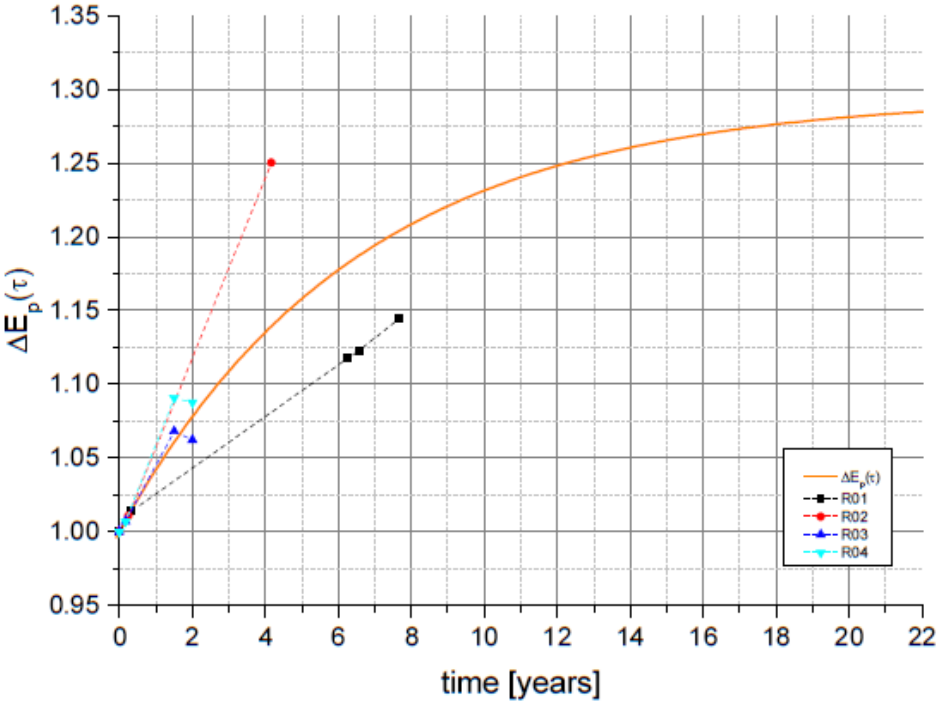

Figure SM2: Corrected energy consumption for the appliances R01 to R04 (symbols) and consolidated aging function $\Delta E_p(\tau)$ (line).

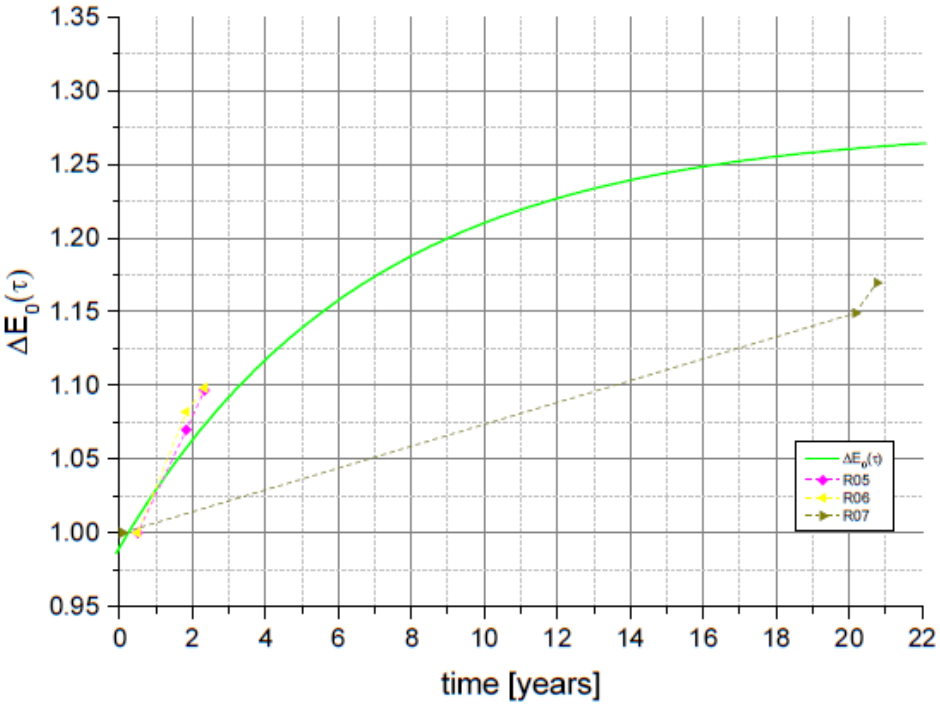

Figure SM3: Normalized energy consumption for the appliances R05 to R07 (symbols) and preliminary aging function (line).

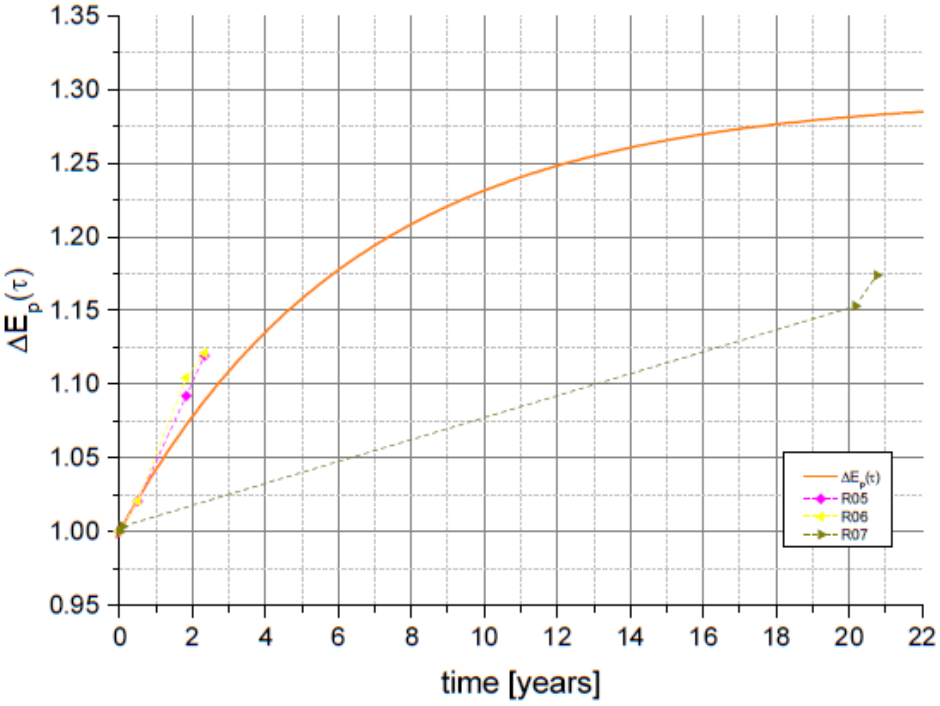

Figure SM4: Corrected energy consumption for the appliances R05 to R07 (symbols) and consolidated aging function $\Delta E_p(\tau)$ (line).

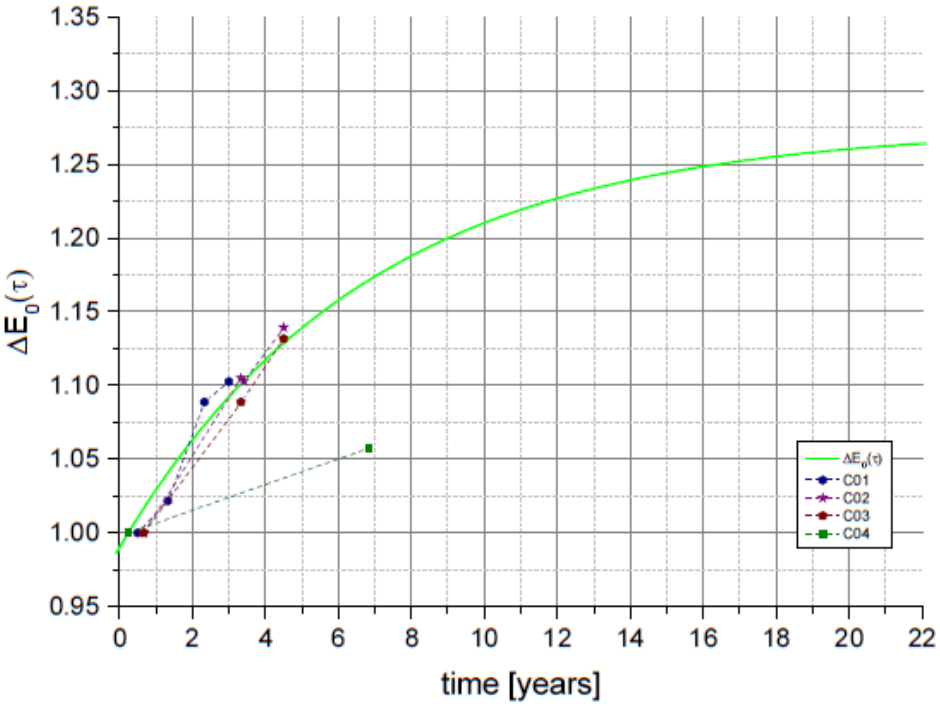

Figure SM5: Normalized energy consumption for the appliances C01 to C04 (symbols) and preliminary aging function (line).

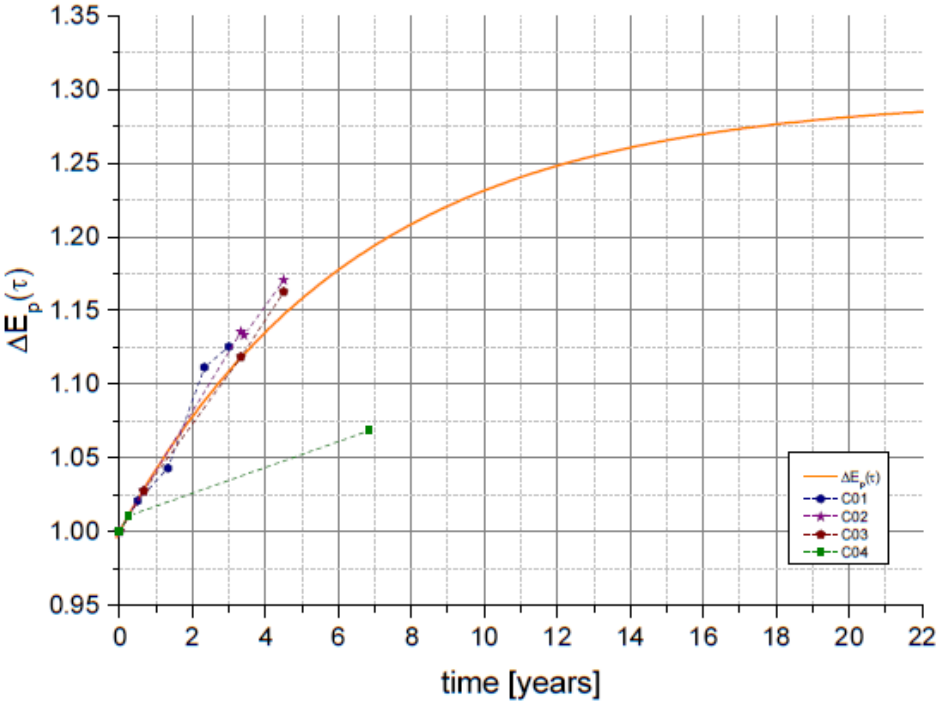

Figure SM6: Corrected energy consumption for the appliances C01 to C04 (symbols) and consolidated aging function $\Delta E_p(\tau)$ (line).

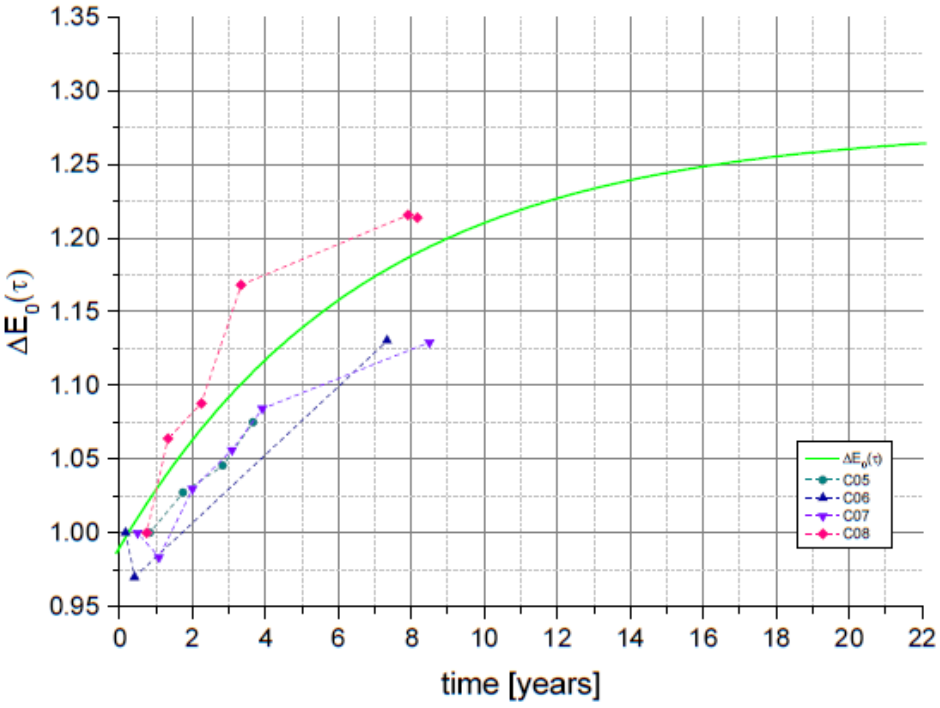

Figure SM7: Normalized energy consumption for the appliances C05 to C08 (symbols) and preliminary aging function (line).

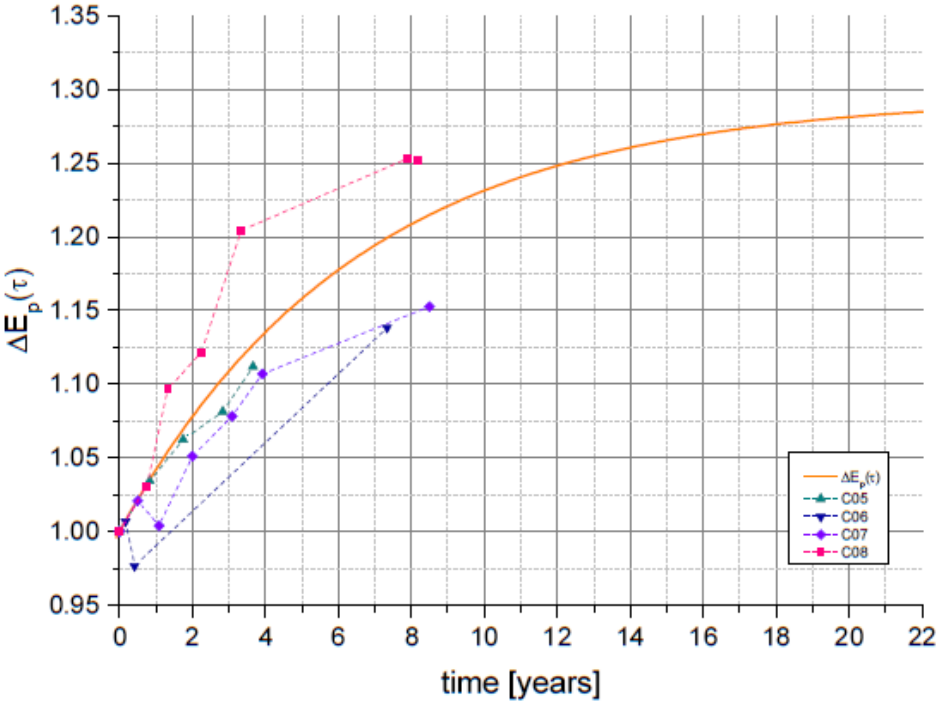

Figure SM8: Corrected energy consumption for the appliances C05 to C08 (symbols) and consolidated aging function $\Delta E_p(\tau)$ (line).

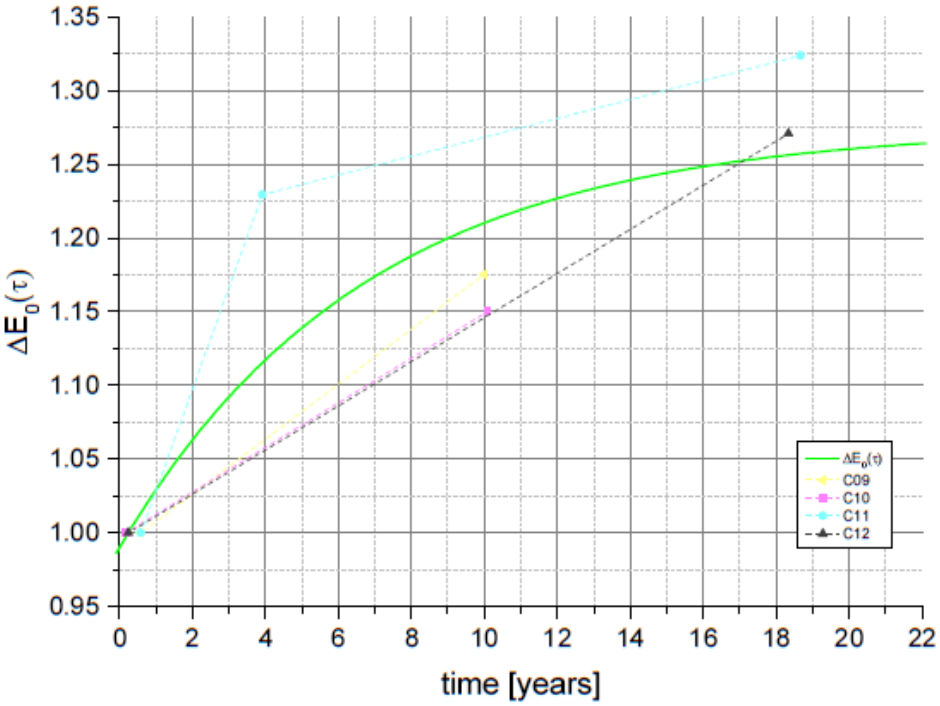

Figure SM9: Normalized energy consumption for the appliances C09 to C12 (symbols) and preliminary aging function (line).

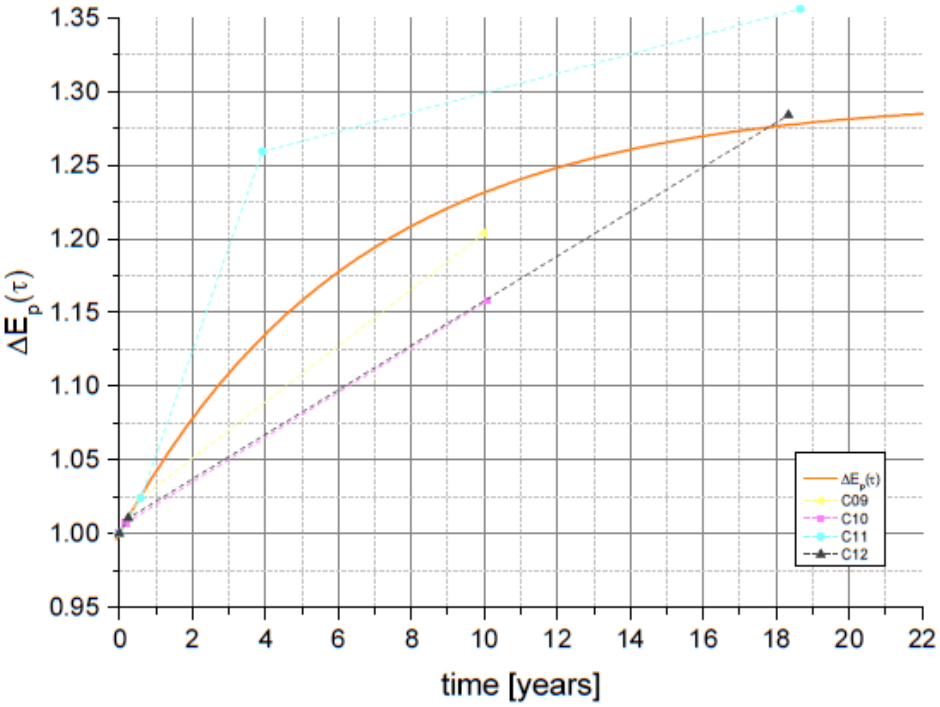

Figure SM10: Corrected energy consumption for the appliances C09 to C12 (symbols) and consolidated aging function $\Delta E_p(\tau)$ (line).

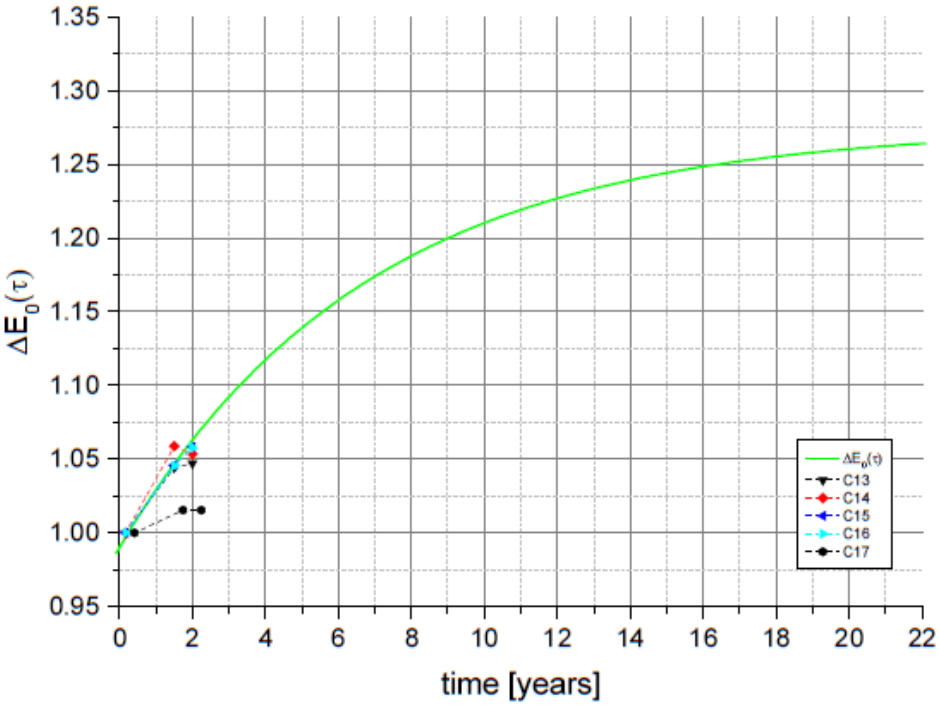

Figure SM11: Normalized energy consumption for the appliances C13 to C17 (symbols) and preliminary aging function (line).

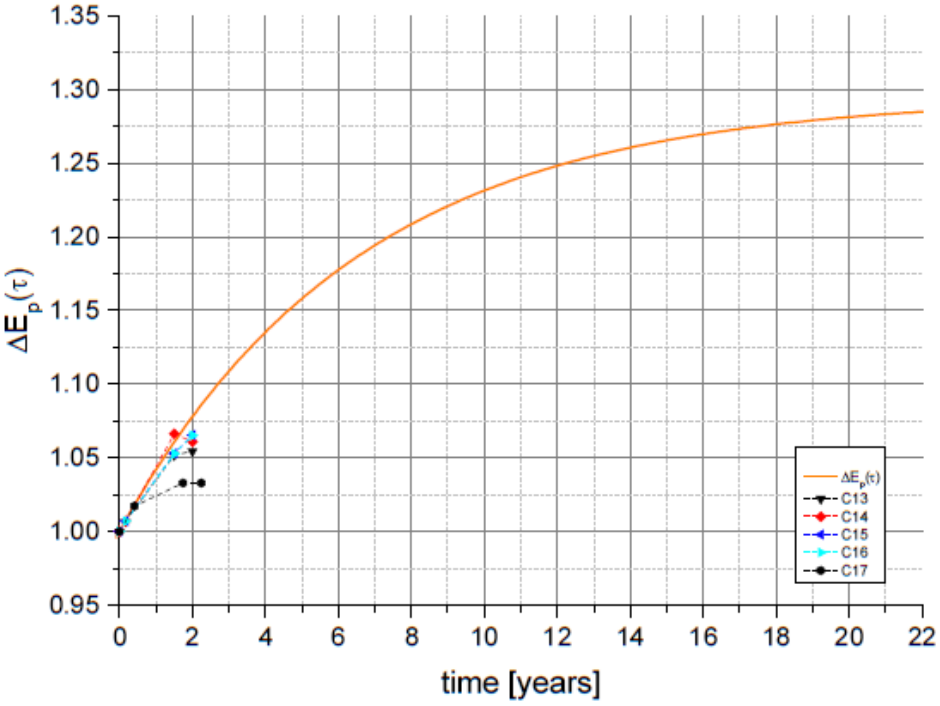

Figure SM12: Corrected energy consumption for the appliances C13 to C17 (symbols) and consolidated aging function $\Delta E_p(\tau)$ (line).

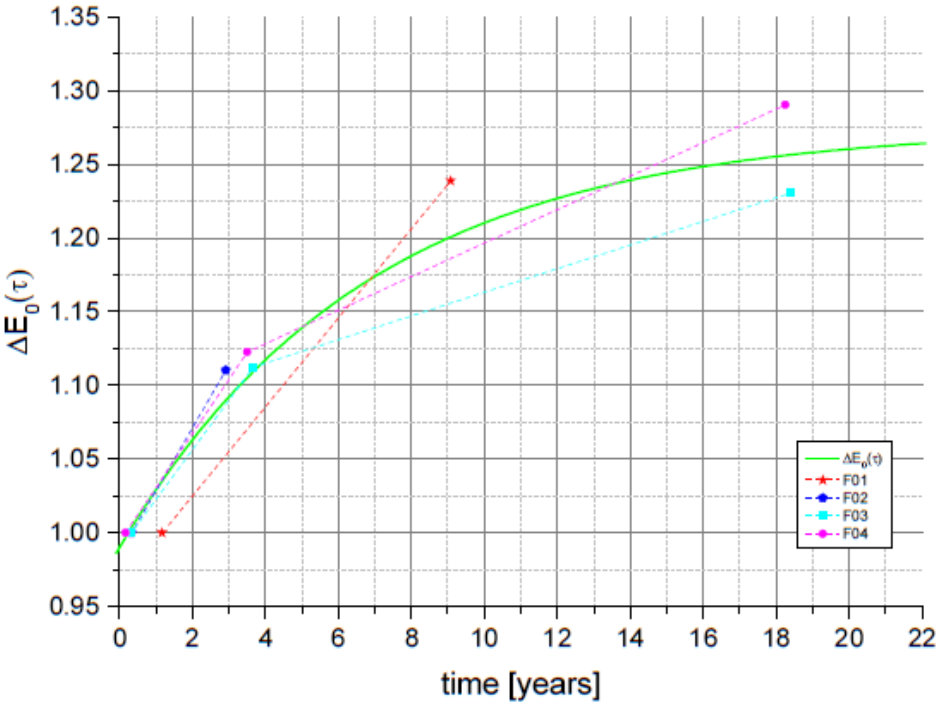

Figure SM13: Normalized energy consumption for the appliances F01 to F04 (symbols) and preliminary aging function (line).

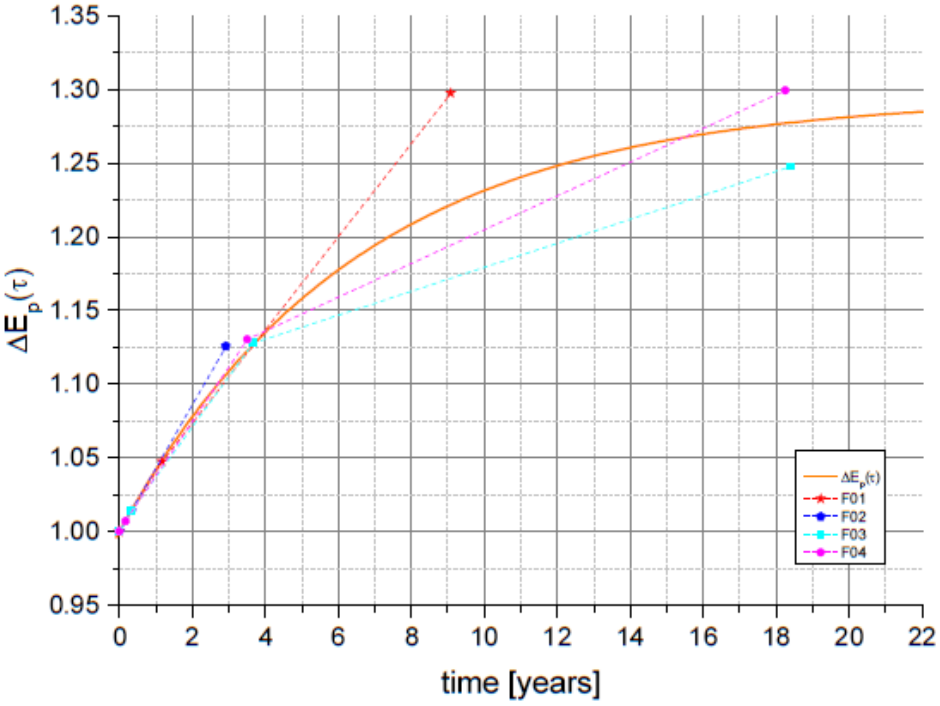

Figure SM14: Corrected energy consumption for the appliances F01 to F04 (symbols) and consolidated aging function $\Delta E_p(\tau)$ (line).

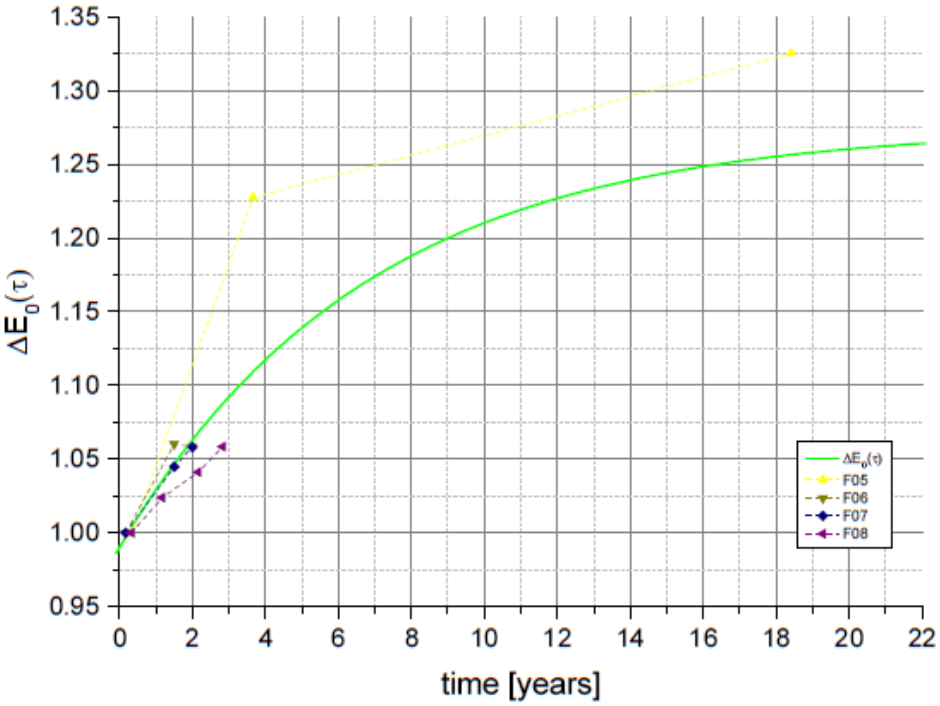

Figure SM15: Normalized energy consumption for the appliances F05 to F08 (symbols) and preliminary aging function (line).

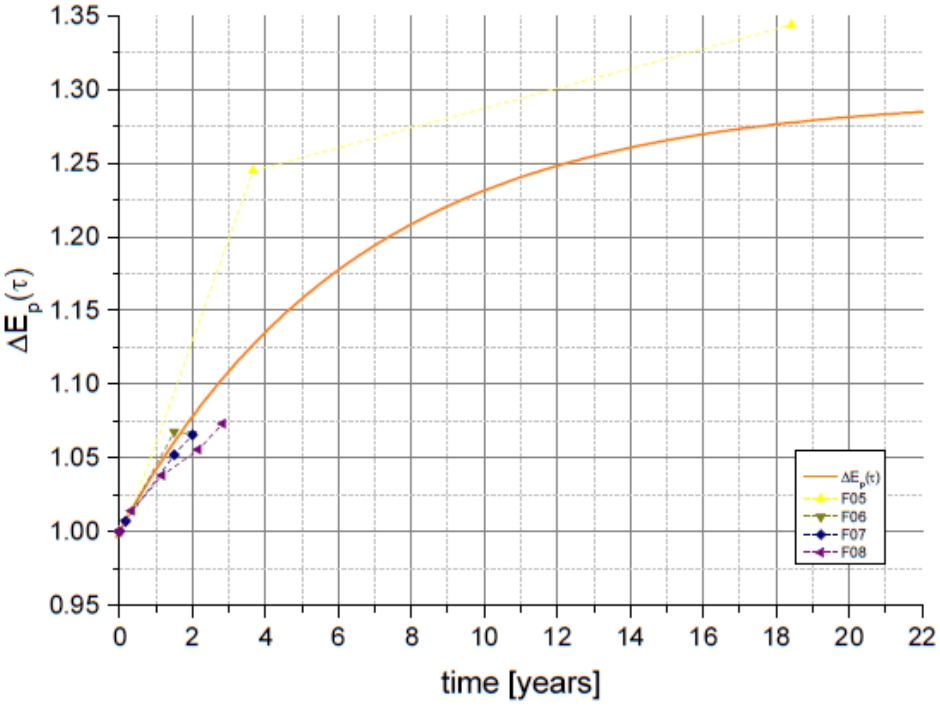

Figure SM16: Corrected energy consumption for the appliances F05 to F08 (symbols) and consolidated aging function $\Delta E_p(\tau)$ (line).

Household refrigerating appliances used for COP measurements

Table SM33: Results of the calorimeter measurements for R03.

Nr.:	R03			
Brand:	Siemens			
Type:	KI81RAD30			
serial number:	258050362166024031			
Compressor type:	DLX4.8KK			
Compressor serial number:	DJ39K180			
Actual appliance operation time	τ_{op}	[a]	2.00	
Measurement:			1	2
Date of measurement:			11.04.2018	14.09.2020
Evaporation temperature	T_{ev}	[°C]	-23	-23
Condensation temperature	T_{cond}	[°C]	55	55
Superheating temperature	T_{sh}	[°C]	32	32
Subcooling temperature	T_{sc}	[°C]	32	32
Ambient temperature	T_a	[°C]	32	32.0
Mains voltage		[V]	230	230
Utility frequency		[Hz]	50	50
Rotation speed		[min^{-1}]	3000	3000
Refrigerant			R600a	R600a
Electrical drive Power	P_{el}	[W]	45.0	44.4
Evaporator heat flow	$\dot{Q}_{ev}$	[W]	79.6	81.3
Coefficient of performance	COP		1.771	1.831
Improvement of the COP	ΔCOP	[%]	3.44	
Note: Also used for the investigation of the energy consumption.				

Table SM34: Results of the calorimeter measurements for R08.

Nr.:	R08			
Brand:	Siemens			
Type:	KI81RAD30			
serial number:	258050362166024048			
Compressor type:	DLX4.8KK			
Compressor serial number:	DJ3A4009			
Actual appliance operation time	τ_{op}	[a]	2.17	
Measurement:			1	2
Date of measurement:			11.04.2018	07.09.2020
Evaporation temperature	T_{ev}	[°C]	-23	-23
Condensation temperature	T_{cond}	[°C]	55	55
Superheating temperature	T_{sh}	[°C]	32	32
Subcooling temperature	T_{sc}	[°C]	32	32
Ambient temperature	T_a	[°C]	32	32.0
Mains voltage		[V]	230	231
Utility frequency		[Hz]	50	50
Rotation speed		[min^{-1}]	3000	3000
Refrigerant			R600a	R600a
Electrical drive Power	P_{el}	[W]	45.4	44.5
Evaporator heat flow	$\dot{Q}_{ev}$	[W]	79.9	81.7
Coefficient of performance	COP		1.761	1.835
Improvement of the COP	ΔCOP	[%]	4.19	
Note:				

Table SM35: Results of the calorimeter measurements for R09.

Nr.:	R09			
Brand:	Siemens			
Type:	KI81RAD30			
serial number:	258050362166024055			
Compressor type:	DLX4.8KK			
Compressor serial number:	DJ3A7121			
Actual appliance operation time	τ_{op}	[a]	2.17	
Measurement:			1	2
Date of measurement:			11.04.2018	07.09.2020
Evaporation temperature	T_{ev}	[°C]	-23	-23
Condensation temperature	T_{cond}	[°C]	55	55
Superheating temperature	T_{sh}	[°C]	32	32
Subcooling temperature	T_{sc}	[°C]	32	32
Ambient temperature	T_a	[°C]	32	32.0
Mains voltage		[V]	230	230
Utility frequency		[Hz]	50	50
Rotation speed		[min^{-1}]	3000	3000
Refrigerant			R600a	R600a
Electrical drive Power	P_{el}	[W]	44.1	43.4
Evaporator heat flow	$\dot{Q}_{ev}$	[W]	77.5	76.1
Coefficient of performance	COP		1.756	1.754
Improvement of the COP	ΔCOP	[%]	-0.11	
Note:				

Table SM36: Results of the calorimeter measurements for C18.

Nr.:	C18			
Brand:	Bosch			
Type:	KIS86AF30			
serial number:	258050270702003641			
Compressor type:	DLX7.5KK			
Compressor serial number:	DHBDA053			
Actual appliance operation time	τ_{op}	[a]	2.17	
Measurement:			1	2
Date of measurement:			08.03.2018	03.09.2020
Evaporation temperature	T_{ev}	[°C]	-23	-23
Condensation temperature	T_{cond}	[°C]	45	45
Superheating temperature	T_{sh}	[°C]	32	32
Subcooling temperature	T_{sc}	[°C]	32	32
Ambient temperature	T_a	[°C]	32	32.0
Mains voltage		[V]	230	231
Utility frequency		[Hz]	50	50
Rotation speed		[min^{-1}]	3000	3000
Refrigerant			R600a	R600a
Electrical drive Power	P_{el}	[W]	65.1	67.9
Evaporator heat flow	$\dot{Q}_{ev}$	[W]	129.1	134.9
Coefficient of performance	COP		1.983	1.987
Improvement of the COP	ΔCOP	[%]	0.19	
Note:				

Table SM37: Results of the calorimeter measurements for C19.

Nr.:	C19			
Brand:	Bosch			
Type:	KIS86AF30			
serial number:	258050270702003610			
Compressor type:	DLX7.5KK			
Compressor serial number:	DHBDA038			
Actual appliance operation time	τ_{op}	[a]	2.17	
Measurement:			1	2
Date of measurement:			08.03.2018	03.09.2020
Evaporation temperature	T_{ev}	[°C]	-23	-23
Condensation temperature	T_{cond}	[°C]	45	45
Superheating temperature	T_{sh}	[°C]	32	32
Subcooling temperature	T_{sc}	[°C]	32	32
Ambient temperature	T_a	[°C]	32	32.0
Mains voltage		[V]	230	230
Utility frequency		[Hz]	50	50
Rotation speed		[min^{-1}]	3000	3000
Refrigerant			R600a	R600a
Electrical drive Power	P_{el}	[W]	64.1	65.5
Evaporator heat flow	$\dot{Q}_{ev}$	[W]	126.7	129.5
Coefficient of performance	COP		1.977	1.978
Improvement of the COP	ΔCOP	[%]	0.05	
Note:				

Table SM38: Results of the calorimeter measurements for F06.

Nr.:	F06			
Brand:	Siemens			
Type:	GS36NVW3V			
serial number:	508050381845002197			
Compressor type:	HZK95AA			
Compressor serial number:	9 313 0004018 5			
Actual appliance operation time	τ_{op}	[a]	2.00	
Measurement:			1	2
Date of measurement:			09.05.2017	15.09.2020
Evaporation temperature	T_{ev}	[°C]	-23	-23
Condensation temperature	T_{cond}	[°C]	55	55
Superheating temperature	T_{sh}	[°C]	32	32
Subcooling temperature	T_{sc}	[°C]	32	32
Ambient temperature	T_a	[°C]	32	32.0
Mains voltage		[V]	230	230
Utility frequency		[Hz]	50	50
Rotation speed		[min^{-1}]	3000	3000
Refrigerant			R600a	R600a
Electrical drive Power	P_{el}	[W]	87.3	88.1
Evaporator heat flow	$\dot{Q}_{ev}$	[W]	168.6	172.5
Coefficient of performance	COP		1.931	1.957
Improvement of the COP	ΔCOP	[%]	1.35	
Note: Also used for the investigation of the energy consumption.				

Table SM39: Results of the calorimeter measurements for F09.

Nr.:	F09			
Brand:	Siemens			
Type:	GS36NVW3V			
serial number:	508050381845002203			
Compressor type:	HZK95AA			
Compressor serial number:	9 313 00040192			
Actual appliance operation time	τ_{op}	[a]	2.17	
Measurement:			1	2
Date of measurement:			10.05.2017	03.09.2020
Evaporation temperature	T_{ev}	[°C]	-23	-23
Condensation temperature	T_{cond}	[°C]	55	55
Superheating temperature	T_{sh}	[°C]	32	32
Subcooling temperature	T_{sc}	[°C]	32	32
Ambient temperature	T_a	[°C]	32	32.0
Mains voltage		[V]	230	230
Utility frequency		[Hz]	50	50
Rotation speed		[min^{-1}]	3000	3000
Refrigerant			R600a	R600a
Electrical drive Power	P_{el}	[W]	86.8	87.2
Evaporator heat flow	$\dot{Q}_{ev}$	[W]	168.8	167.1
Coefficient of performance	COP		1.945	1.916
Improvement of the COP	ΔCOP	[%]	-1.49	
Note:				

Table SM40: Results of the calorimeter measurements for F10.

Nr.:	F108			
Brand:	Siemens			
Type:	GS36NVW3V			
serial number:	508050381845002180			
Compressor type:	HZK95AA			
Compressor serial number:	9 313 00040178			
Actual appliance operation time	τ_{op}	[a]	2.17	
Measurement:			1	2
Date of measurement:			10.05.2017	03.09.2020
Evaporation temperature	T_{ev}	[°C]	-23	-23
Condensation temperature	T_{cond}	[°C]	55	55
Superheating temperature	T_{sh}	[°C]	32	32
Subcooling temperature	T_{sc}	[°C]	32	32
Ambient temperature	T_a	[°C]	32	32.0
Mains voltage		[V]	230	230
Utility frequency		[Hz]	50	50
Rotation speed		[min^{-1}]	3000	3000
Refrigerant			R600a	R600a
Electrical drive Power	P_{el}	[W]	88.6	89.4
Evaporator heat flow	$\dot{Q}_{ev}$	[W]	170.4	172.3
Coefficient of performance	COP		1.925	1.926
Improvement of the COP	ΔCOP	[%]	0.05	
Note:				

Figure SM17: Climatic chamber.

Figure SM18: Principal measurement setups:

a) Freezer loaded with test packages according to DIN EN 15502:2006 or DIN EN 62552:2013.
b) Air temperature measurement points in empty freezer compartment according to IEC 62552:2015.
c) Air temperature measurement points in freezer compartment with drawers according to IEC 62552:2015.
d) Air temperature measurement points in fresh food compartment[1].

[1] The basic measurement setup in the fresh food compartment differs only in the vertical position of the air temperature measurement points between the standards.

6.2 Investigating the real life energy consumption of refrigeration appliances in Germany: Dynamic modelling of consumer behaviour

Hueppe, C., Geppert, J., Moenninghoff-Juessen, J., Wolff. L., Stamminger, R., Paul, A., Elsner, A., Vrabec, J., Wagner, H., Hoelscher, H., Becker, W., Gries, U., Freiberger, A., 2021. Energy Policy 155, 112275.

Die Entwicklung eines dynamischen Modells zur Bestimmung der Energieaufnahme von Haushaltskältegeräten in Abhängigkeit des Verbraucherverhaltens war das Ziel dieser Publikation. Dies wurde durch die Anpassung von verschiedenen Modellparametern für das direkte und indirekte Verbraucherverhalten an die Ergebnisse einer Verbraucherbefragung realisiert. An dieser Befragung nahmen 706 Probanden aus Deutschland teil. Die Ergebnisse der Untersuchung zeigen, dass bis zu 32,5 % der Energieaufnahme auf das Verbraucherverhalten zurückzuführen sind.

Der Autor dieser Dissertation hat bei der Ausarbeitung der vorliegenden Publikation mitgewirkt, insbesondere hat er bei der Erstellung des Fragenkatalogs der Verbraucherbefragung und durch die Übernahme administrativer Aufgaben unterstützt. Christian Hüppe hat die Publikation verfasst, die Verbraucherbefragung vorbereitet, durchgeführt und ausgewertet. Jasmin Geppert, Julia Mönninghoff-Jüssen und Lena Wolff habe bei der Durchführung der Verbraucherbefragung unterstützt. Andreas Elsner, Heike Hölscher, Hendrik Wagner, Ulrich Gries, Alfred Freiberger und Wolfgang Becker unterstützten die Arbeiten zu dieser Publikation im Rahmen des Forschungsprojekts ALGE. An der Überarbeitung des Manuskripts war Jadran Vrabec beteiligt. Während der gesamten Arbeit wurden die Autoren von Rainer Stamminger und Jadran Vrabec betreut.

Energy Policy 155 (2021) 112275

Contents lists available at ScienceDirect

Energy Policy

journal homepage: http://www.elsevier.com/locate/enpol

Research Article

Investigating the real life energy consumption of refrigeration appliances in Germany: Are present policies sufficient?

Christian Hueppe [a,*], Jasmin Geppert [a], Julia Moenninghoff-Juessen [a], Lena Wolff [a], Rainer Stamminger [a], Andreas Paul [b,c], Andreas Elsner [b], Jadran Vrabec [c], Hendrik Wagner [d], Heike Hoelscher [d], Wolfgang Becker [e], Ulrich Gries [f], Alfred Freiberger [g]

[a] University of Bonn, Institute of Agricultural Engineering – Section Household and Appliance Engineering, Nussallee 5, 53115 Bonn, Germany
[b] Paderborn University, Thermodynamics and Energy Technology, Warburger Straße 100, 33098 Paderborn, Germany
[c] Technical University of Berlin, Thermodynamics and Process Engineering, Ernst-Reuter-Platz 1, 10587 Berlin, Germany
[d] BASF Polyurethanes GmbH, Elastogranstraße 60, 49448 Lemförde, Germany
[e] BSH Home Appliances GmbH, Robert-Bosch-Straße 100, 89537 Giengen an der Brenz, Germany
[f] Secop GmbH, Mads-Clausen-Str. 7, 24939 Flensburg, Germany
[g] Secop Austria GmbH, Jahnstraße 30, 8280 Fürstenfeld, Austria

ARTICLE INFO

Keywords:
Energy efficiency
Refrigeration appliances
Dynamic modelling
Degradation
Consumer behaviour
Energy savings

ABSTRACT

Domestic refrigeration appliances are standard household commodities. Although policies, such as the energy labelling, prompted technical improvements and decreased appliance energy consumption throughout recent decades, important parameters were disregarded. These refer to the efficiency loss over time and the consumer behaviour. The objective of this contribution was to develop a dynamic energy model to determine the power consumption of refrigeration appliances considering degradation factors and behaviour. These were included by model parameters for direct consumer interactions, such as the storage behaviour, door openings and temperature setting, as well as indirect actions, e.g. exposing an appliance to specific temperature conditions at an installation site. For this, an online-survey was conducted to evaluate the consumer behaviour. A total of 706 consumers participated in the national questionnaire, serving as input for the dynamic energy model. It was found that the efficiency loss increases the power consumption by at least 1% annually, leading to an excess of 10% after 10 years of usage. Another important finding was that 32.5% of appliance's power consumption results from consumer behaviour, whereas the promotion of behavioural changes leads to a significant decrease of the consumer-induced consumption. Consequently, this study provides a tool to evaluate the impact of policies targeting refrigeration appliances, stressing that efficiency loss and behaviour should be integrated into future policy approaches.

1. Introduction

Energy efficiency has become increasingly important in recent decades. In 2018, the German residential sector accounted for roughly 25% of the total energy demand, making energy savings in private homes a key to minimise the future use of natural resources and to protect the environment [Federal Environmental Agency of Germany, 2018; German Federal Ministry of Economics and Energy, 2019]. In this light, the efficiency of domestic refrigeration appliances plays a crucial role. Refrigeration appliances are indispensable to preserve perishable food and usually operate continuously throughout their service life, rendering refrigerators (*Rf*), freezers (*Fr*) and fridge-freezer combinations (*RFC*) among the largest energy users in the residential sector. To address the increasing electricity demand of households, the *EU* introduced the energy consumption (*EC*) labelling for white goods and light bulbs via the directive 92/75/EEC in 1992, making a letter-grade labelling system visible to all *EU* consumers since 1995 [Baldini et al., 2018; EU, 1992; EU, 2017]. Clearly visible labels aimed at increasing the consumer awareness of *EC* [Baldini et al., 2018]. Referring to

* Corresponding author.
E-mail addresses: chueppe@uni-bonn.de (C. Hueppe), jgeppert@uni-bonn.de (J. Geppert), julia.moenninghoff-juessen@uni-bonn.de (J. Moenninghoff-Juessen), lena.wolff-mail@web.de (L. Wolff), stamminger@uni-bonn.de (R. Stamminger), apaul@mail.upb.de (A. Paul), elsner@thet.uni-paderborn.de (A. Elsner), vrabec@tu-berlin.de (J. Vrabec), hendrik.wagner@basf.com (H. Wagner), heike.hoelscher@basf.com (H. Hoelscher), wolfgang.becker@bshg.com (W. Becker), ulrich.gries@secop.com (U. Gries), a.freiberger@secop.com (A. Freiberger).

https://doi.org/10.1016/j.enpol.2021.112275
Received 13 August 2020; Received in revised form 17 March 2021; Accepted 20 March 2021
Available online 18 May 2021

Nomenclature

EC	energy consumption
Rf	refrigerator
Fr	freezer
RFC	refrigerator-freezer combination
DUB	consumer's direct using behaviour in the interaction with household cooling appliances
IUB	consumer's indirect using behaviour in the interaction with household cooling appliances
PUR	polyurethane foam insulation
T_a	ambient temperature (in °C)
T_{in}	internal compartment temperature (in °C)
λ	thermal conductivity (in W/m*K)
TA	test appliances: sample appliances exposed to dynamic temperature fluctuations
RA	reference appliances: sample appliances exposed to constant temperatures
τ_I	test value of a testing procedure determining insulation properties (in min^{-1})

Dynamic energy model

P_{off}	stand-by power consumption (in W)
t_i	hours of a year (assumed to be constant, 8760 h)
ε	impact of external heat sources on energy consumption (in %)
η^*	efficiency factor (in W/K)
a	substitution factor
Q_{input_i}	consumer heat input in year i (in Wh)
d_λ	temperature-based degradation parameter
d_λ^{cc}	annual insulation degradation under a given thermal load (in %)
g_i	ageing-based degradation parameter
$T^c_{a\_maximum}$	maximum ambient temperature at the installation site of a consumer household (in K)
x	temperature difference between the ambient and the condenser surface (in K)
y	temperature difference between the compartment and the evaporator surface (in K)
α	weighting factor (in %)
DF	attenuation factor
$n_{door\_opening}$	total number of refrigeration appliance door openings (per day)
n_{food_frequ}	frequency of warm food storages (per year)
n_{food}	total number of food portions stored in a refrigeration appliance (per storage)
n_{bev}	total amount of beverages stored in a refrigeration appliance (in litres per week)
V_{net}	net volume of a refrigeration appliance (in m^3)

Subscripts

i	year of interest ($i \in 1,\ldots,n$)
d	door, i.e. related to door openings
f	food, i.e. related to food storage
b	beverages, i.e. related to the storage of beverages
c	installation site at a respective consumer household
pc	regional weather condition based on the postcode of a consumer
cb	climatic boxes

refrigeration appliances, such policies prompted technological progress and increased efficiency [Kim et al, 2006;Lu 2006; Vine et al., 2001; Wada et al., 2012]. Heap found that the energy labelling led to significant energy savings in the *UK*, i.e. a reduction of 26% in consumption per refrigerator within ten years [Heap, 2001; James et al 2017]. However, it can be doubted whether efficiency improvements translate into actual savings at the households, especially due to appliance's degradation over time and behaviour.

Policies paid no attention to the fact that the efficiency of refrigeration appliances diminishes with progressive use [Berardi and Madzarevic, 2020]. From a technical point of view, refrigeration appliances are subject to mechanical and thermal wear upon ageing, partially because they are exposed to daily and seasonal ambient temperature (T_a) fluctuations [Hasanuzzaman et al., 2009]. Although some system components, such as the door gasket, can be replaced, other components, e.g. the polyurethane foam insulation (*PUR*), must stay in place, i.e. the original efficiency cannot be restored [Kim et al., 2006; Weiss et al., 2010]. *PUR* rigid foam is commonly used as thermal insulation to minimise the heat flow through the appliance walls. Some studies indicate that the degradation of the thermal insulation has a significant impact on the increasing *EC*. Due to concentration differences between the inside of the *PUR* foam cells and the ambient, cell gas diffuses out of the insulation and is partially replaced by ambient air, resulting in degrading insulation properties [Albrecht, 2000; Albrecht, 2004; Khoukhi et al., 2016]. In addition to the efficiency loss, consumer behaviour further influences the *EC* of cooling appliances. Previous research pointed out that behaviour, i.e. the interaction of consumers with their refrigeration appliances by storing food, number of daily door openings etc., appears to have remained unchanged over recent decades [James et al., 2008; Mc Donald and Schrattenholz, 2007; Young, 2008].

Consumer behaviour can be separated in two categories, direct using behaviour (*DUB*) and indirect using behaviour (*IUB*). *DUB* describes direct interactions with refrigeration appliances, e.g. by door openings, whereas *IUB* refers to the environmental impact exposed on appliances, depending on the installation site. For instance, Gemmell et al. (2017) conducted a survey study questioning a total of 766 householders across England about frequently performed interactions with their appliances in 2015 with its results further analysed by Biglia et al. (2018) in 2018 [Gemmel et al., 2017; Biglia et al., 2018]. In a broader context, the cold storage of groceries itself can also be regarded as a *DUB*. Although refrigeration appliances are indispensable to preserve perishable food, the cold storage of food is an important aspect from a sustainability point of view [Masson et al., 2017; Marklinder et al., 2004]. This is especially because shelves, drawers and compartments form different temperature zones (for appliances with a static cooling), providing varying cold storage options. The incorrect storage of groceries in a *Rf* or *RFC* might accelerate their perishability, consequently safety issues arise if the spoilage remains undetected or at least food waste increases [Terpstra et al., 2005; Marklinder et al., 2004]. Regarding the *DUB*, researchers focused on the temperature setting, number of door openings and warm food placements, whereas special attention was paid to the T_a as an *IUB*. The mean internal compartment temperature (T_{in}) was 5.3 °C and survey results indicated that 50% of the respondents opened their appliances more than five times a day, while only 8% occasionally stored warm food in their appliances [Biglia et al., 2018]. On average, the T_a at the installation site was 18.5 °C, and found to vary significantly for different seasons [Biglia et al., 2018]. Building on the findings of the 2015 project, the data were revisited by Foster (2019) to investigate key factors that impact appliance's *EC*, stating that besides the usage, age and the environment in which an appliance is kept influence consumption [Foster, 2019]. Another questionnaire was conducted by Geppert and Stamminger (2010), surveying a total of 1011 consumers in four European countries, namely Germany, France, Great Britain and Spain [Geppert and Stamminger, 2010]. The average T_{in} for all countries

was 4.5 °C, but the temperature setting in Germany with 5.8 °C was found to be significantly higher than in Great Britain with 4 °C. Regarding the *IUB*, the mean T_a at the installation site was 16–23 °C [Geppert and Stamminger, 2010].

A number of experimental studies was conducted to define the influence of *DUB* and *IUB* on the *EC*. With respect to the *DUB*, Saidur et al. (2002) investigated the effect of changes in thermostat setting on two *RFC* and found that the *EC* increases by 7.8% for each degree Celsius temperature reduction [Saidur et al., 2002]. Independent on the temperature setting, each door opening leads to an increase of T_{in} due to air exchange between the appliance's interior and the surrounding. Liu et al. (2004) conducted comparative measurements and found that the *EC* increases by 10% in the event of 65 door openings [Liu et al., 2004]. Additionally, T_{in} is influenced by the storage of food and beverages, i.e. the *EC* increases to dissipate the heat load introduced by stored food [Geppert and Stamminger, 2010; Hasanuzzaman et al., 2009]. Referring to the *IUB*, previous research stated that T_a is a dominant factor in the *EC* of refrigeration appliances [Björk and Palm, 2006; Greenblatt et al., 2013; Harrington et al., 2018]. Throughout a range of different experimental approaches, it was found that door openings, temperature setting and placement of warm food are the most dominant actions of the *DUB*. These interactions were found to influence appliance's *EC* more pronounced than other *DUB* factors (e.g. seasonal storage of large food quantities) [Geppert 2011; Saidur et al. 2002]. The same applies to the *IUB*, with experimental studies identifying the impact of the T_a on appliance's *EC* to be most pronounced [Geppert 2011; Hasanuzzaman et al., 2009; Saidur et al. 2002]. However, the T_a is a generic term that includes varying specifications, e.g. seasonal and daily fluctuations as well as long-term high or low temperature periods. Other interactions defined as *IUB*, such as the exposure of appliances to sunlight or dirt contamination of distinct components, were either found to have no clear influence on the *EC* or to be considerably inferior to that of the T_a.

Furthermore, up to now no models exist that can be used to determine the *EC* of refrigeration appliances. Recent models follow static approaches, do not include the dynamic degradation and examine only limited aspects of consumer behaviour [Dale et al., 2009; De Melo and de Martino Jannuzzi, 2010; Gottwalt et al., 2011; Hermes et al., 2009; Vendrusculo et al., 2009]. However, a better understanding of the degradation and the impact of behaviour on the *EC* are critical topics for policy makers, manufacturers and consumers alike. The primary objective of this contribution is therefore to develop a dynamic model that determines the *EC* of refrigeration appliances under real life conditions. Thereby, the sufficiency of existing policies targeting the efficiency of refrigeration appliances can be evaluated.

2. Methodology

Fig. 1 exemplifies the collection and processing of different data incorporated in the dynamic energy model and serves as a generic overview of processed data.

2.1. Survey development and application

An extensive online-survey was conducted across Germany to monitor consumer's day-to-day interactions with their mainly used refrigeration appliance and appliance installation conditions. This national survey was carried out in collaboration with TOLUNA Germany GmbH, a globally operating market research institute. Before the actual survey was conducted, a comprehensive pretesting phase was undertaken. Three main stages were included. First, several reviews to examine the comprehensibility of survey questions, subsequent revisions of critically reviewed questions and a pre-test (pilot study) with 20 randomly selected consumers. The final survey comprised 22 questions and was conducted over a 14-day field period in January and February 2020. Survey participants were selected from an online panel provided by TOLUNA Germany GmbH. The panel was designed to be representative for the German population and respected demographic characteristics. Participation conditions were pre-programmed to ensure the following. Age groups between 20 and 70 years participated, a balance between male and female interviewees prevailed, different household sizes were covered and answers were gathered from all 95 German postcode regions. All consumers participating in the final survey had to meet certain eligibility criteria (requirements), cf. Table 1.

Eligibility criteria set minimum requirements each interviewee needed to fulfil to participate and, thus, ensured that the information could subsequently be processed. The criteria did not diminish the representativeness of the collected data which was accounted for by the pre-programmed participation conditions. On the one hand, only consumers owning appliances with digital temperature displays could respond the actual T_{in}. Survey participants with a manual temperature setting (e.g. a dial) would have reported estimates of T_{in}, subject to a high degree of uncertainty, and were therefore excluded from the survey. On the other hand, it is impossible for consumers to report the actual age of their appliances and estimates are rather imprecise. Thus, a decoding table was developed to determine the production date of each appliance (Table A1).[1] Since the decoding constitutes sensitive manufacturer information, Table A1 presents only an extract that exemplifies the general approach how the production dates were evaluated. Depending on the appliance manufacturer, each survey participant had to copy specific number and letter codes from the nameplate to pre-programmed survey input fields. The decoding table encompassed 13 manufacturers of refrigeration appliances. Each survey respondent who indicated that his/her appliance was either from a manufacturer not listed in Table A1 or left blank (−) was automatically excluded from the survey.

2.2. Supplementary data collection

Parallel to the design and implementation of the survey, an extensive literature review was conducted to compile a list of approaches that promote an energy-efficient interaction with refrigeration appliances. This list of *best practices* covers both *DUB* and *IUB* (Table A2). However, the listed strategies form behavioural approaches that can only be recommended as *best practices* from an energy-saving point of view. For instance, the recommended storage of perishable food under proper T_{in} is a sensitive part of the cold chain and is ambiguously discussed in the literature. Many studies advise temperatures below 5 °C to prevent microbiological contamination [Roccato et al., 2017; U.S. Food and Drug Administration, 2003; Ceuppens et al., 2016], whereas other studies state that storage temperatures of 7 °C for the refrigerator and −16 °C to −18 °C for the freezer compartment are sufficient [Terpstra et al., 2005; Federal Environmental Agency of Germany, 2013]. Referring to energy savings through behavioural changes, the upper limit is food safety. In this light, the *best practice* regarding the T_{in}^{Rf} is 7 °C and −16 °C for the T_{in}^{RFC}. The above described example shows that each formulation of a *best practice* required a difficult balancing of different parameters [Lu, 2006]. The proposed *best practices* were implemented into the modelling approach to analyse end-use energy saving potentials through consumer behaviour.

Due to the distribution of interviewees all over Germany, regional variations in T_a could be taken into account. The German Metrological Institute provided a comprehensive data record of 99 weather stations distributed across the 95 German postcode areas. The data record re-

[1] On-site visits to household appliance and electronics stores in Germany, manufacturer interviews and an extensive online research were conducted to develop the decoding table, Table A1. The decoding of specific number-letter codes (given on the nameplates) was essential to identify an appliance model, age and to process the data for the dynamic energy model. Consequently, appliances from manufacturers with codes that could not be decoded were excluded because their informat ion could not be further processed.

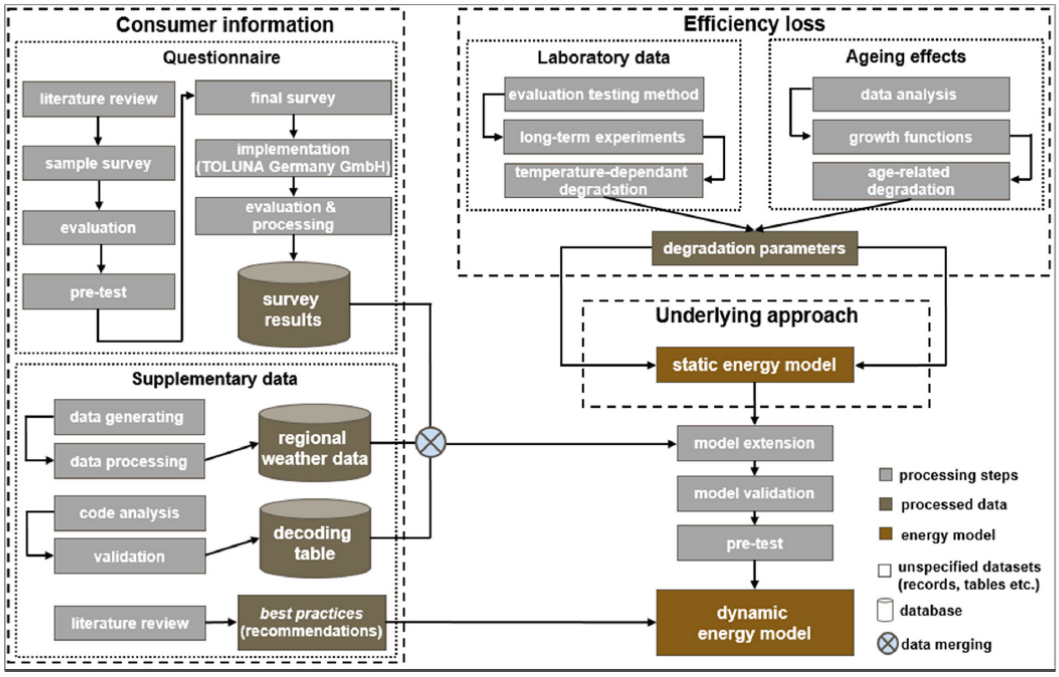

Fig. 1. Generic overview of applied and processed data.

Table 1
Eligibility criteria (set of requirements).

- Only appliances with digital temperature displays
- Only appliances from a specific group of manufacturers
- Only *Rf* and *RFC*
- Only appliances with clearly legible nameplates

ported the T_a of each station for two measuring points. Each measuring point recorded independently weather and temperature data at 10 min intervals throughout the year 2017, serving as a reference year in the following.[2] The temperature data of the year 2017 were used in the modelling approach to specify regional weather conditions at a consumer's domicile (T_a^{pc}). After data processing, each participant was ascribed to a weather station based on the given postcode.

2.3. Modelling approach

The following sections deal with the experimental evaluation of appliance's efficiency loss and how degradation parameters were deduced.

2.3.1. Investigating changes in insulation properties

A non-destructive testing method was applied in a series of experiments to sample appliances to determine the functional relationship between insulation degradation and increasing *EC* over time. The method investigates a temperature rise from T_{in} towards T_a after a cooling appliance was disconnected from the power supply. Since the drain hole and door gasket(s) were sealed, mass flow between the interior and the surrounding was minimised. Consequently, the heat flow that leads to the temperature rise was constituted by the temperature difference to the ambient. In this context, a testing value (τ_I) defined the quality of the insulation at the time of test application (in min^{-1}) [Hueppe et al., 2020]. An insulation degradation was reflected by changes in τ_I over time. The method was applied to ten initially new appliances, including *Rf* and *RFC*, for which τ_I was determined at regular intervals over the course of 1.5 years. All sample appliances incorporated a *PUR* rigid foam insulation which is at present the most frequently used insulation material for refrigeration appliances. Consequently, cooling appliances with varying insulation technologies, e.g. vacuum insulated panels (*VIP*) were disregarded. Two appliances of identical construction were obtained per model and clustered either as test appliances (*TA*) and reference appliances (*RA*). One appliance of each model was assigned as *TA*, whereas the other one was grouped as *RA* (Table 2).

Table 2
Specification of sample appliances.

Type[a]	Production date[b]	Installation site
cooling-freezing (07)	May 2018	*TA*
cooling-freezing (07)	May 2018	*RA*
cooling-freezing (07)	February 2018	*TA*
cooling-freezing (07)	February 2018	*RA*
refrigerator (01)	May 2018	*TA*
refrigerator (01)	May 2018	*RA*
refrigerator (01)	January 2018	*TA*
refrigerator (01)	January 2018	*RA*
cooling-freezing (07)	January 2019	*TA*
cooling-freezing (07)	January 2019	*RA*

[a] Appliance type according to the coding system of the delegate regulation (EU) 1060/2010.
[b] The production date of each appliance was determined according to Table A1 in the **Appendix**.

[2] Temperature and weather data for the years 2017 and 2018 were sourced for this study. 2017 was chosen as a reference year because conditions were in line with previous years, whereas 2018 was exceptionally warm in Germany and would have biased the data basis and output of the dynamic energy model.

Apart from the time of test application, all sample appliances were continuously switched on and operated at the lowest T_{in}. *TA* operated in climatic boxes between test applications, whereas the *RA* counterparts were placed in a machine laboratory. The climatic boxes were specifically designed to perform dynamic changes in T_a between 20 °C and 40 °C in 12 hour intervals. The imposed temperature fluctuations simulated daily and annual T_a variations and, thus, accelerated the ageing process [Bhattacharjee et al., 1994]. Dynamic temperature changes were regulated by a fan heater connected to a timer that was located on the boxes' external cladding, whereas an axial fan ensured air circulation to prevent temperature stratification within the climatic boxes (cf. Fig. 2). In contrast to the climatic boxes, the T_a in the machine laboratory was at 20 °C with daily and annual fluctuations below 2 *K* and 5 *K*, respectively. Consequently, *RA* experienced no accelerated ageing and it was expected that the degradation of a *TA* is above that of its *RA* counterpart.

Lascar electronics EasyLog EL-USB-1 were used for long-term recording of temperature data between two measurements. For each sample appliance, one logger was used to record T_a and one logger per appliance compartment to record T_{in}. Temperature sensors were placed at specific positions that marked the geometric centre of a compartment. Chosen sensors operated within a temperature range from −35 °C to 80 °C with a ±0.5 *K* accuracy and were set to record every minute. The testing method was applied simultaneously to a *TA* and *RA* of the same construction type. For this purpose, both appliances were placed in a laboratory with a constant T_a of 20 °C ± 1 *K*. The test application followed the methodological approach described by Hueppe et al. (2020) [Hueppe et al., 2020].

Changes of τ_I over time were determined for each sample appliance by the increase from the initial to the last measurement and related to one year ($\Delta\tau/a$), given in percent. The application of the non-destructive testing method over the course of 1.5 years resulted in two major findings. First, changes of insulation quality were detected for all appliances, regardless of the installation site. Throughout the investigation, $\Delta\tau/\ a$ was at least 3.5%, i.e. the heat flow through the insulation increased because of deteriorating insulation properties. Consequently, not only a temperature-dependent degradation took place, but also an ageing-based that was independent of the T_a. Second, *TA* suffered a more severe degradation than their *RA* counterparts. On average, τ_I increased for all *TA* by 8.5% and for all *RA* by 4.0% per year.

2.3.2. Modelling of degradation parameters

Two degradation parameters were developed based on the experimental findings to consider both the impact of temperature fluctuations and ageing effects. Temperature-based degradation influences the variable d_λ, whereas the variable g_i presents the ageing-based degradation. d_λ is subject to the ambient conditions at the installation site. Depending on the location, the environmental impact, i.e. temperature changes and exposure to high temperatures, can be extreme. d_λ constitutes a unitless factor denoting the annual increase in the thermal conductivity of *PUR* due to the temperature-dependent degradation of the insulation, calculated according to Equation (1).

$$d_\lambda = \frac{TL^c}{TL^{cb}} * d_\lambda^{cc} \tag{1}$$

TL^{cb} gives the total thermal load, defined as the sum of all temperature increases within the climatic boxes over one year (9767 *K*). Further, d_λ^{cc} constitutes the experimentally determined average annual insulation degradation under given installation conditions over all sample appliances (Table 2), resembling the changes in τ_I over time. TL^c reflects the annual thermal load of the actual installation conditions at the consumer households (in *K*), calculated with Equation (2).

$$TL^c = DF * TL^{pc} \tag{2}$$

TL^{pc} denotes the total ambient thermal load at the domicile of a consumer (in *K*). Question 22 in the survey asked for the postcode of each participant so that consumers could be assigned to the nearest weather station and the corresponding temperature data were evaluated. However, an attenuation factor (*DF*) was formulated to reduce the effect of the ambient thermal load on TL^c, since only appliances outside consumer homes, i.e. exposed unsheltered to the ambient, would suffer the total TL^{pc}. The *DF* of each appliance was established based on the information of a respective survey participant.

Unlike d_λ, g_i is independent of the temperature-based degradation and describes the age-related efficiency loss over time. g_i is a function from a set of four growth functions, namely linear (*lin*), exponential (*exp*), limited exponential (*limexp*) or sigmoid (*sig*). Since the actual efficiency loss of refrigeration appliances throughout their service life is yet unknown, the growth functions represent possible courses of how the degradation might impact the *EC* with progressive use. The set of growth functions is presented in Table 3.

β is a dimensionless factor resembling the ageing-based gradient over time and differs for each growth function. In contrast, p constitutes a limitation factor that depends on the chosen functional form, whereas q determines the shift of the turning point in the sigmoid growth function. To achieve comparability between the different functions, g_i depends on a condition formulated according to Equation (3).

$$EC_{15} = EC_0 * (1 + g_{15}) = EC_0 * 1.2 \tag{3}$$

An ageing-based increase in *EC* by 20% 15 years after appliance production was assumed, i.e. the *EC* of an appliance at the age of 15 (EC_{15}) is 20% above the consumption within the first year after production (EC_0). Although the functional course of the efficiency is yet unknown, the assumption bases on previous studies [Warentest, 2013]. Since the functional condition is variable, it can be adjusted to future

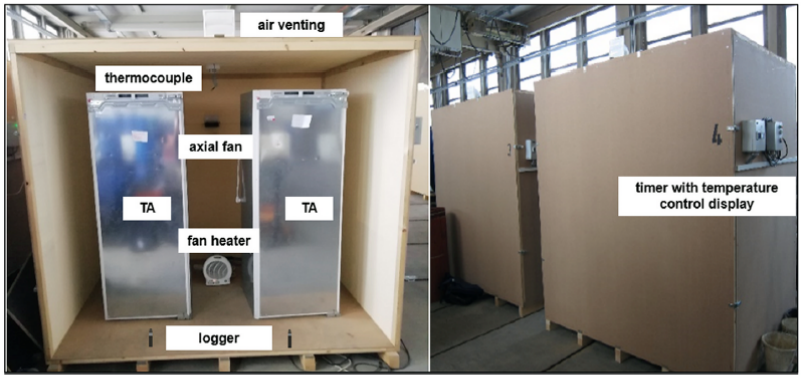

Fig. 2. Climatic boxes, interior view (left) and closed view (right).

Table 3
Growth functions.

g_i *lin*	$\beta_{lin}{}^{*}i$
g_i *exp*	$p_{exp}{}^{*}e^{\beta_{exp}i} - p_{exp}$
g_i *limexp*	$p_{limexp}{}^{*}(1 - e^{-\tau_{limexp}i})$
g_i *sig*	$\left(\frac{1}{p_{sig}{}^{*}(1+e^{-\tau_{sig}(i-a_{sig})})}\right) - \left(\frac{1}{p_{sig}{}^{*}(1+e^{a_{sig}i})}\right)$

findings without much effort. Subsequently, three scenarios, namely BASE, POSITIVE and NEGATIVE, were developed to investigate the impact of the efficiency loss on the *EC* over time. For this purpose, the above described functional condition remained, whereas the annual insulation degradation changed per scenario, i.e. based on the experimental results each scenario included a different d_i^{cc}. The BASE scenario reflected the realistic case, assuming a d_i^{cc} of 6%, whereas the POSITIVE and NEGATIVE scenarios assumed 4% and 8.5%, respectively.

2.3.3. Dynamic energy model

Based on previous experimental research regarding the impact of varying consumer interactions on refrigeration appliance's *EC*, the temperature setting (T_{in}), daily door openings (n_{door_open}), placements of warm food (n_{food} and n_{food_frequ}) as well as the storage of beverages (n_{bev}) were included as *DUB* parameters. Since the ambient temperature at the installation site (T_a^c) is by far the most influential *IUB* parameter, it was implemented in the dynamic model. Different characteristics, e.g. daily and seasonal temperature fluctuations, were respected. The present modelling approach is an extension of a previous model derived by Geppert (2011) to calculate domestic refrigerator's *EC* under real life conditions in Europe. The model is based on a concept to calculate the work input required for a Carnot refrigerator, constitutes a static approach and is presented by Figure A1 [Geppert, 2011]. The model was extended to a dynamic approach quantifying the *EC* of *Rf* and *RFC* based on appliance construction, efficiency loss and consumer behaviour. To increase its comprehensibility, the dynamic model is introduced on the basis of its three sections for an exemplary *Rf* at first. Subsequently, the sections are assembled to form the dynamic approach.

The first section considers that the construction of cooling appliances determines the basic *EC*, presented by

$$P_{off}^{Rf} * t_i$$

P_{off}^{Rf} describes the power consumption of a *Rf* during the compressor off-cycle (in *W*), i.e. the stand-by power and power needed for the control unit. Assuming that each year within a given period has the same length, t_i represents the number of hours (8760) per year of interest ($i \in 1, \ldots, n$).

The second section incorporates the efficiency loss, the *IUB* and components of the *DUB*, expressed by

$$(1+\varepsilon) * \frac{a^{Rf}}{\eta^*} * (1+d_\lambda)^i * (1+g_i) * \frac{\left[T_a^c + x^{Rf}\right] - \left[T_{in}^{Rf} - y^{Rf}\right]}{\left[T_{in}^{Rf} - y^{Rf}\right]} * \left[T_a^c - T_{in}^{Rf}\right] * t_i$$

Question 17 in the survey asked the participants whether their appliance was installed in close proximity to external heat sources (ε), e. g. an oven. This proximity leads to an annual surplus in *EC* of at least 0.9% of the labelled *EC*, depending on to what extent the T_a adjacent to the appliance is increased [Lepthien, 2001]. ε was modelled as a binary variable ($\varepsilon \in [0; 0.009]$). a^{Rf}/η^* describes an efficiency factor that is assembled by two appliance-specific values, the variables a and η^*. It was assumed that the absorbed heat of an appliance is partially dependent on the heat flux per unit area. This process is given by a, substituting the constant term $A{*}\lambda/\Delta\delta$. A is the appliance's surface area (m^2), λ gives the insulation's thermal conductivity (0.025 $W/m{*}K$) and $\Delta\delta$ the wall thickness (m), averaged to 0.04 and 0.05 m regarding *Rf* and *RFC*, respectively. In the case of model extension to introduce appliances with *VIP*, these parameters would have to be modified. The reduced efficiency of the cooling process due to the heat input from the ambient is described by η^*. The efficiency loss was included based on the aforementioned degradation parameters, d_λ and g_i. Regarding the influence of T_a on the *EC*, the installation conditions at consumer homes play an important role and were, therefore, covered by a series of survey questions. Question 6 asked the participants whether their appliances were installed in heated or unheated surroundings, whereas questions 14 and 15 were designed to survey the average T_a^c for different seasons and the maximum perceived T_a^c within a year ($T_{a\_maximum}^c$). x^{Rf} and y^{Rf} are constant parameters constituting the temperature difference between T_a^c and the condenser surface (in *K*) as well as between the T_{in}^{Rf} and the evaporator surface (in *K*), respectively. It was assumed that $x^{Rf} = x^{Pr}$ and $y^{Rf} = y^{Pr}$.

The third section of the dynamic model, constituting most of the *DUB*, is presented by

$$\frac{1}{\eta^*}^{Rf} * Q_{input\_i}^{Rf}$$

$Q_{input\_i}^{Rf}$ determines the annual consumer-induced heat input (*Wh*), derived from three mutually independent model parameters (Equation (4)).

$$Q_{input\_i}^{Rf} = Q_{input\_i}^{d\_Rf} + Q_{input\_i}^{f\_Rf} + Q_{input\_i}^{b\_Rf} \quad (4)$$

$Q_{input\_i}^{d\_Rf}$ gives the heat input through door openings in year i (*Wh*). Based on survey question 9, the participants were asked to estimate how often the appliance door(s) were opened per day (considering all residents), providing the daily $n_{door\_opening}$ per household. In conjunction with other consumer information, $Q_{input\_i}^{d\_Rf}$ was calculated according to Equation (5).

$$Q_{input\_i}^{d\_Rf} = V_{net}^{Rf} * \zeta * c_{air} * n_{door\_opening} * \left(n_{days}^{S} * \Delta T^{S} + n_{days}^{W} * \Delta T^{W}\right) \quad (5)$$

V_{net}^{Rf} is the net volume of the respective *Rf* (m^3) and c_{air} the volumetric heat capacity of air ($kJ/m^2{*}K$). Since the heat gain with each door opening is partially related to the load of the appliance, a weighting factor (ζ) was introduced (monitored by survey question 10). Additionally, the heat input per door opening depends on T_a^c at the time of the opening and is thus related to seasonal temperature changes. The total days per season are given by n_{days}^{s} (n = 183) and n_{days}^{w} (n = 182) subdivided according to German heating periods. Similarly, ΔT denotes the temperature difference between T_a^c and T_{in}^{Rf} in the summer and winter seasons (*K*), respectively.

The impact of the consumer-induced heat input through the storage of warm food is given by Equation (5.1).

$$Q_{input\_i}^{f\_Rf} = m^f * c^f * \Delta T^f \quad (5.1)$$

Since the storage of warm food differs per consumer and for each storage, c^f denotes the average specific heat capacity of different foods commonly stored (3.5 $kJ/m^2{*}K$). It was assumed that if participants stated that they place warm food in the refrigerator, the stored food was placed at a temperature of 323 *K* (50 °C). Consequently, ΔT^f gives the temperature difference between the inserted warm food and the T_{in}^{Rf}. The frequency of warm food storages per year (n_{food_freq}) and the associated number of food portions n_{food} (250 g per portion) were surveyed by questions 11 and 13. Consequently, the mass of stored warm food (m^f) could be calculated (Equation (5.1.1))

$$m^f = 0.25\ \text{kg} * n_{food} * n_{food\_freq} \quad (5.1.1)$$

The consumer impact on the *EC* through the storage of beverages is given by Equation (5.2).

$$Q_{input\_i}^{b\_Rf} = m^b * c^b * \Delta T^b \quad (5.2)$$

Beverages are stored at respective T_a^c conditions, which is why ΔT^b resembles the temperature difference between the inserted beverages and the T_{in}^{Rf}. Similar to the storage of warm food, the exact storage of each beverage cannot be surveyed, which is why c^b was gives the specific heat capacity of water ($1.0\ kJ/m^{2*}K$). Each consumer was asked to estimate the total amount of beverages stored in the mainly used refrigeration appliance in litres per week (n_{bev}) (question 11), used to estimate the stored mass of beverages (Equation (5.2.1)).

$$m^b = 1\ \text{kg} * n_{bev} * 52 \quad (5.2.1)$$

Assembling the previous terms of the approach results in the dynamic energy model for a *Rf*, presented by Equation (6).

$$Work_i^{Rf} = P_{off}^{Rf} * t_i + (1+\varepsilon) * \frac{a^{Rf}}{\eta^*} * (1+d_\lambda)^i * (1+g_i) * \frac{\left[T_a^c + x^{Rf}\right] - \left[T_{in}^{Rf} - x^{Rf}\right]}{\left[T_{in}^{Rf} - x^{Rf}\right]} * \left[T_a^c - T_{in}^{Rf}\right] * t_i + \frac{1^{Rf}}{\eta^*} * Q_{input\_i}^{Rf} \quad (6)$$

$Work_i^{Rf}$ gives the annual *EC* of a household refrigerator for one year of service (*Wh*) depending on construction, dynamic efficiency loss and consumer behaviour. Consequently, the total *EC* throughout its service life was calculated according to Equation (7).

$$Work_{i_{total}}^{Rf} = \sum_{i=1}^{n} Work_i^{Rf} \quad (7)$$

Similarly to *Rf*, the dynamic model for *RFC* is presented by Equation (8).

$$Work_i^{RFC} = P_{off}^{RFC} * t_i + (1+\varepsilon) * \alpha * \frac{a^{RFC}}{\eta^*} * (1+d_\lambda)^i * (1+g_i) * \frac{\left[T_a^c + x^{Rf}\right] - \left[T_{in}^{Rf} - y^{Rf}\right]}{\left[T_{in}^{Rf} - y^{Rf}\right]} * \left[T_a^c - T_{in}^{Rf}\right] * t_i + \frac{1^{RFC}}{\eta^*} *$$
$$Q_{input\_i}^{RFC} + (1+\varepsilon) * (1-\alpha) * \frac{a^{RFC}}{\eta^*} * (1+d_\lambda)^i * (1+g_i) * \frac{\left[T_a^c + x^{Fr}\right] - \left[T_{in}^{Fr} - y^{Fr}\right]}{\left[T_{in}^{Fr} - y^{Fr}\right]} * \left[T_a^c - T_{in}^{Fr}\right] * t_i \quad (8)$$

α constitutes a weighting factor that expresses the ratio of the net volume of the freezer compartment (V_{net}^{Fr}) to V_{net}. Similar to refrigerators, the total *EC* of a *RFC* is determined by the sum of each year of usage. Since the energy model uses the processed information of each monitored appliance as an input, the calculated annual *EC* in the event of standard conditions [DIN EN 62552:2013] gives the labelled *EC* of an appliance. A sensitivity analysis was carried out to validate the dynamic model against real life energy consumption measurements and to determine its accuracy. Table A3 summarises the most important tests of the model validation. All consistency checks were positive, i.e. no output errors were produced by the dynamic model. Consequently, it was deemed valid and the consumer information implemented.

3. Results

3.1. Characteristics of monitored appliances

A total of 936 consumers participated in the national survey. 230 were discarded within the first data evaluation following the data cleaning. For the remaining 706 survey participants, the production date of each appliance could be determined and the actual age be calculated. It was found that most of the appliances were between 2 and 5 years (37.5%) and 6–10 years (28.9%) old. A relatively large fraction of the reported appliances was estimated to be aged 1 year or younger (16.4%) and almost one in ten appliances was between 11 and 15 years (9.9%) old. On average, the appliance age constituted to 6.3 years. The appliance age estimated by each consumer was rather imprecise, i.e. interviewees estimated their appliances, on average, two years younger than they actually were. The difference between the actual ages and consumer estimations could be partly due to the time gap between production and purchase.[3]

Table A4 shows the processed survey data and summarises relevant empirical findings. The survey results of Table A4 relate to all 706 valid responses. 364 men (51.6%) and 342 women (48.4%) were among the 706 participants. The average age was 47 years and a majority of survey participants either lived in a household with two (41.9%) or three residents (21.8%). A majority of 540 out of 706 householders stated to have a *RFC* as the mainly used cooling appliance. Regarding the *IUB*, a majority of 78% declared not to have their mainly used appliance placed in direct proximity to a heat source. More than 60% indicated that the average T_a^c in the summer season was within the range of 21–26 °C, whereas more than 70% estimated the average T_a^c in the winter season between 18 and 23 °C. Besides the seasonal shift in T_a^c, about 10% of the participants indicated that their appliances suffer from high temperature peaks in the summer ($T_{a\_maximum}^c$). Regarding the *DUB*, 523 consumers (74.1%) stated that the T_{in}^{Rf} was between 5 and 8 °C and more than 70% set the T_{in}^{RFC} below −17 °C. A majority of roughly 54% stated to open appliance door(s) on average 6–15 times per day, and more than 60% declared to store between 4 and 10 L beverages per week. 383 consumers (54.2%) noted that they never placed warm food in their appliances, whereas 199 of the remaining 323 participants replied that if warm food was stored, 2–3 portions are placed at once.

3.2. Dynamic model: impact of the efficiency loss

At first, the modelled static *EC*, i.e. without efficiency loss, was determined for all 706 appliances and compared to the model output regarding the dynamic *EC* with degradation afterwards. Fig. 3a and Fig. 3b show the distribution of the calculated static *EC* for one

[3] On-site visits to a range of household appliance and electronics stores in Germany revealed that some appliances stayed in the stores for half a year up to a year after production before being sold as a new appliance.

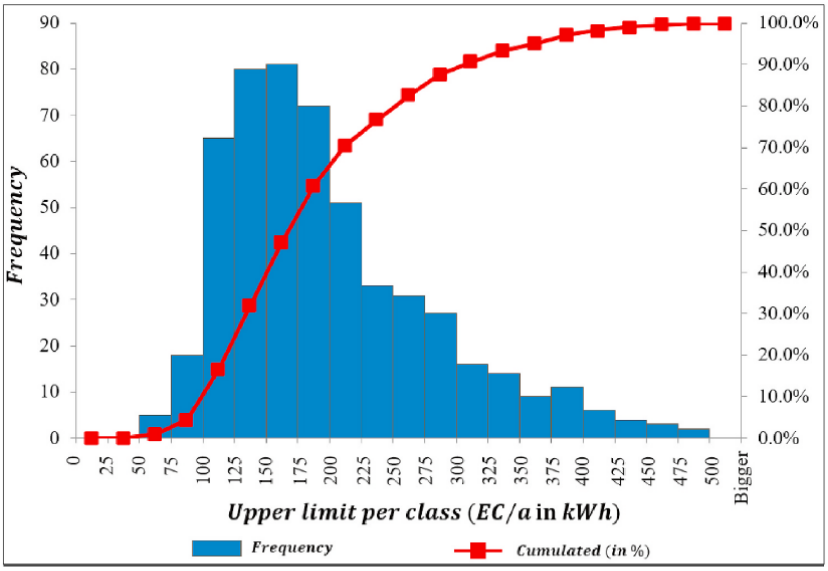

Fig. 3a. Distribution of calculated annual *EC* of sampled *RFC*.

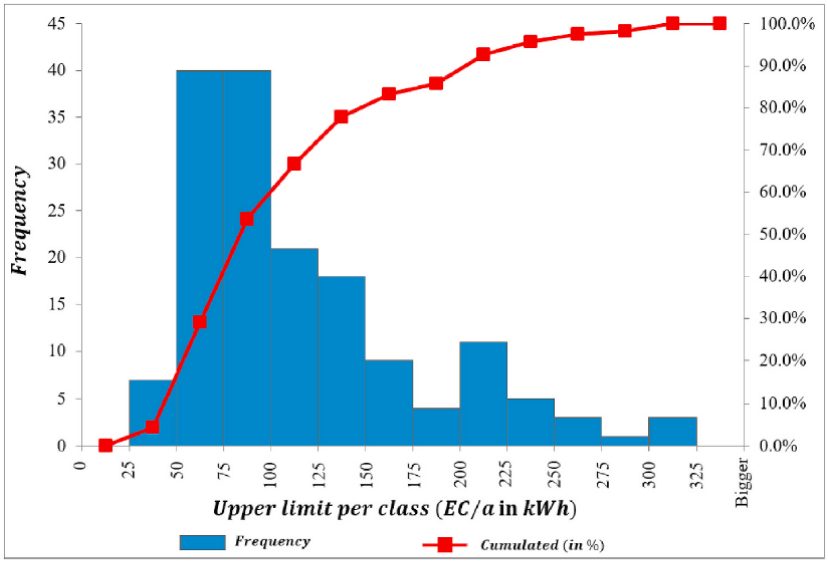

Fig. 3b. Distribution of calculated annual *EC* of sampled *Rf*.

respective year of usage.

The average *EC* of the 540 monitored *RFC* (Fig. 3a) constituted 199.7 *kWh* throughout one respective year of usage. However, a large variation around the mean consumption was found. The highest calculated *EC* was assigned to consumer 173 with a calculated annual *EC* of roughly 488.5 *kWh*, whereas the *RFC* of consumer 176 constituted the lower limit with 55.5 *kWh*. Referring to Fig. 3b, the mean annual *EC* of all *Rf* was roughly 116.9 *kWh* with a large variation around the mean consumption.

In total, the annual static *EC* of all 706 monitored appliances sums up to 127.5 *MWh*. The static *EC* of some appliances was found to be considerably above the labelled consumption, whereas that of others was below the labelled values. Therefore, the total static *EC* approximated to that of the total labelled *EC*, constituting roughly 130 *MWh*. Subsequently, the efficiency loss was activated based on the degradation parameters d_λ and g_i. d_λ^{ec} took the BASE value of 6%, i.e. an annual increase in insulation degradation of 6%, and the functional condition outlined in Equation (3) was applied. Fig. 4 shows the impact of the efficiency loss on the *EC*, assuming the age of monitored appliances to be 15 years.

Fig. 4 indicates that the total *EC* changes significantly if the degradation parameters are activated. Comparing the total annual *EC* of the aforementioned static approach (127.5 *MWh*/*a*) to the dynamic (163.5 *MWh*/*a*) results in an increase of 28%, corresponding to an increase of the labelled consumption from 130.0 *MWh* to 165.5 *MWh*.

To increase the comprehensibility, the results of the scenario analysis

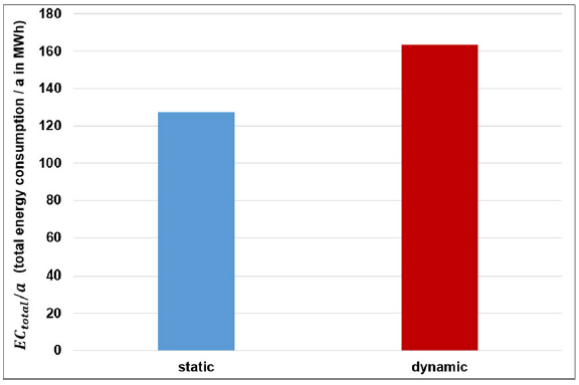

Fig. 4. Impact of efficiency loss on the *EC* at $g_{15} = 0.2$.

are subsequently explained on the example of a single monitored appliance before they are presented for all survey participants. The sample appliance is the 11th *RFC* that was monitored, referred to as RFC_{11} in the following. Fig. 5a shows the output of the dynamic model for an anticipated use phase of 25 years regarding RFC_{11} in the POSITIVE scenario, whereas Fig. 5b presents the model output of RFC_{11} for the NEGATIVE scenario.

Dotted black lines mark the intersection of the *EC* in Fig. 5a and Fig. 5b at the age of 15, respectively. In the POSITIVE scenario, the *EC* of RFC_{11} is 295 kWh/a for all functional courses in year 15, whereas the *EC* amounts to 311 kWh/a within the NEGATIVE scenario. In this light, the increase of d_i^{cc} leads to an increase of 16 kWh, i.e. an annual excess consumption of more than 1 kWh/a. However, as soon as other years are considered, the courses of the *EC* show that varying growth functions lead to significant differences in consumption. For instance, g_i exp *lim* indicates an *EC* of RFC_{11} that is more than 7% above that of g_i *sig* at an appliance age of five years, whereas the *EC* with g_i *sig* is roughly 3% above g_i exp *lim* at an appliance age of 20 years. Fig. 6 summarises the output of the scenario analysis in percentage change of the *EC* for three respective years out of anticipated appliance ages of 25 years. All 706 monitored appliances were taken into account.

For an use phase of ten years, the analysis shows that the increase of *EC* due to decreasing appliance efficiency would be smallest if the course resembles that of g_i *sig*. In contrast, the percentage change in *EC* is largest for all three scenarios in the case of g_i exp *lim* up to an appliance age of 10 years. After appliances aged 15 years, an efficiency loss resembling the g_i*exp* would lead to the largest increase of *EC*, i.e. at least 24% above the consumption in the initial year of usage (g_i*exp* POSITIVE scenario). With progressive use, i.e. the older appliances get, the higher the annual excess of consumption. Even in the most positive case of the scenario analysis, appliances aged 25 years would consume almost 32% more than in their initial state (g_i exp *lim*).

3.3. Dynamic model: impact of consumer behaviour

Fig. 7 shows the proportions of the behavioural influence on the *EC* determined over all 706 monitored appliances for one year (anticipated appliance age = 15 years).

Relating to Fig. 4, the left half of Fig. 7 indicates the total *EC* within the 15th year of appliance lifetime, constituting roughly 163.5 *MWh*. The basic consumption denotes the principal *EC*, depending on construction, stand-by consumption and, for an anticipated age of 15 years, the surplus due to efficiency losses. Unlike the consumer-induced proportion of the *EC*, the basic consumption is independent of behaviour. Approximately 53.1 out of 163.5 *MWh* are consumer-induced, i.e. 32.5% of the total *EC* results from consumer behaviour. A higher level of resolution (right-hand bar of the left half in Fig. 7) shows that the consumer-induced *EC* results from 18.7% of *IUB* and 13.8% of *DUB*, whereas the *DUB* amounts to 9.3% from T_{in} and 4.5% from Q_{input_i}. No further subdivision was attempted for the *IUB*, since 18.6% is constituted by the T_a and only 0.2% by ε. The right half of Fig. 7 shows the calculated total *EC* over all 706 appliances in the event that the surveyed consumers followed the *best practices* (Table A2). The implementation of the *best practices* reduces the *EC* significantly, from initially 163.5 to 138.1 *MWh* due to a decrease of consumer-induced *EC* from 53.1 to 27.8 *MWh*.

4. Discussion

The survey to investigate the interaction of consumers with their refrigeration appliances constitutes one of the most comprehensive studies on the daily use of such devices in Germany. It was found that the average age of monitored appliances was 6.3 years. Up to date, no other

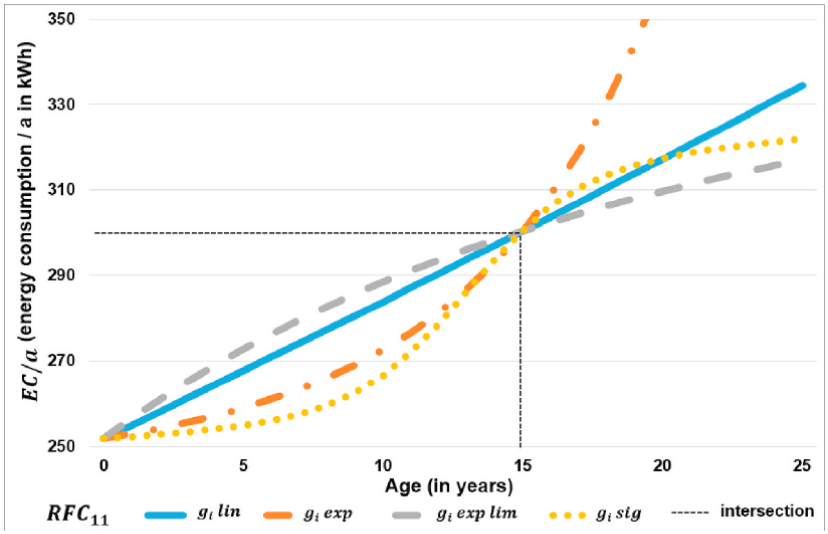

Fig. 5a. POSITIVE scenario of RFC_{11}.

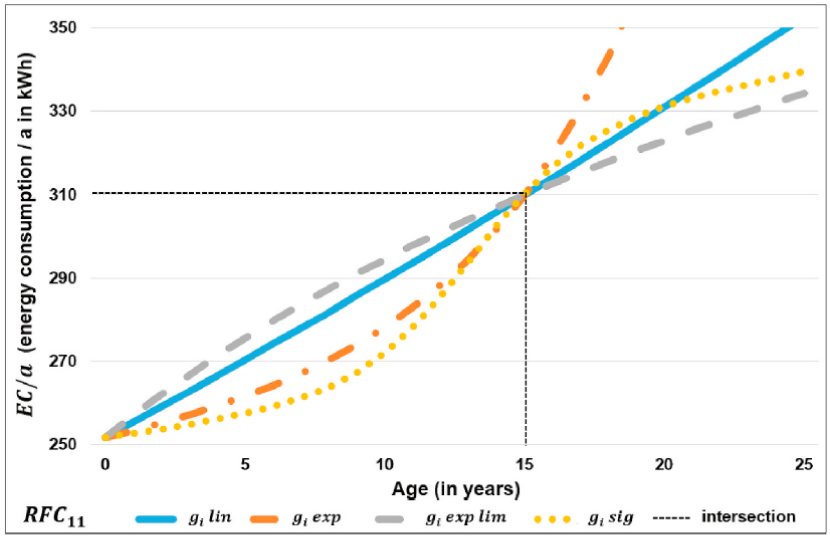

Fig. 5b. NEGATIVE scenario of RFC_{11}.

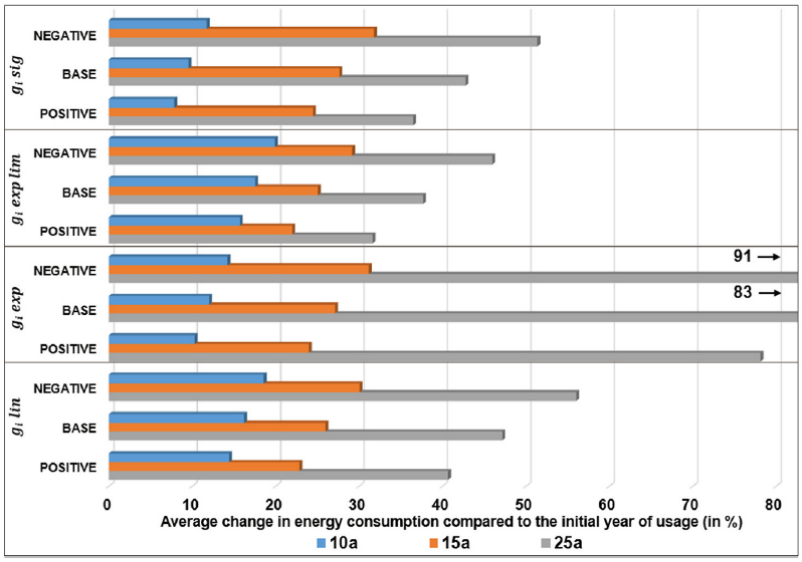

Fig. 6. Scenario analysis – Average change of *EC*.

study investigated the actual age and age distribution of operating refrigeration appliances in Germany, which is why comparative data from similar studies exist only for other countries. Biglia et al. (2018) found in their survey a mean appliance age of seven years [Biglia et al., 2018] and the local 'Domestic Fridge Survey' in New South Wales indicated that most appliances were either between five to ten years old or older than ten years [NSW, 2009]. However, other studies reported the appliance age based on estimations of the survey participants. Comparing the actual appliance ages to consumer estimations highlighted that householders often misjudge the age of their appliances. Referring to the *IUB*, the empirical results are in line with the study of Geppert et al. (2010), stating that T_a at the installation site ranges between 18 and 24 °C, whereas the T_a^* was with 22 °C for this study higher than that found for English households by Biglia et al. (2018) with 18.5 °C [Biglia et al., 2018; Geppert and Stamminger, 2010]. With regard to the *DUB*, results of the T_{in} agree with those of Geppert et al. (2010) and Nauta et al. (2003) [Geppert and Stamminger, 2010; Nauta et al., 2003]. Similarly to the survey study of Biglia et al. (2018), only a minority of participants placed warm food (i.e. with an estimated temperature of 50 °C) into the refrigerator, whereas the $n_{door\_opening}$ was found to be higher with 12 openings, compared to only five for English households [Biglia et al., 2018].

Based on the survey and experiments, a dynamic model was developed. A plurality of data from different sources was processed to derive the model (Fig. 1) and some imprecisions form the basis for future research. On the one hand, only selected consumer actions were integrated into the model. Other parameters referring to the *DUB* and *IUB*, such as the seasonal storage of large food quantities or the exposure of

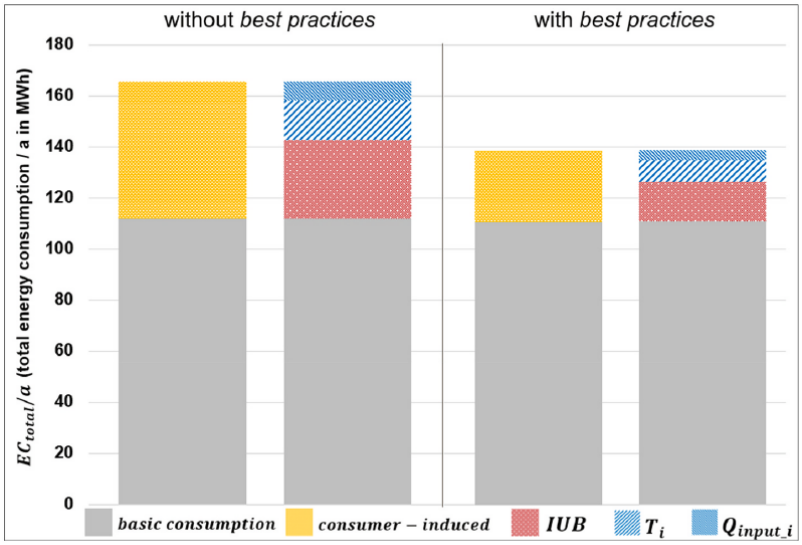

Fig. 7. Consumer impact on the *EC* of cooling appliances.

appliances to direct sunlight, additionally impact the *EC* of refrigeration appliances. Factors different from the chosen parameters were either found to have a negligible impact on appliance's *EC* or were, up to now, not investigated by previous experimental approaches. On the other hand, the extension of the formerly static model to a dynamic one considers the efficiency loss over time. Since d_λ^{cc} results from a series of long-term measurements regarding the insulation degradation, the impact of other system components' degradation that might have occurred simultaneously was ignored. Hueppe et al. (2020) indicated some limitations of the *Bonn method* regarding the derivation of the test value (τ_I) or construction-specific restraints. τ_I reflects an estimate of the overall heat transfer coefficient, considering not only the heat conductivity through a planar refrigerator wall, but also other heat fluxes that depend on the construction and current appliance state [Hueppe et al., 2020]. Minor deviations regarding the degradation factor might have occurred, influenced the d_λ^{cc} and, thus, the modelled impact of the degradation on appliances *EC*. Nevertheless, Hueppe et al. (2020) reported that limitations were small and the validation of the test method indicated a negligible impact on measurement results [Hueppe et al., 2020]. With regard to g_i, the growth functions display possible courses of the excess consumption due to efficiency losses, but cannot claim to reflect the real courses. Since the actual increase in consumption with progressive use is yet unknown, the growth functions show probabilistic courses.

The results of the dynamic energy model indicate that the T_a^c considerably impacts the *EC* of household cooling appliances. It was found that almost 18.5% of the total *EC* is determined by T_a conditions, constituting the largest consumer-induced impact factor. The results are in line with experimental studies of Saidur et al. (2002) [Saidur et al., 2002] and Hazanuzzaman et al. (2004) [Hasanuzzaman et al., 2009], stressing that the T_a is the dominant impact factor on the *EC*. In contrast to T_a, the influence of ε on the *EC* was almost negligible. Lepthien [Lepthien, 2001] stated that the proximity of refrigeration appliances to heat sources (e.g. oven, stove) increases the *EC* by at least 0.9% per year compared to the labelled consumption. However, particularly built-in appliances are covered by an outer casing, such as a wooden frame, that increases the distance of appliances, even though they are installed in direct proximity to a heat source, and diminishes the thermal load from the surrounding. Similarly to the *IUB*, the results of the dynamic model show that *DUB* parameters significantly impact the *EC*, i.e. about 14% of the total *EC* result from direct behavioural interactions. Results indicate that the influence of T_{in} is the largest impact factor among the *DUB*. Previous research conducted by Geppert and Stamminger (2013) concluded that a 1 °C change in T_{in} causes a 6–8% change in consumption [Geppert and Stamminger, 2013]. However, as outlined in section 2.2, *best practices* can only be recommended from an energy-saving point of view and especially the storage of perishable food under proper T_{in} is one of the most sensitive parts of the cold chain. The *best practice* T_{in} for *Rf* of 7 °C might accelerate the perishability of groceries compared to a T_{in} of 4 °C, thus, its implementation potentially leads to an increasing food waste despite energy savings. The effect of door openings on the *EC* was found to be rather small with a share of about 2% in total consumption. However, unlike Liu et al. (2004) who determined a 10% increase of *EC* in the event of 65 door openings, an average of 12 openings per day, as indicated by the interviewees, is more moderate [Liu et al., 2004]. The dynamic energy model only investigated the impact of single behavioural *DUB* and *IUB* parameters on refrigeration appliance's *EC* but did not attempt to further investigate intermediate effects. For instance, if a consumer reduces the n_{bev} according to the *best practices* the $n_{door\_openings}$, is likely to decrease as well. Interestingly, the excess consumption due to the efficiency loss for an anticipated appliance at the age of 20 is within the range of the reductions in energy use due to appliance replacement, estimated by Belshe and Kinney to be between 50 and 70% [Kinney and Belshe, 2001; Arroyo-Cabañas et al., 2009]. Concerning the results of the implementation of *best practices* listed in Table A2, it was highlighted that significant energy savings occur from an energy efficient behaviour. In this light, advice and recommendations have to be promoted much more and the behaviour integrated into future policies. Nevertheless, issues such as food safety and food waste additionally need to be addressed in

the light of sustainability. This is particularly impotant because the consumer acts as a key player in the preservation and use of groceries, limiting the risk of food-borne illnesses, such as listeria or salmonella, and unnecessary food waste by a forward-looking and proactive behaviour. For instance, food should be stored at the proper places (side- and storage compartments) and under correct conditions in a *Rf* or *RFC* to minimise its perishability along with its safety and food waste aspects.

The current dynamic energy model addresses refrigeration appliances with a *PUR* rigid foam insulation which is at present the most frequently used refrigerator insulation material. However, in the future, the model can be extended to incorporate *VIP* to conduct comparative analyses.

5. Conclusions and policy implications

Policies prompted an efficiency increase of household refrigeration appliances, but in-depth research and tools to evaluate the initiated policies were lacking. The present study provides an unprecedented approach by jointly considering technical aspects and consumer interactions in one dynamic energy model to test the sufficiency of policies targeting the efficiency of refrigeration appliances. One important finding of this study is that the efficiency loss increases appliance's *EC* over time. Based on the dynamic energy model, three different scenarios were derived for an anticipated appliance use phase of 10, 15 and 25 years, respectively. Even in the POSITIVE scenario, the impact of the efficiency loss was found to increase the annual average *EC* by no less than 1%, i.e. an excess of at least 10% of *EC* after 10 years of usage. However, present policies, such as the energy labelling, do not incorporate degradation aspects and may thus misinform consumers because an appliance's labelled efficiency potentially decreases several classes throughout its use phase. Another important finding of this study concerns the significant impact of consumer behaviour. It was found that the share of *DUB* in the total *EC* of a daily used refrigeration appliance amounts to more than 13.5% within one year of usage. The *IUB* was found to be larger than the *DUB*. Especially the impact of the T_a at consumer homes was identified to account for an average of roughly 18.5% of appliance's total *EC*. The implementation of *best practices* exemplified multiple initiatives to reduce the *EC* and is feasible for most consumers. Unlike the *DUB*, *best practices* regarding the external influences may not be feasible for all consumers. This is especially because some conditions, such as the T_a^c, are not only affected by behaviour, but also by external factors, e.g. the housing insulation or the location of an apartment in a multi-story building. However, in case that all formulated *best practices* can be implemented, the results of this study highlight a reduction of almost half of the consumer-induced *EC* by behavioural changes.

The results of this study indicate that present policy approaches regarding refrigeration appliances are insufficient. Since neither appliance's efficiency loss over time, nor the impact of consumer behaviour were considered in past policies, the real life *EC* throughout an appliance's lifetime is not outlined to consumers. In fact, the results of this study show that, depending on the degree of efficiency loss, the labelled efficiency class of an appliance may decrease by several classes throughout its service life, whereas an energy-saving behaviour can counteract degradation. A better understanding of the degrading efficiency and the promotion of energy saving behaviour are therefore critical topics that affect multiple stakeholders. For instance, information of impact factors on appliance's *EC* can be presented to consumers by an energy-saving label that is placed next to the energy label. Such a label was, among others, already designed by Lepthien (2001) but never implemented [Lepthien, 2001]. In the future, the dynamic energy model should be extended by further variables to increase the validity of its output and, thus, approximate a universal model. The exposure of appliances to direct sunlight and the dirt contamination of varying components over time, e.g. gradual loosening of the door gasket and dust accumulation on the condenser surface, could be included as additional *IUB* parameters. Further experimental approaches first have to be conducted to determine their impact on appliance's *EC*. The model could be applied to test the sufficiency of policies that aim to improve refrigeration appliance's efficiency. Furthermore, recommendations regarding an energy-saving behaviour have to be promoted much more, since consumers often seem to be unaware of the correct interaction with refrigeration appliances. These should especially refer to the T_{in}, T_a^c and advice on the $n_{door\_opening}$. The basis for such recommendations could be the list of *best practices* (Table A2) that could be graphically processed to a label and applied to refrigeration appliances next to the Energy Label, making it visible to all consumers.

CRediT authorship contribution statement

Christian Hueppe: Conceptualization, Methodology, Software, Validation, Formal analysis, Investigation, Resources, Data curation, Writing – original draft, Writing – review & editing, Visualization, Supervision, Project administration. **Jasmin Geppert:** Conceptualization, Methodology, Resources, Writing – review & editing, Funding acquisition. **Julia Moenninghoff-Juessen:** Conceptualization, Methodology, Software, Validation, Investigation, Resources, Data curation, Writing – review & editing. **Lena Wolff:** Conceptualization, Methodology, Software, Validation, Investigation, Resources, Writing – review & editing, Visualization. **Rainer Stamminger:** Conceptualization, Methodology, Resources, Writing – review & editing, Project administration, Funding acquisition. **Andreas Paul:** Writing – review & editing, Funding acquisition. **Andreas Elsner:** Writing – review & editing. **Jadran Vrabec:** Funding acquisition, Writing – review & editing. **Hendrik Wagner:** Writing – review & editing. **Heike Hoelscher:** Writing – review & editing. **Wolfgang Becker:** Writing – review & editing. **Ulrich Gries:** Writing – review & editing. **Alfred Freiberger:** Writing – review & editing.

Declaration of competing interest

The authors declare that they have no known competing financial interests or personal relationships that could have appeared to influence the work reported in this paper.

Acknowledgement

This work was funded and supported by the German Federal Ministry for Economic Affairs and Energy (BMWi), project 'ALGE' (03ET1544A-E).

Figure A1: Static model to determine the ***EC*** of refrigeration appliances.

Appendix

Table A1
Decoding table (extract)

Manufacturer/Brand	Identification model	Identification production date	Comments
AEG; Electrolux; Zanker; Juno; Zanussi; Progress	**Model** Declared as Modell/Model	**Serial number** Declared as Ser.Nr./Ser.No./Nr.	• The code comprises only the year, not the corresponding decade.
Bauknech; Whirlpool; Privileg	**Model** Indicated by SERVICE and/or a sequence of numbers	**Serial number** Declared as S/N/Serial number	• The sequence of numbers specifying the model has 12 digits, starting with 85 or 86. • The serial number is usually a 12-digit number sequence.
Bosch; Siemens (BSH); Constructa; Neff; Junker	**Model number** Declared as E-Nr.	**Production date** Declared as FD	• The production date is a 4-digit number sequence.
Beko	**Model** Declared as Model/Modell	**Serial number** Declared as SERIAL NUMBER/SERIAL NO	• The number sequence can be written with and without hyphens. • Same coding system as Grundig.
Blomberg*	–	–	–
Bomann*	–	–	–
EXQUISIT	**Model** Declared as Modell	**Production date** Declared as Batch	• Alphabetic coding, i.e. one letter for the production year. • Same coding system as OK.
Gorenje	**Model** Declared as MODEL/MODELL	**Serial number** Declared as SER. N°/Serial number	• Same coding system as AEG.
Grundig	**Model** Declared as MODELL/MODEL	**Serial number** Declared as SERIENNUMMER/Serie Number	• The number sequence can be written with and without hyphens. • Same coding system as Beko.
Haier	**Model** Declared as MODEL	**Serial number** Declared as Serial Number	• Alphabetic coding, i.e. one letter for the production year, number-letter coding for the production month(s) • Similar to SAMSUNG.
Hisense*	–	–	–
Hoover (Candy)*	–	–	–
LG (LG Electronics)	**Model** Declared as Model/Modell/Modello	**Serial Number** Declared as Serial No. or combination of numbers and letters under the barcode	• The number-letter code specifying the serial number is often a 12-digit sequence. • The code comprises only the year, not the corresponding decade.
LIEBHERR	**Model** Declared as Service-no./No.-Service	**Production date** Declared by three-digit code or Serial-Nr.	• If the three-digit code (left-bottom corner on the nameplate) is not given, the customer service evaluates the production date using the 9-digit serial number. • Similar coding system as Miele.
OK.	**Model** Declared as Model	**Production date** Declared as Batch	• Alphabetic coding, i.e. one letter for the production year. • Same coding system as EXQUISIT.
Miele	**Model** Declared as combination of letters and numbers	**Production date** Declared by three-digit code, or letter-number combination (starting with Nr.)	• If the three-digit code (left-bottom corner on the nameplate) is not given, the customer service evaluates the production date using the letter-number combination. • Similar coding system as LIEBHERR.
SAMSUNG	**Model** Declared as MODEL	**Serial number** Declared as S/N/S/no.	• Usually 15-digit number-letter code. • Alphabetic coding, i.e. one letter for the production year, number-letter coding for the production month(s). • Similar to Haier.
Other *	–	–	–

*No freely available data exist to decode the production date of appliances of these manufacturers/brands. Consumers with such appliances were automatically discarded from the survey.

Table A2
Best practices

	Direct using behaviour (DUB)
I.) T_i[a]	Refrigerator compartment: 7 °C Freezer compartment: 16 °C References: Böhmer and Wicke (1998); Ceuppens et al. (2016); Cravitio et al. (2017); James et al. (2008); Federal Environmental Agency of Germany, 2013); Federal Ministry for Economic Affairs and Energy (2020); Preparatory Studies for Eco-design Requirements of EUPs, 2007; Roccato et al. (2017); Terpstra et al. (2005)
II.) $n_{door\_opening}$	$R_f \leq 10$ openings/day $RFC \leq 12$ openings/day References: Böhmer and Wicke (1998); Federal Ministry for Economic Affairs and Energy (2020); Federal Ministry for the Environment, Nature Conservation and Nuclear safety, 2019; Geppert and Stamminger (2010); James and Evans (1992); Saidur et al. (2002)
III.) n_{food}	No storage of warm food References: Böhmer and Wicke (1998); Federal Ministry for Economic Affairs and Energy (2020); Federal Ministry for the Environment, Nature Conservation and Nuclear safety, 2019; Geppert and Stamminger,2010;
IV.) n_{bev} [b]	Storing ≤ 10 l of beverages per week Reference: Böhmer and Wicke (1998)
Indirect using behaviour (IUB)	
I.) T_a [c]	$T_a \approx 19$ °C T_a fluctuation: $T_a^{max} \leq 25$ °C $T_a^{min} \geq 16$ °C Temperature fluctuations should be as small as possible and appliances kept at approximately constant T_aReferences: Böhmer and Wicke (1998); Federal Ministry for Economic Affairs and Energy (2020); Federal Ministry for the Environment, Nature Conservation and Nuclear safety, 2019; James et al. (2017); Hasanuzzaman et al. (2009); Preparatory Studies for Eco-design Requirements of EUPs, 2007
II.) e	No proximity to heat sources: $e = 0$ References: Federal Ministry for Economic Affairs and Energy (2020); Lepthien (2001)

Some *DUB* and *IUB* parameters are unchangeable, such as the T_a at the installation site. Due to the household conditions, a consumer may have no influence on this parameter.
Most advice on the energy-saving handling of refrigeration appliances was gathered from governmental institutions, academic research or consumer information boards. Recommendations are inconsistent for different countries (see chapter 2.2), thus deviations among single advice exist for varying regions.

[a] Depending on the country or region, the energy–saving advice regarding the T_{in} varies for Rf between 5 °C and 7 °C and for RFC from −18 °C to −16 °C. Since 7 °C and −16 °C constitute the upper limits, these were chosen as best *practices* regarding the T_{in} and implemented to the dynamic energy model.

[b] Non-perishable beverages do not have to be stored in the refrigerator (water, soft drinks etc.). Best practice requires a forward-looking and well-planned shopping of beverages. Best practice partially depends on appliance type and household size.

[c] An ambient temperature of 16 °C forms the lower limit of the climatic classes. Temperatures below 16 °C may activate the appliance's winter switch at *RFC*, causing additional energy consumption or lead to a stop of the compressor and subsequent warming-up of stored food.

$$Work^{Rf}_{t_{total}} = P_{off} * t_{total} + \frac{1}{\eta^*} * \int_0^{t_{total}} \frac{[T_{out}(t) + x^{Rf}] - [T^{Rf}_{in}(t) - y^{Rf}]}{[T^{Rf}_{in}(t) - y^{Rf}]} * \left\{ [T_{out}(t) - T^{Rf}_{in}(t)] * a + \frac{Q^{Rf}_{input}}{t_{total}} \right\} dt$$

Stand-by power | **External impact** | **Consumer impact**

$Work^{Rf}_{t_{total}}$	= EC (refrigerator) per year (in Wh)	a	= Substitution factor $\left(\frac{\lambda * A}{\Delta \delta}\right)$ in (W/K)	x^{Rf}	= ΔT_a condenser surface (in K)
P_{off}	= Power (in W)	$T_{out}(t)$	= T_a at time t	y^{Rf}	= ΔT_i evaporator surface (in K)
η^*	= Efficiency factor	$T^{Rf}_{in}(t)$	= T_i at time t	Q^{Rf}_{input}	= Consumer heat input (in kJ)

Fig. A1. Static energy consumption model derived by Geppert (2011).

The static approach consists of three main sections. The first refers to the stand-by power, the second to the external impact exerted on appliances by the environment, e.g. the T_a, whereas the third section comprises the interactions of consumers with their household refrigeration appliances on a daily basis. Geppert's (2011) static approach was extended by the integration of degradation factors (d_i and g_i), additional behavioural parameters (e.g. the proximity to heating sources (ε)) and modified to make it applicable for the introduction of real life consumer information (see section 2.1 and 2.2).

Table A3
Model validation

Model validation and consistency	
1	Model results ($Work^{Rf,RFC}_{i=1}$) have to be equal to the labelled EC under standard conditions for the first year after production (cf. DIN EN 62552:2013). Model input (test specification): a) Age-related efficiency loss: $g_i = 0; d_i = 0$ b) Standard conditions: (Q abbreviates 'question', i.e. survey answers that would have led to the labelled consumption)Q6 = heated; Q9 = 0; Q10 = empty; Q11 = 1 L (equals 0 in this case); Q12 = never; Q13 = 1 portion (equals 0 in this case); Q14 = 24–26 °C (each); Q15 = 25 °C (each); Q17 = no; Q18 = 4 °C T^{Rf}_{in}, −18 °C $T^{RFC,Fr}_{in}$
2	Temperature changes (ambient temperature at the installation site T^{e}_{a} and changes to the temperature setting $T^{Rf,RFC}_{in}$) only impact the second and third section of the equation underlying the dynamic energy model. Model input (test specification): a) All parameters are formulated as in **1.**), but Q14 and Q18 either increase or decrease
3	Increases to $T^{Rf,RFC}_{in}$ decrease $Work^{Rf,RFC}_{1,\ldots,n}$, whereas decreases to $T^{Rf,RFC}_{in}$ increase $Work^{Rf,RFC}_{1,\ldots,n}$ Model input (test specification): a) All parameters are formulated as in 1.), but $T^{Rf,RFC}_{in}$ increases b) All parameters are formulated as in 1.),but $T^{Rf,RFC}_{in}$ decreases
4	Increases of T_a / T^{e}_{a} increase $Work^{Rf,RFC}_{1,\ldots,n}$, whereas decreases of T_a / T^{e}_{a} decrease $Work^{Rf,RFC}_{1,\ldots,n}$ Model input (test specification): a) All parameters are formulated as in 1.), but T_a / T^{e}_{a} increases b) All parameters are formulated as in 1.),but T_a / T^{e}_{a} decreases
Model validation (ambient influence)	
5	Changes to d_i only impact the second section of the equation underlying the dynamic energy model. Model input (test specification): → All parameters are formulated as in **1.**), but d_i increases (to a positive value).
6	Changes to g_i only impact the second section of the equation underlying the dynamic energy model. Model input (test specification): → All parameters are formulated as in **1.**), but g_i either increases or decreases.
7	Changes to ε (Q17) only impact the second section of the equation underlying the dynamic energy model. Model input (test specification): → All parameters are formulated as in **1.**), but ε is either positive (0.009) or zero.
Model validation (consumer influence)	
8	Changes to n_{door} (Q9) only impact the third section of the equation underlying the dynamic energy model. Model input (test specification): → All parameters are formulated as in **1.**), but n_{door} either increases or decreases.
9	Changes to n_{bev} (Q11) only impact the third section of the equation underlying the dynamic energy model. Model input (test specification): → All parameters are formulated as in **1.**), but n_{bev} either increases or decreases.
10	Changes to n_{flood_freq} (Q12) only impact the third section of the equation underlying the dynamic energy model. Model input (test specification): → All parameters are formulated as in **1.**), but n_{bev} either increases or decreases.

Table A4
Summary of empirical results regarding survey participants and monitored appliances

Participants	Household size	1 resident	2 residents	3 residents	4 residents	More than 4 residents	Σ
		105 (14.9%)	296 (41.9%)	154 (21.8%)	115 (16.3%)	36 (5.1%)	706 (100%)
	Age	20–29 years	30–39 years	40–49 years	50–59 years	60–74 years	Σ
		70 (9.9%)	156 (22.1%)	162 (22.9%)	146 (20.7%)	172 (24.4%)	706 (100%)
	Gender	male			female		Σ
		364 (51.6%)			342 (48.4%)		706 (100%)
Appliance characteristics	Type	refrigerator			refrigerator-freezer combination		Σ
		166 (23.5%)			540 (76.5%)		706 (100%)
	Brand [a]	BSH	SAMSUNG	LIEBHERR	AEG	LG	Bauknecht	OTHERS	Σ
		300 (42.5%)	106 (15.0%)	85 (12.0%)	61 (8.6%)	52 (7.4%)	26 (3.7%)	76 (10.8%)	706 (100%)
IUB	Installation site	heated			unheated				Σ
		495 (70.1%)			211 (29.9%)				706 (100%)
	ε	proximity to external heat sources			no proximity to external heat sources				Σ
		156 (22.1%)			550 (77.9%)				706 (100%)
	T_a^c summer	less than 15 °C	15–17 °C	18–20 °C	21–23 °C	24–26 °C	27–29 °C	more than 29 °C	Σ
		36 (5.1%)	28 (4.0%)	85 (12.0%)	253 (35.8%)	234 (33.2%)	53 (7.5%)	17 (2.4%)	706 (100%)
	$T_{a\_maximum}^c$	less than 15 °C	15–20 °C	20–25 °C	26–30 °C	31–35 °C	36–40 °C	more than 40 °C	Σ
		1 (0.1%)	33 (4.7%)	316 (44.8%)	287 (40.7%)	49 (6.9%)	19 (2.7%)	1 (0.1%)	706 (100%)
	T_a^c winter	less than 12 °C	12–14 °C	15–17 °C	18–20 °C	21–23 °C	24–26 °C	more than 26 °C	Σ
		26 (3.7%)	28 (4.0%)	90 (12.8%)	271 (38.4%)	265 (37.5%)	22 (3.1%)	4 (0.5%)	706 (100%)
DUB	T_i cooling [b]	below 3 °C	3–4 °C	5–6 °C	7–8 °C	above 8 °C	Σ
		20 (2.8%)	142 (20.1%)	269 (38.1%)	254 (36.0%)	21 (3.0%)	706(100%)
	T_i freezing [b]	below -20 °C	-20 to -19 °C	-18 to -17 °C	-16 to -15 °C	above -15°C	Σ
		42 (6.9%)	88 (14.4%)	306 (50.1%)	102 (16.7%)	73 (11.9%)	611(100%)
	$n_{door\_opening}$ [c]	less than 6 per day	6–15 per day	16–25 per day	26–35 per day	more than 35 per day	Σ
		98 (13.9%)	381 (53.9%)	160 (22.7%)	38 (5.4%)	29 (4.1%)	706(100%)
	n_{food_frequ}	almost) daily	once a month	weekly	quarterly	never	Σ
		81 (11.5%)	32 (4.5%)	139 (19.7%)	71 (10.1%)	383 (54.2%)	706 (100%)
	n_{food} [d]	1 portion	2 – 3 portions	more than 3 portions	Σ
		111 (34.4%)	199 (61.6%)	13 (4.0%)	323 (100%)
	n_{bev}	1l / week	2–3l / week	4–6l / week	7–10l / week	11–15l / week	more than 15l / week	Σ
		19 (2.7%)	177 (25.1%)	271 (38.4%)	158 (22.4%)	65 (9.2%)	16 (2.2%)	706 (100%)

[a] BSH (BOSCH, SIEMENS) additionaly includes appliances branded as Constructa, Neff, Junker.
AEG additionally includes appliances branded as Electrolux, Zanker, Juno, Zanussi, Progress.
Bauknecht additionally includes appliances branded as Whirlpool.
OTHERS group appliance brands or manufacturer of those brands for which no decoding of the actual production date could be done.

[b] The lines present temperature classes for cooling- and freezing compartments, i.e. all monitored appliances have at least one cooling compartment.
Low-temperature compartments with adjustable internal temperature are thus given within the freezing values.

[c] This table does not differentiate between refrigerators and refrigerator-freezer combinations.

[d] Only those participants who actually placed warm food into their refrigeration appliances are listed, i.e. 706 less 382 participants who stated to never place warm food into their appliances.

References

Albrecht, W., 2000. Cell-gas composition – an important factor in the evaluation of long-term thermal conductivity in closed-cell foamed plastics. Cell. Polym. 19, 319–331.

Albrecht, W., 2004. Change over time in the thermal conductivity of ten-year-old PUR rigid foam boards with diffusion-open facings. Cell. Polym. 23, 161–172. https://doi.org/10.1177/026248930402300303.

Arroyo-Cabañas, F.G., Aguillón-Martínez, J.E., Ambríz-García, J.J., Canizal, G., 2009. Electric energy saving potential by substitution of domestic refrigerators in Mexico. Energy Pol. 37, 4737–4742. https://doi.org/10.1016/j.enpol.2009.06.032.

Baldini, M., Trivella, A., Wente, J.W., 2018. The impact of socioeconomic and behavioural factors for purchasing energy efficient household appliances: a case study for Denmark. Energy Pol. 120, 503–513. https://doi.org/10.1016/j.enpol.2018.05.048.

Berardi, U., Madzarevic, J., 2020. Microstructural analysis and blowing agent concentration in aged polyurethane and polyisocyanurate foams. Appl. Therm. Eng. 164, 114440. https://doi.org/10.1016/j.applthermaleng.2019.114440.

Bhattacharjee, D., Irwin, P.W., Booth, J.R., Grimes, J.T., 1994. The acceleration of foam aging by thin-slicing: some interpretations and limitations. J. Build. Phys. 17, 219–237. https://doi.org/10.1177/109719639401700305.

Biglia, A., Gemmell, A.J., Foster, H.J., Evans, J.A., 2018. Temperature and energy performance of domestic cold appliances in households in England. Int. J. Refrig. 87, 172–184. https://doi.org/10.1016/j.ijrefrig.2017.10.022.

Björk, E., Palm, B., 2006. Performance of a domestic refrigerator under influence of varied expansion device capacity, refrigerant charge and ambient temperature. Int. J. Refrig. 29, 789–798. https://doi.org/10.1016/j.ijrefrig.2005.11.008.

Böhmer, T., Wicke, L., 1998. Energiesparen im Haushalt: So schonen Sie Umwelt und Geldbeutel. DTV-Beck, Munich.

Ceuppens, S., Van Boxtael, S., Westyn, A., Devlighere, F., Uyttendaele, M., 2016. The heterogeneity in the type of shelf life label and storage instructions on refrigerated foods in supermarkets in Belgium and illustration of its impact on assessing the Listeria monocytogenes threshold level of 100 CFU/g. Food Contr. 59, 377–385. https://doi.org/10.1016/j.foodcont.2015.06.009.

Cravitio, J., Yasunaga, R., Yamasue, E., 2017. Comparative analysis of average time of use of home appliances. Procedia CIRP 61, 657–662. https://doi.org/10.1016/j.procir.2016.11.248.

Dale, L., Antinori, C., Mc Neil, M., Mc Mahon, J.E., Fujita, K.S., 2009. Retrospective evaluation of appliance price trends. Energy Pol. 37, 597–605. https://doi.org/10.1016/j.enpol.2008.09.087.

De Melo, C.A., de Martino Jannuzzi, G., 2010. Energy efficiency standards for refrigerators in Brazil: a methodology for impact evaluation. Energy Pol. 38, 6545–6550. https://doi.org/10.1016/j.enpol.2010.07.032.

Din En 62552:2013, Household Refrigerating Appliances–Characteristics and Test Methods (IEC 62552:2007, Modified+corrigendum Mar. 2008), Beuth Verlag, 2013, Berlin.

EU, 1992. Council Directive 92/75/EEC on the Indication by Labelling and Standard Product Information of the Consumption of Energy and Other Resources by Household Appliances. https://eur-lex.europa.eu/legal-content/EN/ALL/?uri=CELEX%3A31992L0075. accessed: 05.08.2020.

EU, 2017. European Commission - energy efficient products. https://ec.europa.eu/info/energy-climate-change-environment/standards-tools-and-labels/products-labelling-rules-and-requirements/energy-label-and-ecodesign_en. (Accessed 5 August 2020).

Federal Environmental Agency of Germany, 2013. Energy Saving in Households. https://www.umweltbundesamt.de/sites/default/files/medien/381/publikationen/energiesparen-im-haushalt.pdf. (Accessed 12 May 2020).

Federal Environmental Agency of Germany, 2018. Energy Consumption of Private Households. https://www.umweltbundesamt.de/daten/private-haushalte-konsum/wohnen/energieverbrauch-privater-haushalte#endenergieverbrauch-der-privaten-haushalte. (Accessed 2 April 2020).

Federal Ministry for Economic Affairs and Energy, 2020. 10 coole Tipps , wie Sie mit Ihrem Kühlschrank Energie sparen. URL: https://www.deutschland-machts-effizient.de/KAENEF/Redaktion/DE/NTRI/Standardartikel/galerie-kuehltipps.html. accessed: 07.06.2020.

Federal Ministry for the Environment. Nature conservation and nuclear safety. Stromverbrauch beim kühlschrank: tipps zum gebrauch & kaufberatung. https://www.co2online.de/energie-sparen/strom-sparen/strom-sparen-stromspartipps/kuehlschrank/. (Accessed 7 June 2020).

Foster, Helen. Factors affecting the energy efficiency of cold appliances. ECEEE Summer Study Proceedings, pp. 1593-1601. https://www.eceee.org/library/conference_proceedings/eceee_Summer_Studies/2019/9-improving-energy-efficiency-in-ict-appliances-and-products/factors-affecting-the-energy-efficiency-of-cold-appliances/. (Accessed 18 June 2020).

Gemmell, Andrew; Foster, Helen; Siyanbola, Busola; Evans, Judith: Study of Over-consuming Household Cold Appliances, Building Research Establishment Ltd. (BRE). URL: https://assets.publishing.service.gov.uk/government/uploads/system/uploads/attachment_data/file/5 85520/Cold_appliances_field_trial_report_FINAL_230117_2_.pdf (accessed: 12.05.2020).

Geppert, J., 2011. Modelling of Domestic Refrigerators' Energy Consumption under Real Life Conditions in Europe. Rheinische Friedrich-Wilhelms-Universität Bonn, Institut für Landtechnik. Dissertation, 2011.

Geppert, J., Stamminger, R., 2010. Do consumers act in a sustainable way using their refrigerator? The influence of consumer real life behaviour on the energy consumption of cooling appliances. Int. J. Consum. Stud. 34, 219–227. https://doi.org/10.1111/j.1470-6431.2009.00837.x.

Geppert, J., Stamminger, R., 2011. Modelling of Domestic Refrigerators' Energy Consumption under Real Life Conditions in Europe. Shaker Verlag, Bonn.

Geppert, J., Stamminger, R., 2013. Analysis of effecting factors on domestic refrigerator's energy consumption in use. Energy Convers. Manag. 76, 794–800. https://doi.org/10.1016/J.ENCONMAN.2013.08.027.

Energy Efficiency in Numbers, 2019. German Federal Ministry of Economics and Energy. https://www.bmwi.de/Redaktion/DE/Publikationen/Energie/energieeffizienz-in-zahlen-2019.pdf?_blob=publicationFile&v=72. accessed: 02.04.2020.

Gottwalt, S., Ketter, W., Block, C., Collins, J., Weinhardt, C., 2011. Demand side management - a simulation of household behavior under variable prices. Energy Pol. 39, 8163–8174. https://doi.org/10.1016/j.enpol.2011.10.016.

Greenblatt, J., Hopkins, A., Letschert, V.E., Blasnik, M., 2013. Energy use of US residential refrigerators and freezers: function derivation based on household and climate characteristics. Energy Efficiency 6, 135–162. https://doi.org/10.1007/s12053-012-9158-6.

Harrington, L., Aye, L., Fuller, B., 2018. Impact of room temperature on energy consumption of household refrigerators: lessons from analysis of field and laboratory data. Appl. Energy 211, 346–357. https://doi.org/10.1016/j.apenergy.2017.11.060.

Hasanuzzaman, M., Saidur, R., Masjuki, H.H., 2009. Effects of operating variables on heat transfer and energy consumption of a household refrigerator-freezer during closed door operation. Energy 34, 196–198. https://doi.org/10.1016/j.energy.2008.11.003.

Heap, R.D., 2001. Refrigeration and Air Conditioning – the Response to Climate Change. Bulletin of the IIR No 2001-5. Paris.

Hermes, C.J., Melo, C., Knabben, F.T., Goncalves, J.M., 2009. Prediction of the energy consumption of household refrigerators and freezers via steady-state simulation. Appl. Energy 86, 1311–1319. https://doi.org/10.1016/j.apenergy.2008.10.008.

Hueppe, C., Geppert, J., Stamminger, R., Paul, A., Elsner, A., Wagner, H., Hoelscher, H., Vrabec, J., Becker, W., Gries, U., Freiberger, A., 2020. Age-related efficiency loss of household refrigeration appliances: Development of an approach to measure the degradation of insulation properties. Appl. Therm. Eng. 173, 115113. https://doi.org/10.1016/j.applthermaleng.2020.115113.

James, S.J., Evans, J., 1992. The temperature performance of domestic refrigerators. Int. J. Refrig. 15, 313–319. https://doi.org/10.1016/0140-7007(92)90047-X.

James, S.J., Evans, J., James, C., 2008. A review of the performance of domestic refrigerators. J. Food Eng. 87, 2–10. https://doi.org/10.1016/j.jfoodeng.2007.03.032.

James, C., Onarinde, B.A., James, S.J., 2017. The use and performance of household refrigerators: a review. Compr. Rev. Food Sci. Food Saf. 16, 160–179. https://doi.org/10.1111/1541-4337.12242.

Khoukhi, M., Fezzioui, N., Draoui, B., Salah, L., 2016. The impact of changes in thermal conductivity of polystyrene insulation material under different operating temperatures on the heat transfer through the building envelope. Appl. Therm. Eng. 105, 669–674. https://doi.org/10.1016/j.applthermaleng.2016.03.065.

Kim, H.C., Keoleian, A., Horic, Y.A., 2006. Optimal household refrigerator replacement policy for life cycle energy, greenhouse gas emissions, and cost. Energy Pol. 34, 2310–2323. https://doi.org/10.1016/j.enpol.2005.04.004.

Kinney, L., Belshe, R., 2001. Refrigerator Replacement in the Weatherization Program: Putting a Chill on Energy Waste. *E Source*. https://www.larryweingarten.com/uploads/1/0/7/3/107350339/kinney_fridge_replacement.pdf. (Accessed 20 June 2020).

Lepthien, K., 2001. Umweltschonende Nutzung des Kühlgerätes im Haushalt. Shaker Verlag, Bonn.

Liu, D.-Y., Chang, W.-R., Lin, J.-Y., 2004. Performance comparison with effect of door opening on variable and fixed frequency refrigerators/freezers. Appl. Therm. Eng. 24, 2281–2292. https://doi.org/10.1016/j.applthermaleng.2004.01.009.

Lu, W., 2006. Potential energy savings and environmental impact by implementing energy efficiency standard for household refrigerators in China. Energy Pol. 34, 1583–1589. https://doi.org/10.1016/j.enpol.2004.12.012.

Marklinder, I.M., Lindblad, M., Eriksson, L.M., Finnson, A.M., Lindqvist, R., 2004. Home storage temperatures and consumer handling of refrigerated foods in Sweden. J. Food Protect. 67, 2570–2577. https://doi.org/10.4315/0362-028x-67.11.2570.

Masson, M., Delarue, J., Blumenthal, D., 2017. An observational study of refrigerator food storage by consumers in controlled conditions. Food Qual. Prefer. 56, 294–300. https://doi.org/10.1016/j.foodqual.2016.06.010.

Mc Donald, A., Schrattenholz, L., 2007. Learning rates for energy technologies. Energy Pol. 29, 255–261. https://doi.org/10.1016/S0301-4215(00)00122-1.

Nauta, M.J., Litman, S., Barker, G.C., Carlin, F., 2003. A retail and consumer phase model for exposure assessment of Bacillus cereus. Int. J. Food Microbiol. 83, 205–218. https://doi.org/10.1016/s0168-1605(02)00374-4.

Domestic Fridge Survey, NSW/FA/CP039/0912, 2009. NSW (New Sout Wales) Food Authority. https://www.foodauthority.nsw.gov.au/_Documents/scienceandtechnical/Domestic_%20Fridge_Survey.pdf. accessed: 02.06.2020.

Preparatory Studies, 2007. For Eco-Design Requirements of EUPs (Tender TREN/D1/49-2007). https://www.eup-network.de/fileadmin/user_upload/Lot_13_Final_Report_Taks_3-5.pdf. (Accessed 20 June 2020).

Roccato, A., Uyttendalaele, M., Membré, J.-M., 2017. Analysis of domestic refrigerator temperatures and home storage time distributions for shelf-life studies and food safety risk assessment. Food Res. Int. 96, 171–181. https://doi.org/10.1016/j.foodres.2017.02.017.

Saidur, R., Masjuki, H.H., Choudhury, I.A., 2002. Role of ambient temperature, door opening, thermostat setting position and their combined effect on refrigerator-freezer energy consumption. Energy Convers. Manag. 43, 845–854. https://doi.org/10.1016/S0196-8904(01)00069-3.

Terpstra, M.J., Steenbekkers, L.P.A., de Maetelaere, N.C.M., Niijhuis, S., 2005. Food storage and disposal: consumer practices and knowledge. Br. Food J. 7, 526–533. https://doi.org/10.1108/00070700510606918.

U.S. Food and Drug Administration, 2003. Quantitative Assessment of the Relative Risk to Public Health from Foodborne Listeria Monocytogenes Among Selected Categories of RTE Foods. http://www.foodsafety.gov/dms/lmr2-toc.html. (Accessed 15 June 2020).

Vendrusculo, E.A., Queiroz, G.C., Jannuzzi, G.D.M., 2009. Life cycle cost analysis of energy efficiency design options for refrigerators in Brazil. Energy Efficiency 2, 271–286. https://doi.org/10.1007/s12053-008-9034-6.

Vine, E., Du Pont, P., Waide, P., 2001. Evaluating the impact of appliance efficiency labelling programs and standards: process, impact, and market transformation evaluations. Energy 26, 1041–1059. https://doi.org/10.1016/S0360-5442(01)00053-6.

Wada, K., Akimoto, K., Sano, F., Oda, J., Homma, T., 2012. Energy efficiency opportunities in the residential sector and their feasibility. Energy 48, 5–10. https://doi.org/10.1016/j.energy.2012.01.046.

Warentest, Stiftung, 2013. Stromhunger Wächst, Test. 2013 60. https://www.test.de/Kuehl-und-Gefriergeraete-Stromhunger-waechst-4579954-0/. (Accessed 20 December 2019).

Weiss, M., Patel, M.K., Junginger, M., Blok, K., 2010. Analyzing price and efficiency dynamics of large appliances with the experience curve approach. Energy Pol. 38, 770–783. https://doi.org/10.1016/j.enpol.2009.10.022.

Young, 2008. Who pays for the 'beer fridge'? Evidence from Canada. Energy Pol. 36, 553–560. https://doi.org/10.1016/j.enpol.2007.09.034.

6.3 Determining the heat flow through the cabinet walls of household refrigerating appliances

Paul, A., Baumhögger, E., Elsner, A., Moczarski, L., Reineke, M., Sonnenrein, G., Hueppe, C., Stamminger, R., Hoelscher, H., Wagner, H., Gries, U., Freiberger, A., Becker, W., Vrabec, J., 2021. International Journal of Refrigeration 121, 235-242

In dieser Studie wurde der zeitliche Anstieg des in das Gehäuse eines Haushaltskältegeräts einfallenden Wärmestroms untersucht. Hierfür wurde ein neues Messverfahren, die Latent-Heat-Sink-Methode, entwickelt, mit dessen Hilfe der $k \cdot A$-Wert des Gehäuses zerstörungsfrei bestimmt werden kann. Diese neue Messmethode beruht auf einer als umspültes Eiswasserbad ausgeführte latente Wärmesenke. Mit dieser Methode wurde der $k \cdot A$-Wert von vier Haushaltskältegeräten über einen Zeitraum von 14 Monaten bestimmt. Der $k \cdot A$-Wert der Geräte stieg in diesem Zeitraum zwischen 3,6 % und 11,5 % an.

Der Autor dieser Dissertation hat die vorliegende Publikation verfasst, den Versuchsaufbau ausgearbeitet, die Versuche durchgeführt und ausgewertet. Lukas Moczarski und Michael Reineke haben die Durchführung der Versuche unterstützt. Bei der Mess- und Regelungstechnik für die Versuchsdurchführung wirkten Andreas Elsner und Elmar Baumhögger mit. In die Ausarbeitung des Versuchsaufbaus waren Andreas Elsner, Elmar Baumhögger und Gerrit Sonnenrein involviert. Die Haushaltskältegeräte wurden durch Wolfgang Becker von der BSH Hausgeräte GmbH bereitgestellt. Christian Hüppe, Rainer Stamminger, Heike Hölscher, Hendrik Wagner, Ulrich Gries und Alfred Freiberger unterstützten die Arbeiten zu dieser Publikation im Rahmen des Forschungsprojekts ALGE. An der Überarbeitung des Manuskripts waren Andreas Elsner und Jadran Vrabec beteiligt. Während der gesamten Arbeit wurde der Autor von Jadran Vrabec betreut.

International Journal of Refrigeration 121 (2021) 235–242

Contents lists available at ScienceDirect

International Journal of Refrigeration

journal homepage: www.elsevier.com/locate/ijrefrig

Determining the heat flow through the cabinet walls of household refrigerating appliances

Andreas Paul[a,b], Elmar Baumhögger[a], Andreas Elsner[a], Lukas Moczarski[a,b], Michael Reineke[a], Gerrit Sonnenrein[a], Christian Hueppe[c], Rainer Stamminger[c], Heike Hoelscher[d], Hendrik Wagner[d], Ulrich Gries[e], Alfred Freiberger[f], Wolfgang Becker[g], Jadran Vrabec[b,*]

[a] Thermodynamics and Energy Technology, University of Paderborn, Warburger Straße 100, 33098 Paderborn, Germany
[b] Thermodynamics and Process Engineering, Technical University of Berlin, Ernst-Reuter-Platz 1, 10587 Berlin, Germany
[c] Institute of Agricultural Engineering - Section Household and Appliance Engineering, University of Bonn, Nussallee 5, 53115 Bonn, Germany
[d] BASF Polyurethanes GmbH, Elastogranstraße 60, 49448 Lemförde, Germany
[e] Secop GmbH, Mads-Clausen-Straße 7, 24939 Flensburg, Germany
[f] Secop Austria GmbH, Jahnstraße 30, 8280 Fürstenfeld, Austria
[g] BSH Home Appliances GmbH, Robert-Bosch-Straße 100, 89537 Giengen an der Brenz, Germany

ARTICLE INFO

Article history:
Received 2 July 2020
Revised 14 September 2020
Accepted 5 October 2020
Available online 7 October 2020

Keywords:
Household refrigerating appliances
PUR foam
$k \cdot A$ value
Insulation
Measurement method

ABSTRACT

The increase of the thermal conductivity of PUR foam in the insulation of the cabinet is an important cause for aging processes of household refrigerating appliances. To determine the influence of the PUR foam aging on energy consumption, the development of a new measurement method is necessary because current methods influence the aging behavior of household refrigerators and are therefore not applicable in general. Based on a latent heat sink, constructed as an ice water bucket, a new measurement method is developed to determine the $k \cdot A$ value over time. With this method, the $k \cdot A$ value of four household refrigerating appliances was determined over an interval of 14 months. The $k \cdot A$ value increased between 3.6% and 11.5% during this period.

Détermination du transport thermique à travers les parois/cloisons des appareils de froid domestique

Mots-clés: Appareils de froid domestique; Mousse PUR; Valeur k·A; Isolation; Méthode de mesurage

1. Introduction

Due to the increasing customer awareness of global warming and the necessary reduction of greenhouse gas emissions, the EU energy label has become an essential selling point for modern household refrigerating appliances (Statista, 2018). It compares household refrigerating appliances with respect to their energy consumption, storage volume as well as construction type and classifies them according to their energy efficiency. For this purpose, standardized measuring methods are used to sample these quantities of new household refrigerating appliances. However, like any technical system, household refrigerating appliances are subject to considerable technical degeneration over their lifespan of up to 20 years in some cases. An Australian study from 1990 on household refrigerating appliances, most likely with CFC-containing PUR foams, showed no aging influence on energy consumption in the first two years (Australian Consumers' Association, 1990). Typically, CFC-11 was used in PUR foams at the time when that study was carried out (Kjeldsen and Jensen, 2001; Scheutz and Kjeldsen, 2002; Yazici et al., 2014). First prototypes

* Corresponding author.
E-mail address: vrabec@tu-berlin.de (J. Vrabec).

https://doi.org/10.1016/j.ijrefrig.2020.10.007
0140-7007/

Nomenclature

A	surface (m^2)
A_a	outer surface (m^2)
A_i	inner surface (m^2)
A_j	average surface of material layer j (m^2)
$c_{v,\,ice}$	specific isochoric heat capacity of ice (kJ/(kg K))
d_j	material thickness of layer j (mm)
k	heat transfer coefficient (W/(m^2 K))
$(k\cdot A)_{total}$	$k\cdot A$ value related to the ice water bucket (W/K)
$(k\cdot A)_{ffc}$	$k\cdot A$ value related to the fresh food compartment (W/K)
m_{ice}	mass of ice of the second addition (kg)
P_{pump}	power of pump (W)
$\dot{Q}_{ice}$	heat flow absorbed by the ice (W)
$\dot{Q}_{cab.}$	heat flow through the cabinet (W)
$\dot{Q}_{total}$	heat flow related to the ice water bucket (W)
$\dot{Q}_{ffc}$	heat flow related to the fresh food compartment (W)
T_a	ambient temperature (°C)
T_{ice}	time averaged ice temperature (°C)
$T_{ice,\,i}$	instantaneous ice temperature (°C)
$T_{ice,\,1}$	storage temperature of the ice (°C)
T_i	temperature inside (°C)
T_{ma}	time averaged temperature of heat sink measurements (°C)
T_1	temperature at measurement point 1 (°C)
T_2	temperature at measurement point 2 (°C)
T_3	temperature at measurement point 3 (°C)
α_a	heat transfer coefficient outside (W/(m^2 K))
α_i	heat transfer coefficient inside (W/(m^2 K))
Δh_m	enthalpy of fusion of ice (kJ/kg)
$\Delta(k\cdot A)_{total}$	measurement error related to the ice water bucket (%)
$\Delta(k\cdot A)_{ffc}$	measurement error related to the fresh food compartment (%)
$\Delta(k\cdot A)_{max}$	maximum measurement error (%)
$\Delta\tau_m$	melting time (s)
ΔT	temperature difference (K)
λ_j	thermal conductivity of material layer (W/(m K))
λ_{PS}	thermal conductivity of HIPS (W/(m K))
λ_{PUR}	thermal conductivity of PUR foam (W/(m K))
λ_{ST}	thermal conductivity of steel (W/(m K))

of CFC-free household refrigerating appliances were developed in 1992 (Meyer, 1993). Around 1994, the first models of this appliance type were brought into the market in significant numbers (Stiftung Warentest, 1994a,b). Due to a low water content in the raw materials, CFC-containing PUR foams are typically less susceptible to aging processes than current state-of-the-art cyclopentane-blown PUR foams (Delebecq et al., 2013). Elsner et al. showed an increase of energy consumption between 20% and 35% over a period of 18 years for household refrigerating appliances with PUR foams that do not contain CFC (Elsner et al., 2013). Harrington examined the influence of the energy saving potential by replacing old appliances through modern appliances (Harrington, 2017). The study showed that the replacement of older appliances has an energy saving potential of about 60%. In his dissertation, Harrington (2018) examined the influence of consumer behavior on energy consumption of household refrigerating appliances. Among others, he determined the influence of temperature and humidity in the storage room, ambient temperature, evaporator defrosting, door openings and the general choice of the model. Wagner developed methods to simulate heat transfer through PUR foam as a part of his dissertation (Wagner, 2002).

The method described in this paper is part of a larger project, which aims to determine the energy consumption increase of new household refrigerators over a period of three years with non-destructive measurement methods.

1.1. Aging of PUR foams

With a share of 45% to 55%, the heat flow entering the storage room through the cabinet represents the largest driver for the energy consumption of a household refrigerating appliance (ASHRAE Handbook, 2010). The cabinet essentially consists of an approximately 1 mm layer of galvanized sheet steel on the outside, a 40-60 mm thick core made of PUR foam and an approximately 0.6-2 mm layer of high impact polystyrene (HIPS) on the inside towards the storage room. During the manufacturing process, isocyanates and polyols react in a polyaddition reaction to PUR. A second blowing reaction between isocyanates and water leads to CO_2-formation. The CO_2 and the additional physical blowing agent cyclopentane (or isopentane) cause foam rise of the PUR. After the manufacturing process, the cell gas of the PUR foam primarily consists of CO_2 and cyclopentane. Through diffusion processes, CO_2 is replaced over time by nitrogen and oxygen from the ambient air (Delebecq et al., 2013; Engels et al., 2013; Tucker, 1992; Berardi and Madzarevic, 2020). This leads to an increase of the thermal conductivity of the PUR foam (λ_{PUR}) and thus to an increase of the energy consumption of household refrigerating appliances (Wilkes et al., 1997, 1999, 2001, 2002, 2003; Albrecht, 2003). This process is strongly dependent on the temperature that the PUR foam is exposed to (Wilkes et al., 1997, 1999, 2001, 2002, 2003). Current research projects are examining the replacement of the blowing agent pentane with CO_2-water mixtures. However, this would not prevent aging due to diffusion processes, since CO_2 is also present in these PUR foam cells as a reaction product (Berardi and Madzarevic, 2020). Instead, the aging problem would be exacerbated with a CO_2-water mixture as a blowing agent.

1.2. Heat transfer through the cabinet walls

The heat flow through the cabinet walls ($\dot{Q}_{cab.}$) can be expressed as a product of the heat transfer coefficient (k), the surface area over which the heat transfer takes place (A) and the temperature difference (ΔT) between the ambient (T_a) and the temperature inside the cabinet (T_i) of the household refrigerating appliance.

$$\dot{Q}_{cab.} = k\cdot A\cdot\Delta T = k\cdot A\cdot(T_a - T_i) \tag{1}$$

The heat transfer coefficient k is constituted by the convective heat transfer coefficients on the outside (α_a) and inside (α_i) surface of the cabinet, the material thicknesses of the various layers of the wall structure (d_j) and the thermal conductivity of the materials (λ_j). Eq. (2) also considers the typically different surface sizes of the outside (A_a) and inside (A_i) of the cabinet and the middle surfaces of the different material layers (A_j).

$$\frac{1}{k\cdot A} = \frac{1}{\alpha_a\cdot A_a} + \sum_{j=1}^{n}\frac{d_j}{\lambda_j\cdot A_j} + \frac{1}{\alpha_i\cdot A_i} \tag{2}$$

A schematic of the cabinet walls and the resulting temperature profile is shown in Fig. 1. With increasing usage time, the thermal conductivity of the PUR foam (λ_{PUR}) increases, while the thermal conductivity of the galvanized steel sheet (λ_{ST}) on the outside and that of the HIPS inliner (λ_{PS}) remain constant. Consequently, the heat flow entering the cabinet increases and so does the energy consumption of the refrigeration process (Fig. 1).

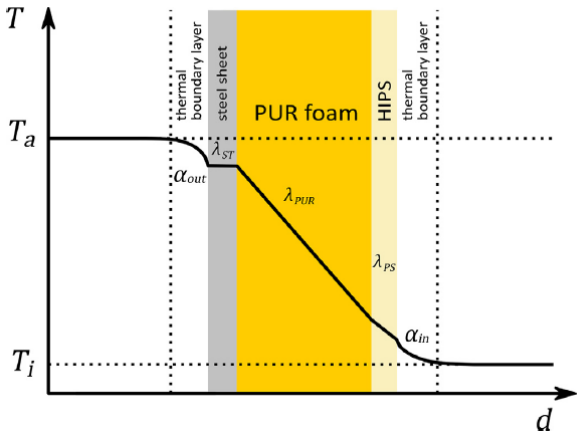

Fig. 1. Schematic of the cabinet wall structure of a household refrigerating appliance with a qualitative temperature profile.

1.3. Measurement methods for the k·A value

Several measurement methods to determine the heat flow through the refrigerating appliance cabinet walls have been proposed. Among them, the reverse heat leak method should be mentioned in particular. Various authors have reported on their investigations, modifications and improvements of the reverse heat leak method (Stovall, 2012; Melo et al., 2000; Lieghton, 2011; Sim and Ha, 2011; Hermes et al., 2013), which is also used in R&D departments of refrigerating appliance manufacturers.

In contrast to the usual temperature conditions in the storage room of a refrigerating appliance, heat is supplied to the interior of the cabinet by means of an electric heater, while the ambient temperature is reduced, so that a heat flow occurs from the inside out. The electrical heating power needed to maintain a stable temperature inside the cabinet is directly related to the heat flow through the cabinet walls.

However, in practice, there are several problems with this experimental setup:

- Using the reverse heat leak method repeatedly over a period of several years can theoretically lead to accelerated aging, as cell gas diffusion is temperature dependent and progresses more rapidly at elevated temperatures.
- In order to prevent temperature stratification in the interior, fans are used in the reverse heat leak method to achieve a more homogeneous temperature distribution. However, the fans create a forced air flow that differs from natural convection in real household use. This results in a larger convective heat transfer coefficient and the aging-dependent thermal conductivity of the PUR foam can be falsified.
- The temperature difference between the storage room and the ambient differs from real household use, where the largest temperature difference occurs at the lower part of the storage room of the refrigerator, while the largest temperature difference at in the upper part of the storage room when using the reverse heat leak method, cf. Fig. 2.

The heat flow can also be determined with heat flow sensors which are selectively placed on the cabinet. The functionality of the heat flow sensors was described by Lassue et al. (1993). Melo et al. investigated the use of heat flow sensors and compared the results with the reverse heat leak method (Melo et al., 2000). This measuring method was further refined by Thiessen et al. (2014).

However, the heat flow sensor measurement method also turned out to be unsuitable for the present project. Each refrigerating appliance has an individual cabinet design, depending on the manufacturer, brand, appliance type and condenser position arrangement. Cables and refrigerant pipes, which run through the PUR foam at various places, would have a strong impact on the results of this method.

Hueppe et al. (2020) developed another measurement method. They determined the k·A value through the duration of a temperature rise in the storage compartments with a temperature rise test. In addition, aging tests on PUR foam samples have been published and show an increase of thermal conductivity of the PUR foam from 19.5 mW/(m K) to 22.5 mW/(m K) in 420 days.

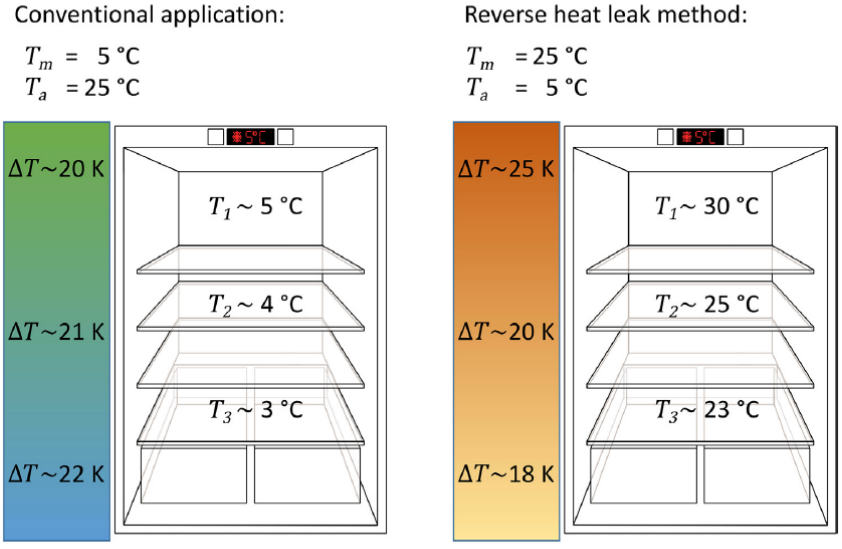

Fig. 2. Representation of the temperature gradient over a fresh food compartment during conventional use and reverse heat leak method measurement.

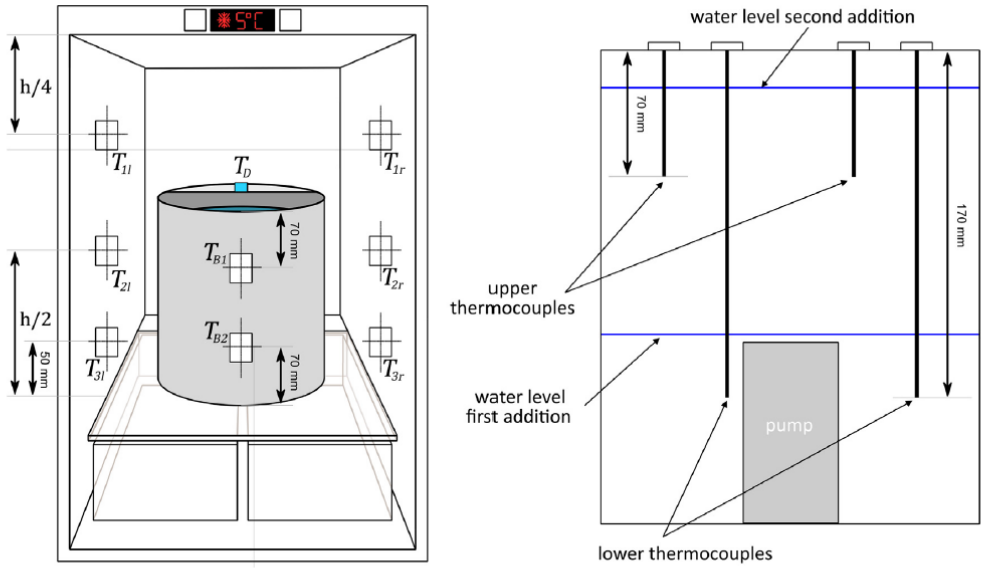

Fig. 3. Basic measurement setup in the fresh food compartment (left) and in the ice water bucket (right).

2. Test setup

A non-destructive measuring method for the $k \cdot A$ value was developed in this work with the following aims:

The natural temperature stratification in the storage room of the refrigerating appliances and the temperature differences between the storage room and the ambient should be maintained as far as possible, natural convection should prevail in the storage room of the appliances and the measurement method should be integratable into the existing measurement setup of the standard energy consumption test according to the standard series IEC 62552:2015 (part 1 – part 3) with as little effort as possible (IEC 62552:2015, 2015a,b,c).

2.1. Methodology

In the present latent heat sink measuring method, the refrigeration cycle of the appliance does not operate. Instead, the storage room of the appliance is cooled by a heat sink in the form of an ice water bucket (height 210 mm, diameter 254 mm) with a volume of 10.64 liters, cf. Figs. 3 and 4. To achieve a homogeneous temperature distribution of the entire bucket surface, several cooling fins were attached to the lid, which protruded into the ice water. To avoid temperature stratification in the ice water, a pump was installed at the bottom of the tank to enforce circulation. The electrical power consumed by the pump was measured and taken into account in the energy balance for the calculation of the $k \cdot A$ value. To monitor the melting process of the ice water, four thermocouples were attached to the container, which protruded into the ice water at two different heights. Furthermore, surface temperatures of the tank were measured with two thermocouples and that of the lid with a third thermocouple.

Before the actual start of the experiment, the refrigerating appliance was operating at a time averaged fresh food compartment temperature of $T_{ma} = 4\,°C$ to 5 °C, which was determined as the mean value of the six temperature measuring points (T_{1r} to T_{3r} and T_{1l} to T_{3l}) located on both sides of the ice water bucket, cf. Fig. 3. The measurements were made at ambient temperatures of 16 °C, 25 °C and 32 °C following the IEC 62552:2015 series of standards (part 1 and 3) (IEC 62552:2015, 2015a,c). Depending on the ambient temperature, the ice water bucket was filled with an amount of liquid water as shown in Table 1 at the start of each measurement.

In principle, the experiment should measure the time required for the ice melting process, where the water temperature remains constant. The point in time at which there is no longer a temperature of 0 °C at all measuring points in the ice water can be seen as an increase in the temperature curve, cf. Fig. 5. However, since there may still be residual ice in the bucket at this point in time, a solution had to be found to ensure that the amount of residual ice is the same at the start and the end of the measurement period. For this purpose, two ice additions were made.

First, a smaller amount of ice was added to the ice bucket. A relatively constant time period for the first melting phase could be achieved by varying this ice amount depending on the various ambient temperatures (cf. Table 1). During this phase of the experiment, the water level in the bucket only reaches the lower thermocouples, cf. Fig. 3.

When the lower thermocouples indicated that the temperature of the ice water had risen by 0.2 K, a second quantity of ice was added to the bucket and the actual measurement was initiated. The evaluation period ended when the average temperature of all ice water thermocouples again rose by 0.2 K. The difference between start and end of the evaluation period was the melting time ($\Delta\tau_m$). Fig. 5 shows the temperature profile of the ice water over the course of a measurement.

Validation tests were performed with a mass of 3500 g ice for the second addition and the measurements of the aging studies were performed with 3000 g to avoid overly long total measurement times.

2.2. Evaluation

By determining the time interval that the ice needs to melt ($\Delta\tau_m$), employing the enthalpy of fusion of water ($\Delta h_m = 333.5$ kJ/kg) and the mass of ice at the second ice addition (m_{ice}), the heat flow ($\dot{Q}_{ice}$) is given by Eq. (3). Since the

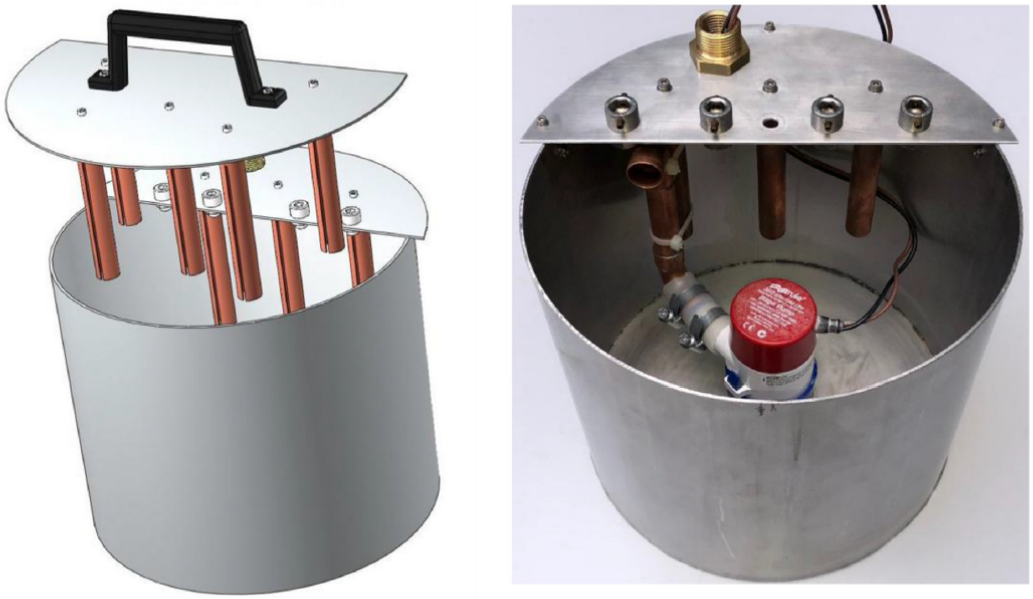

Fig. 4. Ice water bucket: technical drawing (left) and photo of the device (right).

Table 1
Comparison of the test parameters of the first ice addition under different ambient temperatures.

Ambient temperature	16 °C	25 °C	32 °C
Mass of liquid water in the ice water bucket	4000 ± 20 g	3500 ± 20 g	3000 ± 20 g
Mass of the first addition of ice	1000 ± 20 g	1500 ± 20 g	2000 ± 20 g
Time of the first melting phase	7.00–7.75 h	6.75–7.50 h	7.00–7.75 h

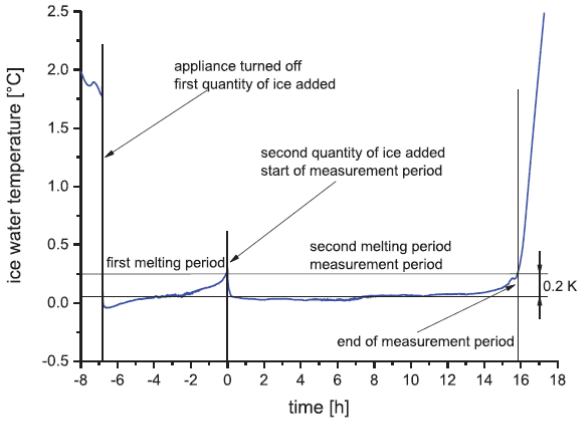

Fig. 5. Ice water temperature over time.

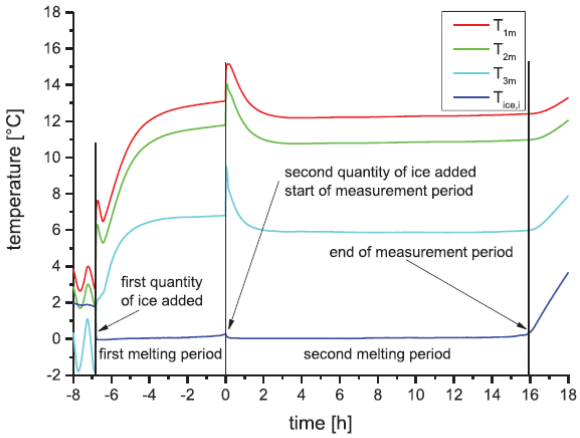

Fig. 6. Temperature at the measuring points in the fresh food compartment over time.

ice was stored at temperatures below 0 °C ($T_{ice,1}$), the according enthalpy contribution was taken into account via the isochoric heat capacity of the ice ($c_{v,ice} = 2.204$ kJ/(kg K)). The electrical power of the pump (P_{pump}) is dissipated by the circulation of the ice water and must be considered in the energy balance.

$$(k \cdot A)_{total} = \frac{m_{ice} \cdot (\Delta h_m + c_{v,ice} \cdot (T_{ice} - T_{ice,1}))}{(T_a - T_{ice}) \cdot \Delta\tau_m} - \frac{P_{pump}}{(T_a - T_{ice})} \quad (3)$$

The equations presented in this way describe the $(k \cdot A)_{total}$ value for the heat flow entering the ice water through the appliance cabinet and the storage room. As shown in Fig. 6, almost constant instantaneous temperatures (T_{ma}) were present in the storage room of the fresh food compartment during the tests. The balance between the heat flows $\dot{Q}_{cab.}$ and $\dot{Q}_{ice}$ remained practically constant until the end of the second melting phase. During the first

Table 2
Technical data of the studied refrigerating appliances.

Test device		V1	V2	R1	R2	R3	R4
Refrigerator model		K12020 S-1	KI81RAD 30/04	KS 16-1 RVA+++	KS 16-1 RVA+++	KI81RAD 30/04	KI81RAD 30/04
Manufacturer		Miele	Siemens	Exquisit	Exquisit	Siemens	Siemens
Refrigerator type		table-height refrigerator	built-in refrigerator	table-height refrigerator	table-height refrigerator	built-in refrigerator	built-in refrigerator
Dimensions (HxWxD)	[mm]	850 × 601 × 628	1775 × 560 × 550	845 × 555 × 575	845 × 555 × 575	1775 × 560 × 550	1775 × 560 × 550
Total storage volume	[l]	167	319	134	134	319	319
Refrigerant		22 g R600a	46 g R600a	26 g R600a	26 g R600a	46 g R600a	46 g R600a
Energy label		A+	A++	A+++	A+++	A++	A++

melting phase, there was an increase of the instantaneous temperatures until a balance between the heat flow entering the storage room through the cabinet and the heat flow entering the ice water bucket from the storage room was established. The slightly lower instantaneous temperatures during the second melting phase can be explained by the higher degree of filling in the ice water bucket and the resulting larger surface of the bucket wetted by ice water.

Constant instantaneous temperatures in the fresh food compartment allow for the replacement of the ice water temperature with the instantaneous temperature of the fresh food compartment in Eq. (3) so that the $(k \cdot A)_{ffc}$ value related to the refrigerating appliance cabinet can be determined, cf. Eq. (4). For this purpose, the ice water temperature in the denominator is replaced with the average fresh food compartment temperature.

$$(k \cdot A)_{ffc} = \frac{m_{ice} \cdot (\Delta h_m + c_{v,ice} \cdot (T_{ice} - T_{ice,1}))}{(T_a - T_{ma}) \cdot \Delta \tau_m} - \frac{P_{pump}}{(T_a - T_{ma})} \quad (4)$$

2.3. Refrigerating appliances

For a validation of the present measurement method, a commercially available table-height refrigerator (Miele, type K12020 S-1) was used. This appliance (V1) was chosen due to its age of five years. The investigations discussed in Section 1 show that the most pronounced aging effects occur in the first three years (Elsner et al., 2013; Wilkes et al., 1997, 1999, 2001, 2002, 2003; Albrecht, 2003). Thus, only small changes of the $k \cdot A$ value were expected for this appliance. In addition, aging tests were carried out for four refrigerators (R1 to R4), cf. Table 2. Contrary to the requirements of the standard IEC 62552–1:2015, part 1, (IEC 62552:2015, 2015a) the built-in refrigerators were operated without wooden cabinets in order to exclude any influences of the wood on the measurement results.

2.4. Measurement system and measurement error analysis

The mass of water and ice was measured with a laboratory scale DE350.5D (Kern & Sohn GmbH) with an accuracy of ± 2.5 g. Temperatures were sampled by thermocouple differential measurements, where each measuring point had its own reference junction in a separate ice water bath. The measurement signal of the thermocouples was processed by a combination of a pre-amplifier LTC1050 (Linear Technologies) with adjusted gain of 1000 and a digital-to-analog converter system OMB-DAQ 55/56 (Omega Technologies), limiting the offset drift to ± 0.025 K. By calibrating each thermocouple individually and applying a polynomial correction, the measurement error was reduced from ± 1% x ΔT to ± 0.5% x ΔT. All measurements were carried out in a climatic chamber with an ambient temperature fluctuation of ± 0.5 K and an air humidity of 50%. The supply voltage of the pumps was provided by BT-305 laboratory power supplies (BASETech) with ± 1% + 0.02 V accuracy and the electric current with ± 2% + 0.02 A. Due to cable length, the supply voltage at the pump was 1% lower than the output of the power supply, which was taken into account in the calculations. The pumps (Bilge pump 360GPH) were operated with a supply voltage of 5 V. In preliminary tests, this turned out to be the best compromise between the heat introduced by the pump and the necessary circulation of the ice water to prevent temperature stratification in the bucket.

Table 3
Measured properties and their uncertainties.

Measured quantity	Measuring device	Uncertainty
Temperature	Thermocouples	± 0.1 K
Voltage	Laboratory power supplies	± 1% + 0.02 V
Electric current	Laboratory power supplies	± 2% + 0.02 A
Time	Personal computer	± 0.1 s/day
Mass	Laboratory scale	± 2.5 g

The measurement errors of the various devices are summarized in Table 3. The fluctuation of the ice storage temperature ($T_{ice,1}$) was assumed to be ± 1 K due to transportation and handling of the ice prior to the addition process. The measurement errors $\Delta(k \cdot A)_{total}$ and $\Delta(k \cdot A)_{ffc}$ were calculated with the error propagation law.

3. Results and discussion

3.1. Validation

For validation, five measurements for each ambient temperature of 16 °C, 25 °C and 32 °C were carried out with refrigerating appliance V1. The aim was to check the reproducibility and the influence of the ambient temperature on the results. In addition to the measured properties and the results for the $k \cdot A$ values of the individual measurements, the total measurement errors $\Delta(k \cdot A)_{total}$ and $\Delta(k \cdot A)_{ffc}$ are specified in the following.

Overall, the data show a homogeneous distribution of the measurement results with a scatter on the same order of magnitude as the overall measurement error. As shown in Table 4, no influence of the ambient temperature on the measurement results was found.

Despite the relatively constant results at different ambient temperatures, an ambient temperature of 25 °C was preferred for this measurement method. At an ambient temperature of 16 °C there are significantly higher measurement errors (± 1.9%) and a time of more than 24 h for an entire test (first and second addition of ice) leads to additional organizational effort in labor operation. In addition, only for this ambient temperature, it was observed that

Table 4
Results of the validation test series with varying ambient temperature.

Test series			16 °C	25 °C	32 °C
Ambient temperature	T_a	[°C]	15.7	24.8	31.8
Mass of the second addition of ice	m_{ice}	[g]	3489.0	3490.5	3493.5
Evaluation period	$\Delta\tau_m$	[h]	22.81	15.83	12.90
Average fresh food compartment temperature	T_{ma}	[°C]	6.3	9.8	12.8
Power of the pump	P_{pump}	[W]	4.35	4.35	4.29
$(k \cdot A)_{total}$		[W/K]	0.74	0.75	0.75
$\Delta(k \cdot A)_{total}$		[%]	1.9	1.2	0.9
$(k \cdot A)_{ffc}$		[W/K]	1.22	1.24	1.25
$\Delta(k \cdot A)_{ffc}$		[%]	1.3	0.8	0.6

Table 5
Evaluation for the selection of the ambient temperature.

Ambient temperature	16 °C	16 °C	25 °C	32 °C
Measurement error	$\Delta(k \cdot A)_{max}$	± 1.9% –	± 1.2% 0	± 0.9% +
Measurement time	second melting interval ($\Delta\tau_m$) total	22.80 h 30.50 h –	15.63 h 23.00 h 0	12.90 h 20.50 h +
Ice layer on the water surface		yes –	no +	no +
Average fresh food compartment temperature	T_{ma}	6.3 °C +	9.9 °C 0	12.8 °C –

Table 6
Results of the aging study of refrigerating appliances.

Test device			R1	R2	R3	R4
Refrigerator model Manufacturer			KS 16–1 RVA+++ Exquisit	KS 16–1 RVA+ Exquisit	KI81RAD 30/04 Siemens	KI81RAD 30/04 Siemens
$(k \cdot A)_{total}$	new	[W/K]	0.56	0.53	0.82	0.78
	after 14 months	[W/K]	0.58	0.58	0.88	0.87
	difference	[W/K]	+ 0.02	+ 0.05	+ 0.06	+ 0.09
		[%]	+ 3.6%	+ 9.4%	+ 7.3%	+ 11.5%
$(k \cdot A)_{ffc}$	new	[W/K]	0.82	0.78	1.65	1.60
	after 14 months	[W/K]	0.87	0.86	1.79	1.78
	difference	[W/K]	+ 0.05	+ 0.08	+ 0.14	+ 0.18
		[%]	+ 6.1%	+ 10.3%	+ 8.5%	+ 11.3%

an ice layer formed in the bucket on the water surface. A comparison of the ambient temperatures of 25 °C and 32 °C shows that the measurement error is lower at 32 °C, but the internal temperatures were significantly higher than in regular refrigerator operation. Table 5 shows the selection criteria mentioned for the evaluation of the three ambient temperatures.

3.2. Aging studies

With the present measuring method, the aging of commercially available refrigerating appliances was investigated shortly after their manufacturing. For this purpose, two tests per appliance were carried out on four appliances at an interval of 14 months and the $k \cdot A$ value was determined. The results are listed in Table 6. Fig. 7 shows the results for the $(k \cdot A)_{total}$ value and the $(k \cdot A)_{ffc}$ value. The results indicate an increase between 3.6% and 11.5% for $(k \cdot A)_{total}$ and an increase between 6.1% and 11.3% for $(k \cdot A)_{ffc}$. These differences between the $k \cdot A$ values are significantly larger than the measurement error ($\Delta(k \cdot A)_{max} < 2\%$). Hueppe et al. (2020) investigated the change over time of the thermal conductivity of PUR foam samples and observed an increase of about 15% over a period of 420 days. The determined increase of the $k \cdot A$ value of real refrigerating appliances is of similar magnitude.

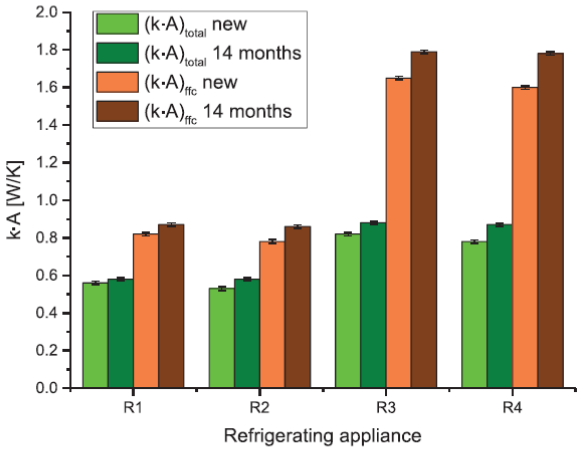

Fig. 7. Results of the aging study for $(k \cdot A)_{total}$ (green) and $(k \cdot A)_{ffc}$ (brown). (For interpretation of the references to color in this figure legend, the reader is referred to the web version of this article.)

4. Conclusions

The presented experimental method with a latent heat sink is a suitable alternative to the reverse heat leak method for determining the heat flow into the cabinet of a refrigerating appliance. The advantage of the latent heat sink method is that the air flow and the temperatures in the storage room are comparable to the real operating conditions. The usage of fans in the reverse heat leak method generates locally turbulent flows, which increase convective heat transfer. The temperature gradient between the storage room and the ambient is also more realistic.

An ambient temperature of 25 °C was found to be optimal for using the latent heat sink method. Application-related temperatures are reached in the storage compartments, the measurement error is small and the total measurement time can be integrated into a 24 h cycle. An ambient temperature of 32 °C should not be chosen due to the higher storage temperature in the compartment and 16 °C should not be chosen due to the possible formation of ice layers.

By measuring the $k \cdot A$ value of new refrigerating appliances over time, an increase of 8.2% (± 2.1%) for the table-high refrigerators and 9.9% (± 1.4%) for the large built-in refrigerators was found over a period of 14 months. This result is consistent with the literature for the increase of the thermal conductivity of PUR foam.

Declaration of Competing Interest

The authors declare that they have no known competing financial interests or personal relationships that could have appeared to influence the work reported in this paper.

Acknowledgments

This work was carried out as part of the ALGE research project funded by the German Federal Ministry for Economic Affairs and Energy as part of the 6th energy research program (project funding reference number: 03ET1544A-E).

References

Albrecht, W., 2003. Änderung der Wärmeleitfähigkeit von zehn Jahre alten PUR-Hartschaumplatten mit gasdiffusionsoffenen Deckschichten. Bauphysik 25, 317–319.
Australian Consumers' Association, 1990. Energy Consumption of Refrigerators and Freezers Used Under Normal Conditions of Use. Choice, Sydney, Australia.
Berardi, U., Madzarevic, J., 2020. Microstructural analysis and blowing agent concentration in aged polyurethane and polyisocyanurate foams. Appl. Therm. Eng. 164, 114440.
Delebecq, E., Pascault, J.-P., Boutevin, B., Ganachaud, F., 2013. On the versatility of urethane/urea bonds: reversibility, blocked isocyanate, and non-isocyanate polyurethane. Chem. Rev. 113, 80–118.
Elsner, A., Müller, M., Paul, A., Vrabec, J., 2013. Zunahme des Stromverbrauchs von Haushaltskältegeräten durch Alterung. Deutsche Kälte-Klima Tagung 40, Hannover, Germany 20–22
Engels, H.-W., Pirkl, H.-G., Albers, R., Albach, R.W., Krause, J., Hoffmann, A., Casselmann, H., Dormish, J., 2013. Polyurethane: vielseitige materialien und nachhaltige problemlöser für aktuelle anforderungen. Angew. Chem. 125, 9596–9616.
Harrington, L., 2017. Quantifying energy savings from replacement of old refrigerators. Energy Procedia 121, 49–56.
Harrington, L., 2018. Prediction of the Energy Consumption of Refrigerators During Use. Melbourne, Australia.
Hermes, C., Melo, C., Knabben, F., 2013. Alternative test method to assess the energy performance of frost-free refrigerating appliances. Appl. Therm. Eng. 50, 1029–1034.
Hueppe, C., Geppert, J., Stamminger, R., Wagner, H., Hoelscher, H., Vrabec, J., Paul, A., Elsner, A., Becker, W., Gries, U., Freiberger, A., 2020. Age-related efficiency loss of household refrigeration appliances: development of an approach to measure the degradation of insulation properties. Appl. Therm. Eng. 173, 115113.
IEC 62552:2015, 2015a. IEC 62552-1:2015 Household Refrigerating Appliances – Characteristics and Test Methods – Part 1: General Requirements. International Electrotechnical Commission (IEC).
IEC 62552-2:2015, 2015b. IEC 62552-2:2015 Household Refrigerating Appliances – Characteristics and Test Methods – Part 2: Performance Requirements. International Electrotechnical Commission (IEC).
IEC 62552:2015, 2015c. IEC 62552-3:2015 Household Refrigerating Appliances – Characteristics and Test Methods Part 3: Energy Consumption and Volumes. International Electrotechnical Commission (IEC).
Kjeldsen, P., Jensen, M.H., 2001. Release of CFC-11 from disposal of polyurethane foam waste. Environ. Sci. Technol. 35, 3055–3063.
Lassue, S., Guths, S., Leclercq, D., Duthoit, B., 1993. Contribution to the experimental study of natural convection by heat flux measurement an anemometry using thermoelectric effects. Exp. Heat Transf. Fluid Mech. Thermodyn. 1993, 831–838.
Lieghton, D.L., 2011. Investigation of Household Refrigerator With Alternative Low Global Warming Potential Refrigerants Master thesis. University of Maryland, USA.
Melo, C., da Selva, L.W., Pereira, R.H., 2000. Experimental evaluation of the heat transfer through the walls of household refrigerators. In: Proceedings of the Eighth International Refrigeration Conference at Purdue University, West Lafayette, IN, USA, pp. 353–360.
Meyer, A, 1993. Der FCKW-freie kuehlschrank der FORON-hausgeraete gmbH - ein beitrag fuer eine bessere umwelt. Luft- und kaeltetechnik 29, Nr. 1, 3–4.
Scheutz, C., Kjeldsen, P., 2002. Determination of the fraction of blowing agent released from refrigerator/freezer foam after decommissioning the product. Environment and Resources DTU. Technical University of Denmark.
Sim, J.S., Ha, J.S., 2011. Experimental study of heat transfer characteristics for a refrigerator by using reverse heat loss method. Int. Commun. Heat Mass Transf. 38, 572–576.
Statista: Haushaltsgroßgeräte. 2018, URL: https://de.statista.com/statistik/studie/id/7683/dokument/haushaltsgrossgeraete-statista-dossier/.
Stiftung Warentest, 1994. Umwelt geschont – strom gespart. Test, Nr.3, 36–39.
Stiftung Warentest, 1994. Auch ohne ozonkiller. Test, Nr.6, 24–25.
, 2010. ASHRAE Handbook 2010: Refrigeration, SI edition ASHRAE, Atlanta, GA ISBN 1933742828.
Stovall, T., 2012. Closed Cell Foam Insulation: A Review of Long Term Thermal Performance. Oak Ridge National Laboratory Report ORNL/TM-2012/583.
Thiessen, S., Knabben, F.T., Melop, C., 2014. Experimental evaluation of the heat fluxes through the walls of a domestic refrigerator. In: Proceedings of the 15th Brazilian Congress of Thermal Sciences an Engineering. Belem, PA, Brazil.
Tucker, B.W., 1992. Rigid polyurethane foams with low thermal conductivities, Patent document, US005169877A, PCT, 08.12.1992.
Wagner, K-E., 2002. Simulation und Optimierung des Wärmedämmvermögens von PUR Hartschaum, Wärme- und Stofftransport sowie mechanische Verformung. Stuttgart, Germany doi:10.18419/opus-1579.
Wilkes, K.E., Yarbrough, D.W., Weaver, F.J., 1997. Aging of polyurethane foam insulation in simulated refrigerator walls. In: Proceedings of the International Conference on Ozone Protection Technologies, Baltimore Maryland, pp. 12–13.
Wilkes, K.E., Gabbard, W.A., Weaver, F.J., 1999. Aging of Polyurethane Foam Insulation in Simulated Refrigerator Panels: One-year Results With Third-generation Blowing Agents. The Earth Technologies Forum, Washington D.C., pp. 27–29.
Wilkes, K.E., Gabbard, W.A., Weaver, F.J., Booth, J.R., 2001. Aging of polyurethane foam insulation in simulated refrigerator panels: two-year results with third–generation blowing agents. J. Cell. Plast. 37, 400–428.
Wilkes, K.E., Yarbrough, D.W., Gabbard, W.A., Nelson, G.E., Booth, J.R., 2002. Aging of polyurethane foam insulation in simulated refrigerator panels: three-year results with third-generation blowing agents. J. Cell. Plast. 38, 317–339.
Wilkes, K.E., Yarbrough, D.W., Nelson, G.E., Booth, J.R., 2003. Aging of Polyurethane Foam Insulation in Simulated Refrigerator Panels: Four-year Results With Third–generation Blowing Agents. The Earth Technologies Forum, Washington D.C..
Yazici, B., Can, Z.s., Calli, B., 2014. Prediction of future disposal of end-of-life refrigerators containing CFC-11. Waste Manag. 34, 162–166.

6.4 Age-related efficiency loss of household refrigeration appliances: Development of an approach to measure the degradation of insulation properties

Hueppe, C., Geppert, J., Stamminger, R., Wagner, H., Hoelscher, H., Vrabec, J., Paul, A., Elsner, A., Becker, W., Gries, U., Freiberger, A., 2020. Applied Thermal Engineering 173, 115113.

Für den alterungsbedingten Anstieg der Energieaufnahme von Haushaltskältegeräten stellte sich der im Gehäuse verbaute Polyurethan-Hartschaum als entscheidende Systemkomponente heraus. Innerhalb dieser Studie wurde ein neuer Ansatz entwickelt, mit dem der alterungsbedingte Verlust der Dämmwirkung zerstörungsfrei untersucht werden kann. Dieses Messverfahren wurde in einer Messreihe an verschiedenen Geräten validiert. Darüber hinaus wurde die Wärmeleitfähigkeit von Polyurethan-Hartschaumstoffproben in einer Messreihe über einen Zeitraum von 13 Monaten gemessen, wobei ein Anstieg von 15 % festgestellt wurde.

Der Autor dieser Dissertation hat bei der Ausarbeitung der vorliegenden Publikation mitgewirkt, insbesondere hat er bei der Erstellung der Versuchsaufbauten und durch die Übernahme administrativer Aufgaben unterstützt. Christian Hüppe hat die Publikation verfasst, den Versuchsaufbau entwickelt und die Versuche durchgeführt. Jasmin Geppert hat die Durchführung der Versuche unterstützt. Die Haushaltskältegeräte wurden durch Wolfgang Becker von der BSH Hausgeräte GmbH bereitgestellt. Andreas Elsner, Heike Hölscher, Hendrik Wagner, Ulrich Gries und Alfred Freiberger unterstützten die Arbeiten zu dieser Publikation im Rahmen des Forschungsprojekts ALGE. An der Überarbeitung des Manuskripts war Jadran Vrabec beteiligt. Während der gesamten Arbeit wurden die Autoren von Rainer Stamminger und Jadran Vrabec betreut.

Applied Thermal Engineering 173 (2020) 115113

Contents lists available at ScienceDirect

Applied Thermal Engineering

journal homepage: www.elsevier.com/locate/apthermeng

Age-related efficiency loss of household refrigeration appliances: Development of an approach to measure the degradation of insulation properties

Christian Hueppe[a,*], Jasmin Geppert[a], Rainer Stamminger[a], Hendrik Wagner[b], Heike Hoelscher[b], Jadran Vrabec[c], Andreas Paul[d], Andreas Elsner[d], Wolfgang Becker[e], Ulrich Gries[f], Alfred Freiberger[g]

[a] University of Bonn, Institute of Agricultural Engineering – Section Household and Appliance Engineering, Nussallee 5, 53115 Bonn, Germany
[b] BASF Polyurethanes GmbH, Elastogranstraße 60, 49448 Lemförde, Germany
[c] Technical University of Berlin, Department of Thermodynamics and Process Engineering, Ernst-Reuter-Platz 1, 10587 Berlin, Germany
[d] Paderborn University, Department of Thermodynamics and Energy Technology (ThET), Warburger Straße 100, 33098 Paderborn, Germany
[e] BSH Home Appliances GmbH, Robert-Bosch-Straße 100, 89537 Giengen an der Brenz, Germany
[f] SECOP GmbH, Mads-Clausen-Str. 7, 24939 Flensburg, Germany
[g] SECOP Austria GmbH, Jahnstraße 30, 8280 Fürstenfeld, Austria

HIGHLIGHTS

- Age-related efficiency loss of domestic refrigeration appliances.
- Increasing energy consumption of refrigeration appliances over time.
- Development of a method to investigate refrigerator insulation degradation.
- Changing thermal conductivity and cell gas composition of foam insulations.
- Successive tests simulating insulation improvements on different refrigerators.

ARTICLE INFO

Keywords:
Household refrigerators
Aging
Insulation degradation
Test method
Heat transfer

ABSTRACT

Despite the omnipresence of household refrigeration appliances, there is still a lack of knowledge about their age-related efficiency loss over time. Past studies provide basic evidence for increasing electricity consumption of cooling appliances with ageing but fail to investigate the associated technical wear. Concentrating on the degradation of the thermal insulation, we first determined the ageing process of sealed samples of polyurethane rigid foam by investigating changes in cell gas composition and thermal conductivity over time. Simultaneously, the main challenge was to develop an approach that investigates the age-related efficiency loss of the insulation without its destruction. This testing procedure is referred to as the *Bonn method*. The non-destructive *Bonn method* was applied to varying refrigerator models in a series of successive experiments to evaluate the insulation degradation over time. Subsequently, the physical relationship between the test value of the *Bonn method* and the heat transfer through the multi-layered compartment walls of domestic refrigeration appliances was established, ultimately characterising the degrading insulation in terms of increasing heat transfer. Our results give substantiated evidence that the efficiency loss of cooling appliances is greatly influenced by insulation degradation over time. The ageing of sealed samples of polyurethane rigid foam indicates a large initial increase of thermal conductivity by 15% within the first year, corresponding to a change in cell gas composition. These results are in line with those of the *Bonn method*, emphasising an increasing heat flow through the multi-layered compartment walls of domestic refrigerators with ageing. Therewith, the present study is of significance to a wide range of stakeholders and forms the basis for future research.

* Corresponding author at: University of Bonn, Institute of Agricultural Engineering – Section Household and Appliance Engineering, Nussallee 5, 53115 Bonn, Germany.
E-mail addresses: chueppe@uni-bonn.de (C. Hueppe), jgeppert@uni-bonn.de (J. Geppert), stamminger@uni-bonn.de (R. Stamminger), hendrik.wagner@basf.com (H. Wagner), heike.hoelscher@basf.com (H. Hoelscher), vrabec@tu-berlin.de (J. Vrabec), apaul@mail.upb.de (A. Paul), elsner@thet.uni-paderborn.de (A. Elsner), Wolfgang.Becker@BSHG.COM (W. Becker), Ulrich.Gries@mail.nidec.com (U. Gries), A.Freiberger@secop.com (A. Freiberger).

https://doi.org/10.1016/j.applthermaleng.2020.115113
Received 28 October 2019; Received in revised form 17 February 2020; Accepted 19 February 2020
Available online 24 February 2020
1359-4311/

Nomenclature

Bonn method	testing procedure of the insulation properties of domestic refrigeration appliances
ABS	acrylonitrile butadiene styrene
HIPS	high impact polystyrene
E1	first layer of additional insulation
E2	second layer of additional insulation
K	kelvin
PUR	polyurethane foam insulation
VIP	vacuum insulation panel
XPS	extruded polystyrene foam
R^2	coefficient of determination
A	cross-sectional surface area (m^2)
A_m	cross-sectional surface area of a specific wall surface (m^2)
x_{cc}	width of the cooling compartment (cm)
x_{fc}	width of the freezer compartment (cm)
y_{cc}	height of the cooling compartment (cm)
y_{fc}	height of the freezer compartment (cm)
z_{cc}	depth of the cooling compartment (cm)
z_{fc}	depth of the freezer compartment (cm)
d	material thickness (mm)
d_{xi}	thickness of the multi-layered compartment inside wall (mm)
d_{yi}	thickness of the multi-layered compartment outside wall (mm)
EC	electricity consumption (Wh)
$\dot{Q}$	heat flow through (composite) compartment walls (W)
C_V	isochoric heat capacity (J/K)
k	heat transfer coefficient ($W/(m^2 * K)$)
$k_{calculated}$	calculated heat transfer coefficient ($W/(m^2 * K)$)
λ	thermal conductivity ($W/(m * K)$)
λ_{PUR}	thermal conductivity of polyurethane foam insulation ($W/(m * K)$)
λ_{XPS}	thermal conductivity of extruded polystyrene foam ($W/(m * K)$)
α_i	heat transition coefficient at inner compartment surface ($W/(m^2 * K)$)
$\alpha_{a,i}$	heat transition coefficient at a specific inner compartment surface ($W/(m^2 * K)$)
α_a	heat transition coefficient at outside compartment surface ($W/(m^2 * K)$)
$\alpha_{a,m}$	heat transition coefficient at a specific outside compartment surface ($W/(m^2 * K)$)
τ_I	test value of the Bonn method (min^{-1})
$\tau_I(t)$	test value at time t within the test interval (min^{-1})
T_a	ambient temperature (°C)
$T_a(0)$	ambient temperature at the start of the test interval (°C)
$T_a(t)$	ambient temperature at time t within the test interval (°C)
T_i	internal compartment temperature (°C)
$T_i measured$	internal compartment temperature measured within the test interval (°C)
$T_i(0)$	internal compartment temperature at the start of the test interval (°C)
$T_i(t)$	internal compartment temperature at time t within the test interval (°C)
$\Delta T_{s,a}$	temperature gradient at outer surface (K)
$\Delta T_{s,i}$	temperature gradient at inner surface (K)

1. Introduction

Domestic cooling appliances are an integral part of our everyday life and are viewed as standard household commodities. However, the market development for refrigeration appliances is regionally diverse and offers a wide range of cooling technologies [1]. The ownership, referring to the total stock over households, in less urbanised countries, such as Peru, was only 45% in 2014, whereas the ownership in the People's Republic of China almost quadruplicated to 90% between 1994 and 2014 [2]. By contrast, the ownership in many European countries often exceeds one appliance per household. Compared to emerging economies, sales in these countries mainly base on replacement with new appliances, motivated by electricity consumption (*EC*) savings and environmental issues [1,3,4]. However, despite the omnipresence of domestic cooling appliances, there is still a lack of knowledge about their age-related efficiency loss over time. This is even more surprising, as a high level of political pressure to reduce the *EC* of refrigeration models exists, for instance, via energy labelling and eco-design measures [5]. Such policy initiatives prompted technological progress and increased the efficiency of new appliances throughout the last decades. Regulations and directives pushed and pulled the market towards more efficient appliances, which is generally why stock appliances consume more than newer models [6,7]. Despite these efforts, little attention has been paid to the fact that the efficiency of refrigeration appliances starts to deteriorate right after the production process [8,9]. Consequently, a profound understanding of the deterioration of domestic cooling appliance's efficiency throughout their lifetime does not exist up to date. A better understanding of the degradation is thus a critical topic for policy makers, consumers and manufacturers alike.

1.1. Degradation of domestic refrigeration appliances over time

To date, limited research has been conducted on the degradation of household refrigeration appliances over time. Previous studies indicated that next to the construction, room temperature, consumer behaviour and age impact the *EC* of refrigeration appliances [10,11]. Harrington et al. [12] discovered that more than 15% of the total *EC* of domestic refrigerators and freezers is due to user interactions. These include day-to-day door openings, the loading of appliances and the impact of room temperature [12]. A survey study conducted by Geppert et al. [13] regarding the influence of consumer behaviour on the *EC* further found that 25% of household refrigeration appliances across Europe operate outside their temperature ranges specified by the climatic classes [13]. However, besides consumer interactions, ageing leads to efficiency loss over time. From a technical point of view, refrigeration appliances are systems that are subject to technical wear throughout their use phase. Biglia et al. [14] conducted a large-scale survey in which 998 cold appliances were monitored in 766 properties in England in 2017. One finding was that the average specific *EC* (kWh/m^3 year) increased significantly for appliances older than 11 years, as compared to younger appliances [14]. Although Biglia et al. [14] did not attempt to explain the reasons for over-consumption, the study showed that appliances older than 11 years disproportionally often suffered from technical wear. Among the sources responsible for over-consumption were broken thermostat controllers, distorted door gaskets and wet insulations. Similar findings were made by Isaacs et al. [15] in New Zealand when monitoring the *EC* of 400 randomly selected houses. Refrigeration appliances accounted for 15% of total household electricity, but 7% of all appliances monitored were found to be faulty and 9% operated marginally [15]. Greenblatt et al. [16] further examined the *EC* of 1467 domestic refrigerators from seven studies over a period of 18 years and conducted multiple regression analysis to

specifically show changes in consumption patterns over time. An average annual increase in consumption between 1% and 2% was concluded [16]. However, while this study shows a degradation of appliance's *EC* with progressive use, uncertainty exists due to a lack of control for user interactions, ambient conditions and the actual operational state of the monitored appliances. Different from other studies, the German Foundation for Product Testing and Consumer's Association (*Stiftung Warentest*) [17] conducted in-depth research on the *EC* of three different refrigeration appliances over a course of 18 years, between 1994 and 2012. The *EC* of these appliances was measured under standardised laboratory conditions after 3 years and 18 years, respectively. One important finding of this study was that the *EC* of all appliances increased at least by 20% within the investigation period. Another finding was that the change in *EC* was most pronounced within the first years of investigation [17,18]. Unlike previous studies that are based on data gathering in the field, the controlled test conditions of this study allowed to assume that the degradation of the foam insulation is a dominant factor for increasing *EC* over time [17,18]. In fact, the effectiveness of foam insulations is highest only after the production process and diminishes from the initial state with progressive use [8,9]. However, differences concerning the ageing of foam insulations produced with varying blowing technologies may exist, especially for previously used trichlorofluoromethane (*CFC-11*) and its nowadays commonly used substitutes [19–21].

Although past studies indicate an ageing-based efficiency loss over time, many failed to investigate the actual reasons. Technical wear affecting system components has rarely been considered to have an impact on the efficiency loss with progressive use and, as a consequence, was not the main focus of previous research [22]. The share of varying system components' degrading impact on changing consumption patterns is thus still unknown and the challenge is to identify which component causes which degree of efficiency loss over time [23–26]. However, neither comprehensive research on the relation between degrading foam insulation and refrigeration appliance's efficiency loss over time exists, nor appropriate testing methods to determine the degradation of built-in insulation materials without destruction. This contribution intends to close this research gap.

1.2. Characteristics and operational properties of foam insulations

Polyurethane (*PUR*) rigid foam is commonly used as a thermal insulation for domestic refrigeration appliances. *PUR*, like other foam insulations, is divided into two groups, either with open or closed-cells. Open-cell foams are distinguished by a high degree of porosity due to the permeability of the cell structure, whereas the cell matrix in closed-cell foams is impermeable and has a more rigid form. Both foam insulations are characterised by their density [9], with closed-cell *PUR* foam commonly used for refrigeration appliances. Foams of high density are created by the expansion of the blowing agent, preventing cells from developing open connections with each other and enclose cell gases within the cell membrane [9,27]. Consequently, closed-cell foam insulations have a higher density than open-cell insulations with roughly 32–48 kg/m^3 compared to 8 kg/m^3, respectively [9,28]. Since the thermal conductivity (λ) of insulation materials partially depends on the material density and porosity, closed-cell insulations typically perform around 0.025 $W/(m * K)$, compared to open-cell insulations with a λ around 0.036 $W/(m * K)$ [9,29]. The thermal conductivity λ is a measure of a material's effectiveness in conducting heat, thus, in the light of thermal performance it is an important property of the refrigerator foam insulation [29]. The structure of the cell matrix determines the heat flux and the λ of the insulation material to a large extent. In closed-cell foams, for instance, the insulation effect originates from the cellular gas within the cells. Due to the impermeability, cell gas is prevented from moving and convective heat transfer is suppressed [28]. Due to the structure finish of closed-cell *PUR* foam matrix, the effect of radiative heat exchange across the insulation is small [30]. Plastic foam insulations, such as *PUR* and polystyrene, commonly use fluorocarbon gases (*PFC*) within the cells to obtain a lowλ performance [28,30,31]. However, the operational properties of foam insulations start to deteriorate right after the manufacturing [8,9].

1.2.1. Ageing effects of the foam insulation

Previous studies investigating ageing effects of foam insulations assumed the diffusion of blowing agents out of the cells and related changes in gas composition to be a main cause for reduced thermal performance [9,30,32,33]. Therefore, the age-related efficiency loss of *PUR* was mostly investigated based on cell gas composition and microstructural analysis in past studies [34–36]. Albrecht and Khoukhi et al. [37–39] and Glouannec et al. [40], for example, conducted comprehensive research on the ageing of *PUR* rigid foam resulting from gas changes over time. Due to concentration differences between the inside of the cells and the ambient, cell gas diffuses out of the insulation and is replaced by ambient air and water vapour [41]. A gradual diffusion process leads to a rise of the thermal conductivity of *PUR* (λ_{PUR}) and impairs the properties of the insulation [42,43]. Gas diffusion rates depend not only on the concentration gradient but also on the tendency of each gas species to diffuse through the matrix, characterised by a diffusion coefficient [44,45].

However, besides the diffusion process, the ambient temperature (T_a) and moisture content are relevant factors degrading insulation properties with progressive use. Budaiwi et al. [29] investigated λ of 32 insulation samples, differing in type, terms of insulating property, facing and intended application. The λ of tested samples was measured at five different operating mean temperatures ranging from 4 °C to 43 °C. Results indicated that various types of insulation material react differently when exposed to high T_a, also depending on the used facing materials [30]. Wilkes et al. [46–48] investigated the degradation of *PUR* foam insulation in simulated refrigerator panels by determining changes of λ_{PUR}. Test specimens were exposed to varying T_a of 90 °F (32.2 °C), 40 °F (4.4 °C) and −10 °F (–23.3 °C). The course of λ_{PUR} was determined at regular time intervals and results were published for two years, three years and four years of ageing. One key finding of Wilkes et al. was that the λ_{PUR} of all test specimens increased throughout the investigation period, regardless of the T_a the test specimens were exposed to [46–48]. Another key finding was that specimens under a high T_a were subject to accelerated ageing compared to specimens aged under a lower T_a [48]. In addition to T_a, condensation and insulation moisture content are factors for degrading efficiency. Condensation occurs within the pores of closed-cell foam insulations as soon as temperatures drop below the dew point of water vapour, which has previously diffused into the cells [27,31,49]. The λ rises as a consequence of the higher conductive property of the liquid phase compared to the gaseous phase [9,31]. Studies investigating the long-term effect of high moisture levels on closed-cell foam insulations found that water vapour is absorbed over time and deteriorates the insulation properties [9,50]. Zhang et al. [51] conducted extensive research on factors, such as humidity and moisture content, affecting changes of λ_{PUR}. The influences of humidity, alternating high and low T_a and atmospheric gas pressure on λ_{PUR} of five *PUR* foam samples were investigated comprehensively. Results show that moist air increases λ_{PUR} between 10% and 18% [51]. However, for some refrigeration appliances with embedded cold wall evaporators moisture can migrate through the foam, aggregate around the evaporator and reduce its performance in the long term, resulting in foam degradation and additional technical wear.

1.2.2. Impact of facings on the ageing of foam insulations

Nowadays, it is a general state of the art that rates of foam insulation degradation are significantly reduced by using facing materials. For instance, the application of metal as a gas diffusion tight facing reduces foam insulation degradation within the lifetime of refrigerators. Plastic materials, such as high impact polystyrene (*HIPS*) or

acrylonitrile butadiene styrene (*ABS*) are potent barrier materials and lower gas diffusion rates of *PUR*. However, *HIPS* or *ABS* still allow gas diffusion to a remarkable extent so that foam ageing and the associated increase of λ_{PUR} cannot be fully avoided. Ozkadi [52], for instance, investigated the impact of ageing on *PUR* systems with different facings by evaluating changes of λ_{PUR} after one year and three years. The λ_{PUR} of unfaced test samples increased from 21 mW/(m ∗ K) to 25 mW/(m ∗ K) within the first year of ageing, whereas λ_{PUR} of fully sealed samples increased from 21 mW/(m ∗ K) to 23 mW/(m ∗ K) after 3 years [52]. Unlike Ozkadi, Fleurent et al. [31] examined the barrier effectiveness of different facing materials on *PUR* test samples to reduce the gas diffusion phenomena and its associated change in the λ_{PUR} over time. Test samples with casing were either covered by a bitumen/glass-fibre facing or sealed by aluminium and, alongside unfaced *PUR* test samples, aged at 23 °C and 70 °C for more than a year [31]. One important finding of Fleurent et al. was that λ_{PUR} of bitumen-faced samples increased from roughly 21 mW/(m ∗ K) to 25.5 mW/(m ∗ K) after 400 days of ageing at 70 °C. This corresponded to the increase of λ_{PUR} of the unfaced sample from 21 mW/(m ∗ K) to 26 mW/(m ∗ K) aged at 70 °C. Another important finding was that the aluminium faced samples increased only by 1.5 mW/(m ∗ K) over a year under the same conditions [31]. Recently, it has been claimed that polyethylenterephthalat (*PET*) holds better barrier properties than other plastic or steel casings and supports to reduce the degradation of the foam insulation performance over time (cf. WO 2019/007829, WO 2019/007030) [53,54]. However, in-depth investigation of the influence of different facing materials on the degradation of insulation properties is an area in which more research would be beneficial.

Past studies point out that λ_{PUR} rises over time, proving an age-related efficiency loss of the insulation material. However, the aforementioned studies formed destructive approaches. Results are based on isolated test specimens, disconnected from the overall refrigeration system. A relationship between the ageing of test samples and changes in *EC* patterns of domestic cooling appliances could, thus, not be drawn. Therefore, the impact of decreasing insulation properties on the age-related efficiency loss of household cooling appliances has never been evaluated thoroughly up to now. In contrast to previous studies, the innovation aspect of this study is to present a non-destructive testing method (*Bonn method*) that determines the overall insulation performance of refrigerating appliances by deriving a time constant test value (τ_I) which is subsequently used to calculate the heat transfer coefficient ($k_{calculated}$) of the multi-layer compartment walls. The *Bonn method* allows the investigation of a refrigeration appliance's insulation degradation over time without influencing the properties of test objects. The method is applicable to different types of domestic refrigeration appliances, fridges, freezers, or fridge-freezer combinations alike. The degradation of different insulation materials, such as *PUR* and vacuum insulated panels (*VIP*) including facing materials and other constructional effects can be tested and changes in performance compared to one another. This is especially important since the ageing of domestic refrigeration appliances is a topic where there is only limited research and data.

1.3. Heat transfer through multi-layer compartment walls

Many researchers stated that the ambient temperature T_a is a dominant factor in the *EC* of domestic refrigerators and freezers [9–12,28,30,38,55]. The reason is that up to 70% of the total thermal load comes by conduction through the compartment walls, considering empty refrigeration appliances as closed rectangular cavities [56,57]. Throughout this paper, the term compartment refers to the enclosed space (or spaces) within a refrigerating appliance, directly accessible through an external door (or doors) [58]. The compartment may itself be divided into sub-compartments with shelves, drawers and other sections. Therewith, the compartment walls relate to the walls of the overall cabinet. Regardless of the actual insulation material, the principle of λ applies to the heat transfer through the thermal insulation of all types of refrigeration appliances. The λ value is generally assumed as a single constant for each material layer and component of the construction [28]. However, the variability of the actual λ through the rigid foam insulation depends on many factors, described in detail in the aforementioned sections. For the multi-layer compartment walls of refrigeration appliances a stationary heat transfer occurs due to temperature differences between T_a and the internal compartment temperature (T_i) [50,55]. Radiative heat exchange occurs between the evaporator and the inside cabinet walls for appliances that are switched on [57–59]. When appliances are switched off the effect diminishes and gradually becomes insignificant, that is, as soon as no more downstream cooling effects are emanated from the evaporator. Unlike convection and conduction, radiative heat exchange has a negligible influence on the heat transfer through the multi-layer compartment walls for T_a of conventional installation conditions, ranging from 10 °C to 43 °C [9,30,50]. Driven by the temperature difference, heat flows through the material layers of the compartment walls and would gradually cause a rise of T_i in the event of non-operation [11,38,56]. Generally, the inside wall (d_{xi}) is comprised of thermoplastic synthetics with different thicknesses made up by *HIPS* and other processed materials. The outer wall consists of consecutive layers of steel sheet,

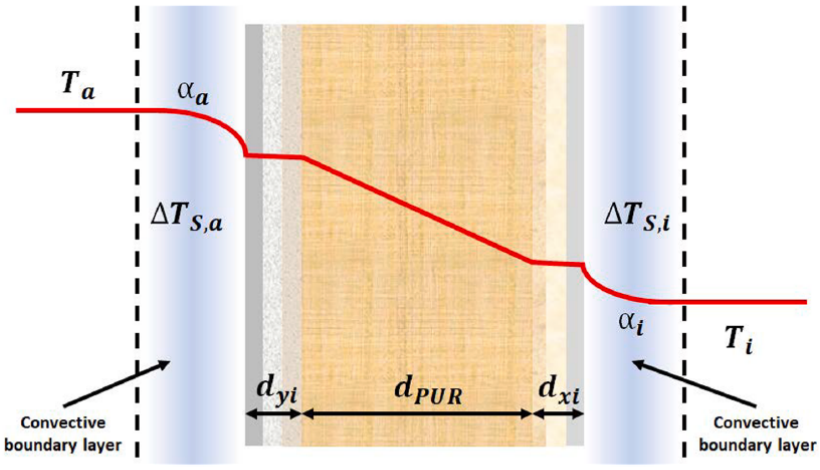

Fig. 1. Temperature profile causing heat transfer through a planar refrigerator wall.

plastic strips and other material, forming the wall exterior (d_{yi}) [60,61]. Insulation materials, such as *PUR* rigid foam, are embedded between the inside and outside walls. *PUR* dominates the components of a multi-layer refrigerating appliance wall, since it is not only important for thermal performance, but also for appliance mechanical stability. The temperature profile through the multi-layer compartment walls is shown in Fig. 1.

Each material layer has a different λ, resulting in successive conductive heat transfers from one layer to the other. This process is described by the heat transfer coefficient (k), given in W/(m² ∗ K), at flat surfaces. Either the definition of a reference surface area or the cross-sectional surface area (A) is required for objects of more complex geometry. This is because the heat transition at the outside wall (α_a) may vary for surface areas due to different oncoming air flow. In the following, the simplification is applied that the heat transfer through the compartment walls of household refrigeration appliances takes place on flat wall surfaces and follows a simple geometry. The calculation of the k for the example given in Fig. 1 is thus expressed by Eq. (1). Without this simplification, varying convective exchanges for different wall surfaces need to be taken into account.

$$\frac{1}{k} = \left(\frac{1}{\alpha_a} + \frac{d_{xi}}{\lambda_{xi}} + \frac{d_{PUR}}{\lambda_{PUR}} + \frac{d_{yi}}{\lambda_{yi}} + \frac{1}{\alpha_i}\right) \quad (1)$$

While the majority of the k value is made up of the effectiveness of the PUR insulation and its facing materials, other factors may influence the heat flow through the multi-layer compartment walls. These refer especially to all physical phenomena that disturb and affect the composition of the *PUR* insulation and its cell structure [31]. Penetrations of the *PUR* insulation can be due to refrigeration piping, heaters and associated wiring, cables, drain holes and other. The actual influence of penetration sources depends on the construction of each appliance and is generally small [49,50].

2. Materials and methods

2.1. Preparation and analysis of sealed samples of PUR rigid foam

To this end, moulded specimens were prepared as individual components representing the insulation foam material of refrigerators. The moulds used during manufacturing are made of metal and faced from the inside with a manually-applied layer of aluminium to fully encase the raw test specimens of *PUR* rigid foam with aluminium foil after subsequent demoulding. The moulded parts were prepared from a polyol mix A with polymeric methylene diphenyl diisocyanate and cyclopentane. The polyol blend admixed with the cyclopentane (13.5 parts in 100 parts of polyol blend) was mixed with the required amount of specified isocyanate using a high-pressure mixing machine with a discharge rate of 250 g/s. The reaction mixture was injected into the previously described moulds (dimensions 2000 × 200 × 50 mm) adjusted to a temperature of 40 °C and demoulded after 5 min. The degree of overpacking was 17.5%, i.e. 17.5% more reaction mixture was used than was necessary to completely foam-fill the moulds. The resulting test specimens, fully covered by aluminium foil, were stored at T_a ranging between 21 °C and 24 °C. All test specimens comprised closed-cell *PUR* only. After storing the test specimens for 24 h a plurality of foam cuboids (positions 10 mm regarding the start of the mould) of dimensions 200 × 200 × 50 mm were cut out from the centre of the specimens and each resulting foam sample entirely enveloped with aluminium foil. Sealed *PUR* foam samples were stored under the aforementioned temperature conditions with humidity ranging between 35% and 70% with an average of about 60% relative humidity. Both cell gas composition and λ_{PUR} were measured at regular time intervals. For this, the top and bottom sides of a part of the sealed foam samples were removed to obtain test specimens of dimensions 200 × 200 × 30 mm. This way, results were obtained for samples that have been entirely covered by aluminium foil during their ageing phase. A gas sample was obtained via a gas-tight syringe from the foam sample for the cell gas analysis. The foam sample was flushed with helium as an inert gas to reduce contamination from the ambient air. The gas samples (15 µl each) were subsequently analysed by gas chromatography equipped with a thermal conductivity detector. The results are an average of two measurements. A Taurus TCA 300 DTX apparatus was used for the identification of λ_{PUR} at an average temperature of 10 °C.

2.2. Development of the Bonn method

This subsection presents the development of the non-destructive *Bonn method* to investigate the insulation degradation intrinsic to household refrigeration appliances.

2.2.1. Theoretical background

The challenge was to develop a non-destructive test procedure that determines changing insulation properties of refrigeration appliances over time without deconstruction. Newton's law of cooling forms the basis of the *Bonn method*. It describes the temperature equalisation

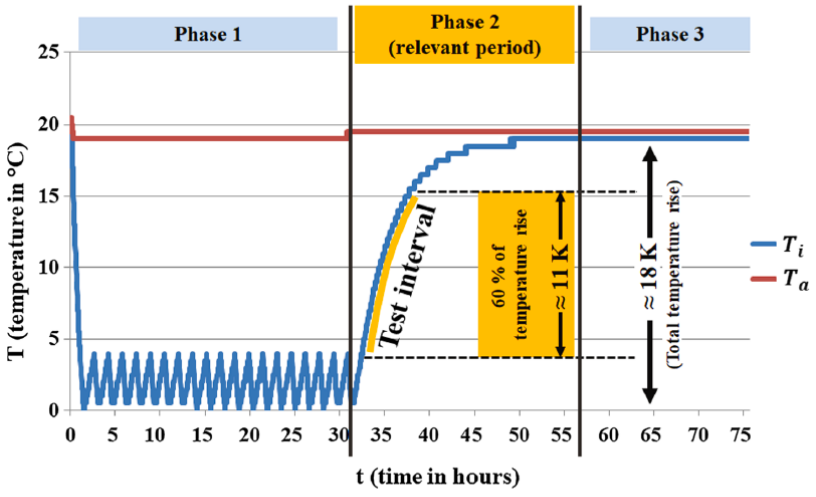

Fig. 2. Temperature profile of a sample appliance throughout the application of the *Bonn method*.

between an object and the ambient in the event of a temperature difference at the boundary level [62]. This initial description was used to investigate the temperature rise of T_i towards T_a after cooling appliances were disconnected from a power supply. Following Newton's law of cooling, the temperature rise is characterised by an exponential increase of T_i towards a boundary value, expressed by T_a [62,63]. The time dependence of this temperature rise is characterised by an exponential function and is independent of T_i and T_a. Assuming that other heat flows through the door gaskets or condensation drain holes are omitted, the heat flow is mostly influenced by the insulation properties of the multi-layered compartment walls [9,31,49,50]. Since the temperature rise is initiated when appliances are switched off, radiative heat exchange emanated from the evaporator on the inside compartment walls can be neglected. This also applies to the radiative heat exchange of the T_a on the *PUR* foam insulation at conventional installation conditions, outlined in the aforementioned sections. The test method can be applied to refrigeration appliances without the need for their deconstruction. When interpreting the ageing of *PUR* as changing heat flow through the insulation material over time, the application of heat flow meters to determine the degradation may offer an alternative approach. However, domestic refrigeration appliances have a complex geometry with foam insulations and facings distributed unevenly among the compartment walls and the door (or doors). The effort to measure the heat transfer through various wall surfaces of the same appliance in order to calculate a uniform value determining the overall insulation performance would be large and the associated value rather imprecise. The IEC 62552-2 (Annex C) [64] reports a temperature rise test for refrigerating appliances with one or more three-star or four-star compartments. The objective is to determine the time necessary for the temperature of test packages (M-packages) to rise from −18 °C to −9 °C after switch-off. However, this test is only applicable to refrigerating appliances with at least one freezer compartment, each compartment needs to be loaded with test packages and measuring points recording the temperature rise are not specifically defined [64]. Due to additional limitations, this test is not applicable for a detailed investigation of refrigerating appliance's insulation degradation over time.

2.2.2. Methodological approach

The theoretical approach was first applied to a sample refrigerator to understand its practical application. Fig. 2 presents the corresponding temperature profiles throughout the *Bonn method*.

Temperature data were measured every minute but is presented in hours to improve the readability of Fig. 2 and the related figures (Fig. 3a, Fig. 3b). The application was conducted under a controlled T_a of 20 ± 1 °C. *Lascar electronics EasyLog EL-USB-1* temperature loggers were used as sensors recording air temperature data (T_a and T_i). Chosen temperature sensors operate at 0.5 °C resolution within an operating temperature range from −35 °C to 80 °C. *VOLTCRAFT ENERGY-LOGGER 4000,* power and energy meters with a resolution of 0.1 W were additionally used to display the power flow throughout the application. First, the overall course of T_i was divided into three subsequent phases. The first section marks the initial phase, the second the relevant measurement period and the third the phasing-out period. The initial phase showed T_i at steady-state conditions reflecting the power on-off cycles of the compressor. The sample test device was disconnected from the power supply when the temperature difference between T_i and T_a was at a maximum. The second phase contains the convergence of T_i towards T_a and is, thus, referred to as the relevant period. This section started after disconnecting the appliance from the power supply. The following phasing-out period reflects the completed temperature equalisation of T_i towards T_a. Fig. 2 shows that the total rise in temperature amounted to approximately 18 K. Second, the test interval of the temperature rise (roughly 11 K) was determined and used for the calculation of the decay constant test value (τ_I), measured in ($1/t$). An amount of 60% of the total temperature rise was used to generate the test interval, disregarding 20% at the beginning and the end of the relevant period, respectively. This is because uncertainties influenced both ends of the temperature rise. Initial values would have been distorted by downstream effects after the sample appliance was disconnected from the power supply, e.g. by downstream cooling effects of the evaporator or pressure equalisation of the refrigeration system. Downstream cooling effects of the evaporator were verified by measuring the surface temperatures of plate evaporators using sheathed thermocouple models with a naked junction between compressor on and off cycles. Resulting temperature profiles of evaporator surfaces indicated that downstream cooling effects only last a few minutes. Additionally, the limited resolution of the temperature sensors employed would have resulted in a large relative uncertainty of T_i and T_a at the end of the temperature rise. The remaining temperature rise provides the test interval. Due to the temperature measuring accuracy of the employed loggers (± 0.5 °C), all data points of T_i recorded within the test interval were smoothed. Subsequent to the derivation of the test interval, the τ_I determining the insulation quality of the sample appliance at the time of test application could be calculated. Newton's law of cooling was used to calculate τ_I, since the test interval reflects a distinct section in the convergence of T_i towards T_a. Its basic formula is given by Eq. (2).

$$T_i(t) = (T_i(0) - T_a(0)) * e^{-\tau_I(t)*t} + T_a(t) \quad (2)$$

τ_I presents the decay constant and, for data measured at every minute, is given in min^{-1}. $T_i(t)$ and $T_a(t)$ give the temperature courses at every point in time throughout the test interval, whereas $T_i(0)$ and $T_a(0)$ resemble the initial values of T_i and T_a at the start of the test interval, respectively. Eq. (2) was transformed to estimate the slope of the temperature rise at every recorded time instance (t in min) within the test interval, shown by Eq. (3).

$$\tau_I(t) = 1/t * ln\frac{T_i(0) - T_a(0)}{T_i(t) - T_a(t)} \quad (3)$$

Based on Eq. (3), $\tau_I(t)$ describes the gradient of all T_i data points measured within the test interval. Referring to Fig. 2, Fig. 3a presents the overall course of $\tau_I(t)$.

τ_I is located at the maximum of all $\tau_I(t)$ within the test interval, determining the state of the thermal insulation. Regarding Fig. 3a, τ_I is at approximately $0.28*10^{-2}$ min^{-1}. The initially steep increase of $\tau_I(t)$ is due to the fact that $T_i(0)$ and $T_i(t)$ are equal at the first measuring point of the test interval. Fig. 3b further shows that T_i measured within the test interval (T_i *measured*) of the sample appliance is best resembled by a regression using the maximum of all τ_I ($0.28*10^{-2}$ min^{-1}) as a constant gradient. The compliance is indicated by a high-quality adaption rate of the regression to T_i *measured* (Fig. 3b), given by a coefficient of determination (R^2) larger than 0.99. Therefore, τ_I is defined as the test value of the *Bonn method*, determining the overall insulation performance of refrigerating appliances through a defined temperature rise in a compartment under specified conditions. Since

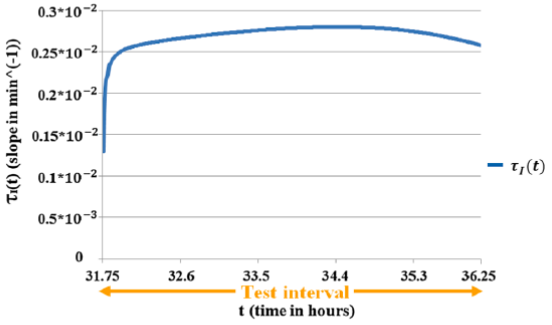

Fig. 3a. Course of $\tau_I(t)$ for a sample appliance.

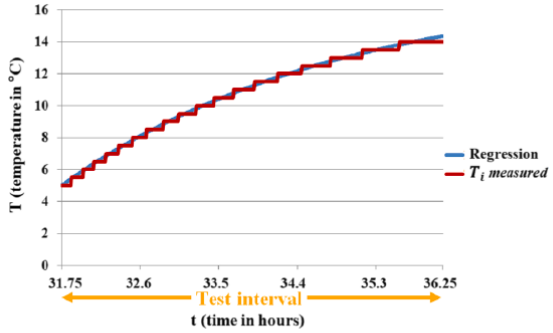

Fig. 3b. Regression with τ_I (max = $\tau_I(t)$) for a sample appliance.

PUR dominates the wall components of domestic refrigerating appliances, a degradation of the insulation dominates changes in τ_I over time. One potential systematic uncertainty of measurement is that not only the direct conductivity of heat through the multi-layer walls is included in τ_I, but also other heat fluxes. To prevent another systematic uncertainty of the *Bonn method*, test parameters (resolution of time and temperature) to record T_i and T_a need to be consistent for all experiments of a test series.

2.2.3. Materials

The *Bonn method* was applied to a range of 15 different domestic refrigeration appliances, including refrigerators, freezers and fridge-freezer combinations. The composition of appliances reflects the German market composition. Consequently, appliances of different construction, price ranges, storage volume and varying insulation material (*VIP* and *PUR*) are under investigation. All appliances were either acquired new or provided directly by the manufacturers. However, in this contribution, the methodological approach of the *Bonn method* was applied to two inventory appliances, in the following referred to as A and B. In contrast to new appliances, A and B were chosen due to their age. In contrast to destructive tests investigating the insulation properties over time, the impact of non-destructive insulation improvements on τ_I and associated changes in *EC* could be simulated. Thus, the impact of the insulation degradation on refrigeration appliance's *EC* over time could be investigated while holding all other ageing impact factors constant. The characteristics of test appliances A and B are specified in Table 1.

Appliances A and B operated on the lowest adjustable temperature level throughout all experiments. The interior equipment of A and B, such as shelves and drawers, was left in place. Both appliances remained unloaded throughout the test application. To receive detailed temperature profiles, both T_a and T_i were measured every minute throughout test applications. The aforementioned temperature sensors used for the practical application on the sample appliance were also used for all subsequent temperature measurements concerning appliances A and B. One sensor was used per compartment. Temperature sensors were placed on determined spots within appliances A and B, located at the geometric centre of each appliance, which is precisely the centre point of the centre shelf within the appliance's cabinet. In the case of fridge-freezer combinations two temperature sensors would be used, located in each compartment as previously described. A detailed positioning of temperature sensors for appliances A and B is given by Fig. 11 in the appendix. For reasons of simplification, the four-star freezer compartment of appliance B is disregarded in the following. Fig. 12 indicates the temperature measuring positions for more complex appliances, such as fridge-freezer combinations, not further specified in this contribution. For appliances A and B, Ramoflex kneading paste 832 (water repellent and temperature resistant) was used to seal the condensate drain holes and OVP lashing straps were used to press the door-sealing on the sill height at every test run. The previously mentioned *VOLTCRAFT ENERGY-LOGGER 4000* was plugged between the power supply and socket of appliances A and B to observe the course of the compressor on-off mode and to measure the *EC*, respectively. Both test appliances were placed in an ambient with constant T_a of 20 ± 1 °C for the implementation of the *Bonn method*. The *EC* measurements were carried out under laboratory conditions with T_a of approximately 25 °C, following DIN EN 62552:2013 [65].

2.2.4. Influence of the T_a on the Bonn method

The *Bonn method* was first applied to A and B in a series of successive tests with different T_a conditions to evaluate the dependence of τ_I on the T_a. Both, T_a and T_i were recorded every minute. A total of six test runs was carried out on appliance A, three at an T_a of 19–21 °C and three at around 31 °C, respectively. Three test runs were conducted for appliance B at the same T_a settings. Fig. 4 shows the distribution of τ_I for A and B at tests with different T_a conditions.

Regarding device A, τ_I remained stable at a mean value of $0.49{*}10^{-2}$ min^{-1} despite a variation of T_a of more than 10 K between test repetitions. Device B remained equally constant at a mean value of $0.87{*}10^{-2}$ min^{-1}. Percentage standard deviations of A and B were 4.6% and 2%, respectively. This indicates an independence of τ_I from T_a and a high degree of reproducibility despite differences in T_a between test repetitions.

2.2.5. Verification of the Bonn method

Conversely to an insulation degradation, an improvement of the insulation was simulated and its influence on τ_I and the *EC* measured for appliances A and B, respectively. Since *PUR* dominates the wall components of domestic refrigerating appliances, the feasibility of the *Bonn method* could be investigated by varying the insulation properties of both appliances. For this, two additional casings per test appliance, each called *E1* and *E2*, were designed and subsequently applied to the surfaces of A and B to simulate an insulation improvement. *E1* and *E2* were constructed of single panels of closed-cell extruded polystyrene foam, commonly referred to as styrofoam or *XPS*. URSA XPS D panels were used for the construction of *E1* and *E2*. Each panel of *XPS* used for construction of *E1* and *E2* had a material thickness (d) of 20 mm and, according to manufacturer product information, a λ of 0.031 W/(m ∗ K). The first casing *(E1)* for each test appliance was specifically designed to fit on the outer surface of its corresponding appliance A or B, whereas the second casing *(E2)* was designed to fit tightly onto *E1*. Both appliances, A and B, had conventional wire tube condensers at the back surfaces. *E1* and *E2* omitted the bottom and back surfaces of A and B, covering four out of six appliance surface areas. Therefore, neither the application of *E1*, nor the subsequent application of *E2* onto *E1* impacted on the ability of the condensers to discharge heat. The *EC* of A and B was measured initially. Afterwards, the *Bonn method* was applied to calculate τ_I without insulation improvement. This state refers to the base case in the following. Given the initial values, *E1* and *E2* were applied successively. Influences of simulated insulation improvements on τ_I and the *EC* could, thus, be examined for both test appliances and relationships drawn. The process was repeated three times for each scenario of simulated insulation improvement. The application of

Table 1
Characteristics of test appliances A and B.

Specifications	Appliance A	Appliance B
Type	Refrigerator, Built-in, No freezer compartment	Refrigerator, Free-standing, One four-star[1] compartment
Age	9 years	33 years
Storage volume	312 L	145 L
Power rating (W)	90	110
Cooling	Dynamic	Static

[1] Refrigerating appliance defined according to IEC 62552-1 (2015).

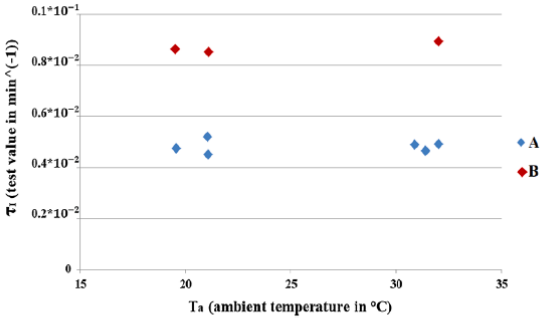

Fig. 4. τ_I for various T_a.

additional casings per test appliance (*E1* and *E2*) is not an integral element of the *Bonn method*, but served the sole purpose to simulate improvements in insulation performance and show resulting changes of τ_I and *EC*.

3. Results

3.1. Ageing of sealed samples of PUR rigid foam

Figs. 5a and 5b refer to the findings regarding the investigation of the stand-alone ageing of moulded parts of *PUR* rigid foam. Fig. 5a shows the cell gas analysis of sealed *PUR* rigid foam samples up to 337 days of storage, while Fig. 5b presents the corresponding λ_{PUR} measurements.

Fig. 5a indicates that the cell gas composition of the sealed samples changes significantly within the first year of investigation. Carbon dioxide initially made up more than 60% of the cell gas volume but started to diffuse out of the test specimens at an early stage. Measurements showed that its gas content declined exponentially throughout the test period and progressed towards zero. In contrast to carbon dioxide, the cell gas contents of nitrogen and oxygen increased from approximately 4% and 1% to 23% and 39%, respectively. Changes in gas composition represent the diffusion of cell gases (carbon dioxide and cyclopentane) and their replacement by ambient air (nitrogen and oxygen). Correspondingly, results indicate an increase in moisture by 15%. Fig. 5b shows the corresponding development in λ_{PUR} of the sealed samples, indicating an increase by roughly 15% within the test period. All sealed samples were encased by aluminium foil during their ageing and the closed-cell content was carefully tested for every specimen so that only foams with nearly 100% closed-cell content have been evaluated within the investigations.

3.2. Relationship between τ_I and EC

Figs. 6 and 7 show results regarding the relationship between τ_I and *EC* in the case of artificial insulation improvement, referring to the subsequent application of *E1* and *E2* to A and B described in the aforementioned sections. The T_a for each test concerning Figs. 6 and 7 is listed in Table 2, given in the appendix.

Fig. 6 indicates that τ_I decreases with the application of additional layers of insulation, corresponding to the decrease of *EC* for A and B, given by Fig. 7. Regarding test appliance A, the mean τ_I of three successive measurements per scenario decreases by roughly 31%, whereas the mean τ_I of appliance B decreases more pronouncedly by 43%. Fig. 7 shows that the *EC* measurements of appliances A and B follow almost congruent courses with the associated τ_I values. The mean *EC* of appliance A decreased by 29%, whereas the mean *EC* of device B decreased by 21% from the base case scenario up to *E2*. Changes in τ_I and *EC* were almost proportional regarding appliance A, whereas a decrease in τ_I led to a lower than proportional reduction of *EC* regarding appliance B. Since A and B are different refrigerator models (Table 1), their results cannot be compared directly with each other. Therefore, preliminary results were further evaluated to investigate whether a correlation between changes of τ_I and the *EC* exists. Fig. 8 shows the correlation between τ_I and the *EC* in the case of simulated insulation improvement for A and B, respectively.

Referring to appliance A, standard deviations of both τ_I and *EC* were small in all three scenarios, whereas the standard deviation of appliance B was large in the base case scenario. This variation of τ_I is also given in Fig. 6. Fig. 8 further presents the linear correlation of A and B for the simulated insulation improvement. The corresponding R^2 of both test appliances shows a distinct correlation between τ_I and the *EC*. Contrary to the simulated insulation improvement, the age-related degradation of a domestic refrigerator's insulation is, therefore, pointed out by an increase of τ_I over time, corresponding to a rising *EC*.

Preliminary results concerning the ageing of detached *PUR* rigid foam samples and τ_I point out important findings. Both approaches emphasize the ageing of the thermal insulation based on increasing heat flow over time. However, the destructive method determines the increase of λ_{PUR} based on sealed *PUR* samples, whereas τ_I reflects the heat flux coefficient k through the multi-layer refrigerator compartment walls. Additionally, preliminary results concerning the *Bonn method* indicate the influence of cover layers and facings on the age-related efficiency loss.

3.3. Relationship between τ_I and k

The heat flow through the multi-layer compartment walls ($\dot{Q}$) was connected to τ_I to indicate the insulation degradation over time. Eq. (4) served as a starting point and $\dot{Q}$ as a link to relate τ_I with k. Eq. (4) gives the heat flow of Newton's law of cooling for an unspecified cross-sectional surface area (A), whereas Eq. (5) gives the heat flow into a heat sink from an ambient at a constant temperature with a given isochoric heat capacity (C_V).

$$\dot{Q} = A * k * (T_a(t) - T_i(t)) \tag{4}$$

$$\dot{Q} = C_V * \frac{d(T_i(t))}{dt} \tag{5}$$

C_V relates to the isochoric heat capacity of all compartment wall built-in material masses (m_i), such as *PUR* rigid foam, bulk and tech plastics. C_V is formally described by Eq. (6).

$$C_V = \sum_i c_v * m_v \tag{6}$$

Inserting Eq. (5) into Eq. (4) results in the physical relationship between τ_I and k, presented by Eq. (7).

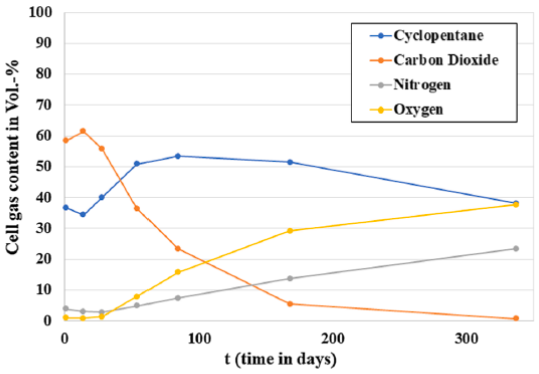

Fig. 5a. Changes in cell gas composition over time.

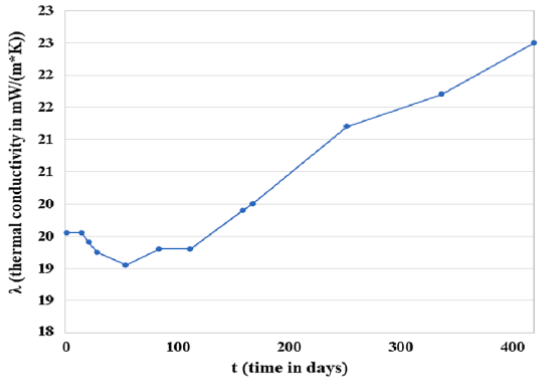

Fig. 5b. Thermal conductivity of *PUR* rigid foam over time.

$$C_V * \frac{dT(t)}{dt} = A * k * (T_a(t) - T_i(t)) \quad (7)$$

Converting Eq. (7) and integrating over time results in Eq. (8).

$$ln\frac{T_i(0) - T_a(0)}{T_i(t) - T_a(t)} = \frac{A * k}{C_V} * t \quad (8)$$

Eq. (8) resembles a modified form of Newton's law of cooling for the calculation of $\tau_I(t)$, previously indicating the gradient of all data points of T_i within the test interval, expressed by Eq. (3). The physical relationship between τ_I and k can thus, be simplified as described by Eq. (9).

$$\tau_I = \frac{A * k}{C_V} \quad (9)$$

Having established the physical relationship between τ_I and k, the heat flow through the multi-layer compartment walls of refrigeration appliances can be calculated. The k was calculated based on the predetermined physical relationship between τ_I and k, therefore, it is referred to as $k_{calculated}$ in the following. A detailed list of materials giving comprehensive information on processed material input was provided by a European manufacturer of domestic refrigeration appliances. Alternatively, some open-source data are available which can be used to assess the material input of the compartment and calculate the associated $k_{calculated}$ [58,60]. The manufacturer information was used in this paper to estimate the d_{xi}, d_{yi} and λ of different materials processed in the multi-layer compartment walls of A and B. Preliminary results for changes of τ_I for appliances A and B with simulated insulation improvement were used to calculate the corresponding k for the different insulation scenarios. Fig. 9 presents $k_{calculated}$ regarding simulated insulation improvement for A and B, respectively.

Fig. 9 shows that $k_{calculated}$ of A and B decreases with the application of additional layers of insulation. Declining k gradually levels out with additional layers of insulation, demonstrated by a flattening course of the $k_{calculated}$ throughout the three scenarios. The mean $k_{calculated}$ of appliance A decreases by 15% between the base case and *E2*. Contrary to appliance A, the mean $k_{calculated}$ of B decreases more pronouncedly with almost 32% throughout successive insulation improvements. Additionally, the standard deviation of the data for appliance B is at least four times larger than that of appliance A for every scenario. Similar to the correlation between τ_I and *EC* in the case of simulated insulation improvement, the correlation between k and the *EC* was further evaluated, as presented in Fig. 10. Again, k is expressed as $k_{calculated}$.

Appliance A shows small standard deviations for both changes of *EC* and $k_{calculated}$ in the event of simulated insulation improvement. Fig. 10 further gives the straight-line correlations for test devices A and B, indicating a high R^2 for both appliances. The fit shows a clear correlation between the $k_{calculated}$ and *EC*. Regarding the age-related efficiency loss of domestic refrigeration appliances, preliminary results imply that the *EC* increases over time due to a rise in heat transfer through the multi-layered compartment walls.

4. Discussion

At first, the degradation of *PUR* rigid foam was investigated based on the stand-alone ageing of sealed samples at a constant T_a for about a year. All samples comprised of closed-cell *PUR* only and were encased by aluminium foil. Both the cell gas composition and λ_{PUR} were determined several times within the investigation period. It was found that cell gases of moulded *PUR* rigid foam samples diffuse out of the

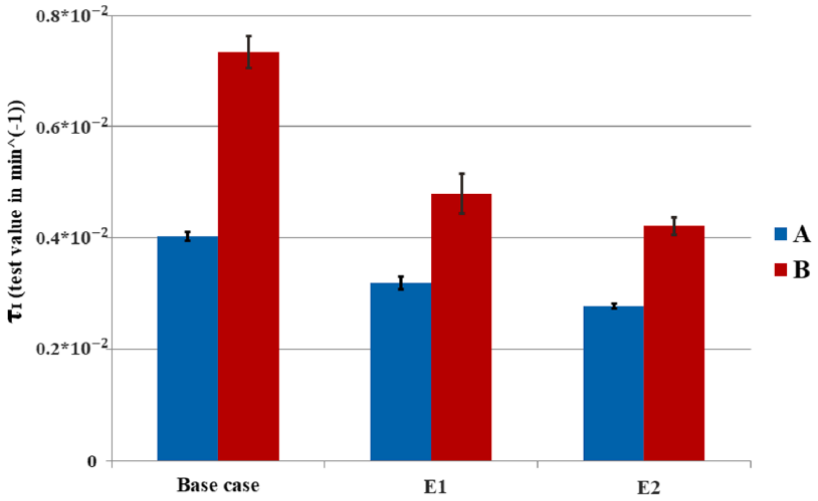

Fig. 6. τ_I values of test appliances A and B.

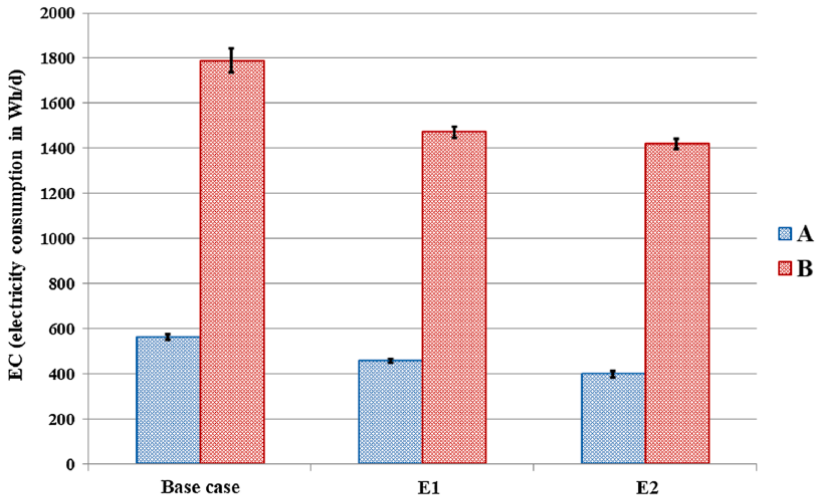

Fig. 7. *EC* of test appliances A and B.

Table 2
Ambient temperatures for successive tests of simulated insulation improvements.

		Fig. 6* Application of the Bonn method	Fig. 7* EC measurements
Cycle 1	Base Case	19.55 °C	24.68 °C
	E1	19.22 °C	24.59 °C
	E2	19.49 °C	24.82 °C
Cycle 2	Base Case	19.10 °C	24.83 °C
	E1	19.56 °C	24.71 °C
	E2	20.00 °C	24.59 °C
Cycle 3	Base Case	19.50 °C	25.12 °C
	E1	19.59 °C	24.73 °C
	E2	20.12 °C	24.84 °C

* Appliances A and B were tested at the same time throughout all experiments concerning simulated insulation improvements (*Bonn method* and *EC* measurements).
All ambient temperatures (T_a) are given as the average measured test room ambient temperature during the test period.

cells and are gradually replaced by nitrogen and oxygen. The λ_{PUR} simultaneously increased by 15% during the investigation period. Wilkes et al. [46–48], Albrecht and Khoukhi et al. [37–39] investigated a similar large initial increase of λ_{PUR} for varying test samples as a result of gas exchange. The results are also in line with the findings of Fleurent et al. [31] for changes of the λ_{PUR} for samples with different facings, such as aluminium. It was further found that if the closed-cell content was below 85%, ageing of the foam insulation performance was quite rapid. The reason for this was a gas-diffusion-controlled, hence, fast exchange of all cell gases (including cyclopentane). According to our own investigations, an open-cell content below 10% leads to an increase of λ_{PUR} from 19.8 mW/(m ∗ K) up to 23.0 mW/(m ∗ K) (storage temperature: 70 °C) within 7 days. In contrast, an open-cell content above 80% leads to an increase of λ_{PUR} up to 32.5 mW/(m ∗ K) within the same storage time of 7 days at 70 °C. The cell gas analysis showed that air was the main cell gas in the latter case. There is evidence that the ageing increases in the event of fluctuating T_a, causing an expansion and contraction of floating gases [29,49,55]. It is anticipated that the increasingλ_{PUR} flattens out after the first couple of years, depending on

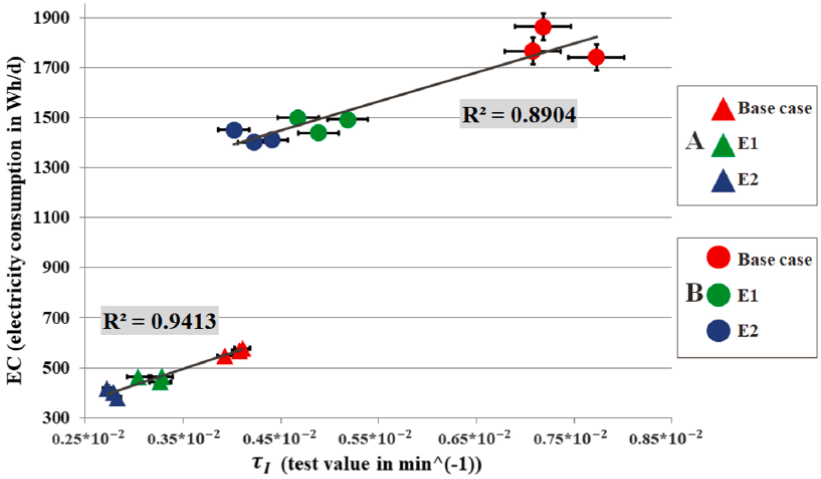

Fig. 8. Correlation between τ_I and *EC* in the case of simulated insulation improvement.

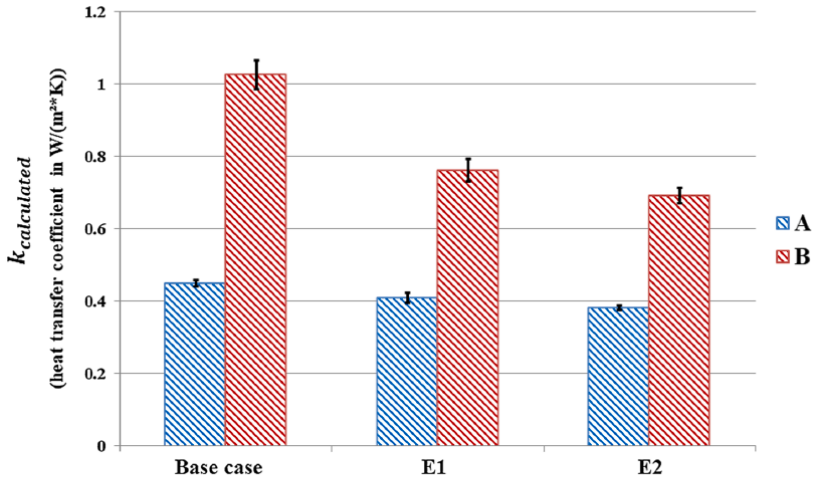

Fig. 9. Mean value and standard deviation of $k_{calculated}$ for appliances A and B.

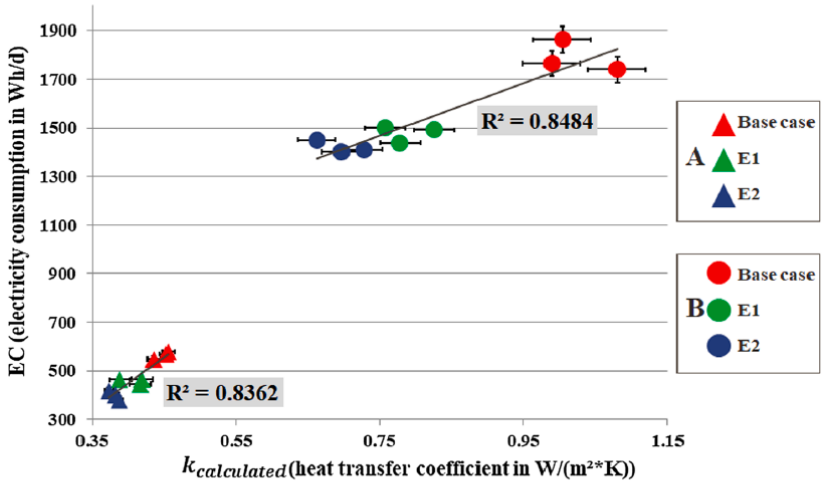

Fig. 10. Correlation between $k_{calculated}$ and *EC* in the case of simulated insulation improvement.

the time it takes the cell gases to reach a stable equilibrium [8,51]. This course would be in line with the previous research results of Wilkes et al. [48], Albrecht [37] and Wu et al. [44].

Second, the main research objective was to develop an innovative approach that specifies the state of insulation degradation intrinsic to household refrigerating appliances. Since the *Bonn method* constitutes an unprecedented approach, some imprecisions form the basis for future research. Regarding the methodological development, Newton's law of cooling (Eq. (2)) was applied to derive a time constant test value (τ_l), subsequently used to calculate the heat transfer coefficient ($k_{calculated}$) through the multi-layer compartment walls of domestic refrigerating appliances. Different from the *temperature rise test* reported in the IEC 62552-2 [64], the main intention of the *Bonn method* is to determine the influence of insulation degradation on the overall efficiency loss of refrigeration appliances over time.

One systematic uncertainty of the approach is related to the derivation of τ_l. The test value does not only consider the heat conductivity through the multi-layer appliance walls, but also involves other heat fluxes. In fact, τ_l reflects an estimate of the overall k of a test appliance. Potential penetrations of the insulation material by piping, heaters and associated wiring, cables, drain hole etc. depend on the type of construction and are likely to lead to additional heat gains. Penetrations are typically difficult to evaluate and can only be distinctly determined by prior deconstruction. The *Bonn method* assumes that these other factors remain constant over time. The effort to determine other factors would be large, especially since it is known that a majority of the k bases on the actual effectiveness of the insulation material and its facings [9,31,49,50]. For instance, most of the electric wiring for appliances with digital temperature display is installed outside of the foam-filled partition walls, whereas single cables of appliances with manual thermostat pass through the partition walls. It is general state of the art that cables and wiring are fixed to the wall insides, having a minimal impact on the insulation effectiveness. Another systematic uncertainty originates from the chosen resolution of time and temperature to record T_i and T_a during the application of the *Bonn method*. Test parameters have to be constant for test repetitions or test series in order to prevent a

variability of the calculated τ_I. Additionally, the range of the test interval to exclude multiple downstream effects after switching an appliance off (Section 2.2.2.) needs to be constant for consecutive tests. The initial period of the test interval was discounted due to ongoing cooling effects of the evaporator, radiative heat exchange between the evaporator and the inside compartment walls, gas migration, pressure equalisation of the refrigeration system and potential condensation accumulation in the evaporator after switch-off. Unlike ongoing cooling effects, other downstream effects could hardly be measured. Excluding the first 20% of all temperature rise data from the relevant period reduces the uncertainty related to the aforementioned downstream effects. However, the duration of downstream effects varies for different types of appliances (refrigerators, freezers, fridge-freezer combinations) and depends on construction. Appliances A and B, for instance, operate on the grounds of hermetic reciprocating compressors and have plate evaporators installed at the interior rear panels. Disregarding 20% of the temperature rise's initial values corresponds to a duration of at least 30 min. To the best of our knowledge, this excludes uncertainties in τ_I. Nevertheless, a deviating delimitation of the test interval would have influenced τ_I.

Regarding the experiments simulating an improvement of the insulation, measurement uncertainties may either have been caused by the construction of *E1* and *E2* or manual fitting to appliances A and B. As casings were constructed of single panels of *XPS*, minor damages to the casings in the assembly process could not be excluded. Additionally, the insulating covers were attached with strap belts and burdened with weights when applied to devices A and B. This ensured a good fit with the surface area. Neither strap belts nor weights have been changed throughout the test repetitions so that the same utilities have been used for fitting the covers to A and B, respectively. The method applied to simulate an improved insulation performance is only applicable to refrigerating appliances with wire tube condensers. It is not applicable to appliances with skin condensers, commonly found on the appliance's back and both sides. For such appliances, the application of additional casings would inhibit the ability of the condensers to reject heat.

Concerning the applicability of the *Bonn* method, the approach can be applied to a range of different types of domestic refrigerating appliances, including refrigerators, freezers and fridge-freezer combinations. To thoroughly evaluate the influence of insulation degradation on the overall efficiency loss of refrigerating appliances, both changes in *EC* and τ_I have to be determined by regular measurements on initially new appliances over several years. In this contribution, however, the Bonn method was applied to two inventory appliances (A and B), chosen due to their age. This way, simulated insulation improvements could be executed to verify the methodological approach on the basis of successive experiments and to indicate which degradation can be expected for new appliances throughout their use phase. The application of the *Bonn method* to different refrigerating models varies slightly, depending on the construction. For instance, the condensation drain hole of fan-forced appliances with a remote evaporator or automatic defrosting, typically freezers, have no manually accessible drainage in the interior cavity. The drain holes of such appliances need to be plugged from the outside, at the back of the appliance over the drainer.

5. Concluding remarks and outlook

The ageing of household refrigeration appliances is caused by multiple sources and leads to degrading efficiency over time. The age-related degradation of the insulation is a key factor of decreasing efficiency. This study was based on experimental measurements concerning both the ageing of sealed samples of *PUR* rigid foam and the development of a non-destructive testing method. The ageing of test samples showed distinct changes in the cell gas composition and λ_{PUR} within the first year of investigation. The cell gas contents of oxygen and nitrogen increased from approximately 4% and 1% to 23% and 39%, respectively, whereas the cell gas content of carbon dioxide dropped to almost zero. Changes in the cell gas composition correspond to the increase of λ_{PUR} by 15% within the investigation period. The main contribution in this paper was the development of the *Bonn method*. The approach determines the overall insulation performance of a refrigerating appliance by deriving a time constant test value (τ_I), used to subsequently calculate the k ($k_{calculated}$) of the multi-layer compartment walls. Preliminary tests regarding the dependence of τ_I on T_a show an independence of the test value from moderate T_a variations. Further experiments simulating successive insulation improvements were conducted to investigate changes of τ_I and *EC* in the event of modified insulation properties, indicating almost congruent courses. The results suggest that a distinct correlation between the *EC* and τ_I exists, validating the non-destructive approach. The physical relationship between τ_I and k was further established. An important finding is the relationship between *EC* and $k_{calculated}$ in the case of simulated insulation improvement, corresponding to the correlation between *EC* and τ_I. Therewith, the results give substantiated evidence that the efficiency loss of cooling appliances is largely influenced by insulation degradation over time.

The comprehensive investigation on the relationship between degrading foam insulation and efficiency loss is important, since the ageing performance of domestic refrigeration appliances is a topic with only limited research. In the future, comparative measurements to other methods (such as $k*A$) are conceivable to determine the general measurement uncertainty of the *Bonn method* and to provide an assessment of impact these might have on results. The *Bonn method* can be used in multiple ways to provide valuable insights into the actual scale of insulation degradation and its associated consequences. One field of future application is to evaluate the effectiveness of varying insulation and facing materials used in the compartment walls to increase efficiency. Another field of application are long-term investigations. Similar to the *Bonn method*, other test methods concerning the degradation of the door gasket and compressor-refrigerant circuit have been developed. A regular application of all three test methods to initially new appliances over several years holds the potential to thoroughly evaluate the extent to which the deterioration of each component affects the efficiency loss of the overall system over time. These are critical topics for many stakeholders and provide the basis for future research.

Declaration of Competing Interest

The authors declare that they have no known competing financial interests or personal relationships that could have appeared to influence the work reported in this paper.

Acknowledgements

This work was funded and supported by the German Federal Ministry for Economic Affairs and Energy (BMWi), project 'ALGE' (03ET1544A-E).

Appendix A

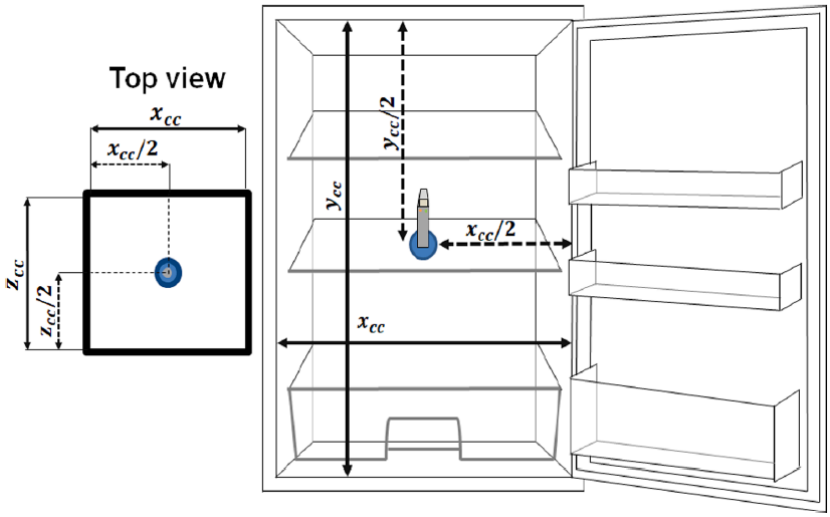

Fig. 11. Positioning of temperature sensors for appliances with one compartment.

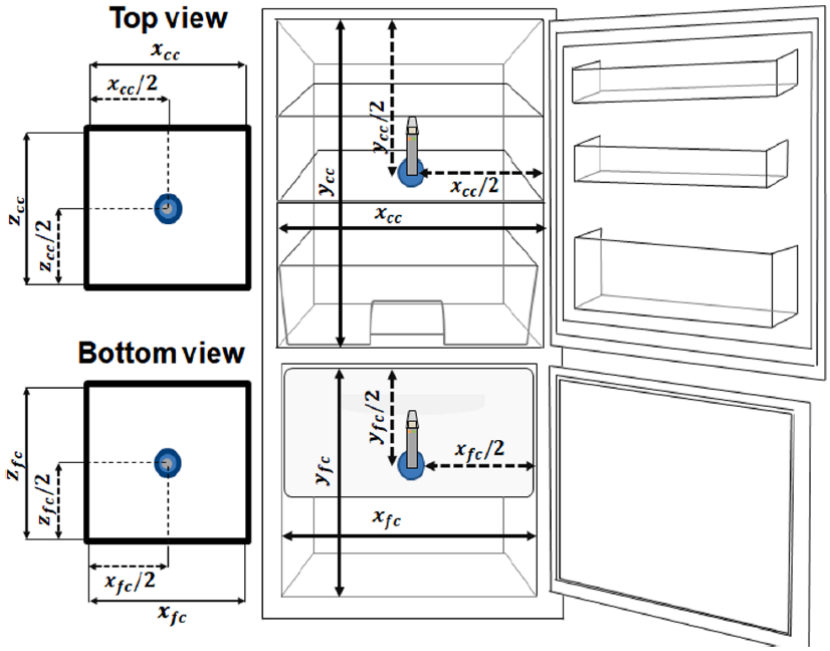

Fig. 12. Positioning of temperature sensors for appliances with multiple compartments.

References

[1] J.S. Brown, P.A. Domanski, Review of alternative cooling technologies, Appl. Therm. Eng. 64 (2014) 252–262, https://doi.org/10.1016/j.applthermaleng.2013.12.014.
[2] C. James, B.A. Onarinde, S.J. James, The use and performance of household refrigerators: a review, Compr. Rev. Food Sci. Food Saf. 16 (2017) 160–179, https://doi.org/10.1111/1541-4337.12242.
[3] R.S. Mithishita, E.M. Barreira, C.O.R. Negrão, C.J.L. Hermes, Thermoeconomic design and optimization of frost-free refrigerators, Appl. Therm. Eng. 50 (2013) 1376–1385, https://doi.org/10.1016/j.applthermaleng.2012.06.024.
[4] German Federal Statistical Office, Equipment of households with electrical household appliances and others. https://www.destatis.de/EN/Themes/Society-

Environment/Income-Consumption-Living-Conditions/Equipment-Consumer-Durables/Tables/liste-equipment-households-electrical–household-appliance-others-germany, 2019 (accessed 22 August 2019).
[5] Official Journal of the European Union, Directive 2009/125/EC of the European Parliament and of the Council of 21 October 2009 establishing a framework for the setting of ecodesign requirements for energy-related products. http://data.europa.eu/eli/dir/2009/125/2012-12-04, 2019 (accessed 21 August 2019).
[6] L.F. Cabeza, D. Urge-Vorsatz, M. Mc Neil, C. Barreneche, S. Serrano, Investigating greenhouse challenge from growing trends of electricity consumption through home appliances in buildings, Renew. Sust. Energ. Rev. 36 (2014) 188–193, https://doi.org/10.1016/j.rser.2014.04.053.
[7] M. Weiss, M.K. Patel, M. Junginger, K. Blok, Analyzing price and efficiency dynamics of large appliances with the experience curve approach, Energ. Pol. 38 (2010) 770–783, https://doi.org/10.1016/j.enpol.2009.10.022.
[8] D. Bhattacharjee, P.W. Irwin, J.R. Booth, J.T. Grimes, The acceleration of foam aging by thin-slicing: some interpretations and limitations, J. Build. Phys. 17 (1994) 219–237, https://doi.org/10.1177/109719639401700305.
[9] U. Berardi, The impact of aging and environmental conditions on the effective thermal conductivity of several foam materials, Energy 182 (2019) 777–794, https://doi.org/10.1016/j.energy.2019.06.022.
[10] J. Geppert, R. Stamminger, Analysis of effecting factors on domestic refrigerators' energy consumption in use, Energ. Convers. Manage. 76 (2013) 794–800, https://doi.org/10.1016/j.enconman.2013.08.027.
[11] L. Harrington, L. Aye, B. Fuller, Impact of room temperature on energy consumption of household refrigerators: lessons from analysis of field and laboratory data, Appl. Energy. 211 (2018) 346–357, https://doi.org/10.1016/j.apenergy.2017.11.060.
[12] L. Harrington, L. Aye, R.J. Fuller, Opening the door on refrigerator energy consumption: quantifying the key drivers in the home, Energ. Effic. 11 (2018) 1519–1539, https://doi.org/10.1007/s12053-018-9642-8.
[13] J. Geppert, R. Stamminger, Do consumers act in a sustainable way using their refrigerator? The influence of consumer real life behaviour on the energy consumption of cooling appliances, Int. J. Consum. Stud. 34 (2010) 219–227, https://doi.org/10.1111/j.1470-6431.2009.00837.x.
[14] A. Biglia, A.J. Gemmell, H.J. Foster, J.A. Evans, Temperature and energy performance of domestic cold appliances in households in England, Int. J. Refrig. 87 (2017) 172–184 https://doi.org/doi:10.1016/j.ijrefrig.2017.10.022.
[15] N. Isaacs, M. Camilleri, L. French, A. Pollard, K. Saville-Smith, R. Fraser, P. Rossouw, J. Jowett, Energy use in New Zealand households – report on the year 10 analysis for the household energy end-use project (HEEP). SR155 (2006), Wellington, New Zealand, http://www.branz.co.nz/books_popup.php?id = 18493.
[16] J. Greenblatt, A. Hopkins, V. Letschert, M. Blasnik, Energy use of US residential refrigerators and freezers: function derivation based on household and climate characteristics, Energ. Effic. 6 (2013) 135–162, https://doi.org/10.1007/s12053-012-9158-6.
[17] Stiftung Warentest, Stromhunger wächst, test. 2013 (2013) 60.
[18] A. Elsner, M. Mueller, A. Paul, J. Vrabec, Zunahme des Stromverbrauchs von Haushaltskühlgeräten durch, Alterung. DKV-Tagung AA II.2 (2013) ISBN:9783932715495.
[19] R. Perkins, L. Cusco, J. Howley, A. Laesecke, S. Matthes, M.L.V. Ramires, Thermal conductivities of alternatives to CFC-11 for foam insulation, J. Chem. Eng. Data. 46 (2001) 428–432, https://doi.org/10.1021/je990337k.
[20] D. Daems, D. Rosbotham, S.N. Singh, M.V. Franco, Factors affecting the long term dimensional stability of rigid foam for the construction industry, J. Cell. Plast. 32 (1996) 485–500, https://doi.org/10.1177/0021955X9603200505.
[21] J.A. King, D.D. Latham, J.C. Ackley, Relationship of k-factor versus density for various appliance foam formulations containing next generation blowing agents, J. Cell. Plast. 32 (1996) 355–366, https://doi.org/10.1177/0021955X9603200403.
[22] J. Cao, C. Chen, G. Gao, H. Yang, Y. Su, M. Bottarelli, M. Cannistraro, G. Pei, Preliminary evaluation of the energy-saving behavior of a novel household refrigerator, J. Renew. Sust. Energ. 11 (2019), https://doi.org/10.1063/1.5054868.
[23] S. Woo, M. Pecht, D.L. O'Neal, Reliability design and case study of a refrigerator compressor subjected to repetitive loads, Int. J. Refrig. 32 (2009) 478–486, https://doi.org/10.1016/j.ijrefrig.2008.07.006.
[24] C. Afonso, M. Castro, Air infiltration in domestic refrigerators: the influence of the magnetic seals conservation, Int. J. Refrig. 33 (2010) 856–867, https://doi.org/10.1016/j.ijrefrig.2009.12.007.
[25] F. Gao, S.S. Naini, J. Wagner, R. Miller, An experimental and numerical study of refrigerator heat leakage at the gasket region, Int. J. Refrig. 73 (2017) 99–110, https://doi.org/10.1016/j.ijrefrig.2016.09.002.
[26] P. Bansal, E. Vineyarda, O. Abdelaziza, Advances in household appliances – a review, Appl. Therm. Eng. 31 (2011) 3748–3760, https://doi.org/10.1016/j.applthermaleng.2011.07.023.
[27] F. Ochs, W. Heidemann, H. Müller-Steinhagen, Effective thermal conductivity of moistened insulation materials as a function of temperature, Int. J. Heat Mass. Transf. 51 (2008) 539–552, https://doi.org/10.1016/j.ijheatmasstransfer.2007.05.005.
[28] U. Berardi, L. Tronchin, M. Manfren, B. Nastasi, On the effects of variation of thermal conductivity in buildings in the Italian construction sector, Energies 11 (2018) 872, https://doi.org/10.3390/en11040872.
[29] M. Budaiwi, A. Abdou, M. Al-Homoud, Variations of thermal conductivity of insulation materials under different operating temperatures: impact on envelope-induced cooling load, J. Archit. Eng. 8 (2002) 125–135, https://doi.org/10.1061/(ASCE)1076-0431(2002) 8:4(125).
[30] M.S. Al-Homoud, Performance characteristics and practical applications of common building thermal insulation materials, Build. Environ. 40 (2005) 353–366, https://doi.org/10.1016/j.buildenv.2004.05.013.
[31] H. Fleurent, S. Thjs, The use of pentanes as blowing agent in rigid polyurethane foam, J. Cell. Plast. 31 (1995) 580–599, https://doi.org/10.1177/0021955X9503100606.
[32] A.A. Abdou, I.M. Budaiwi, Comparison of thermal conductivity measurements of building insulation materials under various operating temperatures, J. Build. Phys. 29 (2005) 171–184, https://doi.org/10.1177/1744259105056291.
[33] K-E. Wagner, Simulation und Optimierung des Wärmedämmvermögens von PUR-Hartschaum, Wärme- und Stofftransport sowie mechanische Verformung, Dissertation, Stuttgart (Germany): I. f. Stuttgart, Ed, 2002. http://dx.doi.org/10.18419/opus-1579.
[34] H. Macchi-Tejeda, H. Opatovà, J. Guilpart, Contribution to the gas chromatographic analysis for both refrigerants composition and cell gas in insulating foams – Part II: Aging of insulating foams, Int. J. Refrig. 30 (2007) 338–344, https://doi.org/10.1016/j.ijrefrig.2006.04.004.
[35] J. Berardia, J. Madzarevic, Microstructural analysis and blowing agent concentration in aged polyurethane and polyisocyanurate foams, Appl. Therm. Eng. 164 (2020) 114440, https://doi.org/10.1016/j.applthermaleng.2019.114440.
[36] J.E. Christian, A. Desjarlais, R. Graves, Five-year field study confirms accelerated thermal aging method for polyisocyanurate insulation, J. Cell. Plast. 34 (1998) 39–64, https://doi.org/10.1177/0021955X9803400103.
[37] W. Albrecht, Change over time in the thermal conductivity of ten-year-old PUR rigid foam boards with diffusion-open facings, Cell. Polym. 23 (2004) 161–172, https://doi.org/10.1177/026248930402300303.
[38] W. Albrecht, Cell-gas composition – An important factor in the evaluation of long-term thermal conductivity in closed-cell foamed plastics, Cell. Polym. 19 (2000) 319–331.
[39] M. Khoukhi, N. Fezzioui, B. Draoui, L. Salah, The impact of changes in thermal conductivity of polystyrene insulation material under different operating temperatures on the heat transfer through the building envelope, Appl. Therm. Eng. 105 (2016) 669–674, https://doi.org/10.1016/j.applthermaleng.2016.03.065.
[40] P. Glouannec, M. Benoit, G. Delamarre, Y. Grohens, Experimental and numerical study of heat transfer across insulation wall of a refrigerated integral panel van, Appl. Therm. Eng. 73 (2014) 196–204, https://doi.org/10.1016/j.applthermaleng.2014.07.044.
[41] H. Seifert, A. Biedermann, Long-term energy efficiency of PU insulation for refrigeration, in: Conference Proceedings, Polyurethanes Conference 2000: Defining the future through technology, CRC Press, Boston (Massachusetts), 2000, pp. 429–435.
[42] G.C.J. Bart, G.M.R. Du Cauzé de Nazelle GMR. Certification of thermal conductivity aging of PUR foam, J. Cell. Plast. 29 (1993) 29–42. https://doi.org/10.1177/0021955X9302900102.
[43] S.A. Al-Ajlan, Measurements of thermal properties of insulation materials by using transient plane source technique, Appl. Therm. Eng. 26 (2006) 2184–2191, https://doi.org/10.1016/j.applthermaleng.2006.04.006.
[44] J.W. Wu, W.F. Sung, H.S. Chu, Thermal conductivity of polyurethane foams, Int. J. Heat Mass Transf. 42 (1999) 2211–2217, https://doi.org/10.1016/S0017-9310(98)00315-9.
[45] A. Galakhova, M. Santiago-Calvo, J. Tirado-Mediavilla, M. Villafañe, A. Rodríguez-Pérez, G. Riess, Identification and quantification of cell gas evolution in rigid polyurethane foams by novel GCMS methodology, Polymers (Basel) 11 (2019) 1192, https://doi.org/10.3390/polym11071192.
[46] K.E. Wilkes, F.J. Weaver, W.A. Gabbard, Aging of polyurethane foam insulation in simulated refrigerator panels –one-year results with third-generation blowing agents, J. Cell. Plast. 37 (2001) 400–428, https://doi.org/10.1106/N9XJ-PKE1-N3UV-DWJQ.
[47] K.E. Wilkes, D.W. Yarbrough, W.A. Gabbard, G.E. Nelson, J.R. Booth, Aging of polyurethane foam insulation in simulated refrigerator panels – three-year results with third-generation blowing agents, J. Cell. Plast. 38 (2002) 317–339, https://doi.org/10.1177/0021955X02038004142.
[48] K.E. Wilkes, D.W. Yarbrough, G. Nelson, Aging of polyurethane foam insulation in simulated refrigerator panels – four-year results with third-generation blowing agents, J. of Cell. Plast. 38 (2003), https://doi.org/10.1177/0021955X02038004142.
[49] M. Bogdan, J. Hoerter, J.O. Moore, Meeting the insulation requirements of the building envelope with polyurethane and polyisocyanurate foam, J. Cell. Plast. 41 (2005) 41–56, https://doi.org/10.1177/0021955X05049869.
[50] M. Pfundstein, R. Gellert, M. Spitzner, A. Rudolphi, Insulating materials – principles, materials, applications, Edition Detail; Walter de Gruyter. Berlin, Germany, 2008.
[51] H. Zhang, W.-Z. Fang, W.-Q. Tao, Y.-M. Li, Experimental study of the thermal conductivity of polyurethane foams, Appl. Therm. Eng. 115 (2017) 528–538, https://doi.org/10.1016/j.applthermaleng.2016.12.057.
[52] F. Ozkadi, 2001. The effect of thermal aging polyurethane to increasing the energy consumption of refrigerator and freezer, in: al., P.B.e. (Ed.), Energy Efficiency in Household Appliances and Lighting. Springer-Verlag, Berlin-Heidelberg, Germany, pp. 114–121.
[53] H. Ozkan, E. Demirtas, U. Kilic, Arcelik Anonim Sirketi, A refrigerator comprising a plastic inner lining, patent document - WO 2019/007829 A1, WIPO | PCT, 10.01.2019.
[54] H. Ozkan, E. Demirtas, M. Sezer, O. Kaymakci, U. Kilic, Arcelik Anonim Sirketi, A refrigerator comprising a plastic inner lining, patent document - WO 2019/007030 A1, WIPO | PCT, 10.01.2019.
[55] M. Khoukhi, A. Hassan, S.A. Saadi, S. Abdelbaqi, A dynamic thermal response on thermal conductivity at different temperature and moisture levels of EPS insulation, Case Stud. Therm. Eng. 14 (2019) 100481, https://doi.org/10.1016/j.csite.2019.

100481.
[56] R. Saidur, H.H. Masjuki, I.A. Choudhury, Role of ambient temperature, door opening, thermostat setting position and their combined effect on refrigerator-freezer energy consumption, Energ. Convers. Manage. 43 (2002) 845–854, https://doi.org/10.1016/S0196-8904(01)00069-3.
[57] O. Laguerre, Heat transfer and air flow in a domestic refrigerator. Mathematical modelling of food processing, Mohammed M. Farid (ed.), CRC Press, 445–474, 2010, Contemp. Food Eng. https://hal.archives-ouvertes.fr/hal-00583230.
[58] Ecodesign & Labelling Review Household Refrigeration - Preparatory/review study, Commission Regulation (EC) No. 643/2009 and Commission (Delegated) Regulation (EU) 1060/2010, https://www.eup-network.de/fileadmin/user_upload/2015/Household_Refrigeration_Review_TASK_1_6_DRAFT_REPORT_20151114.pdf, 2019 (accessed 20.12.2019).
[59] O. Laguerre, D. Flick, Heat transfer by natural convection in domestic refrigerators, J. Food Eng. 62 (2004) 79–88, https://doi.org/10.1016/S0260-8774(03)00173-0.
[60] F. Stefano, M. Presutto, R. Stamminger, R. Scialdoni, W. Mebane, R. Esposito, Preparatory studies for eco-design requirements of EuPs (Tender TREN/D1/40-2005) LOT13: Domestic refrigerators and freezers. https://www.eup-network.de/fileadmin/user_upload/Lot_13_Final_Report_Taks_3-5.pdf, 2019 (accessed 10 Mai 2019).
[61] R. Xiao, Y. Zhang, X. Liu, Z. Yuan, A life-cycle assessment of household refrigerators in China, J. Clean Prod. 95 (2015) 301–310, https://doi.org/10.1016/j.jclepro.2015.02.031.
[62] R.H.S. Winterton, Newton's law of cooling, Contemp. Phys. 40 (1999) 205–212, https://doi.org/10.1080/001075199181549.
[63] M. Vollmer, Newton's Law of Cooling revisited, Eur. J. Phys. 30 (2009) 1063–1084, https://doi.org/10.1088/0143-0807/30/5/014.
[64] IEC 62552-2:2015: Household refrigerating appliances – Characteristics and test methods – Part 2: Performance requirements (Annex C), IEC, 2015, p.37.
[65] DIN EN 62552:2013, Household refrigerating appliances–characteristics and test methods (IEC 62552:2007, modified + corrigendum Mar. 2008), Beuth Verlag, 2013, Berlin.

6.5 Thermal conductivity of solid paraffins and several n-docosane compounds with graphite

Paul, A., Baumhögger, E., Dewerth, M. O., Elsner, A., Dindar, I. H., Sonnenrein, G., Vrabec, J., 2023. Journal of Thermal Analysis and Calorimetry 148, 5687-5694.

Diese Studie befasst sich mit der Wärmeleitfähigkeit von festen Paraffinen als Phasenwechselmaterial. Für die meisten Paraffine wurde in bisherigen Veröffentlichungen lediglich die Wärmeleitfähigkeit der flüssigen Phase ausreichend untersucht. In dieser Studie wurde daher ein Messaufbau basierend auf der modifizierten Guarded-Hot-Plate-Methode entwickelt, mit dem die Messung der Wärmeleitfähigkeit von festen Paraffinen durchgeführt wurde. So wurde reines n-Docosan und seine Verbindungen mit verschiedenen Arten und Anteile von Graphit sowie reines n-Octadecan und n-Eicosan untersucht. Für reines festes n-Docosan konnte eine Wärmeleitfähigkeit von 0,49 W/(m·K) bestimmt werden. Zur Steigerung der Wärmeleitfähigkeit der Paraffine stellten sich Graphite mit einer kugelförmigen Partikelgröße von 200 µm als optimal heraus.

Der Autor dieser Dissertation hat die vorliegende Publikation verfasst, den Versuchsaufbau ausgearbeitet, die Versuche durchgeführt und ausgewertet. Mats-Ole Dewerth und Iman Hami Dindar haben bei der Durchführung der Versuche unterstützt. Bei der Mess- und Regelungstechnik für die Versuchsdurchführung wirkte Elmar Baumhögger mit. Die untersuchten Materialien wurden durch Gerrit Sonnenrein von der Axiotherm GmbH bereitgestellt. An der Überarbeitung des Manuskripts waren Elmar Baumhögger und Jadran Vrabec beteiligt. Während der gesamten Arbeit wurde der Autor von Jadran Vrabec betreut.

Journal of Thermal Analysis and Calorimetry (2023) 148:5687–5694
https://doi.org/10.1007/s10973-023-12107-2

Thermal conductivity of solid paraffins and several n-docosane compounds with graphite

Andreas Paul[1] · Elmar Baumhögger[1] · Mats-Ole Dewerth[1] · Iman Hami Dindar[2] · Gerrit Sonnenrein[3] · Jadran Vrabec[4]

Received: 31 August 2022 / Accepted: 12 March 2023 / Published online: 3 April 2023

Abstract

The technical importance of paraffins as phase change materials (PCM) in heat storage systems increases. Knowledge on the thermal conductivity of paraffins is necessary for the design and optimization of heat storage systems. However, for most paraffins solely the thermal conductivity of the liquid state has been sufficiently investigated. For the solid state, precise thermal conductivity data are only known for a few paraffins, while only generalized values are available for the remainder, some of which contradict each other. In this study, a measurement setup based on the modified guarded hot plate method is developed. It is used to investigate the thermal conductivity of several paraffines in the solid state, including pure n-docosane and its compounds with different types and concentrations of graphite. For n-docosane in the solid state, the thermal conductivity is determined to be 0.49 W m^{-1} K^{-1}. A particle size of 200 µm with a spherical shape turns out to be optimal to increase the thermal conductivity. This allows the thermal conductivity of a compound with 10% graphite to increase by a factor of three compared to the pure paraffin. Furthermore, significant differences to thermal conductivity data from the literature are found.

Keywords Thermal conductivity · Guarded hot plate · n-octadecane · n-eicosane · n-docosane · Phase change materials · Graphite compound

List of symbols

A	Surface area [m^2]
P	Heating power [W]
$\dot{Q}$	Heat flow [W]
s	Thickness [m]
ΔT	Temperature difference [K]
λ	Thermal conductivity [W m^{-1} K^{-1}]
a	Air
f	Heat conducting foil
PCM	Phase change material

✉ Jadran Vrabec
vrabec@tu-berlin.de

[1] Technical Thermodynamics, University of Paderborn, Warburger Str. 100, 33098 Paderborn, Germany

[2] Fluid Process Engineering, University of Paderborn, Warburger Str. 100, 33098 Paderborn, Germany

[3] Competence Centre for Sustainable Energy Technology, University of Paderborn, Warburger Str. 100, 33098 Paderborn, Germany

[4] Thermodynamics, Technical University of Berlin, Ernst-Reuter-Platz 1, 10587 Berlin, Germany

Introduction

The technical importance of phase change materials (PCM) has increased in recent years. PCM are used for the short-term and long-term storage of heat in order to save energy in a wide range of applications, such as household appliances, PV module cooling or heating systems [1, 2]. In particular, the temperature range around the ambient of about −50 to +50 °C is of great technical importance. In this temperature range, a large number of materials, like salt hydrates, water or paraffins, can be used as PCM [3]. In addition to an adequate melting temperature for the given process and a large enthalpy of fusion, further selection criteria, such as cycle stability, corrosivity, volume expansion, toxicity or flammability, have to be met for the design of PCM storage systems [4]. Despite the comparatively low enthalpy of fusion, paraffins offer great advantages for many processes due to the relatively freely selectable melting temperature, excellent cycle stability and non-corrosive behavior. Hasnain published a comprehensive review on the thermophysical properties of numerous PCM, such as density and isobaric heat capacity. However, the thermal conductivity was not dealt with in depth in this review [5].

Especially in processes with short-term heat storage, the thermal conductivity is an important property because it determines how quickly the PCM can be charged and discharged [6]. Technically, this can be optimized with additives that increase the thermal conductivity or the structural design of the PCM container [2]. In practical use, the relatively low thermal conductivity of paraffins is often compensated for by applying the paraffin over a large area with a small layer thickness [7–10]. Furthermore, it should be noted that the thermal conductivity of solid and liquid states differs significantly from one another.

Thermal conductivity of paraffins

In 1969, Bogatov et al. measured the thermal conductivity of n-tetradecane, n-pentadecane and n-hexadecane in the liquid state over a temperature range from 20 to 200 °C and a pressure range from 0.98 to 490 bar [11]. Shortly after that, Naziev et al. investigated the thermal conductivity of n-decane [12]. In 1994, Vargaftik et al. published a comprehensive collection of thermal conductivity data for hydrocarbons in liquid and gaseous states [13].

Investigations of the thermal conductivity of paraffins are listed in Table 1, indicating the melting temperature and enthalpy of fusion. This includes various paraffins from n-decane to n-triacontane, n-tetracontane and n-pentacontane. For most of the paraffins addressed in Table 1, only the thermal conductivity of the liquid state was investigated, or the literature does not indicate which state the values refer to. In 1983, a review article by Abhat assumed that the thermal conductivity of all paraffins from n-tridecane to n-pentacontane is generally $\lambda = 0.21$ W m^{-1} K^{-1}, with the exception of octadecane, $\lambda = 0.15$ W m^{-1} K^{-1} [14]. However, these values contradict other studies. The thermal conductivity of the solid state is only known for n-hexadecane, n-octadecane and n-eicosane. The results for these four paraffins were published by Vélez et al., Sasaguchi et al. and Sharma et al. for n-octadecane [15, 16, 17] and are highlighted in boldface in Table 1. Furthermore, Sharma et al. stated that the thermal conductivity of solid n-dodecane, n-tetradecane, n-hexadecane, n-nonadecane and n-hexacosane is throughout 0.21 W m^{-1} K^{-1}, which partially conflicts with the results discussed above (in italics in Table 1).

Thermal conductivity data for n-docosane from the literature are listed in Table 2. The investigations by Rastorguev et al., Fleming et al. and Vargaftik et al. cover a large temperature range in the liquid state starting from the melting point [13, 18, 19]. On the other hand, the publications by Abhat, Sari et al., Li et al. (2013) and Li et al. (2014) do not indicate the temperature where the thermal conductivity was measured [14, 20–22].

It can be concluded that there is an extensive literature dataset for the thermal conductivity of liquid n-docosane, but the thermal conductivity of this paraffin in its solid state was not addressed yet.

Thermal conductivity of n-docosane with graphite

Composite materials with a higher thermal conductivity can be created by mixing n-docosane with graphite. Using Eshelby's equivalent inclusion method, Hatta derived a theoretical model for the thermal conductivity of composite materials consisting of different phases [23].

Figure 1 shows the results of investigations on the thermal conductivity of graphite-compounded n-docosane by Sari et al. [20] from 2007 and Li et al. (2013) [21] from 2013. In another study by Li et al. (2014), the addition of graphite resulted in an increase of the thermal conductivity from 0.26 to 0.59 W m^{-1} K^{-1}, but the authors did not specify the mass fraction of graphite [22].

Methods for the measurement of thermal conductivity

A large number of methods has been proposed for measuring the thermal conductivity [13].

With the laser point method, a defined amount of radiation energy is introduced into the sample in a temperature-controlled vacuum chamber by means of a pulsed laser or a xenon discharge lamp. A photodiode and a temperature sensor attached to the back of the sample are used to determine the ensuing temperature rise in the sample. With the measured temperature profile, the thermal conductivity of the sample can be calculated. This method can be used for solids, regardless of their surface properties, up to temperatures of 2000 °C. However, applying this method to materials with a melting point close to the ambient temperature can result in melting of the sample at certain points so that it is not usable for paraffins [24].

In the hot wire method, a platinum wire is surrounded by the sample material. The heat introduced thermally into the sample can be determined from the electrical current or voltage and the resistance of the wire. The platinum wire serves simultaneously as a heating element and as a temperature sensor. This method can be used when the thermal conductivity is in the range from 0.005 to 5 W m^{-1} K^{-1} and the evaluation is carried out using either the transient or the periodic method. In the transient method, the thermal conductivity can be calculated from the heating curve, and in the periodic method, it is determined via a frequency analysis of the alternating periods of heating and cooling of the sample [18, 25–28].

The measurement setup of the plate conductivity meter is primarily used to determine the thermal conductivity of materials with a higher heat conduction. In this measurement setup, a cylindrical sample is placed between a heat sink and

Table 1 Thermal conductivity of different paraffins from the literature

Material		Melting temperature/K	Enthalpy of fusion/kJ kg^{-1}	Thermal conductivity/W m^{-1} K^{-1}	Solid/liquid	Ref.
n-decane	$C_{10}H_{22}$	–	–	0.1349 (313.15 K)	Liquid	[12]
n-dodecane	$C_{12}H_{26}$	261.15	–	*0.21*	Solid	[17]
n-tridecane	$C_{13}H_{28}$	267.15	–	–	–	[17]
n-tetradecane	$C_{14}H_{30}$	279.15	230	*0.21*	Solid	[3]
		277.65	165	–	–	[14]
		278.95	–	0.1325 (313.15 K)	Liquid	[11]
n-pentadecane	$C_{15}H_{32}$	283.15	207	0.17	–	[17]
		283.15	212	–	–	[3]
		283.05	–	0.134	–	[11]
n-hexadecane	$C_{16}H_{34}$	291.35	238	*0.21*	Solid	[17]
		291.15	210	0.21	–	[3]
		290.90	235.13	**0.335 (276.15 K)**	Solid	[15]
				0.143 (313.15 K)	Liquid	
		291.35	–	0.137 (313.15 K)	Liquid	[11]
n-heptadecane	$C_{17}H_{36}$	295.15	215	–	–	[17]
		295.15	240	–	–	[3]
n-octadecane	$C_{18}H_{38}$	301.35	245	**0.35**	Solid	[17]
				0.149	Liquid	
		300.65	243.50	**0.358 (298.15 K)**	Solid	[16]
				0.148 (313.15 K)	Liquid	
		300.22	243.68	**0.33 (276.15 K)**	Solid	[15]
				0.148 (313.15 K)	Liquid	
n-nonadecane	$C_{19}H_{40}$	305.05	222	*0.21*	Solid	[17]
n-eicosane	$C_{20}H_{42}$	310.15	247	–	–	[17]
		311.15	283	–	–	[3]
		308.85	247.05	**0.425 (286.15 K)**	Solid	[15]
				0.151 (315.15 K)	Liquid	
		309.55	–	0.144 (333.15 K)	Liquid	[18]
n-heneicosane	$C_{21}H_{44}$	314.15	215	–	–	[17]
		312.75	–	0.147 (333.15 K)	Liquid	[18]
n-tricosane	$C_{23}H_{48}$	320.15	234	–	–	[17]
		320.65	–	0.145 (353.15 K)	Liquid	[18]
n-tetracosane	$C_{24}H_{50}$	324.15	255	–	–	[17]
		323.27	–	0.148 (353.15 K)	Liquid	[18]
n-pentacosane	$C_{25}H_{52}$	327.15	238	–	–	[17]
n-hexacosane	$C_{26}H_{54}$	329.15	257	*0.21*	Solid	[17]
n-heptacosane	$C_{27}H_{56}$	332.15	236	–	–	[17]
n-octacosane	$C_{28}H_{58}$	334.15	255	–	–	[17]
n-nonacosane	$C_{29}H_{60}$	337.15	240	–	–	[17]
n-triacontane	$C_{30}H_{62}$	338.15	252	–	–	[17]
n-tetracontane	$C_{40}H_{82}$	355.15	–	–	–	[3]
n-pentacontane	$C_{50}H_{102}$	368.15	–	–	–	[3]
paraffin wax	n.a	305.15	251	0.514	Solid	[17]
				0.224	Liquid	

a hot plate in a vacuum chamber. The thermal conductivity can be determined by the imposed heating power and the sample geometry. In order to minimize external influences, a protective heater system is also used in the vacuum chamber. Due to the low thermal conductivity of paraffins, this measurement method is not suitable for such materials [29, 30].

For solids with a low thermal conductivity, like insulation materials or paraffins, the guarded hot plate method is used.

Table 2 Thermal conductivity of n-docosane from the literature

Melting temperature/K	Enthalpy of fusion/kJ kg^{-1}	Thermal conductivity/W m^{-1} K^{-1}	Ref.
317.15	–	0.149 (333.15 K)	[18]
–	–	0.21	[14]
–	–	0.151 (330 K) 0.149 (340 K) 0.147 (350 K) 0.145 (360 K) 0.143 (370 K) 0.141 (380 K) 0.139 (390 K) 0.137 (400 K) 0.135 (410 K) 0.133 (420 K) 0.131 (430 K) 0.130 (440 K) 0.128 (450 K) 0.126 (460 K) 0.125 (470 K)	[13]
317.15	249	–	[17]
314.75	194.6	0.22	[20]
313.35	124.49	0.205	[21]
–	–	0.26	[22]
–	–	0.151 (317.41 K) 0.150 (322.59 K) 0.148 (327.04 K) 0.146 (331.85 K) 0.146 (336.30 K) 0.144 (341.48 K) 0.143 (346.30 K) 0.142 (351.48 K)	[19]

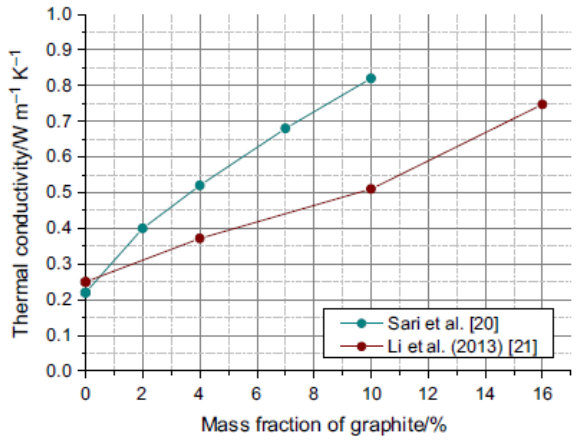

Fig. 1 Increase in the thermal conductivity of n-docosane-graphite compounds as a function of the mass fraction of graphite [20, 21]

The basic measurement setup is shown in Fig. 2. In this symmetrical setup, a temperature gradient ΔT is generated in two identical samples via a centrally located electrical

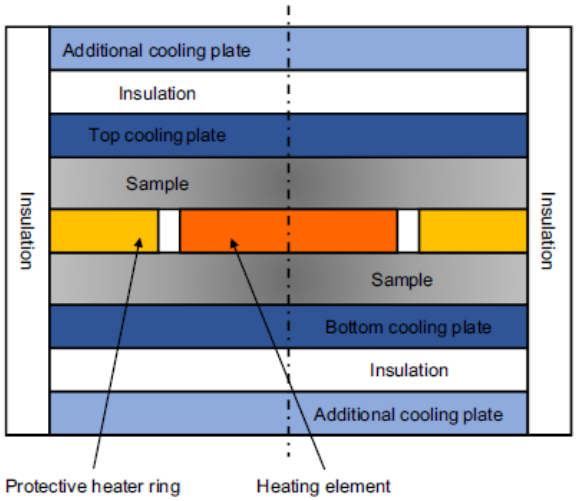

Fig. 2 Basic measurement setup of a guarded hot plate [31]

heating element and cooling plates attached to the top and bottom of the stack. By measuring the power P supplied to the heating element, the thickness of the samples s and the surface area of the heater A, the thermal conductivity λ of the samples can be determined by

$$\lambda = \frac{P\,s}{\Delta T}\,\frac{1}{2\,A} \tag{1}$$

The heating element is surrounded by a ring-shaped protective heater, the temperature of which is regulated to be identical with that of the heating element so that radial heat flow through the sample is prevented. This measurement method can be used for solid materials with a low thermal conductivity of up to 5 W m^{-1} K^{-1} over a wide temperature range [31, 32].

Method

Modified guarded hot plate

A modified guarded hot plate measurement setup was developed for this study. The solid sample was placed between a cooling plate and an inner main heater. By specifying the temperature gradient between the main heater and the cooling plate, a heat flow was generated through the sample. A protective heater cover and a protective heater ring prevented heat loss from the main heater to the ambient. For this purpose, the protective heaters were regulated to the same temperature as the main heater with a closed loop controller. The basic measurement setup is shown in Fig. 3. Compared to other methods, this new measurement setup is characterized by a simple structure and straightforward use.

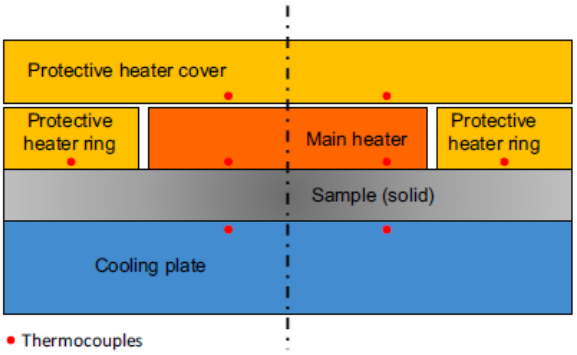

Fig. 3 Modified guarded hot plate measurement setup, this work

The heater had a diameter of 116 mm, the cooling plate had a diameter of 158 mm and the gap between the main heater and the protective heater was 1 mm. The protective heaters had a thickness of 20 mm both in vertical and radial directions.

The solid PCM sample was placed between the heaters and the cooling plate. Since surface roughness of the heater and the sample leads to air pockets between the sample and the heater and also between the sample and the cooling plate, a smooth, soft heat conducting foil was placed on both surfaces of the sample. The foil compensated for the remaining unevenness of the sample surface, thus minimizing the trapped layer of air. The heat conducting foil (SB-HIS-5 from DETAKTA Isolier- und Messtechnik GmbH & Co KG) was made of a silicone glass fabric and had a thermal conductivity of 5 W m^{-1} K^{-1} and a thickness of 0.2 mm.

The heat flow $\dot{Q}$ through the cross-sectional area A of the sample with a thickness s is given by Fourier's law [33]

$$\dot{Q} = P = \frac{1}{2\left(\frac{s_f}{\lambda_f} + \frac{s_a}{\lambda_a}\right) + \frac{s}{\lambda}} \cdot A \cdot \Delta T \tag{2}$$

The thickness of the air s_a summarily represents thin layers of air on top and bottom of each foil. With measurements of samples with a known thermal conductivity and a varying thickness s, the average layer thickness of the air inclusions s_a was found to be 0.8 µm. To adequately deal with the rather uncertain air layer thickness, a large error bar was assigned to it, i.e., $s_a = 0.8 \pm 4$ µm.

By measuring the electrical heating power P of the main heater, the sample thickness s and the temperature gradient ΔT between the main heater and cooling plate, together with thickness and thermal conductivity of foil and air inclusions, the thermal conductivity of the sample λ can be determined by

$$\lambda = \frac{s}{\frac{\Delta T \cdot A}{P} - 2\left(\frac{s_f}{\lambda_f} + \frac{s_a}{\lambda_a}\right)} \tag{3}$$

The electrical heating power was applied and measured over the range from 0 to 200 W with a power supply Agilent E3633A with an accuracy of ± 1% of the measured value. To determine the sample thickness, a caliper gauge with an accuracy of 0.02 mm was used.

With the uncertainties of the individually measured values listed in Table 3, the total uncertainty of the measured thermal conductivity can be determined via the error propagation law by Gauß.

All measurements were carried out at an ambient temperature of 293.15 K and a pressure of 0.1 MPa.

Sample materials

For the measurement of the pure paraffins and compounds of n-docosane with various types and quantities of graphite, cylindrical samples were produced. Once the samples were made, they initially had uneven and curved surfaces. Consequently, these were smoothed in two steps by sandpaper grinding with a grain size of P120 and P320. The n-docosane samples contained an additive to prevent the graphite particles from sinking to the ground of the sample so that they remained homogeneously distributed. Its influence on the thermal conductivity was investigated by a comparative measurement with a pure sample without additive. The difference was 0.06 W m^{-1} K^{-1}, which is negligible compared to the increase of the thermal conductivity due to the presence of graphite. The compositions of the samples are listed in Table 4. The paraffins (pure n-octadecane,

Table 3 Measurement uncertainties

Measured quantity		Measurement uncertainty
PCM sample thickness	s	± 0.2 mm
Heater temperature	T_h	± 0.4 K
Heat sink temperature	T_c	± 0.1 K
Electrical heating power	P	± 1% of the measured value
Thickness of the heat conducting foil	s_f	± 0.02 mm
Thermal conductivity of the heat conducting foil	λ_f	± 0.1 W m^{-1} K^{-1}
Thickness of the air layers	s_a	± 4 µm

Table 4 Composition of the samples

Sample	Paraffin	Graphite powder	Particle form	Mass fraction of graphite/%	D_{50} /µm	Bulk density /g L^{-1}	Carbon content /%	Thermal conductivity /W m^{-1} K^{-1}	Measurement uncertainty /%
A	n-docosane	–	–	0	–	–	–	0.49	3.9
B	n-octadecane	–	–	0	–	–	–	0.36	4.2
C	n-eicosane	–	–	0	–	–	–	0.42	7.2
D5%	n-docosane	GFG5	Spherical	5	5	150	≥95	0.69	3.1
D10%				10				0.67	3.1
E5%	n-docosane	GFG200	Spherical	5	200	100	≥95	0.91	3.3
E10%				10				1.41	3.9
F5%	n-docosane	GFG600	Spherical	5	600	100	≥95	0.77	3.1
F10%				10				1.35	4.2
G5%	n-docosane	GFG1000HD	Rod-shaped	5	1000	350	≥95	0.61	3.2
G10%				10				0.63	2.9

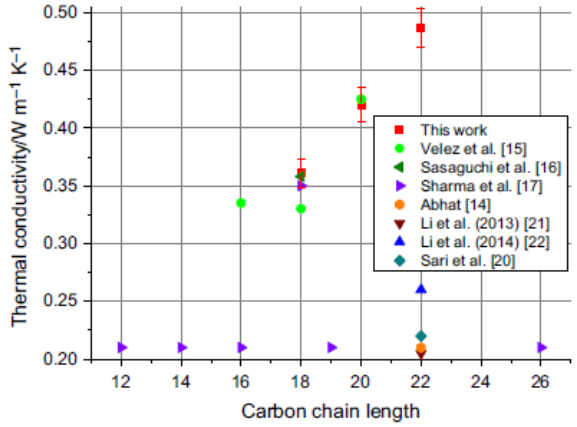

Fig. 4 Thermal conductivity of various pure n-paraffins in the solid state (samples A, B and C) as a function of the carbon chain length

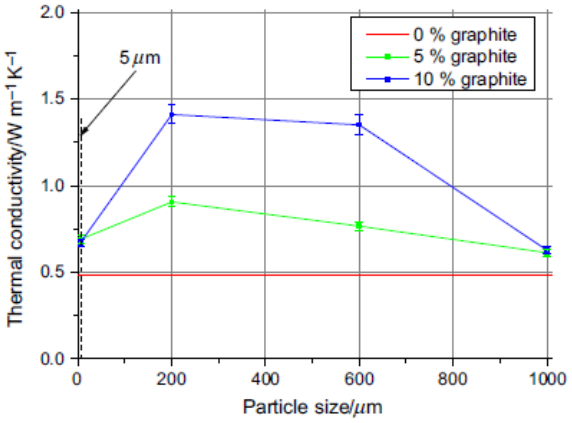

Fig. 5 Thermal conductivity of n-docosane-graphite compounds as a function of particle size and varying graphite content

n-eicosane, n-docosane and n-docosane with additive) were provided by Axiotherm GmbH.

Several expanded graphite powders from Sigratherm® GFG of types GFG5, GFG200, GFG600 and GFG1000HD were used. The technical characteristics of these graphite powders are listed in Table 4.

Results and discussion

The results of this work are compared to literature values for the solid state of the paraffins n-octadecane, n-eicosane and n-docosane in Fig. 4 and are listed in Table 4. The thermal conductivity data for n-octadecane and n-eicosane measured in this study agree well with the results of Vélez et al. [15] and Sasaguchi et al. [16]. All of these data are significantly higher than the results from Sharma et al. [17], Li et al. (2013) [21], Li et al. (2014) [22], Sari et al. [20] and Abhat [14]. From measurements of the thermal conductivity in the liquid state, it is known that it increases with rising carbon chain length [34]. With the thermal conductivity data determined in this study, this can now also be confirmed for the paraffins n-octadecane, n-eicosane and n-docosane in the solid state.

Figures 5 and 6 show the results for the thermal conductivity of n-docosane as a function of the particle size and varying mass fraction of graphite. In the present work, a thermal conductivity of pure n-docosane of 0.49 W m^{-1} K^{-1} was measured, which is indicated by the horizontal line in Fig. 5. The addition of graphite increases the thermal conductivity, while particle size and shape of the graphite were found to have a significant influence. With a mass fraction

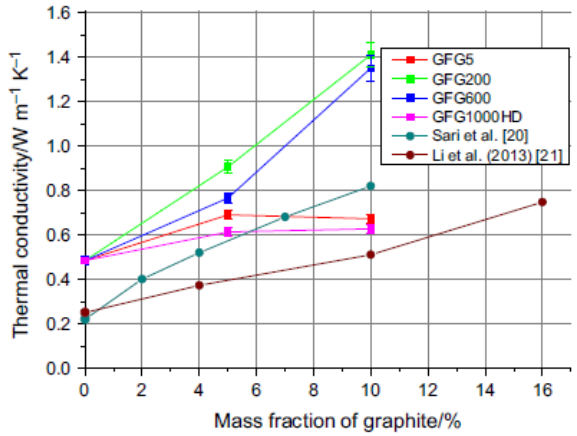

Fig. 6 Comparison of the present results for n-docosane-graphite compounds with literature values

of 10% for the graphite types GFG200 and GFG600, the thermal conductivity increased almost threefold to a value of 1.41 W m^{-1} K^{-1}. The finest graphite GFG5 considered in this study only showed an increase by a factor of ~ 1.4 to a value of 0.67 W m^{-1} K^{-1}. With the largest particle size, the GFG1000HD graphite led to the smallest rise of the thermal conductivity.

Graphite incorporated into the compound creates local thermal bridges that conduct heat within the paraffin. Mathematically, this can be described by a combination of serial and parallel connections of more thermally conductive graphite within the paraffin. Models of Lewis and Nielsen from 1970 that rest on this idea have prevailed in the literature [35].

The results of the paraffin samples compounded with graphite powder with a particle size of 1000 µm show a significantly lower thermal conductivity compared to the smaller particle sizes. This is due to the more rod-shaped form of the GFG1000HD particles. The thermal conductivity deteriorates significantly due to the smaller extent of the rods in transverse direction. With a theoretical arrangement of the rods in longitudinal direction aligned with the heat flow, the thermal conductivity should increase significantly. But such an application is practically impossible, since the graphite particles rearrange themselves with each phase change cycle of the paraffins, resulting in a disordered particle arrangement.

In comparison with the results of Sari et al. [20] and Li et al. (2013) [21], the thermal conductivity measured in this study shows higher values and a larger increase of the thermal conductivity upon the addition of graphite, cf. Figure 6. It should be noted that the temperature of the measurements of Sari et al. [20] and Li et al. (2013) [21] was not clearly defined so that their values may refer to the liquid state.

Conclusions

In addition to the enthalpy of fusion and the melting temperature, the thermal conductivity is an important design parameter for PCM. With the knowledge of these properties, thermal energy storage systems can be adequately designed and the time period of a phase change can be determined. Despite the extensive studies on the thermal conductivity of paraffins in the liquid state from in the 1970s to the early 1990s, the thermal conductivity of paraffins in the solid state has been poorly investigated so far. A thermal conductivity of solid n-docosane between 0.205 and 0.26 W m^{-1} K^{-1} specified in older investigations seems to be too low. The thermal conductivity of solid n-docosane was determined in the present work to be 0.49 W m^{-1} K^{-1}. The results of Vélez et al. and Sasaguchi et al. for the thermal conductivity of n-octadecane and n-eicosane were confirmed in this study.

By adding graphite powder, the thermal conductivity of n-docosane can be significantly increased by more than a factor of three with a graphite mass fraction of 10%. The selection in terms of quantity and shape of the graphite powder has to be optimized so that the desired thermal conductivity is achieved, while minimizing costs. Spherical particles were found to be adequate.

The presented measuring setup is a suitable tool for determining the thermal conductivity of solid paraffins. With this setup, a reliable determination of the thermal conductivity in a range from below 0.2 to 2 W m^{-1} K^{-1} was possible. Since the thermal conductivity of only a few paraffins in the solid state is known, these materials should be further investigated because of their technical relevance.

Acknowledgements This work was carried out within the SoLifE research project fund by the German Federal Ministry for Economic Affairs and Energy as a part of the 6th energy research program (project funding reference number: 0324084A).

Author Contributions AP contributed to conceptualization, methodology, validation, formal analysis, investigation, resources, data curation, writing—original draft, writing—review and editing, visualization, supervision, project administration. EB contributed to conceptualization, methodology, resources, writing—review and editing. MOD contributed to conceptualization, methodology, investigation, resources, writing—review and editing. IHD contributed to conceptualization, methodology, resources, writing—review and editing. GS contributed to writing—review and editing. JV contributed to conceptualization, methodology, resources, writing—review and editing, project administration, funding acquisition.

Funding Open Access funding enabled and organized by Projekt DEAL.

References

1. Helbing BT, Schmitz G. Experimental Analysis of Latent Heat Storages integrated into a Liquid Cooling System for the Cooling of Power Electronics. 16th International Refrigeration and Air Conditioning Conference at Purdue University, West Lafayette, Indiana, USA, July, 2016. p. 11–14, paper 2221.
2. Grabo M, Weber D, Paul A, Klaus T, Bermpohl W, Krauter S, Kenig EY. Numerical investigation of the temperature distribution in PCM-integrated solar modules. Chem Eng Trans. 2019;76:895–900.
3. Mehling H, Cabeza LF. Heat and cold storage with PCM: An up to date introduction into basics and applications. Berlin, Heidelberg: Springer; 2008.
4. Kenisarin M, Mahkamov K. Solar energy storage using phase change materials. Renew Sustain Energy Rev. 2007;11:1913–65.
5. Hasnain SM. Review on sustainable thermal energy storage technologies, part I: heat storage materials and techniques. Energy Convers Manage. 1998;39:1127–38.
6. Himran S, Suwono A, Mansoori GA. Characterization of alkanes and paraffin waxes for application as phase change energy storage medium. Energy Sources. 1994;16:117–28.
7. Sonnenrein G, Elsner A, Baumhögger E, Morbach A, Fieback K, Vrabec J. Reducing the power consumption of household refrigerators through the integration of latent heat storage elements in wire-and-tube condensers. Int J Refrig. 2015;51:154–60.
8. Sonnenrein G, Baumhögger E, Elsner A, Fieback K, Morbach A, Paul A, Vrabec J. Copolymer-bound phase change materials for household refrigerating appliances: experimental investigation of power consumption, temperature distribution and demand side management potential. Int J Refrig. 2015;60:166–73.
9. Sonnenrein G, Baumhögger E, Elsner A, Morbach A, Neukötter M, Paul A, Vrabec J. Improving the performance of household refrigerating appliances through the integration of phase change materials in the context of the new global refrigerator standard IEC 62552:2015. Int J Refrig. 2020;119:448–56.
10. Sharma A, Tyagi VV, Chen CR, Buddhi D. Review on thermal energy storage with phase change materials and applications. Renew Sustain Energy Rev. 2009;13:318–45.
11. Bogatov GF, Rastorguev YL, Grigor'ev BA. Thermal Conductivity of normal hydrocarbons at high pressures and temperatures. State Scientific Institute (GNI). Translated from Khimiya i Tekhnologiya Topliv i Masel, 1969. p. 9, 31–83, September 1969.
12. Naziev YM, Aliev MA. Thermal conductivity and specific heat of n-Decane at various temperatures and pressures. Ch. Il'drym Azerbaidzhan Polytechnic Institute. Baku Translated from Inzhenerno-Fizicheskii Zhurnal. 1973;24:1033–8.
13. Vargaftik NB, Filippov LP, Tarzimanov AA, Totskii EE. Handbook of thermal conductivity of liquids and gases. Boca Raton: CRC Press; 1994.
14. Abhat A. Low temperature latent heat thermal energy storage: heat storage materials. Sol Energy. 1983;30:313–32.
15. Vélez C, Khayet M, Ortiz de Zárate JM. Temperature dependent thermal properties of solid/liquid phase change even-numbered n-alkanes: n-Hexadecane, n-octadecane and n-eicosane. Appl Energy. 2015;143:383–94.
16. Sasaguchi K, Viskanta R. Phase change heat transfer during melting and solidification of melt around cylindrical heat source(s)/sink(s). J Energy Res Technol. 1989;111:43–9.
17. Sharma SD, Sagara K. Latent heat storage materials and systems: a review. Int J Green Energy. 2005;2:1–56.
18. Rastorguev YL, Bogatov GF, Grigor'ev BA. Thermal conductivity of higher n-alkanes. Chem Technol Fuels Oils. 1974;10:728–32.
19. Fleming FP, de Andrade Silva L, dos Santos Vieira Lima G, Herzog, I, Barreto Orlando HR, Daridon JL, Pauly J, Alzuguir Azevedo LF. Thermal conductivity of heavy, even-carbon number n-alkanes (C22 to C32). Fluid Phase Equilib. 2018;477:78–86.
20. Sari A, Karaipekli A. Thermal conductivity and latent heat thermal energy storage characteristics of paraffin/expanded graphite composite as phase change material. Appl Therm Eng. 2007;27:1271–7.
21. Li M, Wu Z. Thermal properties of the graphite/n-docosane composite PCM. J Therm Anal Calorim. 2013;111:77–83.
22. Li JF, Lu W, Zeng YB, Luo ZP. Simultaneous enhancement of latent heat and thermal conductivity of docosane-based phase change material in the presence of spongy graphene. Sol Energy Mater Sol Cells. 2014;128:48–51.
23. Hatta H, Taya M. Equivalent inclusion method for steady state heat conduction in composites. Int J Eng Sci. 1986;24:1159–72.
24. Sölter HJ. Das Laserpunktverfahren zur simultanen Bestimmung der Temperatur- und Wärmeleitfähigkeit von Zweischichtsystemen: Vergleich und Auswerteformalismen und Untersuchungen an plasmagespritzten Schichten. PhD thesis. Universität Stuttgart. 1990.
25. Van der Held EFM, van Drunen FG. A method of measuring the thermal conductivity of liquids. Physica. 1949;15:865–81.
26. Healy JJ, de Groot JJ, Kestin J. The theory of the transient hot-wire method for measuring thermal conductivity. Physica. 1976;82C:392–408.
27. Haran EN, Wakeham WA. A transient hot-wire cell for thermal conductivity measurements over a wide temperature range. J Phys E: Sci Instrum. 1982;15:839–42.
28. Song Y. Das transiente Heißdraht-Verfahren und seine Anwendung zur Messung der Wärmeleitfähigkeit bis nahe an den kritischen Punkt. PhD thesis. Universität Stuttgart. 1992.
29. Kranzmann AE. Wärmeleitfähigkeit von drucklos gesinterten AIN-Substratkeramiken. PhD thesis. Max-Planck-Institut für Metallforschung, Universität Stuttgart. 1988.
30. Kose V, Wagner S. Kohlrausch Praktische Physik, vol. 2. Stuttgart: B. G. Teubner; 1996.
31. Flynn DR, Zarr RR, Healy W, Hahn MH. Design concepts for a new guarded hot plate apparatus for use over an extended temperature range. The fourth symposium on insulations materials: testing and applications. Charleston, S. C., USA, 2002. October 21–22. p. 98–115.
32. Yang I, Kim D, Lee S. Construction and preliminary testing of a guarded hot plate apparatus for thermal conductivity measurements at high temperatures. Int J Heat Mass Transf. 2018;122:1343–52.
33. Baehr HD, Stephan K. Heat and mass transfer. Berlin, Heidelberg: Springer-Verlag; 2011.
34. Poling BE, Prausnitz JM, O´Connell JP. The properties of gases and liquids. New York: McGraw-Hill; 2001.
35. Lewis TB, Nielsen LE. Dynamic mechanical properties of particulate-filled composites. J Appl Polym Sci. 1970;14:1449–71.

6.6 Improving the performance of household refrigerating appliances through the integration of phase change materials in the context of the new global refrigerator standard IEC 62552:2015

Sonnenrein, G., Baumhögger, E., Elsner, A., Neukötter, M., Paul, A., Vrabec, J., 2020. International Journal of Refrigeration 119, 448-456.

Im Rahmen dieser Studie wurde der Einfluss von Latentwärmespeicherelementen im Lagerfach für frische Lebensmittel (Kühlschrank) auf die Kühlleistung und die Zeit eines Temperaturanstiegs bei einer Störung gemäß der Normenreihe IEC 62552:2015 experimentell untersucht. Für die Kühlleistungsversuche wurde ein bestehender Versuchsaufbau aus der IEC 62552-2:2015 verwendet. Da der in der Norm beschriebene Versuchsaufbau zur Bestimmung der Zeit eines Temperaturanstiegs nur für Gefrierfächer definiert ist, wurde auf Grundlage dieses Versuchsaufbaus ein neues Messverfahren entwickelt. Die Ergebnisse zeigen, dass durch den Einsatz von PCM die Kühlleistung um bis zu 33 % steigt und sich auch die Zeit eines kritischen Temperaturanstiegs um bis zu 145 % verlängert. Im Vergleich zu den unmodifizierten Referenzgeräten wurde die Energieaufnahme, der mit PCM ausgestatteten Geräte nicht beeinträchtigt.

Der Autor dieser Dissertation hat bei der Ausarbeitung der Versuchsaufbauten und der Versuchsdurchführung mitgewirkt. Gerrit Sonnenrein hat die vorliegende Publikation verfasst, die Latentwärmespeicherelemente entwickelt, die Versuche durchgeführt und ausgewertet. Moritz Neukötter hat bei der Versuchsdurchführung und Andreas Elsner sowie Elmar Baumhögger haben an der Mess- und Regeltechnik für die Versuchsdurchführung mitgearbeitet. Andreas Morbach, Andreas Elsner und Vrabec haben an der Überarbeitung des Manuskripts mitgewirkt. Während der gesamten Arbeit wurde der Autor von Jadran Vrabec betreut.

International Journal of Refrigeration 119 (2020) 448–456

Contents lists available at ScienceDirect

International Journal of Refrigeration

journal homepage: www.elsevier.com/locate/ijrefrig

Improving the performance of household refrigerating appliances through the integration of phase change materials in the context of the new global refrigerator standard IEC 62552:2015

G. Sonnenrein[a], E. Baumhögger[a], A. Elsner[a], A. Morbach[b], M. Neukötter[a], A. Paul[a], J. Vrabec[c,*]

[a] Thermodynamics and Energy Technology, University of Paderborn, Warburger Str, 100, 33098 Paderborn, Germany
[b] Miele & Cie. KG, Carl-Miele-Str. 29, 33332 Gütersloh, Germany
[c] Thermodynamics and Process Engineering, Technical University of Berlin, Ernst-Reuter-Platz 1, 10587 Berlin, Germany

ARTICLE INFO

Article history:
Received 20 May 2020
Revised 19 July 2020
Accepted 28 July 2020
Available online 1 August 2020

Keywords:
Household refrigerator
Thermal storage
Phase change material
Cooling capacity
Temperature rise

ABSTRACT

The influence of latent heat storage elements on the cooling performance and the temperature rise time of household refrigerating appliances is studied experimentally in the context of the "new global refrigerator standard" IEC 62552:2015. In addition to the daily energy consumption, this international standardization introduced performance tests for cooling capacity and temperature rise time. While the cooling capacity has long been anchored in various test procedures of consumer organizations, the temperature rise time, which has only been tested on freezers so far, will be a decisive factor in the future. Moreover, the need for so-called "smart appliances" that may balance power consumption is increasing since such devices may compensate the volatility of renewable energies and thus stabilize the power grid. Against this background, eight commercial household refrigerators and refrigerator-freezers are equipped with polymer-bound phase change materials (PCM) and their performance is determined under the new standard test conditions. The results show that the introduction of PCM increases the cooling capacity by up to 33 % and also increases the temperature rise time by up to 145 %, without affecting power consumption, as compared to the unmodified refrigeration appliances.

Amélioration des performances des équipements frigorifiques domestiques par l'intégration de matériaux à changement de phase dans le cadre de la nouvelle norme mondiale IEC 62552:2015 relative aux réfrigérateurs

Mots-clés: Réfrigérateur domestique; Accumulation thermique; Matériau à changement de phase; Puissance frigorifique; Élévation de la température

1. Introduction

Although the power consumption of a single household refrigeration appliance appears to be low, the savings potential of the entire fleet is considerable due to the almost complete market penetration and typical continuous operation. In total, over 1.5 billion household refrigerators and freezers are in use worldwide, accounting for approximately 4 % of global electricity consumption (Coloumb et al., 2015), annually causing 480 million tons of CO_2 equivalent (Barthel and Götz, 2012). As a result, test standards with sometimes striking energy labels were developed in many countries from as early as the 1990s. Meanwhile, energy efficiency has become a decisive purchase criterion for consumers (Faberi et al., 2007). However, these often very different standards and regulations require specific tests for the regional distribution of these products, which is costly and time consuming. To mitigate this problem, e.g. Bansal (2003) called for the creation of a single, consolidated testing standard. The development of this so-called "global standard" already began in 2006

* Corresponding author.
E-mail address: vrabec@tu-berlin.de (J. Vrabec).

https://doi.org/10.1016/j.ijrefrig.2020.07.025
0140-7007/

Nomenclature

h	specific enthalpy (kJ kg^{-1})
T	temperature (°C)
TMP_i	temperature measurement point
T_{ama}	time averaged ambient temperature (°C)
T_i	instantaneous refrigerator compartment temperature (°C)
T_{ma}	time averaged refrigerator compartment temperature (°C)
T_{Mi}	instantaneous M-package temperature (°C)
$T_{M,a}$	arithmetic average of all instantaneous M-package temperatures (°C)
$T_{M,max}$	instantaneous temperature of the warmest M-package (°C)
M_i	M-package number

and led to the new IEC 62552:2015 "Household refrigerating appliances – characteristics and test methods", which is currently being adapted into national standards in many countries and regions. In addition to the standardization of power consumption measurement, performance tests for cooling capacity and temperature rise time have recently been introduced. Table 1 provides an overview of the different test conditions for the daily energy consumption measurements of some of the most important international standards.

The positive influence of PCM, both on power consumption and temperature stability of household refrigeration appliances, has been known for a long time and has been the subject of scientific research in recent years, cf. Azzouz et al. (2008, 2009), Khan et al. (2015), Oró et al. (2012a, 2012b), Sonnenrein et al. (2015a, 2015b) and references therein. PCM can absorb large amounts of heat at almost constant temperature and are thus particularly well suited for heat and cold storage. By implementing PCM, temperature fluctuations were reduced successfully in a variety of applications, e.g. transport boxes for sensitive goods or heat sinks for electronic devices. Mehling and Cabeza (2008) provide a general overview.

Already Onyejekwe (1989) attached a simple latent heat accumulator based on an eutectic NaCl/H_2O mixture to the evaporator to increase the coefficient of performance (COP) of a refrigerator. Wang et al. (2007a, 2007b, 2007c) examined the influence of PCM at various locations in the cooling system and were able to raise their prototype's efficiency by 6 % to 8 %. Besides an increase of energy efficiency by 3 % to 4 % through a 1°C increase of evaporator temperature, Cheralathan et al. (2007) were able to prove the potential of load shifting into cost-effective power night-rates of an industrial cooling device. A direct connection of different PCM-layers to the evaporator of a household refrigerator allowed Azzouz et al. (2008, 2009) to achieve a 10 to 15 % increase of the COP through a higher evaporator temperature and simultaneously a considerable reduction of the on/off switch control frequency. Through PCM in contact with the refrigerator compartment evaporator of a domestic refrigerator/freezer appliance, Visek et al. (2014) showed an improvement of about 6 % in terms of energy consumption during the refrigeration cycle.

In a preceding study Sonnenrein et al. (2015) were able to reduce the power consumption by up to 12 % through the integration of polymer-bound PCM into foamed as well as roll-bond evaporators. Yusuffoglu et al. (2015) achieved similar energy savings of about 10 % in their studies on the integration of different PCM in foamed evaporators. Niyai et al. (2017) located PCM in a roll-bond evaporator of a domestic refrigerator

Table 1
Overview of different test conditions for energy consumption measurements.

Region	Europe	Australia / New Zealand	USA	USA	Japan	Global standard
Standard	EN 62552:2013	AS/NZS 4474.1:2007	ANSI/AHAM HRF-1(2007)	AHAM HRF-1(2008)	JIS C 9801 (2006)	IEC 62552:2015
Energy consumption test						
Ambient temperature	25°C	32°C	32.2°C	32.2°C	15°C & 30°C	16°C & 32°C
Fresh food compartment temperature	5°C	3°C	3.3 / 7.22°C	3.9°C	4°C	4°C
Frozen food compartment temperature	-18°C	-15°C	-15/ -17.8°C	-17.8°C	-18°C	-18°C
Loading of frozen food compartment	yes	no	no (No-frost) yes (static cooling)	no (No-frost) yes (static cooling)	no (No-frost) yes (static cooling)	no
Door openings and insertion of warm load	no	no	no	no	yes (No-frost)	no
Performance test at varying ambient temperatures						
Ambient temperature	10/16 to 32/38/43°C	10/32/43°C	12.8/21.1/ 32.2/43.3°C	-	15/30°C	10/16 to 32/38/43°C
Fresh food compartment temperature	0 to 4°C	0.5 to 6°C	1.1 to 5°C	-	0 to 4°C	0 to 4°C
Frozen food compartment temperature	≤-18°C	≤-15°C	≤-15/ -17.8°C	-	≤-18°C	≤-18°C
Loading of frozen food compartment	Yes	yes	yes	-	yes	yes
Freezing test	yes	no	no	no	yes	yes
Temperature rise test	yes	no	yes (freezers only)	no	yes	yes
Pull-down test	no	yes	yes	no	yes	yes
Automatic ice-making test	yes	yes	yes	no	yes	yes

and were able to reduce its compressor running time significantly. Cofré-Toledo et al. (2018) studied the integration of two eutectic PCM and could also show an improved COP through an increase of the evaporator temperature, but the temperature of the refrigerator compartments was affected negatively. Investigations of Berdja et al. (2019) showed similar results. Maiorino et al. (2019) integrated water as a PCM in contact with the evaporator of a household refrigerator and showed a reduced switching frequency and lower temperature fluctuations in the refrigerator compartment. Ben-Abdallah et al. (2019) came to similar conclusions by integrating PCM into the evaporator of an open display cabinet. Although the most commonly studied PCM configuration is the integration into the evaporator, another possibility is the integration into the condenser. Cheng et al. (2011) were able to reduce the power consumption of a refrigerator/freezer combination by up to 12 % through the integration of a paraffin-polyethylene compound on the integrated, i.e. foamed, condenser. In another investigation Sonnenrein et al. (2015) studied different options of sensible and latent heat storage elements integrated into standard wire-and-tube condensers and were able to reduce the power consumption by about 10 % with a newly developed PCM polymer compound.

The third possibility is to integrate PCM inside the freezer or refrigerator to reduce temperature fluctuations or to slow down the temperature rise, e.g. in case of a power failure. Gin et al. (2010a, 2010b) studied the temperature rise in a household freezer with integrated PCM panels during power loss, defrosting cycles as well as door openings and found an improved storage quality and a significantly slower temperature increase inside the freezer. Oró et al. (2012a) found consistent results for commercial freezers and also observed a significantly slower temperature rise in case of a refrigeration system failure (Oró et al., 2012b). Liu et al. (2017) placed a $NaCl/H_2O$ mixture in the freezer and water as a PCM in the air duct of the fresh food chamber of an air-cooled frost-free refrigerator and found a decreased temperature rise in the fresh food and freezing compartments, but noticed an increase of power consumption depending on the operating mode. More studies about the application of PCM in refrigerators/freezers can be found in the reviews of Mastani Joybari et al. (2015) or Bista et al. (2018).

Together, these studies provide a good insight into the general advantages of PCM in refrigerators and freezers, such as the positive influence on COP, temperature fluctuations and on/off ratio. However, none examined the effects on the new standardized functional test procedures introduced internationally by the IEC 62552:2015. With this standard, cooling capacity and temperature rise time can now be quantified in the same way as the energy consumption and will thus play a comparable role in the future. Therefore, this paper studies the effect of a polymer-bound PCM on (1) the cooling capacity and (2) the energy consumption according to the IEC 62552:2015 of eight commercially available household refrigerators. Moreover, the effects on the (3) temperature rise time in the refrigerator compartment were determined. For this purpose, a test procedure was developed that is analogous to the IEC test for freezers in order to examine the refrigerators' suitability as future smart appliances.

2. Test setup

2.1. Methodology

The tests in this study were performed according to the IEC 62552:2015. The cooling capacity test determines the time required to cool a specific load (4.5 kg per 100 l volume) from 25°C down to 10°C; details can be found in Part 2 of the IEC standard. The original temperature rise test in the IEC standard determines the time interval for the temperature of a specific load to increase by a certain amount. In case of a three- or four-star freezer compartment, this would be from -18°C to -9°C, once the operation of the refrigeration system has been interrupted, details can be found in Part 2 of the IEC standard. Analogously, in this study the time interval was determined during which the temperature of a specific load in the refrigerator compartment rises from 8°C to 11°C. Following Part 3 of the IEC standard, all power consumption tests were also performed at an ambient temperature of 25°C. Although the standard mentions energy consumption tests at 16 and 32°C ambient temperature and an interpolation of the measurements results to 25°C, the method can in principle be applied at any other ambient temperature.

Table 2
Measured properties and their uncertainties.

Measured quantity	Measuring device	Uncertainty
Temperature	Thermocouples	±0.1 K
Power	Energy meters	±0.05 W
Time	Personal computer	±0.1 s/day

2.2. Measurement of temperatures and power consumption

The test setup and all executed measurement procedures were in accordance with the IEC standard mentioned above. Fig. 1 schematically shows the standard temperature measurement positions TMP_1, TMP_2 and TMP_3 as well as the filling and distribution of test packages and M-packages (M1 to M6) in a fresh-food compartment.

Temperature sampling was carried out by thermocouple differential measurements, each measuring point with a reference junction in an ice water bath. The utilized acquisition interface OMB-DAQ 55/56 (Omega Technologies) was combined with a preamplifier LTC1050 (Linear Technologies), which limits the offset conditioned by zero-point drift to ±0.025 K. The typical error of thermo-elements of ±1% x ΔT in other work was reduced to ±0.5% x ΔT by batch consistency and polynomial calibration. For determining the power consumption under standard conditions (average temperature of the fresh-food compartment T_{ma} = 4°C, ambient temperature T_{ama} = 25°C and humidity 50 %), energy meters type EZI 1 (Zimmer Electronic Systems) with 25 pulses/Wh were used, leading to a relative measurement error of < 1%. Table 2 summarizes the measured quantities and their associated uncertainties.

2.3. Refrigerating appliances

A total of eight commercially available refrigerators and refrigerator-freezers with volume capacities of the fresh food compartment between 158 l and 320 l were analyzed. Power consumption, cooling capacity and temperature rise tests were first performed with the appliances in their original state and subsequently with PCM. Table 3 summarizes the essential technical data of the examined appliances. Fig. 2 shows the setup of a fresh-food compartment equipped with PCM and M-packages.

2.4. Heat storage materials

High-capacitive, dimensionally stable latent heat storage elements based on polymer-bound organic paraffin derivatives were developed in this study. In contrast to prior approaches, this compound material is dimensionally stable and in its "liquid" state it is secure against leakage and exudation. Therefore, an elaborate encapsulation is not necessary and the PCM compound was processed into foil-laminated sheets and integrated on top of the shelves of the refrigerating appliances, in order to examine their

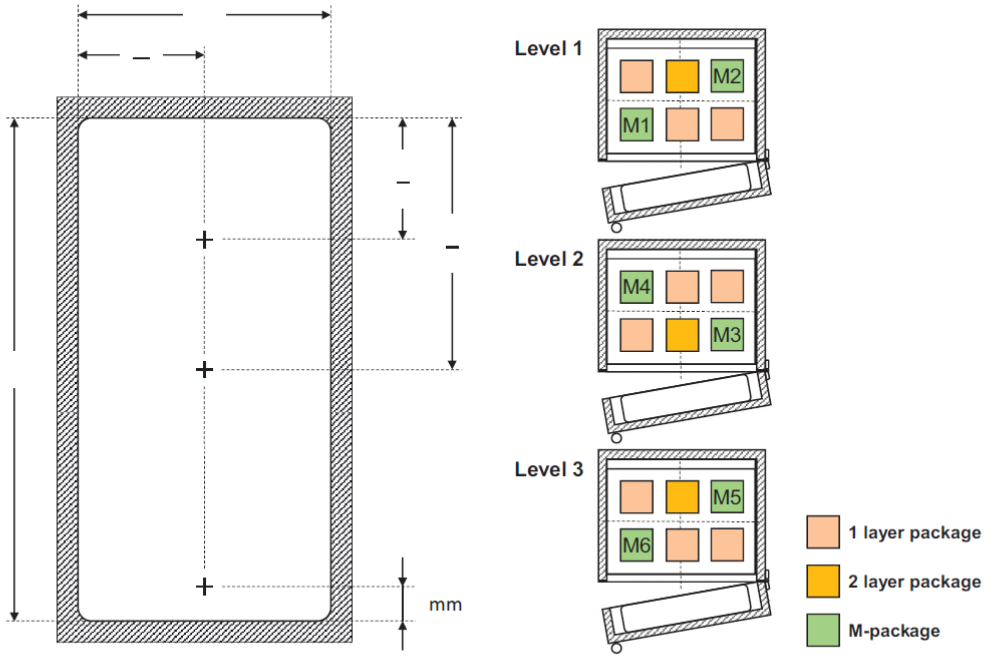

Fig. 1. Standard temperature measurement positions *TMP1*, *TMP2* and *TMP3* (left) and the filling and distribution of test packages and M-packages in a fresh-food compartment (right).

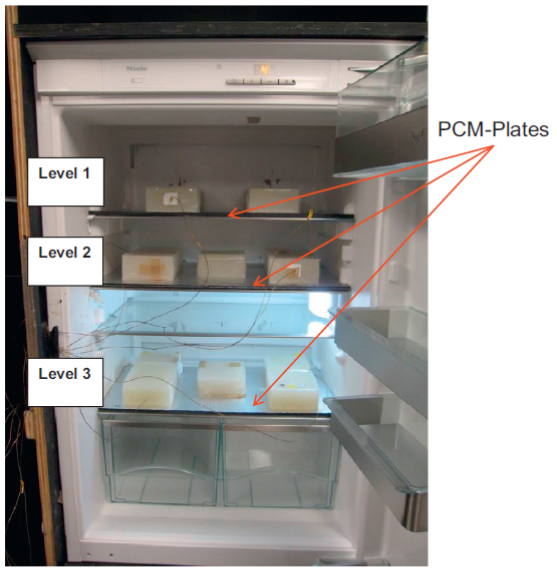

Fig. 2. Fresh-food compartment of a tested appliance equipped with PCM and M-packages.

influence on performance and power consumption. Depending on the size of the fresh-food compartment and the number of shelves, between 1.79 kg and 2.96 kg of PCM were placed in the refrigerating appliances, corresponding to specific PCM densities of 0.72 kg to 1.41 kg per 100 l volume.

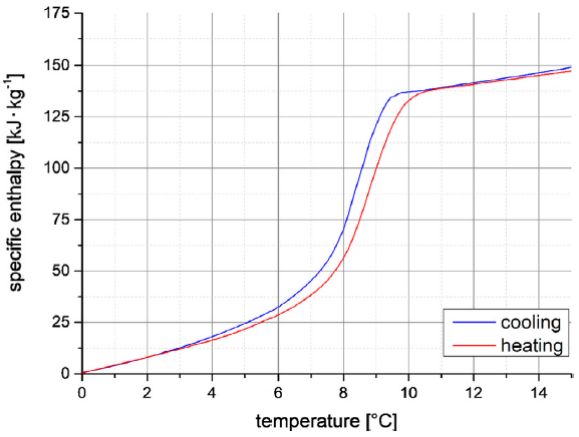

Fig. 3. Specific enthalpy as a function of temperature of the developed PCM polymer compound.

Fig. 3 shows the temperature dependence of the specific enthalpy h of the compound developed for the integration in fresh-food compartments of refrigerating appliances. Measurements were done with Differential Scanning Calorimetry (DSC, SETARAM TG-DSC 111) and also with a heat flow three-layer calorimeter (W&A, WOTKA), developed specifically for analyzing PCM. The latter allows for a considerably larger sample quantity than commercial DSC devices and therefore yields the phase change temperature more precisely. The specific enthalpy h of the dimensionally stable polymer compound in the temperature range of from 0°C to 15°C is about 150 kJ/kg and the phase change temperature is around 9°C.

Table 3
Technical data of the examined refrigerating appliances.

Test device	R1	R2	R3	R4	C1	C2	C3	C4
Combined refrigerator-freezer	no	no	no	no	yes	yes	yes	yes
Refrigerator model	K9252i-1	K12020 S-1	KRIE 2183	K37272 iD	CUPesf 3503	KD12622 S edt/cs	KG39 EAI40	BCD-185TNG
Manu-facturer	Miele	Miele	Bau-knecht	Miele	Liebherr	Miele	Siemens	Haier
Dimensions (HxBxT) [mm]	872 × 540 × 550	850 × 628 × 601	1770 × 535 × 540	1772 × 560 × 550	1817 × 631 × 600	1623 × 637 × 600	2010 × 650 × 600	1900 × 700 × 680
Fridge storage volume [l]	158	167	320	216	232	199	247	185
Total storage volume [l]	158	167	320	216	323	253	339	243
Refrigerant	35 g R600a	22 g R600a	55 g R600a	60 g R600a	90 g R600a	48 g R600a	78 g R600a	42 g R600a
Energy label	A++	A+	A++	A++	A++	A++	A+++	A++

Fig. 4. Transparency of the present polymer compound from solid (top) to liquid (bottom).

Fig. 3 also shows a significant advantage of the present polymer compound compared to the salt-water or glycol solutions often used in other studies. The subcooling that is necessary for initiating solidification of these liquids, i.e. the difference between melting and freezing temperature, is typically between 5 K and 15 K, whereas the present polymer compound does not undergo significant subcooling. This is crucial for the use in the fresh food compartment, where only very small temperature differences are available for solidification and melting of the PCM. A further advantage of the present polymer compound is its transparency (or milky transparency), which also enables simple integration into the (e.g. double-walled) shelves in later practice, cf. Fig. 4.

3. Results and discussion

Experimental tests with eight commercially available household refrigerators and refrigerator-freezers, cf. Table 3, equipped with PCM polymer compound were carried out to investigate the effect

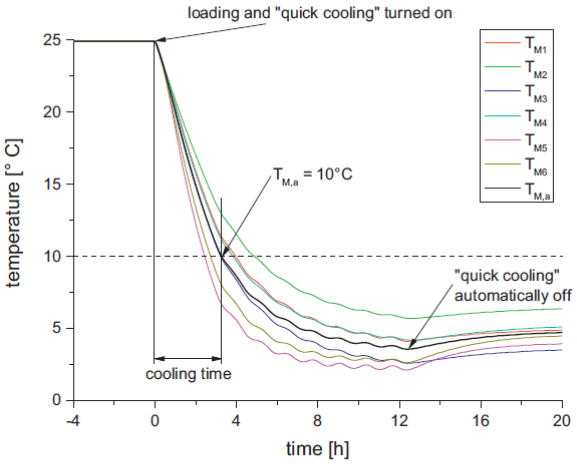

Fig. 5. Temperatures of the M-packages during the cooling capacity test according to IEC 62552:2015.

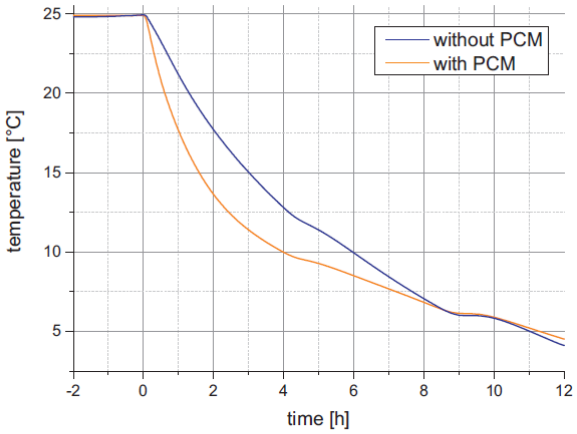

Fig. 6. Mean temperatures of M-packages ($T_{M,a}$) during the cooling capacity test of refrigerating appliance C1 without PCM (blue) and with PCM (orange). Fig. 7 Cooling capacity test of the studied refrigerating appliances without (blue) and with PCM (orange).

on cooling capacity, temperature rise and daily energy consumption following the global standard (IEC 62552:2015, 2015).

3.1. Cooling capacity

The cooling capacity test according to IEC 62552:2015 determines the time required to cool a specific load (4.5 kg per 100 l volume) from 25°C down to 10°C. For this purpose, the refrigerating appliances were each loaded with 4.5 kg per 100 l (fresh-food compartment) volume with defined test- and M-packages (IEC 62552:2015, Part 1, Annex C) according to a defined filling plan (IEC 62552:2015, Part 2, Chapter 7), cf. Fig. 1. Loading started when stable operating conditions with a mean temperature $T_{ma} = +4°C \pm 0.5$ K have been attained. In order to achieve comparable and reproducible results, loading always took place exactly at the start of a compressor cycle. And as defined in the standard, if the appliance had a "quick cooling" function, this was activated at the moment when the load was inserted. Fig. 5 shows an exemplary temperature curve of such a cooling capacity test, where the cooling time was measured by determining the time between loading and when the arithmetic mean of the temperatures of all M-packages ($T_{M,a}$) had reached 10°C.

The influence of the latent heat storage elements integrated into the fresh-food compartment on the cooling time is exemplarily shown in Fig. 6. The cooling time of the refrigerator-freezer C1 equipped with PCM was reduced by 33 % from 5.9 to 3.9 h. Fig. 7 summarizes the results of all cooling capacity measurements. The cooling time could be significantly shortened by the PCM for all refrigerating appliances, i.e. between 0.55 to 2.00 h in absolute terms and between 16 to 33 % in relative terms.

3.2. Temperature rise

The temperature rise time in case of (external) switch-off, only tested on freezers so far, will in the future be a decisive factor in the context of the use of refrigerators as "smart appliances" for energy peak shaving. Although network connectivity of household refrigerators/freezers is currently not a commercial reality, they might play a role here in the future due to their large number. The European Commission is currently engaged in a "horizontal preparatory study" on this subject (LOT 33, 2019). The actual temperature rise test in the IEC standard (IEC 62552:2015, Part 2, Annex C) determines the time taken for the temperature of a specific load in the freezer compartment to rise from -18°C to -9°C after power is disconnected. Analogously, in this study the temperature rise time was determined in which a specific load in the refrigerator compartment rises from X°C to Y°C.

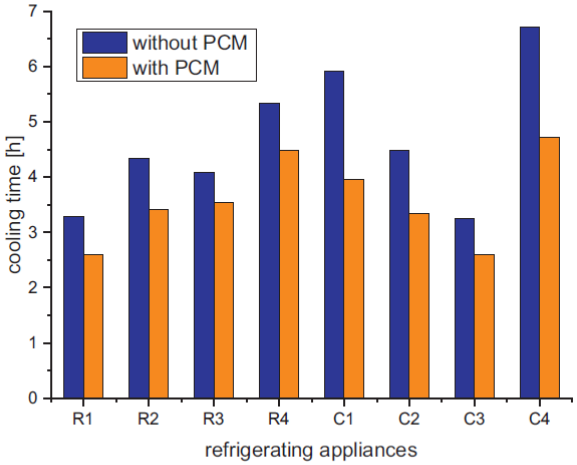

Fig. 7. Cooling capacity test of the studied refrigerating appliances without PCM (blue) and with PCM (orange).

Because -18°C is clearly defined as the maximum permissible temperature in the compartment of a three- or four-star freezer (IEC 62552:2015, Part 2, Table 2), the lower temperature limit (X°C) can be defined analogously as the maximum permissible temperature of 8°C in the fresh-food compartment. The upper temperature limit of -9°C stated in the original freezer test is more or less arbitrary, i.e. not defined anywhere else (two-star freezer < -12°C, one-star freezer < -6°C). The only remaining definition is that during a defrost period, which is comparable to a switch-off, the temperature may rise by up to 3 K. Following this analogy, the upper temperature limit Y°C for determining the temperature rise time in fresh food compartments was set to 11°C in this study. Like in Section 3.1, the refrigerating appliances were loaded with 4.5 kg

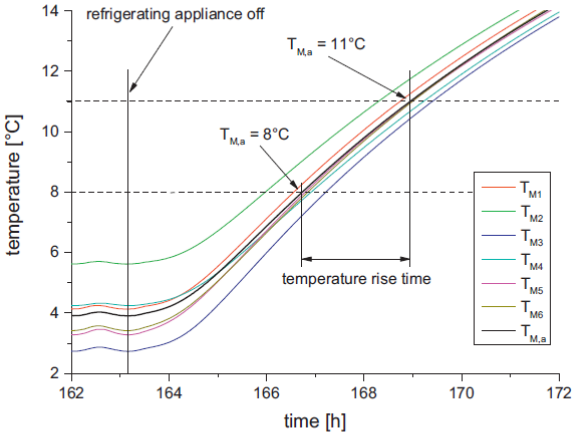

Fig. 8. Temperatures of the M-packages during the temperature rise time test in analogy to IEC 62552:2015.

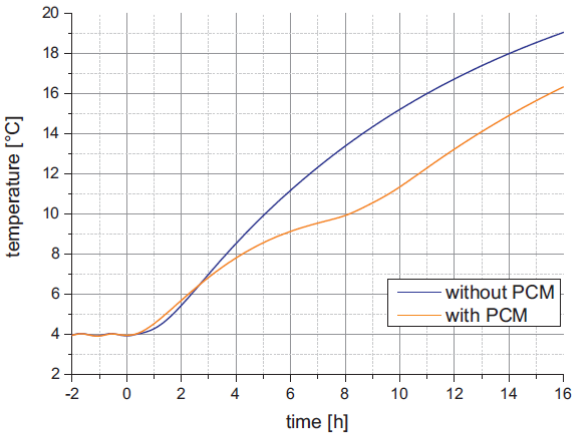

Fig. 9. Mean temperatures of M-packages ($T_{M,a}$) during the temperature rise time test of refrigerating appliance R1 without PCM (blue) and with PCM (orange).

test and M-packages per 100 l (fresh-food compartment) volume according to the filling plan. In analogy to the freezer temperature rise test, the power supply was switched off once stable operating conditions were achieved, and the temperature rise time was determined as the the time during which the arithmetic mean of the temperatures of all M-packages $T_{M,a}$ rises from 8°C to 11°C.

Fig. 8 shows exemplary temperature curves of the M-packages of such a measurement. The influence of the latent heat storage elements integrated into the fresh-food compartment on the temperature rise time is exemplarily shown in Fig. 9. While the temperature of the warmest M-package without PCM rises continuously, the temperature curve with PCM shows a clear temperature plateau in the range of the melting temperature. Thereby, the temperature rise time of refrigerator R1 equipped with PCM was increased by 145 % from 2.2 to 5.4 h. It is also evident that when considering an upper temperature limit of $T_{M,a}$ = 12°C instead of $T_{M,a}$ = 11°C, the increase would even be greater.

Fig. 10 summarizes the results of all temperature rise time measurements. The temperature rise time could be significantly increased by the PCM for all refrigerating appliances, i.e. between

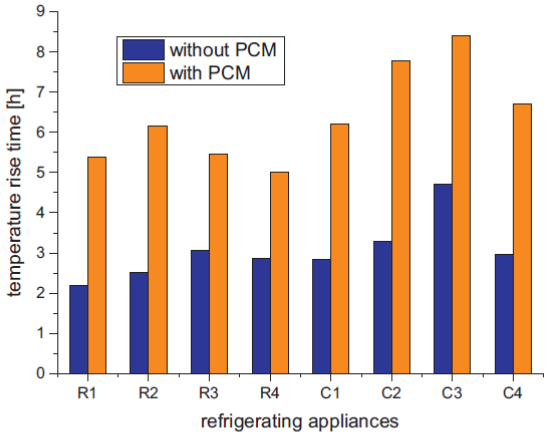

Fig. 10. Temperature rise time of the studied refrigerating appliances without PCM (blue) and with PCM (orange).

2.15 to 4.48 h in absolute terms and between 75 % to 145 % in relative terms.

3.3. Energy consumption

Even though performance tests have now been internationally standardized with the global standard IEC 62552:2015, the daily energy consumption remains the most important technical specification of a refrigerating appliance. Therefore, the effects of all modifications on power consumption were measured to facilitate their later implementation into practice. A summary of the results including the energy consumption measurements obtained with the present experiments is given in Tables 4 and 5. In all cases with PCM, the results show that the cooling capacity as well as temperature rise time was increased without affecting energy consumption. The maximum deviations found here are all within the range of the uncertainty of the energy consumption measurement.

4. Conclusions

A polymer-bound PCM with a phase change temperature around 9°C was developed and integrated into the fresh-food compartment of different commercially available household refrigerating appliances. In this experimental study, their influence on daily energy consumption, cooling capacity and temperature rise time according to the global standard IEC 62552:2015 was studied.

The results show a considerable positive influence on the performance indicators cooling capacity and temperature rise, without negatively impacting energy consumption. Through the integration of PCM into the appliances, the cooling capacity was increased by up to 33 % and temperature rise time even by up to 145 %.

Given that the present polymer compound is leak proof and (milky) transparent, a direct integration into the fresh-food compartment shelves of household refrigerators/freezers can also be easily implemented into practice. It was shown that this also enhances the suitability of refrigerators/freezers as "smart appliances" to meet the growing demand for balancing energy to compensate the growing volatility of renewable energy.

Nevertheless, future work on developing polymer-bound PCM with lower phase change temperatures and evaluating their effects on cooling capacity and temperature rise time has to be done.

Table 4
Test results of the studied refrigerators.

Test device			R1 refrigerator	R2 refrigerator	R3 refrigerator	R4 refrigerator
Fridge storage volume		[l]	158	167	320	216
Thermostat set point			3°C	4°C	3°C	4°C / b5
PCM		[g]	2235	2271	2297	2360
mass		[kg/100l]	1.41	1.36	0.72	1.09
Cooling time	without PCM	[h]	3.28	4.33	4.08	5.33
	with PCM	[h]	2.60	3.42	3.53	4.48
	difference	[h]	-0.68	-0.92	-0.55	-0.85
	relative		126%	127%	116%	119%
Temperature	without PCM	[h]	2.20	2.52	3.05	2.85
rise time	with PCM	[h]	5.38	6.15	5.47	5.00
(average)	difference	[h]	3.18	3.63	2.42	2.15
	relative		245%	244%	179%	175%
Daily energy	without PCM	[kWh/day]	0.377	0.437	0.384	0.375
consumption	with PCM	[kWh/day]	0.371	0.431	0.384	0.379

Table 5
Test results of the studied refrigerator-freezers.

Test device			C1 combination	C2 combination	C3 combination	C4 combination
Fridge storage volume		[l]	232	199	247	185
Thermostat set point			1°C	5	4°C / -16°C	3.6
PCM mass		[g]	2963	2814	2235	1791
		[kg/100l]	1.28	1.41	0.90	0.97
Cooling	without PCM	[h]	5.92	4.48	3.25	6.72
time	with PCM	[h]	3.95	3.35	2.60	4.72
	difference	[h]	-1.97	-1.13	-0.65	-2.00
	relative		150%	134%	125%	142%
Temperature	without PCM	[h]	2.83	3.28	4.72	2.95
rise	with PCM	[h]	6.22	7.77	8.40	6.70
time	difference	[h]	3.38	4.48	3.68	3.75
(average)	relative		219%	237%	178%	227%
Daily energy	without PCM	[kWh/day]	1.146	0.716	0.479	0.426
consumption	with PCM	[kWh/day]	1.164	0.710	0.475	0.423

Declaration of Competing Interest

The authors declare that they have no known competing financial interests or personal relationships that could have appeared to influence the work reported in this paper.Acknowledgements

This work was supported by Deutsche Bundesstiftung Umwelt (DBU, AZ 28626).

References

Azzouz, K., Leducq, D., Gobin, D., 2008. Performance enhancement of a household refrigerator by addition of latent heat storage. Int. J. Refrig. 31, 892–901.
Azzouz, K., Leducq, D., Gobin, D., 2009. Enhancing the performance of household refrigerators with latent heat storage: an experimental investigation. Int. J. Refrig. 32, 1634–1644.
Barthel, C., Götz, T., 2012. The overall worldwide saving potential from domestic refrigerators and freezers. Wuppertal (Germany). http://www.bigee.net/ media/filer _ public/2012/12/04/bigee _ doc _ 2 _ refrigerators _ freezers _ worldwide _ potential _ 20121130.pdf.
Ben-Abdallah, R., Leducq, D., Hoang, H.M., et al., 2019. Experimental investigation of the use of PCM in an open display cabinet for energy management purposes. Energy Conv. Manag. 198.
Berdja, M., Hamid, A., Sari, O., 2019. Characteristics and thickness effect of phase change material and frost on heat transfer and thermal performance of conventional refrigerator: theoretical and experimental investigation. Int. J. Refrig. 97, 108–123.
Bista, S., Hosseini, S.E., Owens, E., Phillips, G., 2018. Performance improvement and energy consumption reduction in refrigeration systems using phase change material (PCM). Appl. Therm. Eng. 142, 723–735.
Cheralathan, M., Velraj, R., Renganarayanan, S., 2007. Performance analysis on industrial refrigeration system integrated with encapsulated PCM-base cool thermal energy storage system. Int. J. Energy Res. 31, 1398–1413.
Cofré-Toledo, J., Vasco, D.A., Isaza-Roldán, C.A., Tangarife, J.A., 2018. Evaluation of an integrated household refrigerator evaporator with two eutectic phase-change materials. Int. J. Refrig. 93, 29–37.
Coulomb, D., Dupon, J.L., Pichard, A., 2015. The role of refrigeration in the global economy. http://www.iifiir.org/clientBookline/service/reference.asp?INSTANCE=exploitation&OUTPUT=PORTAL&DOCID=IFD _ REFDOC _ 0016453&DOCBASE=IFD _ REFDOC _ EN&SETLANGUAGE=EN.
Faberi, S., Esposito, R., Mebane, W., Presutto, M., Sciadoni, R., Stamminger, R., 2007. Preparatory Studies for Eco-design Requirements of EuPs: Final Report Domestic Refrigerators & Freezers. TREN/D1/40-2005.
Gin, B., Farid, M.M., Bansal, P.K., 2010a. Effect of door opening and defrost cycle on a freezer with phase change panels. Energy Convers. Manag. 51, 2698–2706.
Gin, B., Farid, M.M., 2010b. The use of PCM panels to improve storage condition of frozen food. J. Food Eng. 100, 372–376.
IEC 62552:2015, 2015. IEC 62552:2015 Household Refrigerating Appliances –Characteristics and Test Methods. International Electrotechnical Commission (IEC).
Joybari, Mastani, M., Haghighat, F., Moffat, J., Sra, 2015. Heat and cold storage using phase change materials in domestic refrigeration systems: the state-of- the-art review. Energy Build. 106, 111–124.
Khan, I., Afroz, H., 2015. Effect of phase change material on compressor on-off cycling of a household refrigerator. Sci. Technol. Built Environ. 21 (4), 462–468.
Liu, Z., Zhao, D., Wang, Q., Chi, Y., Zhang, L., 2017. Performance study on air-cooled household refrigerator with cold storage phase change materials. Int. J. Refrig. 79, 130–142.
Maiorino, A., Duca, M.G., Mota-Babiloni, A., Greco, A., Aprea, C., 2019. The thermal performances of a refrigerator incorporating a phase change material. Int. J. Refrig. 100, 255–264.
Mehling, H., Cabeza, L.F., 2008. Heat and Cold Storage with PCM. An up to Date Introduction into Basics and Applications. Springer-Verlag, Berlin, Heidelberg.
Onyejekwe, D., 1989. Cold storage using eutectic mixture of NaCl/H2O: an application to photovoltaic compressor vapours freezers. Sol. Wind Tech. 6, 11–18.
Oró, E., Miró, L., Farid, M.M., Cabeza, L.F., 2012a. Improving thermal performance of freezers using phase change materials. Int. J. Refrig. 35, 984–991.

Oró, E., Miró, L., Farid, M.M., Cabeza, L.F., 2012b. Thermal analysis of a low temperature storage unit using phase change materials without refrigeration system. Int. J. Refrig. 35, 1709–1714.

Sonnenrein, G., Baumhögger, E., Elsner, A., Fieback, K., Morbach, A., Paul, A., Vrabec, J., 2015. Copolymer-bound phase change materials for household refrigerating appliances: experimental investigation of power consumption, temperature distribution and demand side management potential. Int. J. Refrig. 60, 166–173.

Sonnenrein, G., Elsner, A., E., Baumhögger, A., Morbach, K., Fieback, Vrabec, J., 2015. Reducing the power consumption of household refrigerators through the integration of latent heat storage elements in wire-and-tube condensers. Int. J. Refrig. 51, 154–160.

Visek, M., Joppolo, C.M., Molinaroli, L., Olivai, A., 2014. Advanced sequential dual evaporator domestic refrigerator/freezer: System energy optimization. Int. J. Refrig. 43, 71–79.

Wang, F., Maidment, G., Missenden, J., Tozer, R., 2007a. The novel use of phase change materials in refrigeration plant. Part 1: experimental investigation. Appl. Therm. Eng 27, 2893–2901.

Wang, F., Maidment, G., Missenden, J., Tozer, R., 2007b. The novel use of phase change materials in refrigeration plant. Part 2: dynamic simulation model for the combined system. Appl. Therm. Eng 27, 2902–2910.

Wang, F., Maidment, G., Missenden, J., Tozer, R., 2007c. The novel use of phase change materials in refrigeration plant. Part 3: PCM for control and energy savings. Appl. Therm. Eng 27, 2911–2918.

Yusufoglu, Y., Apaydin, T., Yilmaz, S., Paksoy, H.O., 2015. Improving performance of household refrigerators by incorporating phase change materials. Int. J. Refrig. 57, 173–185.

7 Weitere Publikationen

Publikationen, die nicht Teil der Dissertation sind:

Sonnenrein, G., Baumhögger, E., Elsner, A., Fieback, K., Morbach, A., Paul, A., Vrabec, J., 2015. Copolymer-bound phase change materials for household refrigerating appliances: experimental investigation of power consumption, temperature distribution and demand side management potential. International Journal of Refrigeration 60, 166-173. DOI: https://doi.org/10.1016/j.ijrefrig.2015.06.030.

Grabo, M., Weber, D., Paul, A., Klaus, T., Bermpohl, W., Krauter, S., Kenig, E. Y., 2019. Numerical investigation of the temperature distribution in PCM-integrated solar modules. Chemical Engineering Transactions 76, 895-900. DOI: 10.3303/CET1976150

8 Wissenschaftliche Vorträge

Elsner, A.; Müller, M.; Paul, A.; Vrabec, J., 2013. Zunahme des Stromverbrauchs von Haushaltskältegeräten durch Alterung. Tagungsbeitrag, Deutsche Kälte-Klima Tagung 40, Hannover, Deutschland, 20.-22. November 2013.

Grabo, M., Weber, D., Paul, A., Klaus, T., Bermpohl, W., Krauter, S., Kenig, E. Y., 2019. Entwicklung eines thermischen 1D-Simulationsmodells zur Bestimmung der Temperaturverteilung in Solarmodulen. Tagungsbeitrag, 2. Regenerative Energietechnik Konferenz (RET.Con 2019), Nordhausen, Deutschland, 07.-08. Februar 2019.

Grabo, M., Weber, D., Paul, A., Klaus, T., Bermpohl W., Kenig, E. Y., 2019. Numerische Untersuchung der Temperaturverteilung in PCM-integrierten Solarmodulen. Tagungsbeitrag, Jahrestreffen der ProcessNet-Fachgruppe Energieverfahrenstechnik und des Arbeitsausschusses Thermische Energiespeicherung, Frankfurt am Main, Deutschland, 06.-07. März 2019.

Paul, A., Moczarski, L., Gieselmann, M., Reineke, M., Elsner, A., Baumhögger, E., Sonnenrein, G., Vrabec, J., 2019. Bestimmung von Wärmeverlusten in Haushaltskältegeräten. Deutsche Kälte-Klima Tagung 45, Ulm, Deutschland, 20.-22. November 2019.

Paul, A., Baumhögger, E., Elsner, A., Reineke, M., Kasper, T., Schumacher, D., Vrabec, J., Hueppe, C., Stamminger, R., Hoelscher, H., Stoll, R., Wagner, H., Gries, U., Becker, W., 2022. Alterungsmechanismen von Haushaltskältegeräten. Deutsche Kälte-Klima Tagung 48, Magdeburg, Deutschland, 16.-18. November 2022.

Erklärung zur Zitation von Inhalten aus studentischen Arbeiten

In Ergänzung zu meinem Antrag auf Zulassung zur Promotion in der Fakultät für Maschinenbau der Universität Paderborn erkläre ich gemäß §11 der Promotionsordnung und unter Beachtung der Regelung zur Zitation studentischer Arbeiten:

Die von mir vorgelegte Dissertation habe ich selbstständig verfasst, und ich habe keine anderen als die dort angegebenen Quellen und Hilfsmittel benutzt. Es sind keine Inhalte studentischen Ursprungs (studentische Arbeiten) in dieser Dissertation enthalten.

Paderborn, 12.05.2023

Abbildungsverzeichnis

Tabellenverzeichnis